Åbo Akademi University

Jani Rahkila

Multivalency in Carbohydrate Chemistry

From Oligosaccharides to Oligovalency and Beyond

Jani Rahkila (born 1987)

M.Sc. in Chemistry, 2012
Åbo Akademi University

Åbo Akademi University Press
Tavastgatan 13, FI-20500 Åbo, Finland
Tel. +358 (0)2 215 3478
E-mail: forlaget@abo.fi

Sales and distribution:
Åbo Akademi University Library
Domkyrkogatan 2–4, FI-20500 Åbo, Finland
Tel. +358 (0)2 -215 4190
E-mail: publikationer@abo.fi

MULTIVALENCY IN CARBOHYDRATE CHEMISTRY

Multivalency in Carbohydrate Chemistry

From Oligosaccharides to Oligovalency and Beyond

Jani Rahkila

Åbo Akademis förlag | Åbo Akademi University Press
Åbo, Finland, 2018

CIP Cataloguing in Publication

Rahkila, Jani.
Multivalency in carbohydrate chemistry : from oligosaccharides to oligovalency and beyond / Jani Rahkila. - Åbo : Åbo Akademi University Press, 2018.
Diss.: Åbo Akademi University.
ISBN 978-951-765-885-0

ISBN 978-951-765-885-0
ISBN 978-951-765-886-7 (digital)
Painosalama Oy
Åbo 2018

There is nothing like looking, if you want to find something.
You certainly usually find something, if you look,
but it is not always quite what you were after.

-J. R. R. Tolkien, The Hobbit

SUPERVISOR AND CUSTOS

Professor Reko Leino
Laboratory of Organic Chemistry
Åbo Akademi University
Åbo, Finland

OPPONENT

Professor David Crich
Department of Chemistry
Wayne State University
Detroit, MI, USA

REVIEWERS

Professor Pasi Virta
Laboratory of Organic Chemistry
University of Turku
Åbo, Finland

and

Professor Pedro Merino
Department of Organic Chemistry
Department of Synthesis and Structure of Biomolecules
University of Zaragoza
Zaragoza, Aragon, Spain

Preface

The work for this thesis was carried out at the Laboratory of Organic Chemistry, Johan Gadolin Process Chemistry Centre, Faculty for Science and Engineering, at Åbo Akademi University from January 2013 to December 2017. Financial support from the Academy of Finland, Stiftelsen för Åbo Akademi, the Magnus Ehrnrooth Foundation, TEKES, and the Johan Gadolin Process Chemistry Centre is gratefully acknowledged. COST action CM1102 *MultiGlycoNano* and Turku Centre for Lifespan Research are thanked for covering the expenses of several short term scientific missions during the work for this thesis.

First of all, I wish to thank my supervisor Professor Reko Leino for giving me the opportunity to work in several interesting carbohydrate-related projects. I am grateful for the support and trust since my time as an undergraduate. Furthermore, I would like to thank Professor Jesús Jiménez-Barbero (Chemical Glycobiology Lab, CIC bioGUNE, Bilbao, Spain) for many fruitful collaborations and allowing me to make several research visits to his laboratory. I also wish to thank Professors Pasi Virta (University of Turku) and Pedro Merino (University of Zaragoza) for reviewing my thesis, and Professor David Crich (Wayne State University) for being my opponent.

I wish to thank my mentor Dr. Filip Ekholm (University of Helsinki), who first introduced me to the world of carbohydrate chemistry, for a nearly endless flow of ideas and brainstorming throughout the years. I also wish to thank Professor Javier Cañada (Centro de Investigaciones Biológicas) and Dr. Ana Ardá (CIC bioGUNE) for their help during my research visits to Spain, and Professor Johannes Savolainen (University of Turku) for lending his expertise in some of the biological aspects. The dynamic duo of the Instrument Centre in Arcanum, Dr. Petri Ingman and Dr Jari Sinkkonen, is thanked for helping solve countless NMR related issues.

I would like to thank my current and past coworkers and good friends at the Laboratory of Organic chemistry, in no particular order: Dr. Patrik Eklund, Dr. Tiina Saloranta-Simell, Professor Leif Kronberg, Dr. Jan-Erik Lönnqvist, Päivi Pennanen, Peter Holmlund, Dr. Ramesh Ekambaram, Professor Jorma Mattinen, Dr. Denys Mavrynsky, Sabine Rendon, Dr. Risto Savela, Dr. Otto Långvik, Jan-Erik Raitanen, Dr Rajib Panchadhayee, Dr. Yury Brusentsev, Patrik Runeberg, Matilda Kråkström, Ewelina Kortesmäki, Dr. Jenny-Maria Brozinski, Andreas Gunell, Juha Forsblom, Robert Lassfolk and Mathilda Råberg as well as the good people of the Laboratory of Polymer Technology for making the daily life

on the fourth floor of Axelia a delight. In particular, I wish to thank Lucas Lagerquist, Ida Mattsson, Axel Meierjohann, Heidi Sundelin and Magnus Perander for numerous wonderful events over the years.

Special thanks go to all the good friends I have acquired over the years, and who have been with me throughout this process. Thank you, my traveling companions, Mathias Östergård, Krister Dalhem, David Eränen, Mika Yrjänä and Otto Jula, for coming with me to see the world. Thank you, Mats Nyfors and Sarah Muscat-Nyfors, for countless parties and get-togethers. Thank you "my friends back home", Jessica Indola, Mia Ylitalo, Johanna Wennström and Maarit Logren, for all the good times. Thank you, Nina Seppola, for bringing daily joy to my life.

Finally, I would like to thank my parents and my brother. I cannot begin to express my appreciation for all the endless support you have offered during my studies and thesis work.

Åbo, December 2017

Jani Rahkila

Abstract

Carbohydrates are among the most abundant biomolecules on earth and can be found in all living things. Their role in nature ranges from structural components such as cellulose in plants and chitin in the exoskeletons of arthropods, to fundamental building blocks of DNA and RNA, to the most important energy storage molecules in organisms in the form of starch and glycogen.

The practically unlimited ways in which individual monosaccharides can be connected make the information storage potential of this class of compounds exponentially greater than that of DNA or proteins. This property does, however, also result in some complications as, while the potential for storing information in carbohydrate structures is great, the process of doing so and reading the information back is complicated by this exact same phenomenon. A majority of the early carbohydrate investigations focused on the elucidation of the structures of carbohydrates and the pioneering work in this field was done by Emil Fischer at the end of the 19th century. Later the focus shifted towards creating glycosidic linkages, and over the years, countless methods have been developed allowing for the preparation of complex structures. The advances in the field have enabled the investigation of the biological roles of this class of compounds.

This thesis explores the world of carbohydrates starting from small oligosaccharides, expanding towards multivalent structures and finally into modification of polysaccharides for preparing well-defined mimics of natural polysaccharides. Potential biological applicability is always a consideration when designing the compound and a recurring theme throughout the thesis are β-(1→2) linked mannosides which are an interesting class of compounds due to their biological impact, their unique structure and problems associated with their synthesis. Particular attention has been paid to the analysis of products by NMR spectroscopy and complete assignment of the spectra. Where feasible, the spectra were simulated by NMR simulation software PERCH to allow a more complete interpretation.

Abstrakt

Kolhydrater tillhör en av de största grupperna av naturligt förekommande biomolekyler. Deras förekomst i naturen sträcker sig från strukturella komponenter såsom cellulosa i växter och chitin i exoskeletten av artropoder, till fundamentala byggnadsblock av DNA och RNA, till stärkelse och glykogen som är de viktigaste molekylerna för energiförvaring.

De praktist taget oändliga sätten att kombinera enskilda monosackarider medför en informationslagringspotential som är exponentiellt större än den hos DNA och proteiner. Denna egenskap leder dock också till vissa komplikationer, emedan potentialen för lagring av information är stor, kompliceras de praktiska aspekten av att göra så av detta exakta fenomen. Majoriteten av de tidiga undersökningarna av kolhydrater var fokuserade på utredning av deras strukturer och de fundamentala grunderna för detta arbete utfördes av Emil Fischer i slutet av 1800-talet. Senare har forskningen skiftat mot skapandet av glykosidiska bindningar och genom åren har otaliga metoder utvecklats vilket har möjliggjort framställning av komplexa strukturer för undersökning av de biologiska rollerna hos denna klass av föreningar.

Denna avhandling utforskar kolhydratlandskapet med början från små oligosackarider varifrån forskningen expanderar mot multivalenta strukturer och senare mot modifiering av polysackarider för att framställa väldefinierade molekyler som imiterar naturliga polysackarider. De potentiella biologiska tillämpningarna hos de framställda molekylerna hålls alltid i tankarna och ett genomgående tema i avhandlingen är β-(1→2) kopplade mannosider som är en intressant klass av föreningar på grund av sina biologiska egenskaper, unika struktur och problemen associerade med deras syntes. Särskild uppmärksamhet har ägnats åt analys och karakterisering av de framställda molekylerna med hjälp av NMR spektroskopi och NMR spektra har i mån av möjlighet simulerats med NMR-simuleringsprogrammet PERCH för att erhålla så mycket information som möjligt.

List of publications and manuscripts

This thesis is based on four original research papers and one review. Additionally concepts and methods from two related publications are applied. Parts of the work in publication III are included in a patent application.

I **Oligosaccharides for Pharmaceutical Applications,** J. Rahkila, T. Saloranta, R. Leino, in *Biomass Sugars for Non-Fuel Applications* (eds. Dmitry Yu. Murzin, Olga Simakova), Royal Society of Chemistry, 2015, Chapter 6, pp 205 – 227.

II **Synthesis and Conformational Analysis of β-(1→2)-Linked Phosphorylated Mannosides,** J. Rahkila, F. S. Ekholm, R. Panchadhayee, A. Ardá, F. J. Cañada, J. Jiménez-Barbero, R. Leino, *Carbohydr. Res.* **2014,** 383, 58 – 68.

III **Acetylated Trivalent Mannobioses – Chemical Modification, Structural Elucidation and Biological Evaluation,** J. Rahkila, R. Panchadhayee, A. Ardá, J. Jiménez-Barbero, J. Savolainen, R. Leino, *ChemMedChem,* **2016,** *11,* 562 – 574.

IV **Mimicking Saccharide Interactions in Nature: NMR Studies of Dextran-Supported Multivalent Molecular Probes Show Distinct Glycan-Lectin Recognition Features,** J. Rahkila, F. S. Ekholm, J. Savolainen, A. Ardá, S. Delgado, J. Jiménez-Barbero, R. Leino, *manuscript submitted.*

V **Cu(I) Mediated Degradation of Polysaccharides Leads to Fragments With Narrow Polydispersities,** J. Rahkila, F. S. Ekholm, R. Leino, *Eur. J. Org. Chem.* **2018,** Accepted manuscript online: 17 Jan 2018, DOI: 10.1002/ejoc.201800033

List of related publications

VI **Glycosylation of 'basic' alcohols: methyl 6-(hydroxymethyl) picolinate as a case study,** S. Wang, D. Lafont, J. Rahkila, B. Picod, R. Leino, S. Vidal, *Carbohydr. Res.* **2013,** 372, 35 – 46

VII **Glycosylation of Phenolic Acceptors Using Benzoylated Glycosyl Trichloroacetimidate Donors,** J. Rahkila, A. K. Misra, L. Guazzelli, R. Leino, in *Carbohydrate Chemistry: Proven Synthetic Methods, Vol. 3* (eds. René Roy, Sébastien Vidal); CRC Press/Taylor & Francis Group, 2015, Chapter 12, pp 97 – 105

VIII **Immunostimulatory Adjuvant And Uses Thereof,** J. Rahkila, J. Savolainen, R. Leino, Fin. Pat. Appl. FI20155997 (to University of Turku and Åbo Akademi University); Int. Appl. PCT/FI2016/050908.

Author contributions

The author of this thesis is the main author of publications I – V and is responsible for the majority of the experimental work, with a few notable exceptions:

- HRMS analysis of prepared compounds was performed by Markku Reunanen at the Laboratory of Wood and Paper Chemistry at Åbo Akademi and Sabine Rendon at the Laboratory of Organic Chemistry at Åbo Akademi
- Original synthesis of trivalent compound **2** in publication III was developed and carried out by Dr. Rajib Panchadhayee.
- Biological studies with PBMCs in publication III were done by Leena Kaven-Honka and Professor Johannes Savolainen at the Department of Pulmonary Disease and Clinical Allergology at the University of Turku.
- TLR ligation screening in publication III was done by InvivoGen, Toulouse, France.
- Copper content analysis by ICP-MS in publication III was done by Paul Ek at the laboratory of Analytical Chemistry at Åbo Akademi.

The conformational studies of molecules presented in publications II and III as well as the binding studies in publication V were performed under supervision of Professor Jesús Jimenez-Barbero.

Abbreviations and symbols

Ac	Acetyl
Ac_2O	Acetic anhydride
$BF_3{\cdot}OEt_2$	Boron trifluoride diethyletherate
Bn	Benzyl
BSP	1-(Phenylsulfinyl)piperidine
DBU	1,8-Diazabicyclo[5.4.0]undec-7-ene
DMF	Dimethylformamide
DOSY	Diffusion Ordered SpectroscopY
DQF-COSY	Double-Quantum Filtered COrrelation SpectroscopY
ESI	Electrospray ionization
Gal-3	Galectin-3
HMBC	Heteronuclear Multiple Bond Correlation
HPSEC	High-pressure size-exclusion chromatography
HRMS	High-resolution mass spectrometry
HSQC	Heteronuclear Single Quantum Coherence
J	Scalar spin-spin coupling constant
LG	Leaving group
MALLS	Multiangle laser light scattering
NBS	N-bromosuccinimide
NIS	N-iodosuccinmide
NMR	Nuclear Magnetic Resonance
NOE	Nuclear Overhauser Effect
NOESY	Nuclear Overhauser Effect SpectroscopY
OBz	Benzoyl
OTf	Triflate, trifluoromethanesulfonate
PERCH	PEak ResearCH
Ph	Phenyl
PMB	*para*-Methoxyphenyl
p-TSA	*para*-Toluenesulfonic acid
ROE	Rotating-frame Overhauser Effect
ROESY	Rotating-frame Overhauser Effect SpectroscopY
TFA	Trifluoroacetic acid
THF	Tetrahydrofuran
TLC	Thin-layer chromatography
TMS	Tetramethylsilane
TMSOTf	Trimethylsilyl trifluoromethanesulfonate
TOCSY	TOtal Correlation SpectroscopY
TTBP	2,4,6-tri-*tert*-butylpyrimidine

Table of Contents

1 Introduction

Carbohydrates are among the most abundant biomolecules on earth and comprise one of the three types of biopolymers, polysaccharides, the other two being polynucleotides (DNA and RNA) and polypeptides. The functions of carbohydrates in nature are many, for example, components for structural integrity such as cellulose in plant cell walls and chitin in the exoskeletons arthropods. Furthermore, ribose and deoxyribose (2-deoxy-D-*erythro*-pentofuranose) are vital parts of the fundamental building blocks of life itself and glucose is the most important molecule for energy storage in living organisms.

The widespread use of carbohydrates in nature, and one of the major differences between polysaccharides and other biopolymers, stems from the large variation of monosaccharide units and ways in which they can be connected.

Both polynucleotides and polypeptides form linear structures with no stereochemistry involved in the linkages between the monomers (technically a stereocenter is involved in the linkage between polypeptides, but only the L enantiomer occurs in nature). Carbohydrates, however, typically have several positions where another carbohydrate unit can be attached which can lead to branching. Furthermore, most of the hydroxyl groups involved in the linkages between two monosaccharides are connected to a stereocenter. A simple disaccharide consisting of two D-glucose units can be constructed in 19 different ways. If the disaccharide consists of two different monosaccharides, such as D-glucose and D-mannose, the total number of molecules that can be constructed is 36.

1.1 Structure and nomenclature of carbohydrates

Early elemental analysis showed that carbohydrates consist of carbon and water in a ratio $C_n(H_2O)_m$ ($n \geq m$) which means that they are hydrates of carbon. The term carbohydrate is derived from the Latin word *carbo* and the ancient Greek word for water (ὕδωρ, húdōr).[1]

Generally, carbohydrates are divided into three groups: monosaccharides consisting of a single carbohydrate unit, oligosaccharides consisting of between two to ten monosaccharide units, and polysaccharides consisting of more than 10 monosaccharide units. The exact definitions of how many monosaccharide units constitute an oligosaccharide or polysaccharide vary between sources though.

Monosaccharides are the simplest carbohydrate structures and even though they are rather small molecules, they offer great structural variation due typically to having several stereocenters. Monosaccharides can further be divided into aldoses that contain an aldehyde functionality and ketoses that contain a ketone.

One of the earliest pioneers in carbohydrate chemistry was Hermann Emil Fischer who, in 1902, was awarded the Nobel Prize in chemistry *"in recognition of the extraordinary services he has rendered by his work on sugar and purine syntheses"*. His most famous achievements are the determination of the absolute stereochemical configuration of all the sugars known at the time as well as the first total synthesis of D-glucose.[2–4] What makes his discoveries even more remarkable is that he, did not have access to modern analytical methods and had to rely heavily on more primitive methods such as measuring the optical rotation and derivatization with phenylhydrazine to form osazones. He also laid the foundations for the nomenclature of sugars[2] and developed the Fischer projection which is still commonly used for visualizing monosaccharides.

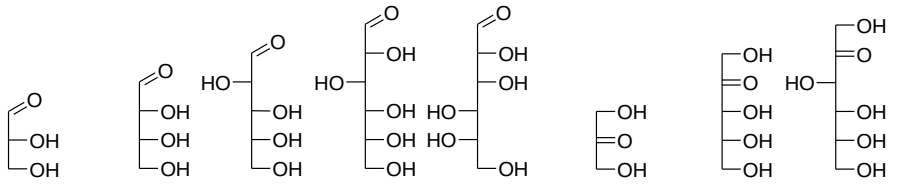

Figure 1.1. Fischer projections of selected monosaccharides.

In the Fischer projection, the monosaccharides are drawn in such a way that the carbon atoms are arranged in a vertical line placing the carbon atom with the lowest number at the top. The hydroxyl groups are drawn out horizontally to the left or to the right. The horizontal bonds come out of the plane of the paper and the vertical bonds go into the plane. This is visualized in Figure 1.1, which shows the Fischer projections of selected monosaccharides.

Monosaccharides are given trivial names by grouping the carbon atoms in groups of a maximum of four, starting from the lowest numbered center of chirality. The first one to three carbon atoms determine the trivial name for that segment, for example *gluco*, *manno*, *galacto* etc. and the fourth determines whether the segment is D or L. If the substituent at that position is on the right side in the Fischer projection, it is denoted D and if it is on the left, it is denoted L.[5]

Monosaccharides can, be named in a systematic way like any other molecules and β-D-glucopyranose could be called (2*R*, 3*R*, 4*S*, 5*S*, 6*R*)-6-(hydroxymethyl)oxane-2,3,4,5-tetraol. This is obviously not practical and thus trivial names are almost exclusively used.

1.1.1 The cyclic structures of monosaccharides

Fischer incorrectly assumed that the monosaccharides occur as linear molecules. Today, we know that monosaccharides prefer to form cyclic structures in the form of hemiacetals (in the case of aldoses) or hemiketals (in the case of ketoses). In an aqueous solution, the linear form typically makes up less than 1% of the total amount. Monosaccharides typically form six-membered pyranose rings or five-membered furanose rings that are in equilibrium with the linear form. This happens when one of the hydroxyl groups attacks the carbonyl carbon to form a hemiacetal or hemiketal. Because the carbonyl carbon has a planar structure, the attack can happen from either side and a new stereocenter is formed. The ring-opening and closing is called mutarotation and is visualized in Scheme 1.1. The configuration of the new stereocenter in the cyclic structure is denoted with α or β and the IUPAC definition for this is as follows (Figure 1.2):[5]

> *The anomeric reference atom is the configurational atom of the parent, unless multiple configurational prefixes are used. If multiple configurational prefixes are used, the anomeric reference atom is the highest-numbered atom of the group of chiral centres next to the anomeric centre that is involved in the heterocyclic ring and specified by a single configurational prefix. In the α anomer, the exocyclic oxygen atom at the anomeric centre is formally cis, in the Fischer projection, to the oxygen attached to the anomeric reference atom; in the β anomer these oxygen atoms are formally trans.*

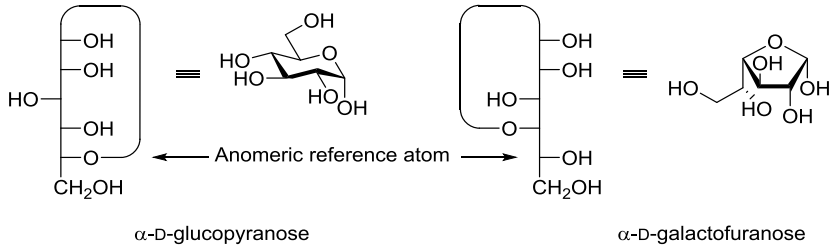

Figure 1.2. Visualization of the IUPAC definition of anomeric configuration.

Here, the configurational atom refers to the chiral center that has the highest location number, *i.e.* the atom that is used to determine whether the monosaccharide has D or L configuration. The anomeric reference atom is that used for determining whether the anomeric configuration is α or β. In the molecules discussed in depth in this thesis, the configurational atom and reference atom will always be the same. Monosaccharides with more than six carbon atoms can have several configurational atoms and in these, the configurational atom and the anomeric reference atom are not necessarily the same, but these do not appear in this thesis.

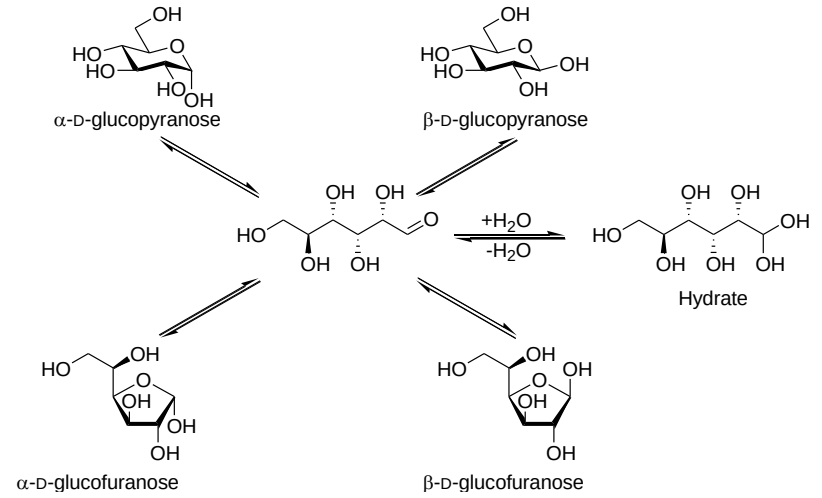

Scheme 1.1. Mutarotation in D-glucose.

In addition to different stereochemical configurations of monosaccharides, the same monosaccharide can exist in a number of different conformations. Technically, a monosaccharide in a furanose or pyranose form can exist in similar conformations as other five- or six-membered structures consisting of sp^3 hybridized atoms (Figure 1.3).

A six-membered ring can be twisted into several different conformations, some more stable than the others. Pyranoses can exist in four different types of ring conformations or variations of these: chair (C), boat (B), skew (S) and half-chair (H). Additionally, when describing a conformation, the atom that is above the plane is indicated with a superscript before the notation and the atom below the plane is indicated with a subscript after the conformation. There are a total of 26 pyranose conformations (two chair, six boat, six skew and twelve half-chair conformations). The furanose forms of monosaccharides can adopt two general ring conformations: envelope (E) and twist (T) with ten variations of each.

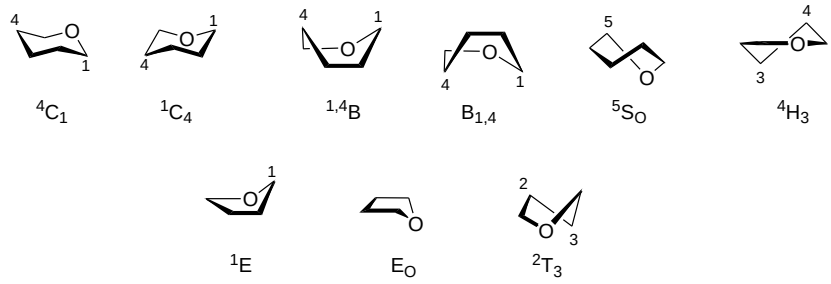

Figure 1.3. Examples of the different conformations of the pyranose (top) and furanose (bottom) conformations.

The preferred conformation of monosaccharides in pyranose form is $^4C_1$ for D-sugars and $^1C_4$ for L-sugars as these conformations minimize the steric interactions between the substituents on the ring (Figure 1.4).

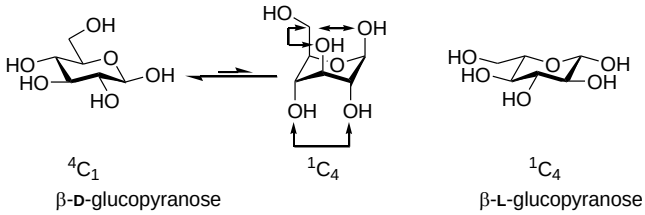

Figure 1.4. Chair conformations of β-D-glucopyranose (left) with steric interactions indicated in the $^1C_4$ conformation and β-L-glucopyranose (right).

In general, monosaccharides that can form a pyranose will prefer that over a furanose form as the ring strain is lower in a six-membered ring than it is in a five-membered ring. Monosaccharides that have several axial substituents regardless of the conformation, however, such as altrose (Figure 1.5) or idose, also exist to a significant degree in the furanose form.[6]

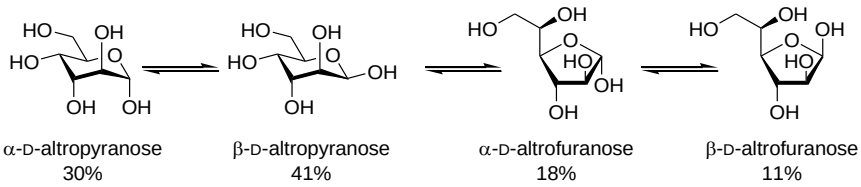

Figure 1.5. The ratios of the different pyranose and furanose forms of D-altropyranose in water at 31 °C.

While the cyclic structures are the dominant ones in aqueous solution, the small amount of aldehyde or ketone present can be used for chemical modifications.

Emil Fischer used the aldehyde for chain extensions by first reacting it with NaCN followed by hydrolysis and finally reduction of the formed lactone with sodium amalgam to create a new monosaccharide with one more carbon atom. This method for extending monosaccharides is known as the Kiliani–Fischer synthesis.[7,8]

1.2 Anomeric effect

In cyclic structures, the preferred conformation can often be explained by steric factors and a common rule is that large substituents prefer an equatorial orientation to minimize steric interactions. An electronegative atom, *e.g.* oxygen or nitrogen, in the ring can, however, have a significant effect on the stability of the orientations of the substituents on the neighboring atoms. Electronegative substituents at the anomeric position have a preference for axial orientation, instead of an equatorial orientation that would be preferred from a sterical point of view. This phenomenon was first described by J. T. Edward in 1955[9] and R. U. Lemieux later coined the term *anomeric effect*.[10] The effect is also sometimes called the Edward-Lemieux effect, and is one of the key factors for determining the conformations of monosaccharides.[9,11] Without the anomeric effect, one would expect that D-glucose exists almost solely in the β-configuration in a solution. In reality, the α:β-ratio is 36:64, and the effect is even more pronounced in D-mannose due to the axial substituent at on C-2, resulting in an α:β-ratio of 69:31.[6]

Some of the most extreme cases, where the anomeric effect drastically changes the low-energy conformation of a monosaccharide are acetylated aldopyranosyl halides. In the case of 2,3,4-tri-*O*-acetyl-α-D-xylopyranosyl chloride, the only conformation found is the expected $^4C_1$ whereas in the corresponding β-anomer, there is an equilibrium between the $^4C_1$ and the $^1C_4$ conformations, with preference for the latter (~80%), even though this results in all the acetyl groups being axial (Figure 1.6).[12,13]

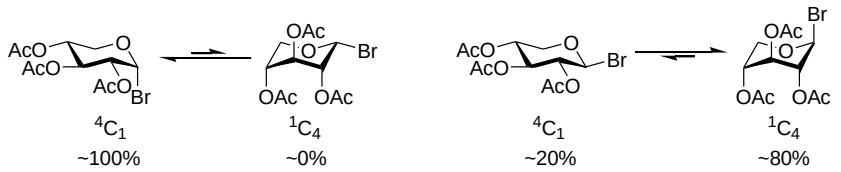

Figure 1.6. Comparison of the preferred conformations of the α and β anomers of acetylated xylopyranosyl bromide.

There are two main reasons for the anomeric effect: hyperconjugation between the axial free electron pair of the ring oxygen and the antibonding orbital of the anomeric C-X bond, and dipolar interaction. Hyperconjugation allows one electron pair from the endocyclic oxygen to be shifted towards the antibonding orbital of the C-X bond at the anomeric center, resulting in a lower energy conformation. Dipolar interaction between the dipoles caused by the endocyclic oxygen and the C-X bond is repulsive if the anomeric substituent is equatorial (Figure 1.7).

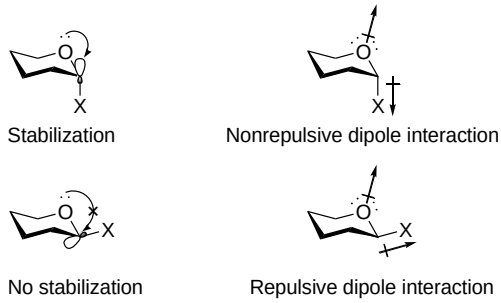

Figure 1.7. Top: Stabilization of the axial substituent by electronic effects. Bottom: An equatorial substituent is not stabilized.

1.3 Reactivity of carbohydrates

Carbohydrates have many reactive sites that can be targeted for modification. These sites are typically hydroxyl groups with very similar reactivities, and require special methods for specific modifications. There are generally three types of functional groups on a monosaccharide: the anomeric center which is a (hemi)acetal or –ketal, secondary hydroxyl groups and primary hydroxyl groups (Figure 1.8). The hydroxyl group at the anomeric center has different reactivity than the rest, and can be selectively manipulated under acidic conditions. Primary hydroxyl groups are more nucleophilic than secondary ones, and typically also less sterically hindered. Under basic conditions, the least hindered primary hydroxyl group can typically be manipulated selectively. Of the secondary hydroxyls, the equatorial ones tend to be more reactive than the axial. The reactivity of the hydroxyl groups can, however, be modified by appropriate selection of protecting groups.

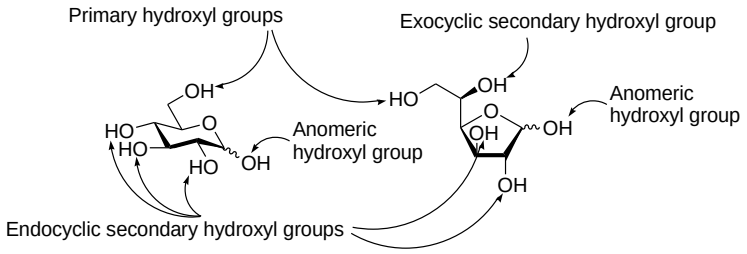

Figure 1.8. The different types of hydroxyl groups in D-glucose.

While manipulations not involving protecting group chemistry would often be preferred, from an atom economical point of view, it is typically not possible due to the very similar reactivities of the hydroxyl groups, which would lead to a complex mixture of products. Because of this, the hydroxyl groups not targeted for the modification typically have to be blocked with protecting groups.

Traditionally, synthetic carbohydrate chemistry relies heavily on protecting groups, and there are several factors that have to be taken into consideration when designing a synthetic strategy, such as stability, order of introduction, and orthogonality. The protecting groups should be stable enough to remain intact during subsequent transformations, but possible to remove without affecting the other protecting groups present.

Protecting groups are generally divided into two categories, permanent and temporary protecting groups. Permanent protecting groups stay on the molecule until the end, when they are preferentially all removed in one single step. Temporary protecting groups are groups that can be removed selectively, without affecting the other protecting groups.

1.4 Creating glycosidic linkages

The perhaps most important aspect of carbohydrate chemistry, is the creation of new glycosidic linkages between carbohydrates, or between a carbohydrate and some other molecule, commonly referred to as an aglycon. There are several ways of preparing these types of linkages, and the earliest example of chemical glycosylation is by Arthur Michael who reacted potassium phenolate with 2,3,4,6-tetra-*O*-acetyl-D-glucopyranosyl chloride to form phenyl D-glucopyranoside.[14]

1.4.1 Enzymatic methods

In nature, glycosidic bonds are created by enzymes, so-called glycosyltransferases, which attach carbohydrates to various other structures, including proteins and other carbohydrates. These enzymes, are highly selective and do not require protecting groups, but each type of linkage requires its own enzyme. During recent years, enzymatic oligosaccharide synthesis has received considerable attention, and a multitude of complex structures have been prepared. A more detailed view of the use of enzymes in synthetic carbohydrate chemistry is beyond the scope of this thesis, but an overview can be found in the reviews by Liang *et. al.*[15] and Lairson *et. al.*[16]

Enzymatic methods are useful, but do suffer from some drawbacks, such as high cost of enzymes and difficult scale up of the synthesis. Because of this, the most reliable method for preparing oligosaccharides for biological purposes is typically traditional carbohydrate synthesis.

1.4.2 Chemical glycosylation

While numerous ways of creating glycosidic linkages have been developed, most of them are based on the same principle. One molecule, called the glycosyl donor, has a good leaving group at the anomeric position. The other molecule involved in the glycosylation, called glycosyl acceptor, has a nucleophilic functionality, such as an alcohol or thiol. The donor is activated by a promotor, typically a Lewis acid, which forms an oxocarbenium ion that is attacked by the nucleophile (Scheme 1.2). One of the most simple examples of chemical glycosylation is the so-called Fischer glycosylation,[17–19] originally reported by Emil Fischer in the 1890s, where an unprotected sugar is dissolved or suspended in a solvent that can also act as the acceptor, such as methanol, in the presence of an acid catalyst. This leads to the formation of a mixture of α and β anomers, where the ratio depends on the thermodynamic stability of the anomers, the α anomer typically being the predominant one.

Later, in 1901, Wilhelm Koenigs and Eduard Knorr reported a new method for glycosylation, using glycosyl halides that could be activated towards glycosylation by heavy metal halophiles, such as silver carbonate.[20] This method, which is still used today, became known as Koenigs-Knorr glycosylation.

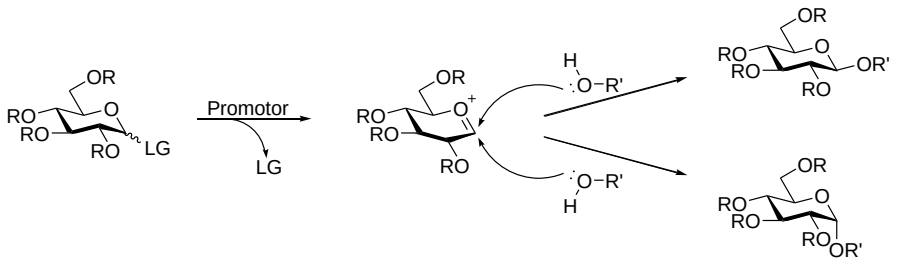

Scheme 1.2. General scheme for a glycosylation reaction.

While both Fischer glycosylations and Koenigs-Knorr glycosylations still find their use today, new methods are constantly being developed and there are a vast number of different reaction protocols suitable for different applications. The most commonly used methods still rely on the same donor/acceptor principles, however. Some selected glycosyl donors can be seen in Figure 1.9.[21]

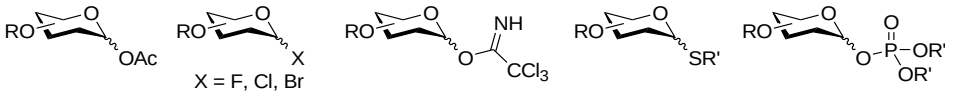

Figure 1.9. Selected glycosyl donors. From left to right: glycosyl acetates, glycosyl halides, glycosyl trichloroacetimidates, thioglycosides, glycosyl phosphates.

The oxocarbenium ion that is initially formed has a planar geometry, and thus the attack of the nucleophile can come from either side and the product can be either an α-glycoside or a β-glycoside. Typically, only one of the stereoisomers is the desired product, and because of this, stereoselective synthetic protocols are required to minimize the formation of unwanted products. Stereoselectivity in glycosylation reactions, has thus over the years been one of the major research areas of chemical glycosylation.

Great care should be taken when designing a protecting group strategy for chemical glycosylation, as it is one of the most powerful ways of controlling the stereochemical outcome of the reaction. Using participating protecting groups, is the simplest way of controlling the anomeric configuration of the final product. A participating group, such as an ester group, on the carbon atom next to the anomeric center can greatly enhance the stereoselectivity of the reaction. The carbonyl functionality of the ester can act as a temporary nucleophile and form a five-membered ring that blocks a nucleophilic attack from one side of the ring (Scheme 1.3).

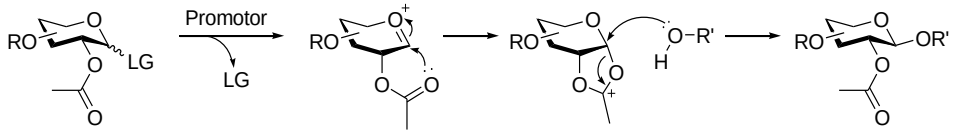

Scheme 1.3. Neighboring group participation used for controlling the stereochemical outcome of a glycosylation reaction.

In some cases, depending on the reaction conditions, the intermediate can form stable orthoesters, in particular when secondary alcohols are used as acceptors.[22] This inevitably leads to some loss of yield.

The use of ester protecting group on C-2 allows for simple preparation of so-called 1,2-*trans* glycosides (although there are some reports[23,24] where they have been used for preparing 1,2-*cis* glycosides as well), where the substituents on carbon atoms 1 and 2 are on opposite sides of the ring. There are, in general, no equally simple methods for preparing 1,2-*cis* glycosides, where the substituents on carbon atoms 1 and 2 are on the same side of the ring. Developing new methods for such reactions is one of the driving forces of progress in synthetic carbohydrate chemistry.

While 1,2-*cis* glycosides are generally considered difficult to prepare, over the years a number of different methodologies have been developed. One of the most important aspects of 1,2-*cis* glycosylation is the glycosyl donor and the intermediate it forms.

Neighboring group participation can also be used for preparing 1,2-*cis* glycosides, as demonstrated by Boons *et. al.*[25,26] who used a particular participating group at carbon two, (*S*)-phenyl-thiomethylbenzyl ether. Upon activation of the donor, the protecting group forms a six-membered ring that blocks the β-face of the activated glucopyranosyl donor, resulting in high selectivity towards α-glucosides.

In addition to neighboring group participation, protecting groups further away from the anomeric center can also have an effect on the glycosylation reaction. Particularly the substituents at C-3 and C-6 have been shown to be able to significantly alter the α:β ratio of the products.[27,28]

The solvent used in the reaction also plays a part in the stereochemical outcome of the reaction. In general, ethereal solvents have been shown to direct the reaction towards the α-glycoside, whereas nitrile solvents favor the formation of β-glycosides. While the effect is typically not very strong,[29,30] it has in some

cases been shown to have a significant effect on stereochemical outcome of the reaction.[31]

A large part of the published research about 1,2-*cis* glycosylations focus on making α-glycosides. In these cases, the anomeric effect helps by making the target product thermodynamically favorable. Making β-linked 1,2-*cis* glycosides, such as β-mannosides, is typically even more difficult. A specific case of such 1,2-*cis* glycosides, β-(1→2) linked mannosides, will be a recurring theme throughout this thesis, and the synthesis will be discussed in more detail in the next chapter.

This has been a short, and in no way complete, overview of some of the methods available for preparing 1,2-*cis* glycosides. For a more comprehensive overview the reader is referred to for example the reviews by S. S. Nigudkar and A. V. Demchenko.[32,33]

1.4.3 Automated synthesis

Automated synthesis of peptides has been available since the 1960s,[34,35] and the first automatic oligonucleotide synthesizer was built in the late 1970s. The linearity, and limited structural variation of these classes of molecules, makes them optimal for an automated process. In essence, one would only need one variation of each building block to make any sequence of peptides or nucleotides. The possibility of branching, and stereochemical variations of carbohydrates, makes oligosaccharides exponentially more complicated. While it is true, that a particular linear oligosaccharide could be made using only single building block, such structures are not always of high biological relevance.

Any polypeptide or polynucleotide can be constructed from 20 or four building blocks respectively. A hexapeptide could thus be constructed in 20^6 (=64 million) different ways, and a hexanucleotide in 4^6 (=4096) different ways. It has been calculated, that a hexasaccharide based on the ten mammalian monosaccharides, however, could due to branching and stereochemical variation, theoretically be constructed in 192 000 000 000 different ways.[36] The number of possible structures for oligosaccharides is, thus, more than three orders of magnitude greater than the number of polypeptides consisting of the same number of monomeric units.

While each new peptide or nucleotide coupling can be made under more or less identical conditions, the creation of different types of glycosidic linkages often requires very different conditions in terms of solvent, temperature and reagent

systems.[37] Contrary to oligopeptides and oligonucleotides, one single variation of a specific monosaccharide is not sufficient for creating all oligosaccharides containing such a monomer unit.[38] One of the largest obstacles in oligosaccharide synthesis is the requirement for a vast library of glycosyl donors, with carefully designed protecting group strategies. It has been estimated, that 36 monosaccharide building blocks would be required for preparing 75% of the mammalian polysaccharides, and to create 90% of the polysaccharides, 65 different monosaccharide building blocks would be required.[36]

The general principle of automated synthesis is that the polysaccharide to be constructed is attached to a support that can be used to easily separate the reaction product from the reaction mixture. Typically, this support is attached to the reducing end of the sugar. The activated donors are highly reactive molecules, and thus more susceptible to undesired side reactions. By attaching the acceptor to the support, the byproducts can more easily be separated from the product. The supports can be divided into soluble[39] and insoluble, of which the insoluble ones have by far been more utilized. Regardless of whether one uses soluble or insoluble tags, the principle for the synthesis is the same, and can be divided into five distinct steps (Scheme 1.4):

1) a) Attachment of a solid or fluorous tag for easy purification.
b) Selective deprotection of one or more hydroxyl groups for further modifications.
2) Chain growth by addition of glycosyl donor and promotor.
3) Selective deprotection of one or more hydroxyl groups for further modifications.
4) Purification of the intermediate by filtration or FSPE.

Steps 2 – 4 are repeated until the oligosaccharide has been assembled.

5) The oligosaccharide is detached from the support, the remaining protecting groups are removed, and the final product is purified, typically by HPLC methods.

Even though the synthesis of oligosaccharides in this manner simplifies the purification of the intermediates, the automated synthesis introduces some new problems regarding the analysis of intermediates, and purification of final products. Typically, all intermediates in oligosaccharide synthesis would as a minimum be analyzed by HRMS and fully characterized by NMR spectroscopic

methods. Insoluble compounds are difficult, if not impossible, to analyze in this manner, which means that an aliquot of reasonable amount of the growing oligosaccharide is typically cleaved from the support and characterized.[40] Furthermore, as very few glycosylation reactions are fully stereoselective, each addition of a new monosaccharide unit will generate two diastereomers. For creating a hexasaccharide as in the previous example, five glycosidic bonds need to be created (excluding the step where the first monosaccharide is attached to the support). As each step creates two compounds, the number of compounds after the final deprotection is 2^5 (=32) of which typically only one is the target compound. In traditional synthesis, the overall number of diastereomers produced would be 2 × 5 (=10), and these would be separated two at a time after each glycosylation reaction, whereas on solid support the unwanted anomers (and other side products, including deletion sequences) accumulate throughout the synthesis.

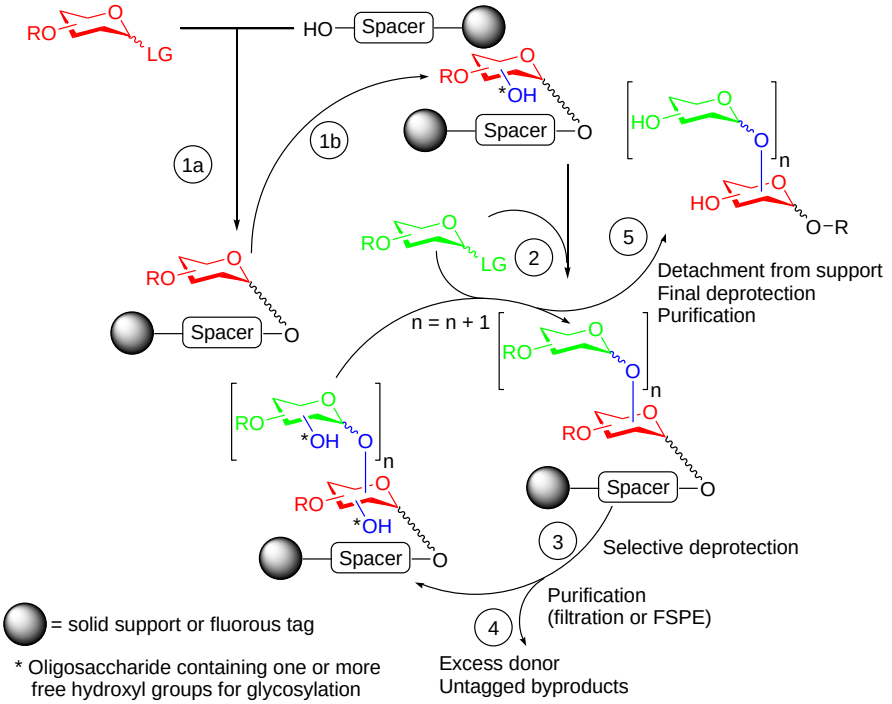

Scheme 1.4. Automated oligosaccharide synthesis.

Automated synthesis has been used to prepare some rather impressive structures, such as for example the fully protected Le^y-Le^x nonasaccharide depicted in Figure 1.10.[41] Many of the challenges with traditional synthesis remain, however. The requirement for a large number of building blocks required for

preparing arbitrary oligosaccharides is an intrinsic one that is not easily overcome.

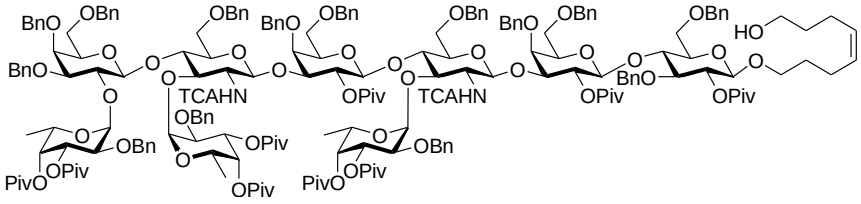

Figure 1.10. Fully protected Le^y-Le^x nonasaccharide prepared by automated synthesis.

1.5 Biological importance of carbohydrates

Carbohydrates are one of the four major classes of biomolecules, the other three being nucleotides, peptides and lipids. While this is the classification that is typically used, the distinction is not always so straightforward. In nature, carbohydrates are often found as glycoconjugates; glycosides covalently bound to other types of molecules, such as proteins or peptides (glycopeptides, glycoproteins and peptidoglycans) and lipids (glycolipids and lipopolysaccharides).

The most abundant biomolecule on earth is cellulose, an important structural component of the cell wall of green plants, consisting of β-(1→4) linked glucose units. A very similar polysaccharide, consisting of N-acetylglucosamine linked in the same fashion, chitin, makes up the exoskeletons of arthropods.

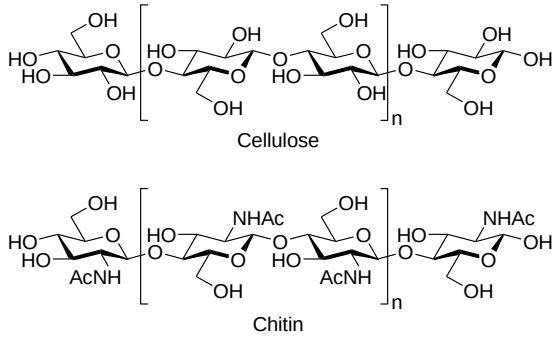

Figure 1.11. Structures of cellulose and chitin.

Carbohydrates mediate and regulate a wide range of critical biological processes, such as cell communication, cell adhesion, inflammation, protein function, fertilization,[42] and many others. Typically, a cell expresses a multitude of different carbohydrates on its surface. Diseases or disorders can cause changes

in the carbohydrates expressed on a cell, which makes carbohydrates excellent biomarkers for tracking changes in living systems.

1.5.1 Carbohydrates as diagnostic tools

The distinction of native and foreign cells in our bodies is largely based on the carbohydrate biomarkers on the surface of cells. One of the most commonly used examples of this, is the ABO blood group system. In a very simplified manner, our blood types can be separated into four categories, (A, B, AB and O) based on the glycans on the surface of our blood cells. Individuals with blood group A, express A antigens on the surface of their blood cells, individuals with blood group B, express B antigens and individuals with blood group AB express both A and B antigens. Individuals with blood group O, express an H antigen on the surface of their blood cells. This H antigen is a disaccharide precursor to the A and B antigens (Figure 1.12).

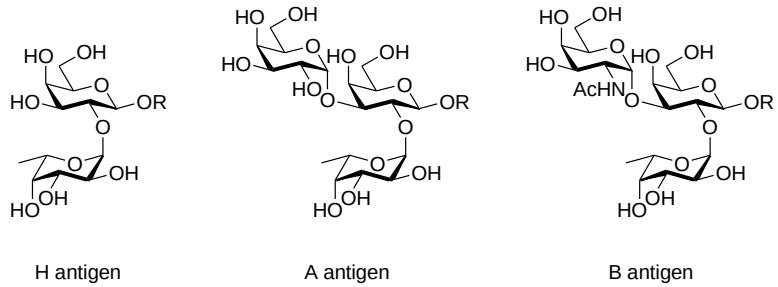

Figure 1.12. ABO blood group antigens.

The existence of different blood groups, was originally discovered in the beginning of the 20th century by Karl Landsteiner, who discovered blood groups A, B and O in 1900[43–45] followed by Alfred von Decastello and Adriano Sturli, who discovered the AB blood type in 1902.[46] A few years later, in 1907 Jan Jaský,[47] and in 1910 William Lorenzo Moss, [48] published similar findings. The discoveries showed that humans could be divided into different categories depending on whether their blood serum contained components that would agglutinate red blood cells from other humans. At the time, it was not known that the antigens were glycans, however, and it was not until the work of Morgan and Watkins in the 1940s and 1950s, that the actual structures were determined.[49–51] Since the discovery of different blood types, the complications associated with blood transfusions have diminished significantly and countless lives are saved on yearly basis. While the ABO classification of blood types is

the most common one, there are, in fact, over 30 different human blood group systems, the majority of which involve carbohydrates.

One of the most active areas of research involving carbohydrate biomarkers is in cancer research. Cancer is a group of diseases associated with abnormal and uncontrolled growth of cells. It is one of the biggest medical problems of the modern world, and according to a report by the World Health Organization there were 14.1 million new cancer cases, and 8.2 million deaths due to cancer in the year 2012.[52] It is the second most common cause of death after cardiovascular and circulatory diseases.[53]

Upon transforming into a cancerous cell, the expression of carbohydrates on the cell surface changes, typically towards overexpression of certain carbohydrates. These carbohydrates, which can stay on the cell surface, or be shed into circulation, are commonly referred to as tumor-associated carbohydrate antigens (TACA). Over the years a number of TACAs have been identified,[54] and the most common of these is the Tn antigen.[55] The Tn antigen was reported as a TACA in the late 1970s,[56] and has since then been the focus of numerous investigations.[55,57,58] Structurally, it is a GalNac moiety α-linked to a serine or threonine residue of a polypeptide, and it has been reported to be found on the cell surface of 90% of solid tumors.[56] The Tn antigen also acts as a precursor for a number of other carbohydrate TACAs, such as sTn, TF, sTF and di-sTF which, in addition to the Tn structural, unit also contain additional galactose and sialic acid residues.

In addition to the Tn-based TACAs, there are a number of others that have been studied extensively, such as Globo H, the Lewis blood group antigens and their sialylated analogues; sLe^a, sLe^x, and Le^y, as well as the ganglioside based structures GM2, GD2, and GD3.[59] Examples of the structures of some TACAs can be seen in Figure 1.13.

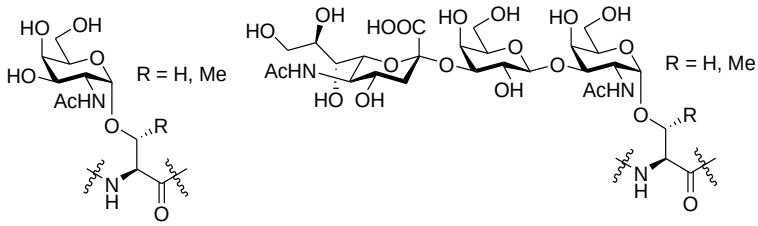

Figure 1.13. Examples of TACAs.

The search for new carbohydrate biomarkers is an ongoing process, and while the majority of research in carbohydrate biomarkers is focused specifically on biomarkers for cancer, there are several promising applications in various metabolic disorders,[60–62] infectious diseases,[55] inflammation etc. The immense effect of minute differences in carbohydrate structures, as exemplified by the violent reaction of our bodies towards foreign blood groups, shows the great potential of carbohydrate biomarkers as diagnostic tools.

Throughout history, bodily fluids have been used for diagnosis of diseases.[63] Even though it was not known at the time, carbohydrates have been used for diagnosing type I diabetes for 3.5 millennia. Urine from persons with diabetes was found to attract ants and flies, which caused Indian physicists to name it *madhumeha* or "honey urine". In 1670 Thomas Willis, an English doctor, found that the urine from diabetes patients tastes sweet, and in 1776 it was shown, by the British physiologist Matthew Dobson, that the sweet taste was caused by sugar.[64] Nowadays measuring the glucose content in urine is not considered reliable, and thus blood is used instead.

Since ancient times the analytical methods have, of course, evolved and today we have access to powerful methods, such as proteomics, antibody screening, mass spectrometry and nuclear magnetic resonance.[65–68] Interdisciplinary collaborations have enabled the detection of smaller amounts, a wider range of different carbohydrate-based biomarkers, as well as accurate structural determination of them.

1.5.2 Pharmaceutical applications and immunological aspects

With carbohydrates being involved in a wide range of biological processes, it is a very logical step to try to take advantage of these properties for treatment of various conditions as well. Carbohydrates do, however, suffer from some severe inherent draw-backs that limit their applicability as pharmaceuticals. The major problem is their high polarity, which limits their uptake due to their inability to passively cross the enterocyte layer of the small intestine. This makes oral administration difficult, if not impossible, in many cases. While the problems with uptake can be circumvented by parenteral administration, the high polarity remains a problem as it leads to fast renal excretion and, consequently, short biological half-lives.[69]

Despite the problems with uptake and pharmacokinetics, carbohydrates and carbohydrate-based structures have, over the years, found widespread clinical

use as antithrombotics, anticoagulants, antibotics, antiviral drugs as well as for treatment of diabetes, epilepsy, osteoarthritis and several other conditions.[70] In this section, a few selected examples of carbohydrate-based pharmaceuticals will be presented.

It is not possible to discuss carbohydrate-based pharmaceuticals without mentioning glycosaminoglycans (GAG). GAGs were first described, almost two centuries ago, by J. Müller who isolated chondrin, (later renamed chondroitic acid) from cartilage. Almost a century later, heparin (Figure 1.14), a highly sulfated GAG consting of alternating glucosamine and uronic acid (iduronic acid and glucuronic acid) units connected via (1→4) linkages, was discovered. The actual discovery is somewhat debated, but typically Jay McLean, working under William Howell at John Hopkins University, is credited. Heparin was found to have significant anticoagulant properties, and became commercially available in the 1920s, making it the oldest carbohydrate-based drug. The original preparation had some significant side-effects, such as headache, fever and nausea and even after development of better isolation procedures, which allowed for a more pure product, problems with a short biological half-life, and side-effects in the form of bleeding and thrombocytopenia remained. Heparin with lower molecular weight, produced by enzymatic fragmentation, was shown to cause significantly fewer side-effects, and after the active component of heparin, a pentasaccharide fragment, was determined the first total syntheses of the fragment were developed in the 1980s.[71,72] In 2002, a fully synthetic heparin pentasaccharide, fondaparinux, marketed under the name Arixtra, entered the market and since then a number of analogues have been developed.[73]

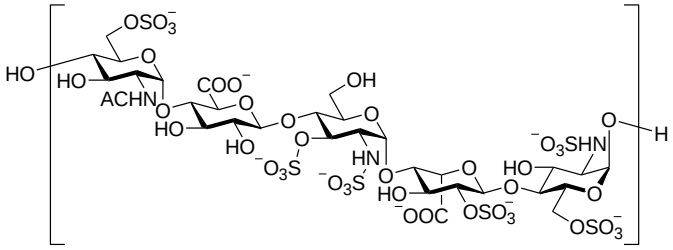

Figure 1.14. The active pentasaccharide fragment of heparin.

Antibiotics are generally defined as a class of compounds of fungal or bacterial origin, which inhibit the growth of other microorganisms.[74] The definition has come to include also semisynthetic and synthetic products.[75] Generally, the carbohydrate-based antibiotics can be divided into two groups: so-called aminoglycoside antibiotics (*e.g.* streptomycin and neomycins),[76] where the

carbohydrates are glycosidically linked to cyclitols or aminocyclitols, and orthosomycins,[77] which consist of polysaccharides where, in addition to normal glycosidic linkages, the monosaccharide units can also be connected via orthoester linkages (*e.g.* flambamycin). In addition to these two main classes of carbohydrate-based antibiotics, this class of compounds contains molecules where carbohydrates are glycosidically linked to non-carbohydrate antibiotics, such as macrolides (*e.g.* erythromycin).[74]

In addition to carbohydrates being used as pharmaceuticals as such, there a many cases where carbohydrates are used as starting points, and selectively modified to eliminate the problems commonly associated with carbohydrate-based pharmaceuticals. One particular example of such glycomimetic drugs, is oseltamivir (Tamiflu), which is based on the structure of Zanamivir, which in turn was developed from *N*-acetylneuraminic acid.[78] While the design of the compound is based on a carbohydrate precursor, the final molecule no longer fits the definition of carbohydrates. Some selected examples of carbohydrate-based and carbohydrate-derived pharmaceuticals can be seen in Figure 1.15 below.

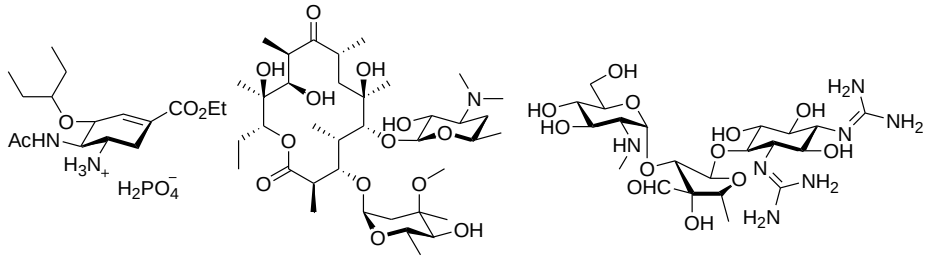

Oseltamivir phosphate Erythromycin Streptomycin

Figure 1.15. Examples of carbohydrate-based and carbohydrate-derived pharmaceuticals.

Most diseases are treated directly by pharmaceuticals and this practice has, over the years, led to serious problems. At least partially due to excessive use of antibiotics, some diseases are becoming increasingly more difficult to treat due to mutations and gene exchange, which has made some bacteria resistant to antibiotics. The development of new antibiotics has not been able to keep up with the speed at which bacteria develop resistance, and there are several strains of life-threatening diseases that are resistant to most, if not all, known antibiotics, for example, *Enterococcus faecalis*,[79] *Mycobacterium tuberculosis*[80] and *Pseudomonas aerudinosa*.[81]

Our immune system is an effective weapon against foreign cells, and is able to eventually defeat most common pathogens. The first time our bodies encounter a specific pathogen, the immune response is a complicated cascade of reactions. A detailed description is beyond the scope of this thesis, but this complex mechanism, while ultimately effective, is rather slow compared to the rate at which the pathogen can multiply, and thus our bodies do not have enough time to defeat certain infections before they become a serious threat to our health. Furthermore, there are pathogens that do not cause a significant immune response, even if present in dangerous amounts. One example is the anaerobic bacterium *Clostridium tetani* that releases tetanospasmin, a potent neurotoxin. The toxin is so potent that even a lethal dose is insufficient to trigger an immune response.[82]

As mentioned earlier, the surface of cells is covered with glycan structures, herein referred to as antigens. The antigens on foreign cells are different than those of native cells. These structures are recognized by the immune system, which produces specific antibodies, also known as immunoglobulins, to target the antigens. These antibodies, bind to the pathogen, deactivating it and marking it for disposal. Some of the cells that produce the specific antibodies develop into so-called memory cells, which can be rapidly activated upon subsequent infection.

One of the most important breakthroughs in medicine throughout history is the invention of vaccines. Vaccines are used to trigger an immune response, in order to teach the immune system to combat a pathogen. This can, in general, be achieved in two ways: using whole cells that have been weakened or killed, or using only the antigenic polysaccharide or protein fragments from the cell surface.[83,84]

The easiest way of preparing vaccines is to use killed or attenuated pathogens. Live microorganisms are typically more efficient than killed ones, due to a stronger immune response as a result of more sustained dose of antigen. There are, however, some problems and risks associated with using whole pathogens as vaccines. The attenuated pathogen might revert back to the virulent form and cause an infection. Furthermore, an entire pathogen will contain more than just the antigens required for the protective response. These additional components might suppress the immune response towards the protective antigens, or in the worst case they might cause side reactions in the form of hypersensitivity.[83] Furthermore, while growing viruses and bacteria in bulk quantities, is in general not very difficult, the same is not true for pathogens such as parasitic worms.

Antigenic fragments, associated with certain pathogens, can be acquired via either purification of samples of biological origin, or by synthetic methods. The glycans on the surface of cells are, however, inherently highly heterogenic, which can cause problems due to the high specificity of antibodies. If an antibody only binds to a specific part of a glycan, heterogeneity will inevitably dilute the response. Furthermore, high heterogeneity induces problems with purification and batch-to-batch variations. Synthetic approaches bypass these problems, and although the synthetic procedures might be laborious, they at least technically allow for large-scale production of highly pure compounds. There are some inherent problems associated with the use of carbohydrate fragments as vaccines, besides those related to the heterogeneity of native polysaccharides. Polysaccharides are typically poorly immunogenic, especially among young children, and have to be conjugated to an immunogenic carrier protein. The interactions between carbohydrates and proteins are generally quite weak, and achieving binding at physiological concentrations is difficult.[83] This problem can, however, often be solved by multivalency, where several antigens are attached to a scaffold, which has been shown to enhance binding to a larger extent than a simple increase in the concentration of the ligand.[85,86]

There are a number of carbohydrate-based vaccines available that offer protection against various pathogens, *e.g. Salmonella typhi*, several strains of *Streptococcus pneumoniae* and *Haemophilus influenzae* type b (hib). In addition, there are a number of carbohydrate-based vaccines in different stages of clinical trials.[87] Of these vaccines, hib vaccine is the most noteworthy as it is based on a fully synthetic carbohydrate antigen.

The goal of this brief discussion about the biological importance of carbohydrates is not to be a comprehensive overview of current literature, but rather to show their importance with selected examples. From the examples presented here, it should be evident that for understanding the biological interactions, knowledge about the structure and behavior of the carbohydrates in a biological environment is crucial. A particular class of oligosaccharides, β-(1→2) linked mannosides, and their biological importance and potential applications will be discussed in more detail in the following chapters.

Modern analytical tools, particularly NMR spectroscopy, allow accurate determination of the structure of carbohydrate structures found in nature. The amount of material available by isolation from biological sources is, however, typically insufficient to be of use in comprehensive biological studies. The

synthetic methods developed over the years, allow chemists to prepare well-defined, pure, compounds for biological studies.

1.6 Outline of this thesis

This thesis is based on the work done by the author at the Laboratory of Organic Chemistry, at Åbo Akademi University from 2013 – 2017. The thesis features all the most common aspects of carbohydrate chemistry: Synthesis, characterization, and biological applications, and tackles the challenges associated with each of these.

Chapter 2 explores in detail the synthesis of β-(1→2) linked mannosides, which are a recurring theme throughout the thesis. Different methods for creating the *cis*-glycosidic linkage from mannose are discussed, and a versatile synthetic protocol, the Crich β-mannosylation reaction, is selected. Key features of the building blocks required for the synthesis are discussed, and different methods for introducing a phosphate group are explored. The methods are then applied for preparation of a β-(1→2) mannotriose and tetraose, with a phosphate group at the reducing end, which are then used for investigating how the phosphate group might affect the unique conformation of this class of compounds. Application of NMR spectroscopy for structural verification and conformational analysis is emphasized.

Chapter 3 applies the concepts of chapter 2 for preparing multivalent structures featuring β-(1→2) linked mannosides, using click chemistry. The compounds are based on a previously discovered biologically active lead molecule, and two new trivalent glycoclusters with varying linker length are prepared, and their biological activity is evaluated to investigate the impact of the linker length. A brief overview of allergic inflammation is provided, and the potential of using the prepared glycoclusters as adjuvants for specific allergen immunotherapy is evaluated. The behavior of the compounds in solution is investigated with NMR spectroscopic and molecular modelling techniques.

Chapter 4 further expands the concept of multivalency by grafting various disaccharide fragments onto a polysaccharide-based backbone, using techniques discussed in chapter 3. The interactions between the modified polysaccharides and a protein, human Galectin-3, are evaluated by NMR spectroscopic techniques. The aim here is to investigate the claims of Gal-3 binding to β-(1→2) linked mannosides, and the general potential of using polysaccharides as scaffolds for carbohydrate-based ligands. An investigation of the applicability of

the click reaction for controlled depolymerization of polysaccharides, prompted by an unexpected decrease in size of the polymers during the reaction, is carried out using three naturally occurring polysaccharides

NMR spectroscopy, which is a particularly powerful analytical tool in carbohydrate chemistry, is heavily featured throughout the thesis. Accurate chemical shifts and coupling constants, are extracted from the spectra by quantum-mechanical simulations using the NMR simulation software PERCH. In addition to structural verification, NMR spectroscopy is used for investigating the conformational behavior of the target molecules, and interactions between polyvalent carbohydrate structures and proteins.

1.7 References

1. Rüdiger, H. & Gabius, H.-J. in *The Sugar Code* (ed. Gabius, H.-J.) 1–14 (WILEY-VCH Verlag, GmbH & Co. KGaA, 2009).

2. Kunz, H. Emil Fischer - Unequalled classicist, master of organic chemistry research, and inspired trailblazer of biological chemistry. *Angew. Chem., Int. Ed.* **41,** 4439–4451 (2002).

3. Hudson, C. S. Emil Fischer's discovery of the configuration of glucose. A semicentennial retrospect. *J. Chem. Educ.* **18,** 353 (1941).

4. Fischer, E. Synthesen in der Zuckergruppe II. *Ber. Dtsch. Chem. Ges.* **27,** 3189–3232 (1894).

5. McNaught, A. D. Nomenclature of Carbohydrates. *Pure Appl. Chem.* **68,** 1919–2008 (1996).

6. Angyal, S. J. & Pickles, V. A. Equilibria between pyranoses and furanoses: II. Aldoses. *Aust. J. Chem.* **25,** 1695–1710 (1972).

7. Kiliani, H. Heinrich Kiliani: Ueber das Cyanohydrin der Lävulose. *Ber. Dtsch. Chem. Ges.* **18,** 3066–3072 (1885).

8. Fischer, E. Emil Fischer: Reduction von säuren der Zuckergruppe. *Ber. Dtsch. Chem. Ges.* **22,** 2204–2205 (1889).

9. Edward, J. T. Stability of Glycosides to Acid Hydrolysis. *Chem. Ind. (London)* 1102–1104 (1955).

10. Lemieux, R. U. in *Molecular Rearrangements* (ed. de Mayo, P.) 709 (Interscience Publishers, 1964).

11. Juaristi, E. & Cuevas, G. Recent studies of the anomeric effect. *Tetrahedron* **48,** 5019–5087 (1992).

12. Lichtenthaler, F. W., Rönninger, S. & Kreis, U. Tetra-0-acetyl-P-D-glucopyranosyl Chloride: Occurrence of. *Liebigs Ann. der Chemie* **1990,** 1001–1006 (1990).

13. Durette, P. L. & D, H. Conformational Studies on Pyranoid Sugar Derivatives by NMR Spectroscopy: The Conformational Equilibria of Some Peracylated Aldepentopyranosyl Halides in Solution. *Carbohydr. Res.* **18,** 57–80 (1971).

14. Michael, A. On the Synthesis of Helicin and Phenolglucoside. *Am. Chem. J.* **1,** 305–312 (1879).

15. Liang, D.-M. *et al.* Glycosyltransferases: mechanisms and applications in natural product development. *Chem. Soc. Rev.* **44,** 8350–74 (2015).

16. Lairson, L. L., Henrissat, B., Davies, G. J. & Withers, S. G. Glycosyl transferases: Structures, functions, and mechanisms. *Annual Review of Biochemistry* **77,** 521–555 (2008).

17. Fischer, E. Ueber die Glucoside der Alkohole. *Ber. Dtsch. Chem. Ges.* **26,** 2400–2412 (1893).

18. Fischer, E. & Beensch, L. Ueber einige synthetische Glucoside. *Ber. Dtsch. Chem. Ges.* **27,** 2478–2486 (1894).

19. Fischer, E. Ueber die Verbindungen der Zucker mit den Alkoholen und Ketonen. *Ber. Dtsch. Chem. Ges.* **28,** 1145–1167 (1895).

20. Koenigs, W. & Knorr, E. Ueber einige Derivate des Traubenzuckers und der Galactose. *Ber. Dtsch. Chem. Ges.* **34,** 957–981 (1901).

21. Demchenko, A. V. in *Handbook of Chemical Glycosylation: Advances in Stereoselectivity and Therapeutic Relevance* (ed. Demchenko, A. V) 1–28 (WILEY-VCH Verlag, GmbH & Co. KGaA, 2008).

22. Igarashi, K. The Koenigs-Knorr Reaction. *Adv. Carbohydr. Chem. Biochem.* **34,** 243–283 (1977).

23. Zeng, Y., Ning, J. & Kong, F. Pure α-linked products can be obtained in high yields in glycosylation with glucosyl trichloroacetimidate donors with a C2 ester capable of neighboring group participation. *Tetrahedron Lett.* **43,** 3729–3733 (2002).

24. Zeng, Y., Ning, J. & Kong, F. Remote control of α- or β-stereoselectivity in (1→3)-glucosylations in the presence of a C-2 ester capable of neighboring-group participation. *Carbohydr. Res.* **338,** 307–311 (2003).

25. Kim, J. H., Yang, H., Park, J. & Boons, G.-J. A general strategy for stereoselective glycosylations. *J. Am. Chem. Soc.* **127,** 12090–12097 (2005).

26. Boltje, T. J., Kim, J. H., Park, J. & Boons, G.-J. Stereoelectronic effects determine oxacarbenium vs β-sulfonium ion mediated glycosylations. *Org. Lett.* **13,** 284–287 (2011).

27. Baek, J. Y., Lee, B. Y., Jo, M. G. & Kim, K. S. β-directing effect of electron-withdrawing groups at O-3, O-4, and O-6 positions and α-directing effect by remote participation of 3-O-acyl and 6-O-acetyl groups of donors in mannopyranosylations. *J. Am. Chem. Soc.* **131,**

17705–17713 (2009).

28. Komarova, B. S., Orekhova, M. V, Tsvetkov, Y. E. & Nifantiev, N. E. Is an acyl group at O-3 in glucosyl donors able to control α-stereoselectivity of glycosylation? the role of conformational mobility and the protecting group at O-6. *Carbohydr. Res.* **384,** 70–76 (2014).

29. Eby, R. & Schuerch, C. The use of 1-O-tosyl-D-glucopyranose derivatives in α-D-glucoside synthesis. *Carbohydr. Res.* **34,** 79–90 (1974).

30. Ishiwata, A., Munemura, Y. & Ito, Y. Synergistic solvent effect in 1,2-cis-glycoside formation. *Tetrahedron* **64,** 92–102 (2008).

31. Shirahata, T. *et al.* Improved catalytic and stereoselective glycosylation with glycosyl N-trichloroacetylcarbamate: application to various 1-hydroxy sugars. *Carbohydr. Res.* **345,** 740–749 (2010).

32. Nigudkar, S. S. & Demchenko, A. V. Stereocontrolled 1,2-cis glycosylation as the driving force of progress in synthetic carbohydrate chemistry. *Chem. Sci.* **6,** 2687–2704 (2015).

33. Demchenko, A. 1,2-cis O-Glycosylation: Methods, Strategies, Principles. *Curr. Org. Chem.* **7,** 35–79 (2003).

34. Merrifield, R. B. Automated Synthesis of Peptides. *Science* **150,** 178–185 (1965).

35. Merrifield, R. B., Stewart, J. M. & Jernberg, N. Instrument for automated synthesis of peptides. *Anal. Chem.* **38,** 1905–1914 (1966).

36. Seeberger, P. H. Automated oligosaccharide synthesis. *Chem. Soc. Rev.* **37,** 19–28 (2008).

37. Hsu, C. H., Hung, S. C., Wu, C. Y. & Wong, C. H. Toward automated oligosaccharide synthesis. *Angew. Chem., Int. Ed.* **50,** 11872–11923 (2011).

38. Bennett, C. S. Principles of modern solid-phase oligosaccharide synthesis. *Org. Biomol. Chem.* **12,** 1686 (2014).

39. Jaipuri, F. A. & Pohl, N. L. Toward solution-phase automated iterative synthesis: fluorous-tag assisted solution-phase synthesis of linear and branched mannose oligomers. *Org. Biomol. Chem.* **6,** 2686–91 (2008).

40. Hahm, H. S. *et al.* Automated glycan assembly using the Glyconeer 2.1 synthesizer. *Proc. Natl. Acad. Sci. U. S. A.* 1–5 (2017).

41. Love, K. R. & Seeberger, P. H. Automated Solid-Phase Synthesis of Protected Tumor-Associated Antigen and Blood Group Determinant Oligosaccharides. *Angew. Chem., Int. Ed.* **43,** 602–605 (2004).

42. Clark, G. F. The role of carbohydrate recognition during human sperm-egg binding. *Hum. Reprod.* **28,** 566–577 (2013).

43. Landsteiner, K. Zur Kenntnis der antifermentativen, lytischen und agglutinierenden Wirkungen des Blutserums und der Lymphe. *Zentralblatt Bakteriol.* **27,** 357–362 (1900).

44. Landsteiner, K. On Agglutination of Normal Human Blood. *Transfusion* **1,** 5–8 (1961).

45. Landsteiner, K. Individual differences in Human blood. *Science* **73,** 403–409 (1931).

46. von Decastello, A. & Sturli, A. Ueber die Isoagglutinine im Serum gesunder und kranker Menschen. *Munchener Medizinische Wochenschrift* **49,** 1090–1095 (1902).

47. Jaský, J. Haematologické studie u. psychotiku. *Sborn. Klin.* **8,** 85–139 (1907).

48. Moss, W. L. 'Studies on isoagglutinins and isohemolysins'. *Bull. Johns Hopkins Hosp.* **21,** 63–70 (1910).

49. Morgan, W. T. J. The human ABO blood group substances. *Experientia* **3,** 257–67 (1947).

50. Watkins, W. M. & Morgan, W. T. Neutralization of the anti-H agglutinin in eel serum by simple sugars. *Nature* **169,** 825–826 (1952).

51. Watkins, W. M. & Morgan, W. T. J. Specific Inhibition Studies Relating to the Lewis Blood-Group System. *Nature* **180,** 1038–1040 (1957).

52. CANCER FACT SHEETS: ALL CANCERS EXCLUDING NON-MELANOMA SKIN CANCER. (2012). at <http://gco.iarc.fr/today/fact-sheets-cancers?cancer=29&type=0&sex=0>

53. Lozano, R. *et al.* Global and regional mortality from 235 causes of death for 20 age groups in 1990 and 2010: A systematic analysis for the Global Burden of Disease Study 2010. *Lancet* **380,** 2095–2128 (2012).

54. Fukuda, M. & Hindsgaul, O. *Molecular and Cellular Glycobiology*. (Oxford University Press, 2000).

55. Wang, B. & Boons, G.-J. *Carbohydrate Recognition: Biological*

Problems, Methods, and Applications. (John Wiley & Sons, Inc, 2011).

56. Springer, G. F., Desai, P. R., Murthy, M. S., TegtMeyer, H. & Scanlon, E. F. Human Carcinoma-Associated Precursor Antigens of the Blood Group MN System and the Host's Immune Responses to Them. *Prog. Allergol.* **26,** 42–96 (1979).

57. Springer, G. T and Tn, general carcinoma autoantigens. *Science* **224,** 1198–1206 (1984).

58. Springer, G. F. Immunoreactive T and Tn epitopes in cancer diagnosis, prognosis, and immunotherapy. *J. Mol. Med.* **75,** 594–602 (1997).

59. Freire, T., Bay, S., Vichier-Guerre, S., Lo-Man, R. & Leclerc, C. Carbohydrate antigens: synthesis aspects and immunological applications in cancer. *Mini Rev. Med. Chem.* **6,** 1357–1373 (2006).

60. Wamelink, M. M. *et al.* Detection of transaldolase deficiency by quantification of novel seven-carbon chain carbohydrate biomarkers in urine. *J. Inherit. Metab. Dis.* **30,** 735–742 (2007).

61. Lawrence, R. *et al.* Disease-specific non–reducing end carbohydrate biomarkers for mucopolysaccharidoses. *Nat. Chem. Biol.* **8,** 197–204 (2012).

62. Lawrence, R. *et al.* Glycan-based biomarkers for mucopolysaccharidoses. *Mol. Genet. Metab.* **111,** 73–83 (2014).

63. Falagas, M. E., Zarkadoulia, E. A., Bliziotis, I. A. & Samonis, G. Science in Greece: from the age of Hippocrates to the age of the genome. *FASEB J.* **20,** 1946–50 (2006).

64. Zajac, J., Shrestha, A., Patel, P. & Poretsky, L. in *Principles of Diabetes Mellitus* (ed. Poretsky, L.) 3–18 (Springer US, 2010).

65. Ueda, K. Glycoproteomic strategies: From discovery to clinical application of cancer carbohydrate biomarkers. *Proteomics - Clin. Appl.* **7,** 607–617 (2013).

66. Dai, C. *et al.* Carbohydrate biomarker recognition using synthetic lectin mimics. *Pure Appl. Chem.* **84,** 2479–2498 (2012).

67. Gebregiworgis, T. & Powers, R. Application of NMR Metabolomics to Search for Human Disease Biomarkers. *Comb. Chem. High Throughput Screen.* **15,** 595–610 (2012).

68. Emwas, A.-H. *et al.* Recommendations and Standardization of Biomarker

Quantification Using NMR-Based Metabolomics with Particular Focus on Urinary Analysis. *Journal of Proteome Research* **15,** 360–373 (2016).

69. Galan, M. C., Benito-Alifonso, D. & Watt, G. M. Carbohydrate chemistry in drug discovery. *Org. Biomol. Chem* **9,** 3598–3610 (2011).

70. Ernst, B. & Magnani, J. L. From carbohydrate leads to glycomimetic drugs. *Nat. Rev. Drug Discov.* **8,** 661–677 (2009).

71. van Boeckel, C. a. a. *et al. Synthesis of a Pentasaccharide Corresponding to the Antithrombin III Binding Fragment of Heparin*. *Journal of Carbohydrate Chemistry* **4,** (1985).

72. Petitou, M. *et al.* Synthesis of heparin fragments. A chemical synthesis of the pentasaccharide ... *Carbohydr. Res.* **147,** 221–236 (1986).

73. Petitou, M. & Van Boeckel, C. A. A. A synthetic antithrombin III binding pentasaccharide is now a drug! What comes next? *Angew. Chem., Int. Ed.* **43,** 3118–3133 (2004).

74. Miljkovic, M. *Carbohydrates: Synthesis, Mechanisms and Stereoelectronic Effects*. (Springer Science+Business Media, LLC, 2009).

75. Ritter, T. K. & Wong, C.-H. Carbohydrate-Based Antibiotics: A New Approach to Tackling the Problem of Resistance. *Angew. Chem, Int. Ed. English* **40,** 3508–3533 (2001).

76. Mingeot-Leclerq, M.-P., Glupczynski, Y. & Tulkens, P. M. MINIREVIEW Aminoglycosides : Activity and Resistance. *Antimicrob. Agents Chemother.* **43,** 727–737 (1999).

77. Wright, D. E. The orthosomycins, a new family of antibiotics. *Tetrahedron* **35,** 1207–1237 (1979).

78. Kim, C. U. *et al.* Influenza neuraminidase inhibitors possessing a novel hydrophobic interaction in the enzyme active site: Design, synthesis, and structural analysis of carbocyclic sialic acid analogues with potent anti-influenza activity. *J. Am. Chem. Soc.* **119,** 681–690 (1997).

79. Genaro, A., Cunha, M. L. R. S. & Lopes, C. A. M. Study on the susceptibility of Enterococcus faecalis from infectious processes to ciprofloxacin and vancomycin. *J. Venom. Anim. Toxins Incl. Trop. Dis.* **11,** 252–260 (2005).

80. Meacci, F. *et al.* Drug Resistance Evolution of a Mycobacterium tuberculosis Strain from a Noncompliant Patient Drug Resistance Evolution of a Mycobacterium tuberculosis Strain from a Noncompliant

Patient. *J. Clin. Microbiol.* **43,** 3114–3120 (2005).

81. Lister, P. D., Wolter, D. J. & Hanson, N. D. Antibacterial-resistant Pseudomonas aeruginosa: Clinical impact and complex regulation of chromosomally encoded resistance mechanisms. *Clin. Microbiol. Rev.* **22,** 582–610 (2009).

82. Farrar, J. J. *et al.* Tetanus. *J. Neurol. Neurosurg. Psychiatry* **69,** 292–301 (2000).

83. Delves, P. J., Martin, S. J., Burton, D. R. & Roitt, I. M. *Roitt's Essential Immunology*. (Wiley-Blackwell, 2011).

84. Plotkin, S. A., Orenstein, W. & Offit, P. A. *Vaccines: Expert Consult*. (Elsevier, 2012).

85. Kiessling, L. L., Gestwicki, J. E. & Strong, L. E. Synthetic multivalent ligands in the exploration of cell-surface interactions. *Curr. Opin. Chem. Biol.* **4,** 696–703 (2000).

86. Mammen, M., Choi, S.-K. & Whitesides, G. M. Polyvalent interactions in biological systems: implications for design and use of multivalent ligands and inhibitors. *Angew. Chem., Int. Ed.* **37,** 2755–2794 (1998).

87. Astronomo, R. D. & Burton, D. R. Carbohydrate vaccines: developing sweet solutions to sticky situations? *Nat. Rev. Drug Discovery* **9,** 308–324 (2010).

2 Oligosaccharides: The almighty mannose

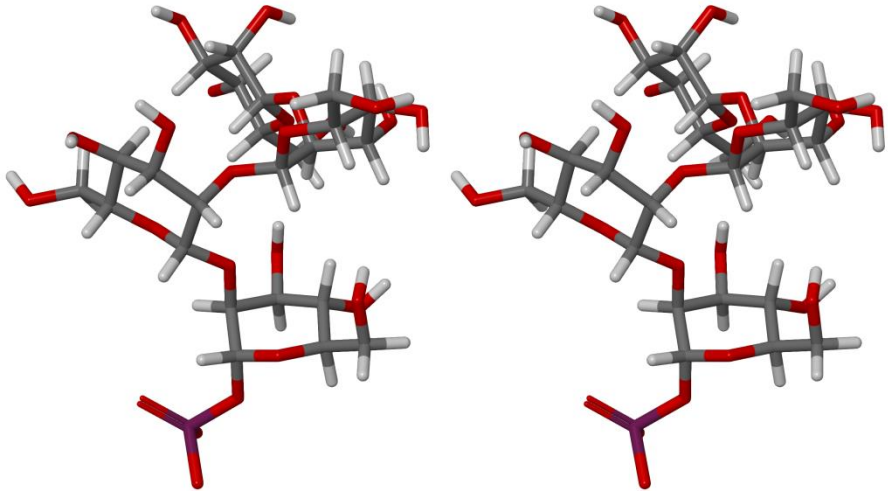

Candida albicans is one of the few organisms that express β-(1→2) linked mannosides on its cell surface. This class of compounds is known to be highly immunogenic, and considerable effort has been focused on developing vaccines against *C. albicans* based on these structures. This chapter explores the synthesis of β-(1→2) linked mannotriose and tetraose with a phosphate group at the reducing end, analogous to the acid-labile mannan portion of the *C. albican*s cell wall polysaccharide. The conformations of the prepared compounds in solution are investigated, and the impact of the charged phosphate group on the conformation is evaluated.

This chapter is based on the previously published paper: **Synthesis and conformational analysis of β-(1→2)-linked phosphorylated mannosides,** J. Rahkila, F. S. Ekholm, R. Panchadhayee, A. Ardá, F. J. Cañada, J. Jiménez-Barbero, R. Leino, *Carbohydr. Res.* **2014,** 383, 58 – 68.

2.1 Introduction

Candida is a genus of fungi, with a large number of species that are responsible for an increasing number of invasive fungal infections. Most people carry these fungi, and they are considered part of the human microbial flora.[1] While they can cause yeast infections in healthy people, these infections do not typically become invasive, or pose any serious threat. In immunocompromised individuals *e.g.* HIV patients,[2] people undergoing prolonged antibiotic treatment, and organ transplant receivers treated with immunosuppressant drugs,[3] however, they can cause serious infections. The infections caused by Candida are commonly called candidosis or candidiasis.

During the last 30 years, there has been a significant increase in invasive fungal infections of which the vast majority, more than 95%, are caused by *Candida spp*. or *Aspergillus spp*.[4,5] One contributing factor to the increased number of invasive infections, is the increasing resistance to antifungal drugs.

The most common species of the *Candida* species is *C. albicans*, the cell wall of which contains a glycoprotein consisting of α-(1→6) linked mannopyranan with branches of α-(1→2), α-(1→3), and additional α-(1→6) linked mannopyranosyl units. What makes the cell wall especially interesting, is the fact that some of the branches terminate in β-(1→2) linked mannopyranosyl fragments (acid stable β-mannan). Additionally, there are β-(1→2) linked mannans connected via a phosphodiester linkage to C-6 on the side chains (acid labile β-mannan). The entire polysaccharide is attached via N-linked glycan core to N-acetyl glucosamine, that is connected to an asparagine residue on the glycoprotein (Figure 2.1).[6–8]

2.2 Immunochemistry of β-(1→2) linked mannosides

The cell wall of *C. albicans* has been found to be highly immunogenic,[9,10] and compelling evidence suggests that it is the β-(1→2) linked mannans that are the main source for the effect. Immunoglobulin M (IgM) monoclonal antibody (MAb) B6.1, has been shown to protect mice from disseminated candidiasis. Another antibody, IgM MAb B6, on the other hand, does not offer such protection.[11] While the antibodies are of the same type and both bind to the cell wall of *C. albicans*, their epitope specificities differ. The protecting IgM MAb B6.1 antibody binds the acid labile fraction of the cell wall mannan, whereas IgM MAb B6 does not. Furthermore, another monoclonal antibody IgG3 MAb C3.1 also offers protection against candidiasis in mice.[12]

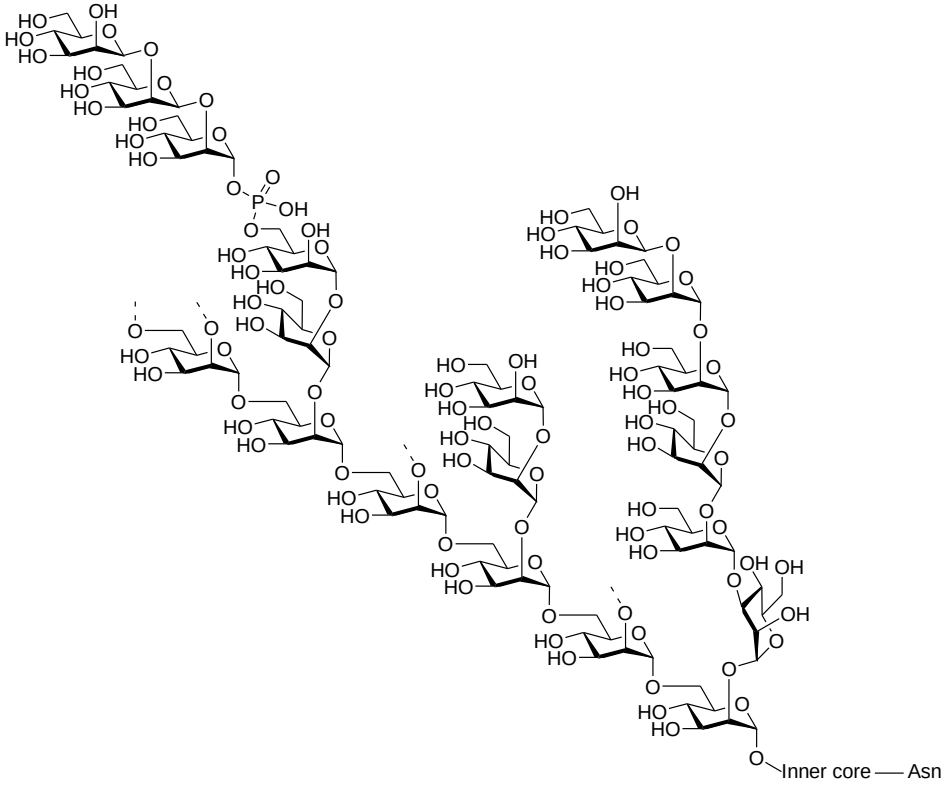

Figure 2.1. Structural representation of the C. albicans cell wall mannan.

The immunogenic activity of the β-(1→2) linked mannans has prompted rigorous investigations towards potentially using them for treatment or prevention of candidiasis. Bundle *et al.* have determined that the affinities of the aforementioned antibodies is greatest towards disaccharides and trisaccharides, and decreases rapidly for larger fragments.[13] This is due to the unique conformation of β-(1→2) linked mannosides, which will be discussed in more detail below. Binding of larger fragments would require energetically unfavorable conformational adjustments of the oligosaccharides. Molecular modelling of a tetrasaccharide fragment (Figure 2.2) spanning the phosphodiester linkage found in the native *C. albicans* mannan suggests that, while the phosphate group is not crucial for the binding, the α-linkage to the phosphate allows the tetrasaccharide to make greater contact with the antibody. Synthesis of the fragment and binding studies indicated, however, that this does not increase the binding affinity.[14]

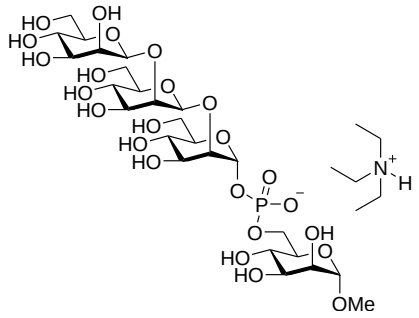

Figure 2.2. Mannotetraose derived from the *C. albicans* cell wall, prepared and investigated by Bundle *et. al.*

The immunochemical properties of β-(1→2) linked mannosides have been studied in detail, and the potential applications of this class of compounds as vaccines have been investigated. As mentioned in the previous chapter, carbohydrates alone are typically not highly immunogenic. Therefore the vaccines have been based on glycoconjugates where the carbohydrate is covalently attached to a protein[12,15,16] or a shorter glycopeptide chain.[17] Immunization with such vaccines has shown to protect mice and rabbits against candidiasis, but they have not yet entered clinical trials.

2.3 Synthesis of β-(1→2) linked mannosides

The preparation of β-mannosides was for long considered one of the greatest challenges in synthetic carbohydrate chemistry,, and still today it is far from trivial. There are several factors that contribute to the particular difficulties associated with the synthesis of this class of compounds. β-Mannosides are *cis* glycosides, which makes the use of neighboring group participation difficult. Furthermore, the stabilizing effect of the anomeric product makes the α-anomer more favorable from a thermodynamic point of view and, finally, the β-face of the oxocarbenium ion transition state is typically more hindered than the α-face, making the α-anomer kinetically favored as well.

Over the years, a number of methods for creating such linkages have been developed.[18–20] While many of these methods are highly creative, it is difficult to find one universal synthetic protocol for preparing these compounds. Many of the published methods are to be regarded with some caution, as they are developed having rather simple or very specific acceptors in mind. These are quite often unsuitable for bulkier and otherwise more complex acceptors, such as monosaccharides or larger carbohydrate structures.

One method that has found widespread use is the preparation of β-glucosides followed by stereochemical inversion of C2 via an oxidation-reduction sequence. This method, originally developed by Lichtenthaler *et al.*[21] has been used extensively by Bundle *et al.* for preparation of β-(1→2) linked mannosides for developing a *C. albicans* vaccine.[22–24] Using glucopyranosyl donors allows for taking advantage of neighboring group participation of an ester protecting group on C2. After the reaction the protecting group is hydrolyzed, and the alcohol is oxidized to a ketone, typically by Swern oxidation,[25] followed by reduction with a bulky reduction agent, such as L-selectride, resulting in hydride addition from the least hindered side, yielding an axial hydroxyl group (Scheme 2.1).

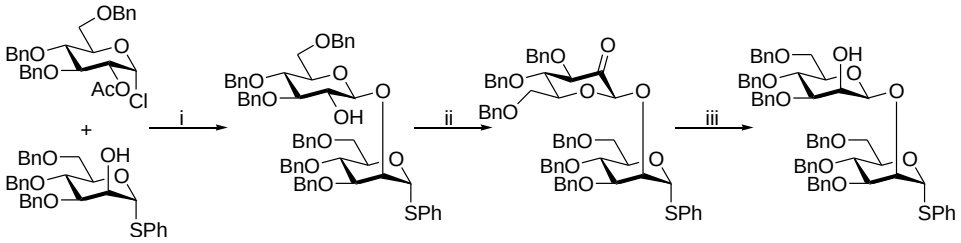

Scheme 2.1 The method for preparation of β-mannosides used by Bundle *et al.*[24] Reagents and conditions: i) 1. AgOTf, 4 Å MS, toluene, CH_2Cl_2, –40 °C (74%), 2. NaOMe, MeOH, rt, (96%); ii) DMSO, $(COCl)_2$, Et_3N; iii) L-selectride, THF (73%).

Many of the modern strategies for preparing β-mannosides are based on modification of the transition state of the activated glycosyl donor. Generally S_N1-like reactions will prefer the α-product, and a shift towards S_N2-type reactions would thus be preferred. Destabilizing the oxocarbenium ion intermediate will favor S_N2-type reactions. This destabilization can be achieved by electronic effects, or physical constraints that prevent the molecule from attaining the $^4H_3$ conformation that is postulated as the preferred one of the oxocarbenium ion.[26] Upon reaction with a nucleophile, the ring will twist into a favored $^4C_1$ conformation or a disfavored $^1S_3$ conformation, depending on if the nucleophile attacks from the α or β-face (Scheme 2.2).[26,27]

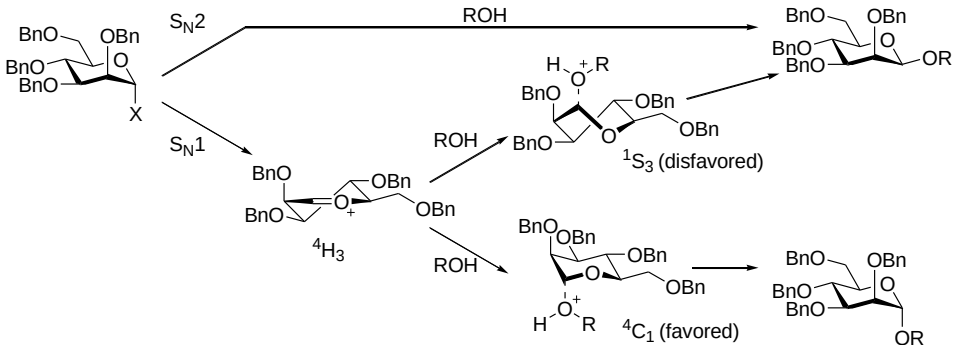

Scheme 2.2. Conformational changes of the oxocarbenium intermediate associated with the S_N1 mechanism.

A popular method, used by several groups, for preventing the intermediate from attaining a $^4H_3$ conformation is to use a 4,6-tether, a second ring structure that fixes the geometry of O5-C5-C6-O6 in a *trans-gauche* (tg) conformation. This also maximizes the electron-withdrawing effect of O6. While the oxocarbenium ion is destabilized by the conformational restriction and the electron-deficiency in the ring, the mechanism of the reaction is shifted towards a synchronized reaction, but is never purely S_N2. The additional benefit of a 4,6-tether is that the oxocarbenium ion that does form, is assumed to have a $B_{2,5}$[28,29] conformation, which makes a nucleophilic attack from the α-face less favored.

Finally, the method selected for this work was the so-called Crich method,[18,30] where an α-triflate is used as the donor in combination with a 4,6-*O*-benzylidene acetal. The electron withdrawing effect of O6 destabilizes the oxocarbenium ion favoring a covalent or contact ion pair α-triflate that can undergo an S_N2-type reaction instead of S_N1. Originally, the method used glycosyl sulfoxides preactivated by triflic anhydride (Tf_2O) to form the α-triflate before adding the acceptor.[31–34] Later, the method was developed further, and thioglycosides are now typically used as donors.[35] The activation protocol typically uses 1-(phenylsulfinyl)-piperidine (BSP) and triflic anhydride, but other sulfoxides, such as diphenylsulfoxide, can be used to reduce the cost, as BSP is rather expensive. During the reaction, one equivalent of triflic acid is formed and to avoid anomerization, or other side reactions, a non-nucleophlic base, such as 2,4,6-tri-*tert*-butylpyrimidine, is used to quench the acid. This method has successfully been used for preparation of various β-(1→2), β-(1→3) and β-(1→4) linked oligomannosides.[36–39] Mechanistic studies by suggest, that the reaction proceeds via a transition state where the α-triflate is in equilibrium with a transient contact ion pair, with the triflate ion in close proximity to the α-face of the oxocarbenium ion (Scheme 2.3).[40,41] NMR spectroscopic studies show,

that the chemical shift of the anomeric carbon is 104.5 ppm instead of ~250 ppm, as would be expected for an oxocarbenium ion. This indicates that the equilibrium is heavily shifted towards the covalent α-triflate.[40] The small amount of α-product often obtained in the reaction, is likely to be due to the presence of a small fraction of a more loosely associated, maybe even solvent separated triflate anion.

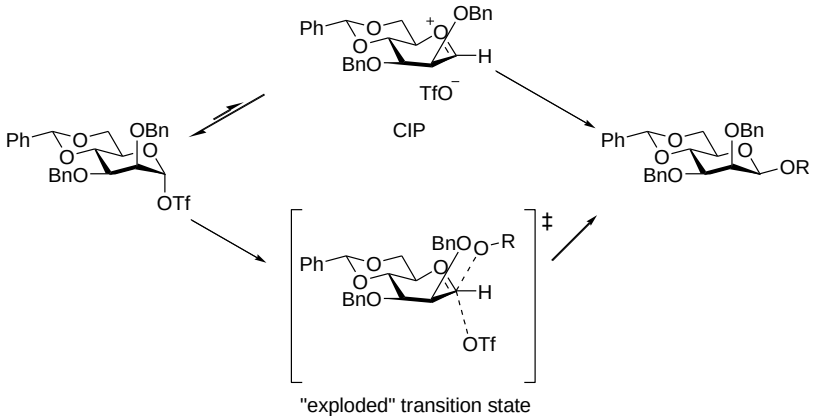

Scheme 2.3. Proposed mechanism of the Crich β-mannosylation.

The preparation of the monosaccharide building blocks used in this work has been described earlier,[39,42] and will not be discussed in detail here but, in short, the synthesis started with acetylation of D-mannose with acetic anhydride in pyridine to afford **1** (Scheme 2.4). The peracetylated mannose was used in a thioglycosylation reaction, with thiophenol as the acceptor and $BF_3{\cdot}OEt_2$ as the activator. In theory, this reaction would only require a catalytic amount of the acid, but even with large excess the reaction typically takes overnight which is why five equivalents were used. The thioglycoside **2** was deprotected under Zemplén conditions,[43] using sodium methoxide in methanol. The 4 and 6 positions of **3** were protected with a benzylidene acetal by using benzaldehyde dimethyl acetal and catalytic *p*-toluenesulfonc acid to yield **4**. At this point, the synthetic path splits in two to make the two final building blocks. The minute difference in reactivity between the axial 2-OH and equatorial 3-OH can be amplified by generating a stannylene acetal using dibutyltin oxide. This acetal could be selectively ring-opened and alkylated at the equatorial position by using a fluoride salt, tetrabutylammonium bromide and an alkyl halide (benzyl bromide in this case) to yield the monobenzylated compound **5**. The last free hydroxyl group was protected by a traditional Williamson ether synthesis using sodium hydride to generate the alkoxide, followed by addition of 4-

methoxybenzyl bromide to afford the finished building block **6**. Finally, building block **7** was prepared in a similar manner by treating **4** with sodium hydride, followed by benzyl bromide (Scheme 2.4).

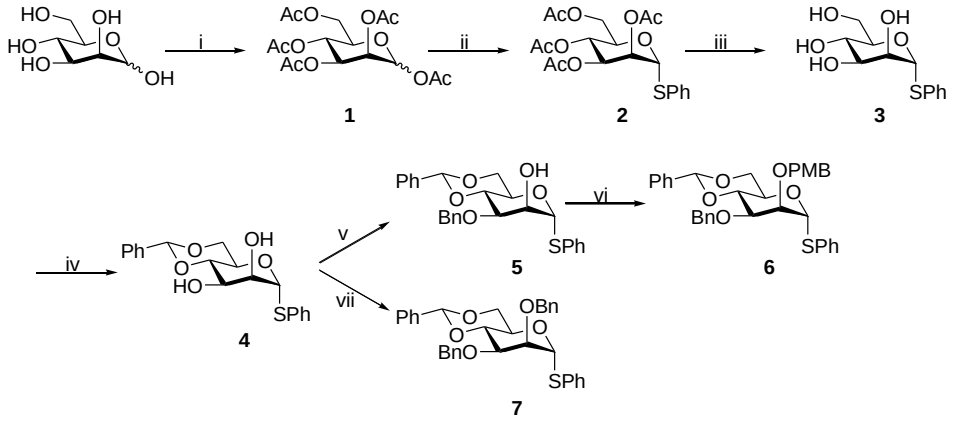

Scheme 2.4. Synthesis of monosaccharide building blocks. Reagents and conditions: i) Ac_2O, pyridine, rt, 2 h (95%); ii) PhSH, $BF_3{\cdot}OEt_2$, CH_2Cl_2, rt, 20 h (90%); iii) NaOMe, MeOH, rt, 18 h (quant), iv) $C_6H_5CH(OCH_3)_2$, *p*-TSA, DMF, 60 °C, 200 mbar, 2 h (91%); v) 1. Bu_2SnO, toluene, 120 °C, 2 h, 2. Bu_4NBr, CsF, BnBr, 120 °C, 3 h (48%); vi) 1. NaH, DMF, 0 °C, 30 min, 2. PMBCl, rt, 1 h (95%); vii) 1. NaH, DMF, 0 °C, 30 min, 2. BnBr, rt, 3 h (95%).

The stability of thioglycosides under a wide range of conditions, and the utilization of a preactivation protocol made it possible to use building block **5** as the reducing end monosaccharide unit without further modification. This particular method was selected for this work due to the robustness of the reaction, and the fact that it allows for a convergent synthesis in the case of a tetrasaccharide. The linear synthesis of larger oligosaccharides is less efficient considering the number of synthetic steps. While the stereoselectivity of the reaction is in general very high, it has been shown to decrease from practically fully selective, to an α:β ratio of approximately 1:4 for larger oligosaccharides.[44]

With all the building blocks prepared, the focus was turned to the preparation of the target oligosaccharides. Using the Crich β-mannosylation protocol, building block **7** was converted to the corresponding α-triflate by Tf_2O and BSP, in the presence of TTBP in freshly distilled CH_2Cl_2 at –60 °C under inert atmosphere. Typically, the activation was complete in less than 15 minutes, but the reaction was stirred at said temperature for 30 min to ensure complete activation. The reaction mixture containing the activated donor was cooled down to –78 °C, and the acceptor, building block **5**, was added dropwise as a solution in freshly distilled CH_2Cl_2. The solution of the acceptor was at room temperature, so a

slow addition was important to avoid localized warmer areas in the reaction mixture. After two hours at –78 °C the reaction was complete according to TLC, and was quenched with triethylphosphine followed by conventional work-up, resulting in a 75% yield of disaccharide **8**. This disaccharide was activated using the same protocol, and glycosylated one more time using acceptor **5** to afford a β-(1→2) linked mannotriose **9** with a thiophenol group at the reducing end in 62% yield (Scheme 2.5).

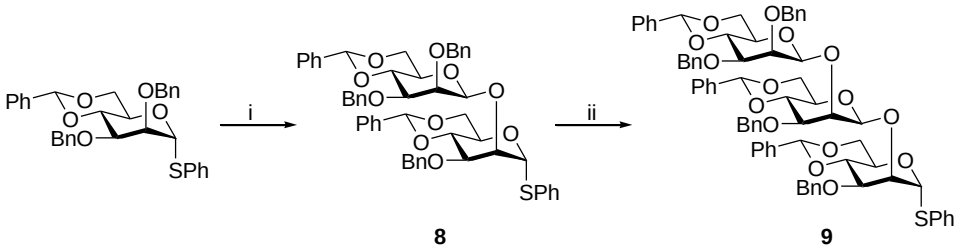

Scheme 2.5. Synthesis of trisaccharide **9**. Reagents and conditions: i) 1. BSP, TTBP, Tf_2O, CH_2Cl_2, –60 °C, 30 min, 2. Acceptor **5**, –78 °C, 2 h (75%); ii) BSP, TTBP, Tf_2O, CH_2Cl_2, –60 °C, 30 min, 2. Acceptor **5**, –78 °C, 2 h (62%).

One could argue, that it would be better to design a synthesis so that the simplest possible molecule (typically a monosaccharide) would be used as a donor. The activated donor is highly reactive, and thus more likely to decompose or undergo side reactions. Because of this, the least valuable molecule should be used as an acceptor. This could have been achieved using building block **6** instead of **7** when preparing the disaccharide. The yields of glycosylations using the more reactive donor **6** were, however, found to be somewhat lower than the yields of **7**. Furthermore, this methodology would have required an extra deprotection step before the second glycosylation. Overall, the benefits of using a disaccharide donor outweigh the disadvantages in this particular case.

The helical conformation of β-(1→2) linked mannosides is already quite evident in a molecule as small as a trisaccharide, which would make the β-face of the activated donor **9** rather sterically hindered, and thus a similar strategy as was used for preparing trisaccharide **9**, is not viable for preparation of an analogous tetrasaccharide. Because of this, a convergent synthetic strategy was selected, and another disaccharide (**10**) was prepared according to the same protocol as previously. The yield of this reaction was, however, slightly lower (57% vs 75%) than when preparing disaccharide **8**. As previously mentioned, this could be due to the somewhat higher reactivity of the donor, owing to the electron-donating properties of the PMB protecting group on C2. After the glycosylation,

the PMB group was selectively cleaved under oxidative conditions using DDQ yielding disaccharide acceptor **11** in fair (50%) yield over two steps. Disaccharide **8** was again used as a donor, and reacted with acceptor **11** to afford tetrasaccharide **12** in 35% yield (Scheme 2.6).

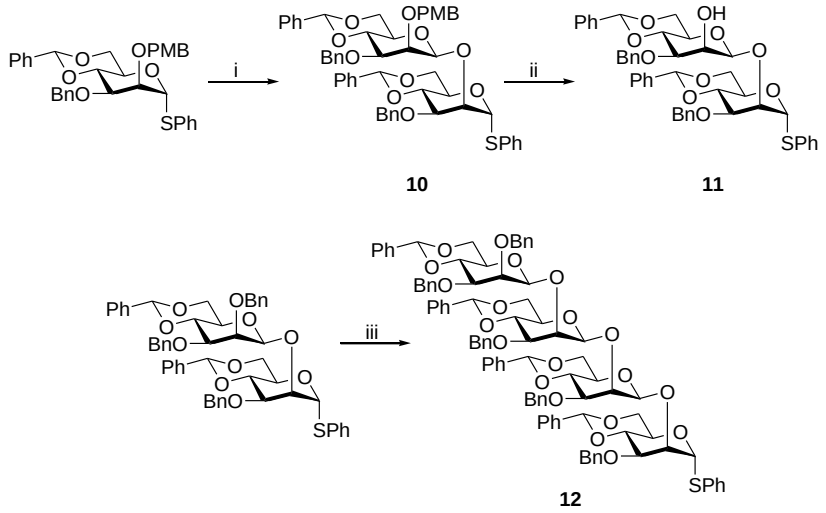

Scheme 2.6. Synthesis of tetrasaccharide **12**. Reagents and conditions: i) 1. BSP, TTBP, Tf_2O, CH_2Cl_2, –60 °C, 30 min, 2. Acceptor **5**, –78 °C, 2 h (57%); ii) DDQ, CH_2Cl_2:H_2O 1:1, 0 °C, 1 h (88%); iii) 1. BSP, TTBP, Tf_2O, CH_2Cl_2, –60 °C, 30 min, 2. Acceptor **11**, –78 °C, 2 h (35%).

With the basic structures for the trisaccharide and tetrasaccharide completed, the next step was to add the phosphate functionality. Similar molecules have been prepared previously,[39] and in the reported method, the thiophenyl group was hydrolyzed by N-bromosuccinimide in acetone/H_2O, followed by reacting the anomeric hydroxyl group with dibenzyl(*N*,*N*-diisopropyl) phosphoramidite in the presence of 1*H*-tetrazole. The phosphite was then oxidized to the corresponding phosphate by *m*-chloroperbenzoic acid. Initially, the same procedure was employed for these molecules as well, but the yields of the hydrolysis of the thiophenyl groups were not satisfactory (28% for both trisaccharide **13** and tetrasaccharide **14**). One reason for the low yield could be that the NBS is able to cleave the benzylidene acetals.[45,46] Despite the low yield of the reaction, the products were phosphorylated with dibenzyl(*N*,*N*-diisopropyl) phosphoramidite and 1*H*-tetrazole, and subsequently oxidized to the corresponding phosphates with *m*-CPBA (Scheme 2.7). The overall yield of this reaction was good but, rather surprisingly, there was almost no stereoselectivity (α:β = 1:1 for trisaccharide **15** and 2:1 for tetrasaccharide **16**). The overall yields

of 11% and 17% over two steps for **15** and **16** respectively prompted to explore an alternative method for preparing these compounds.

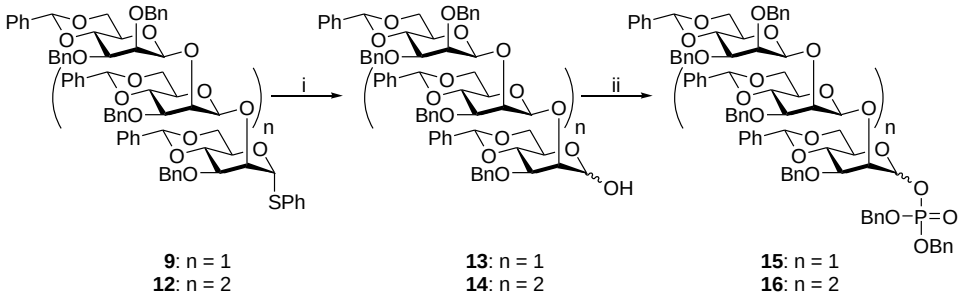

9: n = 1
12: n = 2

13: n = 1
14: n = 2

15: n = 1
16: n = 2

Scheme 2.7. Synthesis of phosphorylated tri and tetrasaccharides **15** and **16**. Reagents and conditions: i) NBS, acetone:H_2O 50:1, 0 °C, 1.5 h (**13**, **14**: 28%); ii) 1. Dibenzyl(*N*,*N*-diisopropyl) phosphoramidite, 1*H*-tetrazole, CH_2Cl_2, 0 °C, 22 h, *m*-CPBA, –60 °C, 2 h (**15**: 41%, α:β ≈ 1:1, **16**: 60%, α:β ≈ 2:1).

Trisaccharide **9** and tetrasaccharide **12** both have a thioglycoside functionality, and can thus act as donors in a glycosylation reaction. Thioglycosides can typically not be activated by using simple Lewis acids like many other glycosyl donors. Stronger electrophiles are needed, and in this case iodonium ions, produced by a reagent system consisting of NIS and TMSOTf or TfOH, were used as promotor, and dibenzyl phosphate as acceptor.[47,48] This makes the reaction proceed via the typical oxocarbenium ion, which should promote the formation of the α-product. It was found, however, that there was practically no stereoselectivity in this reaction either, and both α and β anomers were formed in an approximately 1:1 ratio. The overall yield was excellent, however, and the yields of the α-anomers of **15** and **16** were 42% and 47% respectively, which was a significant improvement over the previous method (Scheme 2.8).

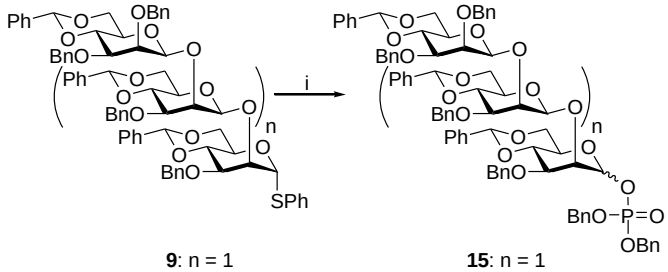

9: n = 1
12: n = 2

15: n = 1
16: n = 2

Scheme 2.8. Direct phosphorylation of **9** and **12**. Reagents and conditions: i) $HOPO(OBn)_2$, NIS, TfOH (**9**) TMSOTf (**12**), CH_2Cl_2, –20 °C → 0 °C, 1 h (**9**), –50 °C → –20 °C, 18 h (**12**), (**15**: 42%, **16**: 47%) α:β ≈ 1:1.

Once the protected trisaccharide and tetrasaccharide had been prepared, the final step that remained was deprotection, which could be performed in a single step due to the protecting group strategy selected for these molecules. Deprotection of benzylic ethers is typically performed by hydrogenation over Pd/C, and this is the strategy that was applied here as well.[49] The protected trisaccharide and tetrasaccharide were deprotected in an autoclave reactor over Pd/C under 2 bar H_2 overnight, which yielded the target trisaccharide in excellent (97%) yield, and the target tetrasaccharide in fair (67%) yield. The only purification required in this step was filtration through celite to remove the Pd/C (Scheme 2.9).

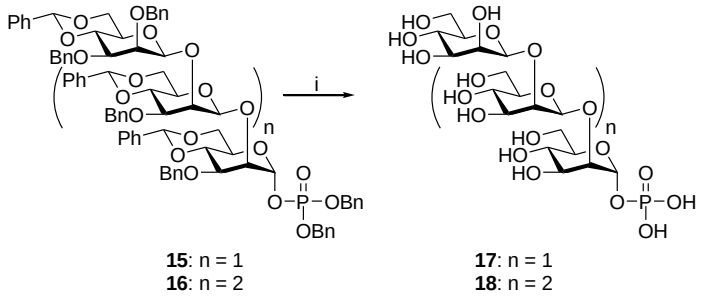

15: n = 1
16: n = 2

17: n = 1
18: n = 2

Scheme 2.9. Deprotection of trisaccharide **15** and tetrasaccharide **16**. Reagents and conditions: i) Pd/C, H_2, MeOH, 2 bar, rt, 19 h (**17**: 97%, **18**: 67%).

2.4 Characterization by NMR spectroscopy

All compounds were thoroughly characterized by NMR spectroscopy to ensure that the correct compounds were formed, and that the purity was acceptable. The compounds were analyzed by a standard set of spectra: ^{1}H, ^{13}C, and ^{31}P NMR (for the phosphorylated compounds), COSY, HSQC (both coupled and decoupled) and HMBC.

The analysis of NMR spectra of carbohydrates can often be rather complicated, as most of the protons are in rather similar chemical environments. In fact, most of the signals in the ^{1}H NMR spectra appear in the range of 3 – 4.5 ppm (excluding anomeric signals). This causes severe overlapping in the spectra, making the analysis difficult. Fortunately the spectra can be simplified by using the selective 1D-TOCSY experiment, which reduces the complexity to a monosaccharide level. The 1D-TOCSY experiment requires only one signal from a spin system to be separated from others. This signal can then be used to spread the magnetization to the entire spin system giving, in this case, separate ^{1}H spectra for each of the monosaccharide units.

Determining the anomeric configuration of monosaccharides, is often achieved by measuring the coupling constant J_{H1-H2} between the anomeric proton and the proton on C2. In mannopyranosyl units, the difference between the coupling constants in the α and β-anomers is very small though, making this method inapplicable. In addition, the chemical shifts of H3 and H5 are typically somewhat affected by the anomeric configuration. In the α anomer, the protons are closer in space to the anomeric oxygen, and will thus typically appear at higher chemical shifts than those of the corresponding β anomer, where they are located further away from the anomeric oxygen.[37] In the case of **18**, the chemical shift of H5A was found to be 3.84 ppm, and the chemical shifts of H5B, H5C and H5D were found to be 3.42, 3.38 and 3.39 ppm respectively. The chemical shift of H3A was found to be 4.00 ppm, and the chemical shifts of H3B, H3C and H3D were found to be 3.73, 3.66 and 3.62 ppm respectively. These values are in accordance with the expected values for the anomeric configurations

While the $J_{H1,H2}$ coupling constant and chemical shifts of H3 and H5 might provide some indication of the anomeric configuration, they are not universally true (as will be seen in the following chapter). NOE and ROE experiments can be used for determining the anomeric configuration, but typically it is achieved by measuring the $^1J_{C1-H1}$ between C1 and H1. A coupling constant of >170 Hz is considered indicative of α-configuration, and ~160 Hz or below is considered indicative of β.[50] Measuring the coupling constants in a coupled ^{13}C could prove to be difficult due to the anomeric signals being fairly close to each other. Because of this, coupled HSQC spectra, which show the coupling along the ^1H axis, was used instead. In the case of **18**, the coupling constants were found to be 172.1, 159.9, 162.0 and 160.6 Hz for $J_{C1A-H1A}$, $J_{C1B-H1B}$, $J_{C1C-H1C}$ and $J_{C1D-H1D}$ respectively. From these values it can be concluded that the anomeric configurations in the molecule are as reported.

The ^1H NMR spectra were analyzed in detail by employing the NMR simulation software PERCH, which by iterative quantum mechanical calculations allows for determination of accurate chemical shifts and coupling constants which, in many cases, would be difficult to obtain by conventional, manual, spectral analysis. The spectral simulation showed, that the coupling constants $J_{H2,H3}$, $J_{H3,H4}$ and $J_{H4,H5}$ were 3.0 – 3.5 Hz, 9 – 10 Hz and 9 – 10 Hz respectively which suggested that the individual monosaccharide units are in $^4C_1$ conformations as expected. Especially this information obtained from the coupling constants is important later for the conformational analysis of the molecules. Figure 2.3 shows experimental and simulated spectra of tetrasaccharide **18**.

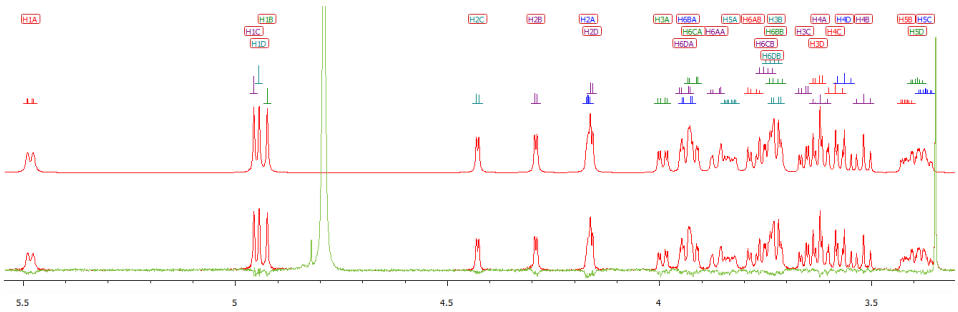

Figure 2.3. ^{1}H NMR spectrum of **18** (bottom) and simulated spectrum (top). The difference between the observed and simulated spectra is shown in green.

2.5 Conformational studies

The glycosidic bonds in oligosaccharides can rotate which allows the molecules to adopt a number of different conformations. Naturally, not all of these conformations are equally likely, as some will be more favored due to steric and electronic effects. The low-energy conformations of oligosaccharides can be important from a biological point of view, as they might affect how the oligosaccharide can interact with biological receptors.

The conformation around a glycosidic linkage can be described by two parameters: The dihedral angle defined by H1B–C1B–O1B–C2A (ϕ^{H}_{1}) and the dihedral angle defined by C1B–O1B–C2A–H2A (ψ^{H}_{1}) (Figure 2.4). The lower index indicates which glycosidic bond the angle refers to (*i.e.* 1, 2, or 3 in the molecules discussed herein), and the upper index 'H' indicates that the angle includes a hydrogen atom. As all the angles discussed herein will include a hydrogen atom, the upper indices will be omitted for clarity.

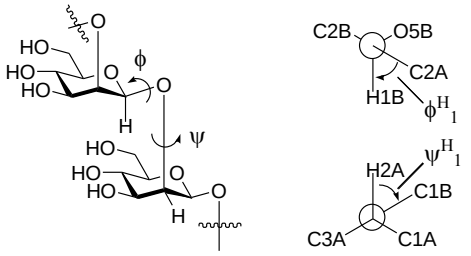

Figure 2.4. Definitions of the dihedral angles across glycosidic linkages.

The conformations of β-(1→2) linked mannosides have been studied extensively, and already in the 1970s, calculations using empirically derived force fields were used to predict that this class of compounds would adopt folded

conformations.[51] Further evidence for these types of structures has been obtained for oligomannosides capped at the reducing end by various alkyl chains, as well as for fully unprotected oligomannosides, and it has been shown that the molecules form a contorted helical structure with approximately 3 – 4 mannose residues per revolution.[13,37,52,53] The focus of this work was, thus, to determine how a charged phosphate group at the reducing end would impact the conformation. It could be reasoned, that a phosphate group could affect the conformation due to its ability to form hydrogen bonds.

When available, crystal structures obtained by X-ray crystallographic methods are valuable sources for conformational information as they, more or less, give a direct image of the molecule in question. In a crystal, the molecules are locked in a specific conformation. This, however, may or may not be of biological importance. In a solution, however, the molecules can switch between different conformations. Because of this, it is often more useful to investigate how the molecules behave in solution, instead of simply finding the conformation with the lowest energy.

The behavior of a molecule in solution over time can be investigated by performing molecular dynamics (MD) simulations. Such simulations predict the conformational changes in a molecule based on a set of physical rules. Depending on the wanted result, and the amount of computing power available, different levels of detail can be applied. Typically MD simulations are carried out by solving Newton's equations of motion for a system of particles, *i.e.* the molecule to be investigated. The other alternatives are quantum-mechanical or hybrid approaches, which are significantly more resource intensive in terms of computing power. These methods are not applied in this thesis, and will thus not be discussed in detail here.

Newton's equations of motion can typically not be solved analytically, except for trivial cases, which is why numerical methods are needed. This inevitably leads to cumulative errors, which can be minimized by using so-called force fields, *i.e.* parameter sets that describe the potentials of clusters of atoms. These force fields are derived from physical experiments or by quantum-mechanical calculations.

One important aspect to consider in molecular modeling is how to treat the solvent. Basically there are three approaches: 1) no solvent, 2) a homogeneous medium described by electrical properties (implicit solvation, continuum solvation), and 3) explicit solvation where the molecule to be investigated is

surrounded by a large number of actual solvent molecules. It is easy to understand that the last alternative is the most demanding in terms of computing power. Here, an implicit solvation model based on the relative permittivity of water (ε = 80) was used.

While the MD simulations can give good approximations of the conformational behavior of a molecule, verifying that the calculations give realistic results is recommended. In other words, the calculated result should be compared to experimentally obtained parameters. This can be done by applying NMR techniques such as NOESY (Nuclear Overhauser Effect SpectroscopY) and ROESY (Rotating-frame Overhauser Effect SpectroscopY). These experiments give information about the distance between atoms in three-dimensional space. Similar to most NMR techniques these two also give only relative information, which means that for quantitative results, a reference is needed. The intensities of NOE/ROE correlations are proportional to $1/r^6$, which means that, if the distance between to protons A and B in the molecule is known, the intensity of that correlation can be used for calculating the distance between two other protons, C and D, according to equation 1 below.

$$\frac{NOE_{AB}}{NOE_{CD}} = \frac{r_{CD}^6}{r_{AB}^6} \Rightarrow r_{CD} = \sqrt[6]{\frac{NOE_{AB} \cdot r_{AB}^6}{NOE_{CD}}} \qquad [1]$$

The distance between 1,3-diaxial protons in a chair conformation of cyclohexane is known to be approximately 2.6 Å.[54] Since the individual monosaccharide units in **17** and **18** were shown to be in $^4C_1$ conformations, this means that the correlations between 1,3-diaxial protons H1, H3 and H5 can be used to calculate other distances in the molecules.

For small molecules that tumble rapidly in solution, the NOE effect is positive, *i.e.* the intensity of a signal is increased by a nearby proton, whereas for large molecules that tumble more slowly, the NOE effect is negative which means that the signal intensity is decreased by a nearby proton. A consequence of this is, that for molecules of intermediate size, the signal intensity remains unaffected by nearby protons. What this means in practice is that no NOE effect is observed for molecules of this size. The region where this zero-crossing happens is approximately 400 – 1500 Da, which for oligosaccharides means approximately disaccharides to pentasaccharides. This is, however, also dependent on the specific molecule in question. In addition to the tumbling rate, the zero-crossing also depends on the spectrometer frequency. The tumbling rate can be somewhat affected by temperature, but changing the spectrometer frequency (*i.e.* moving to

a spectrometer with higher or lower field) is not always possible. Furthermore, NOESY can suffer from indirect NOE correlations where two protons far away from each other can appear to be close if they are both close to a third proton. These correlations are typically indistinguishable from direct NOE correlations.

ROESY, another NMR technique that gives information about distances between atoms, does not suffer as severely from the drawbacks associated with NOESY. Indirect ROE correlations are not as common as indirect NOE correlations, and if they appear, they are distinguished by having opposite phase of direct ROE correlations. Since ROESY relies on a spin-lock pulse, TOCSY artifacts can occasionally be seen in the spectra. The spin-lock pulse in the ROESY experiment is, however, much weaker than in the TOCSY experiment, and because of this, such artifacts are not very common. If the artifacts appear, however, they can still be distinguished by having opposite phase of real ROE correlations.

NOESY spectra of tetrasaccharide **18** were recorded at 5 °C on a 700 MHz instrument, which made the observed NOE signals enter the negative regime. For trisaccharide **17**, however, the NOE correlations were very weak, which is in accordance with a smaller size, and therefore slightly faster tumbling. Because of this, the conformation of **17** was investigated using ROESY instead of NOESY.

2.5.1 Conformation of trisaccharide 17

The ROESY spectrum of trisaccharide **17** showed correlations across the glycosidic bonds (H2A–H1B and H2B–H1C), which further confirmed the correct sequential assignment. The important correlations for the conformational analysis, however, were the correlations between H4A and H1C as well as between H4A and H2C (Figure 2.5). These correlations between protons from non-contiguous residues indicate that the molecule prefers a well-defined, folded, conformation. Unfortunately, not all correlations could be properly quantified due to overlapping in the spectrum and disappearance of the signals in the direct dimension due to solvent suppression. The fact that a correlation is found, however, shows that the protons are within 4 Å, which is the approximate maximum range at which NOE/ROE correlations can be seen in molecules of this size.

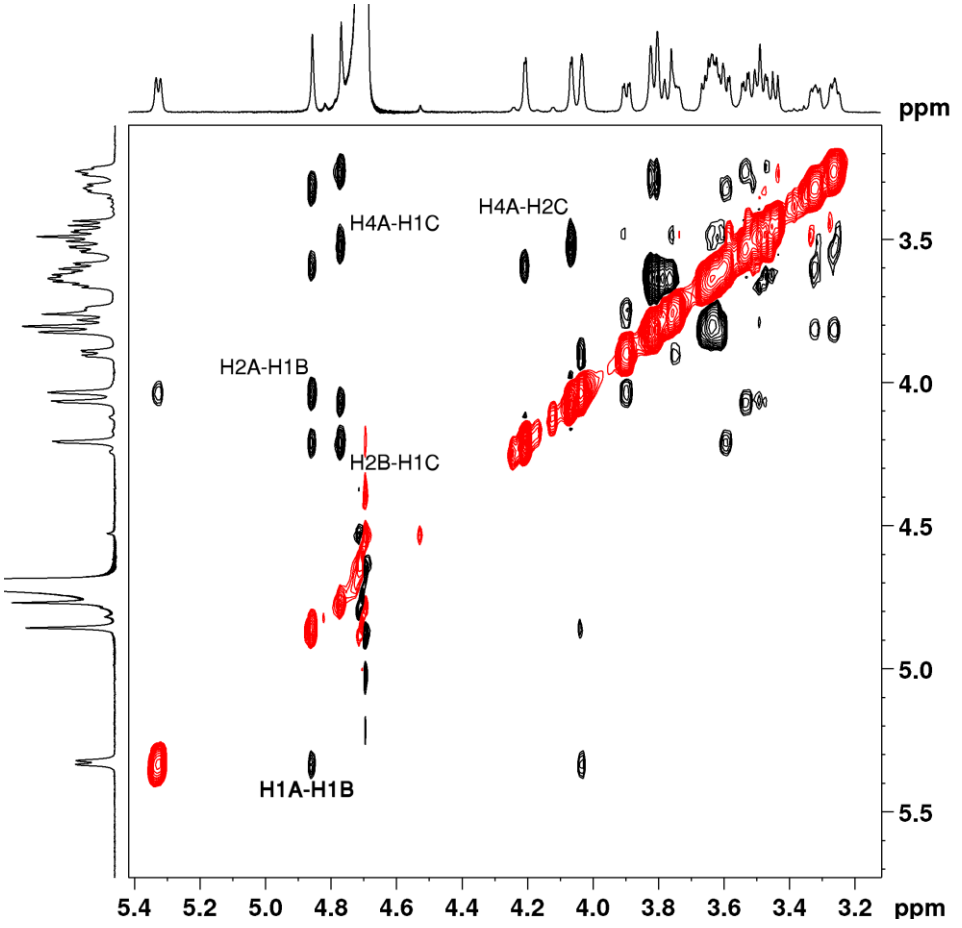

Figure 2.5. ROESY spectrum of **17** (300 ms mixing time, 500 MHz, 298 K). Key inter-residual cross peaks are labeled.

During the MD simulation, the dihedral angles ϕ and ψ, as well as key intermolecular distances in **17** were monitored. The glycosidic ϕ angles remained mostly at around 60° (Figure 2.6) in accordance with the exo-anomeric effect, which states that the O5B-C1B-O1B-O2A dihedral angle prefers a gauche conformation, which minimizes the repulsive interaction of the dipoles created by the lone pairs of the two oxygen atoms, over the typically less sterically hindered trans (antiperiplanar) conformation. The ψ angles, however, seemed to prefer eclipsed syn-type conformations, with values between 0 and 30° (Figure 2.6). While these values represent the majority of conformations over the course of the MD simulation, a number of minor conformations were observed. Although these conformations exist only for a short amount of time, they show that the molecule is not trapped in a local minimum, but able to find the global minimum energy conformation. Key intermolecular distances calculated from the MD simulation and the ROESY spectrum, are shown in Table 1, and the

most abundant conformational family, where $\phi_1 = 58°$, $\psi_1 = 41°$, $\phi_2 = 56°$ and $\psi_2 = -1°$, is represented in Figure 2.7.

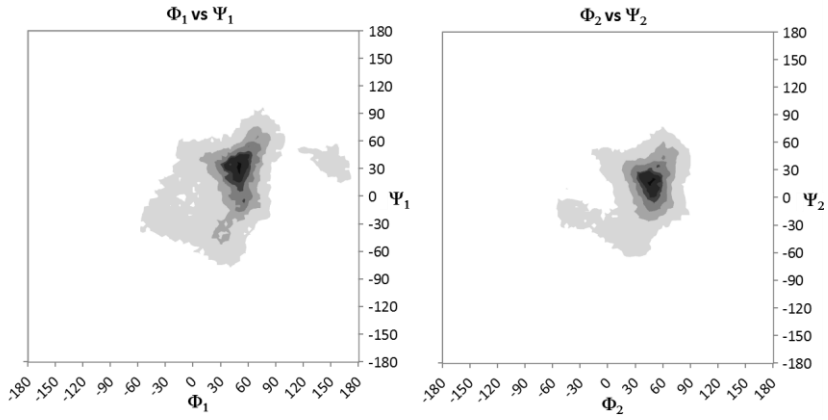

Figure 2.6. Populations of ϕ_1/ψ_1 and ϕ_2/ψ_2 angles for **17** during the MD simulation.

Table 1. Key intramolecular distances for **17** calculated from the MD simulation (weighted) and from NMR data.

Correlation	MD (Å)	NMR (Å)
H2A,H1B	2.3	2.5
H1A,H1B	2.3	2.8
H2B,H1C	2.3	2.4
H4A,H1C	2.7	2.8
H4A,H2C	2.7	n.d.

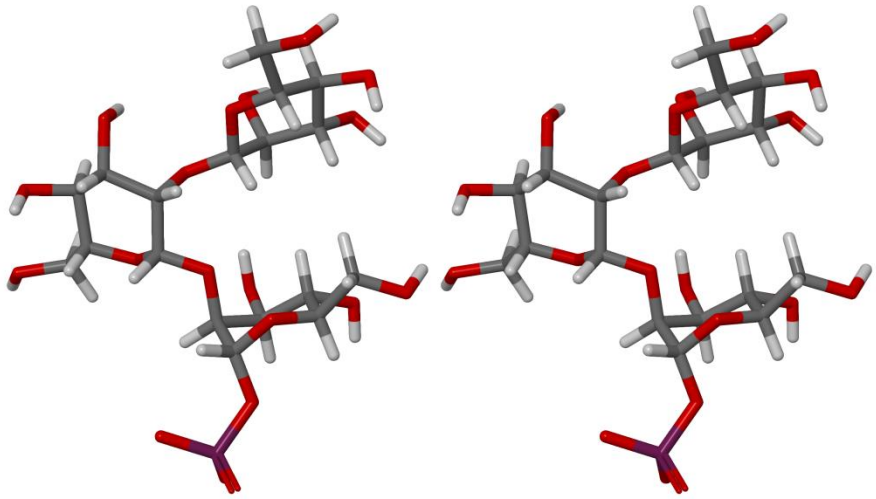

Figure 2.7. Stereoscopic representation of **17**.

2.5.2 Conformation of tetrasaccharide 18

The NOESY spectrum of **18** (Figure 2.8) shows similar trends as the ROESY spectrum of **17**. Vicinal correlations across the glycosidic linkages can be seen, but quantification is impossible due to severe overlapping of the anomeric proton signals. Correlations between non-contiguous residues separated by one mannose unit, can again be seen from H4A to H1C and H2C, as well as from H4B to H2D.

The ϕ and ψ again display similar behavior as in **17**, and all ϕ angles are in good agreement with the exo-anomeric effect. The ψ_1 and ψ_3 angles strongly prefer a syn-type geometry like in **17**, but the ψ_2 angle has a somewhat significant population in the opposite direction as well (ca. –15°), which suggests that the helical conformation can be oriented in both directions (Figure 2.9).

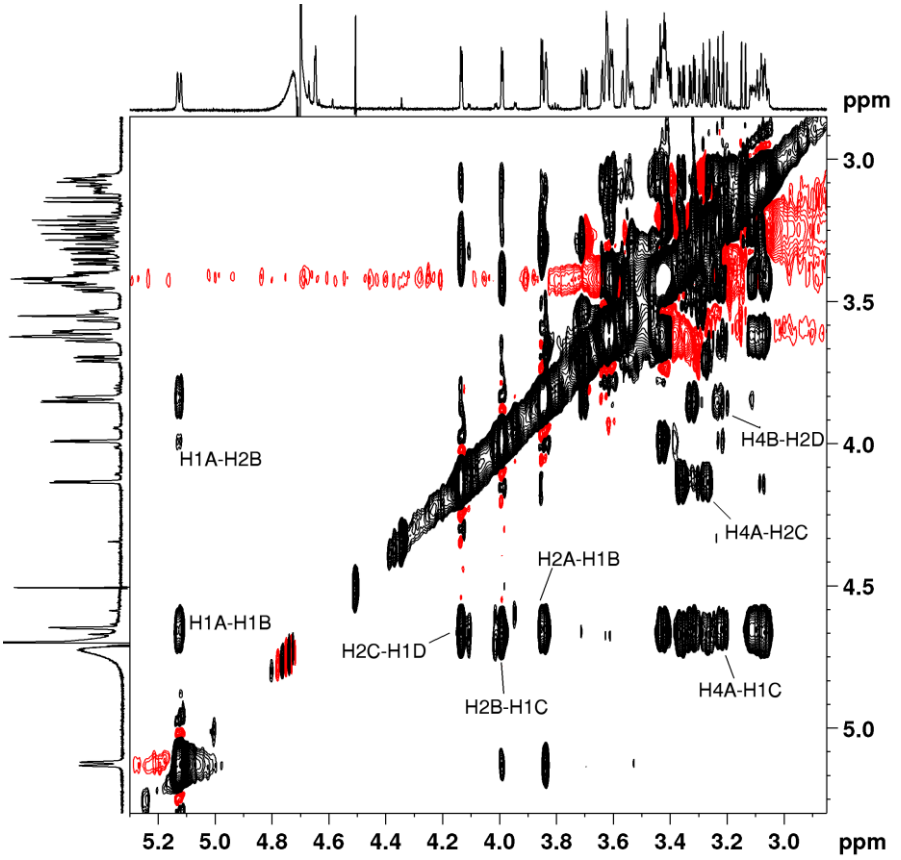

Figure 2.8. NOESY spectrum of **18** (250 ms mixing time, 700 MHz, 278 K) Key inter-residual crosspeaks are labeled.

Table 2. Key intramolecular distances for **18** calculated from the MD simulation (weighted) and from NMR data.

Correlation	MD (Å)	NMR (Å)
H1A,H2B	3.0	3.3
H1A,H1B	2.3	2.6
H4A,H1C	2.7	n.d.
H4A,H2C	2.6	3.0
H4B,H2D	2.7	3.4

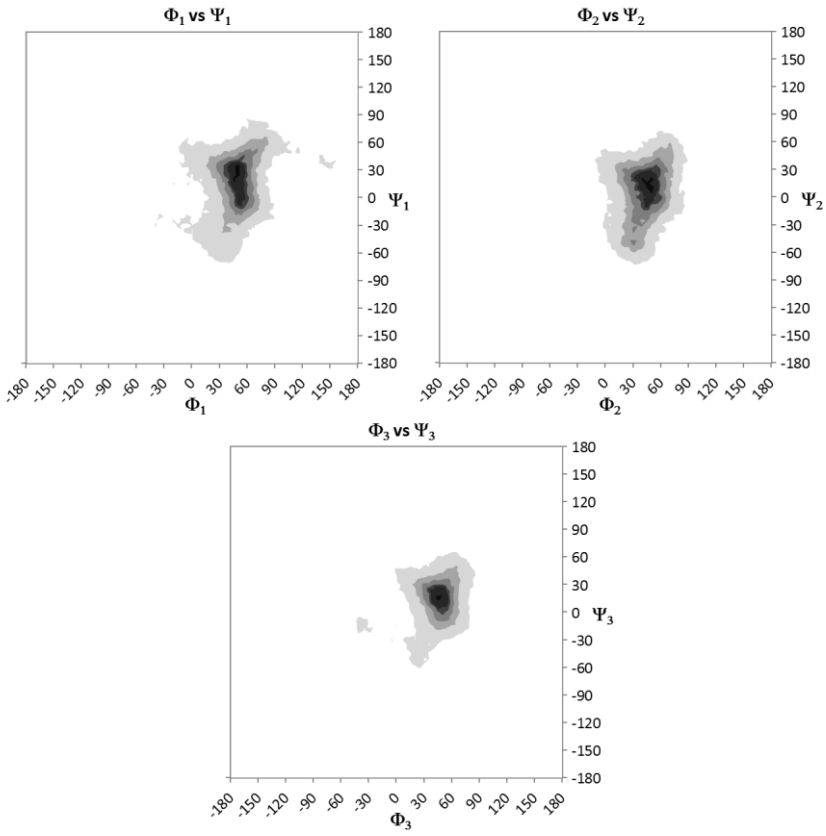

Figure 2.9. Populations of ϕ_1/ψ_1, ϕ_2/ψ_2 and ϕ_3/ψ_3 angles for **17** during the MD simulation.

The distances extracted from the MD simulation data, and those calculated from the intensities of the correlations in the NOESY spectrum are in good agreement (Table 2). This indicates that the MD simulation is a realistic representation of the behavior of the molecule. Nevertheless, for a large molecule like this, with several degrees of freedom in terms of rotation around the glycosidic bonds, a

large number of minor conformations, which differ significantly from the minimum-energy conformation, are possible. The most populated conformation, with $\phi_1 = 58°$, $\psi_1 = 17°$, $\phi_2 = 31°$, $\psi_2 = 8°$, $\phi_3 = 51°$ and $\psi_3 = 16°$ is, however, depicted in Figure 2.10.

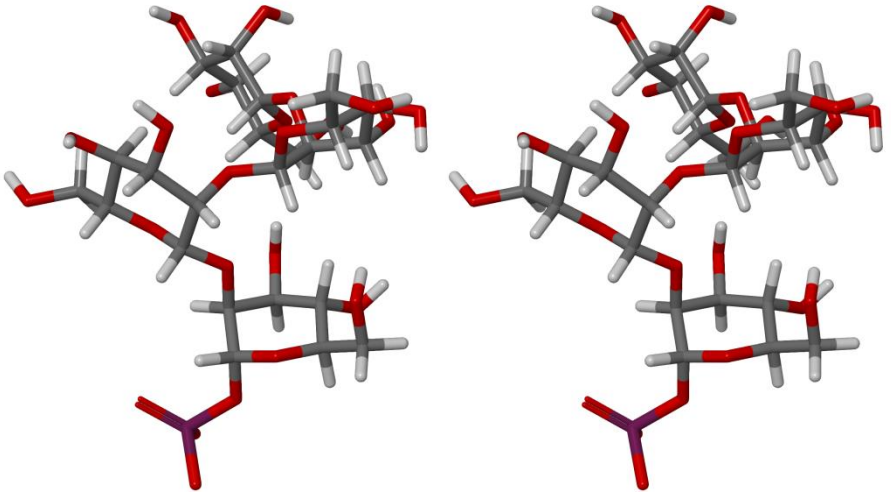

Figure 2.10. Stereoscopic representation of **18**.

In addition to the behavior of individual molecules, the interactions between the molecules and their ability to form larger, structured, complexes in solution were investigated. Theoretically, this could be possible if several molecules were to form clusters with water molecules trapped inside them, or by interactions between the charged oxygen atoms of the phosphate group and hydroxyl groups at other positions in the molecules. The first alternative is not possible to study by NMR in D_2O, due to the rapid association/dissociation and proton/deuterium exchange between the solvent and the hydroxyl groups of the molecule. This investigation, focused on the possibility of forming P–O–H–O bonds, was carried out by measuring ^{1}H and ^{31}P spectra of the molecules at different concentrations. If the interactions were sufficiently strong for the molecules to prefer larger structures, slight chemical shift perturbation should be expected of the signals involved in the interactions. No differences in the spectra recorded at different concentrations were observed for either the trisaccharide **17** or tetrasaccharide **18**, which suggests that no larger aggregates are formed. This is not very surprising due to the large excess of water molecules compared to the carbohydrate molecules. Water likely causes any eventual interactions between the phosphate group and hydroxyl groups to be dominated by interactions with water, thus negating any ability to form larger aggregates.

2.6 Conclusions

Phosphorylated β-(1→2) linked mannosides analogous to the *C. albicans* cell wall polysaccharide were prepared and thoroughly characterized by NMR spectroscopic methods. Their behavior in solution was investigated by MD simulations and NMR spectroscopic techniques, and the impact of a charged phosphate group was evaluated by comparing the obtained data to that of non-phosphorylated analogues. The conformation of trisaccharide **17** and tetrasaccharide **18** are very similar, as expected, and no significant differences in the geometries of the phosphorylated mannosides compared to the non-phosphorylated analogues were observed,[14,22,23,37,52] i.e. the phosphate group does not significantly alter the conformation of the molecules. When inspecting the three-dimensional structures of the molecules, the reason for this is evident: The phosphate group in α-position is located outside of the helical structure, and is thus not sufficiently close to interact with, for example, hydroxyl groups within the molecule.

2.7 Experimental section

2.7.1 Instrumental and general details

All reagents were purchased from Sigma-Aldrich and used without further purification. Dry solvents were either distilled (CH_2Cl_2 Over CaH_2 and toluene over Na/benzophenone) or purchased as anhydrous and stored over molecular sieves (DMF and MeOH). TLC was performed on aluminum sheets precoated with Silica gel 60 F_{254} (Merck) and the spots were visualized by UV and charred by using a 1:4 solution of H_2SO_4 in MeOH, followed by heating. Column chromatography was carried out using Silica gel 60 (0.040 – 0.060 mm, Merck).

Optical rotations were measured with a Perkin-Elmer 241 polarimeter equipped with a sodium lamp operating at 589 nm at 24 °C, unless mentioned otherwise. HRMS were recorded on a Bruker Micro Q-ToF instrument with electrospray ionisation operating in positive or negative mode.

NMR data was recorded using a Bruker Avance spectrometer operating at 600.13 MHz for ^{1}H, 150.90 MHz for ^{13}C and 242.93 MHz for ^{31}P. NOESY spectra (250 ms mixing time) of tetrasaccharide **18** were recorded using a Bruker Avance spectrometer with a proton resonance frequency of 700.17 MHz. The complete assignment of proton and carbon spectra was carried out by using a standard set of NMR experiments, ^{1}H NMR, ^{13}C NMR, ^{31}P NMR, DQF-COSY,

HSQC (both coupled and decoupled), HMBC. As previously indicated, 1D-TOCSY was utilized for simplification of the 1H NMR spectra. In addition, 2D ROESY (300 ms mixing time, for the trisaccharide) and 2D NOESY (for the tetrasaccharide) experiments were performed to assist in the conformational analysis. Chemical shifts are expressed on the δ (ppm) scale, referenced to signals from TMS (tetramethylsilane, δH = 0.0 ppm, δC = 0.0 ppm), HOD (δH = 4.79 ppm) or residual solvent signals. ^{31}P NMR spectra were referenced to an external standard, a 0.0485 M solution of PPh_3 in acetone-[d_6], (δP = –17.90 ppm). Coupling constants in the NMR data are reported only the first time they are encountered to avoid unnecessary bloating of the NMR data. Accurate chemical shifts and coupling constants were obtained with the NMR simulation software PERCH.[55]

Modelling of the molecules was carried out using Maestro,[55] and the energy minimizations and molecular dynamics simulations with Impact.[56] First, the models were drawn, simply in order to create the atoms and bonds, after which an iterative energy minimization was performed for obtaining a starting point for the dynamics simulation. The acquired models were visually inspected in order to verify that they were realistic. The minimizations and molecular dynamics simulations were performed using the OPLS_2005 force field, with a constant dielectricity 80 (the relative permeability for water). The calculations were carried out with continuum solvation with implicit solvent using a surface generalized Born model. The algorithm used for the minimization was a truncated Newton model. After the minimization, a molecular dynamics simulation was performed in 1 000 000 steps, each 2 fs to obtain a total simulation time of 2 ns. The force field, electrostatic treatment and solvation model were all the similar to those used for the minimization. The equations of motion were integrated using the r-RESPA algorithm, and the structure was stored every fifth step. From the molecular dynamics simulations, the dihedral angles between the mannose units were then recorded and plotted in order to provide a model for flexibility of the molecules. The low energy conformations obtained by molecular modelling were then compared with the NMR data of these compounds in order to verify that the simulations correctly represent the molecular structures.

2.7.2 Synthetic procedures

General procedure for β-mannosylation

To a solution of the donor (1 equiv.) in dry CH_2Cl_2 (5 mL/0.1 mmol donor) under argon at –60 °C (acetone dry ice) was added pre-activated 4 Å molecular sieves, BSP (1.20 equiv.), TTBP (1.5 equiv.) and Tf_2O (1.3 equiv.). The reaction mixture was stirred for 30 minutes until the activation was complete (confirmed by TLC), after which 1-octene (1 equiv.) was added and the reaction mixture was stirred for another 15 minutes. The reaction mixture was then cooled down to –78 °C and a solution of the acceptor (1.15 equiv.) in dry CH_2Cl_2 (1 mL/0.1 mmol) was added dropwise. The reaction mixture was stirred for 2 h, at –78 °C and, after the reaction was complete, quenched by adding triethylphosphite (3 equiv.) and stirred for 1 h. The reaction mixture was then warmed to room temperature and diluted with CH_2Cl_2 (30 mL/100 mg) and washed with a saturated solution of $NaHCO_3$ in H_2O (30 mL/100 mg). The water layer was extracted with CH_2Cl_2 (2 × 30 mL/100 mg) after which the combined organic layers were washed with brine (30 mL/100 mg) and dried over Na_2SO_4. The solvent was removed and the crude product was purified by column chromatography to yield the β-coupled product.

General procedure for hydrogenolysis of benzyl and benzylidene protecting groups

To a solution of the protected sugar molecule in dry MeOH (1.5 mL/10 mg protected sugar) was added Pd/C 10% w/w (2 equiv. by mass) and the mixture was stirred in an autoclave under H_2 (2 bar) overnight. The reaction mixture was then filtered through celite and evaporated to dryness to yield the corresponding unprotected product.

Phenyl *O*-(2,3-di-*O*-benzyl-4,6-*O*-benzylidene-β-D-mannopyranosyl)-(1→2)-*O*-(3-*O*-benzyl-4,6-*O*-benzylidene-β-D-mannopyranosyl)-(1→2)-3-*O*-benzyl-4,6-*O*-benzylidene-1-thio-α-D-mannopyranoside (9): Synthesized from donor **8** (200 mg, 0.2 mmol, 1 equiv.) and acceptor **5** (107 mg, 0.24 mmol, 1.2 equiv.) according to the general procedure for β-mannosylation. The product was purified by column chromatography (hexane:EtOAc 2:1, R_f = 0.45) to yield pure **9** as a white foam. Yield: 166 mg (62%). $[\alpha]_D^{24}$ = – 51,5° (c = 1.0, CH_2Cl_2). ^{1}H NMR (600.13 MHz, $CDCl_3$, 25 °C): δ = 7.25 – 6.90 (m, 40 H, arom. H), 5.60 (s, 1 H, 4B,6B-OC*H*Ph), 5.57 (s, 1 H, 4A,6A-OC*H*Ph), 5.51 (d, 1 H, $J_{H1A, H2A}$ = 1.4 Hz, H1A), 5.37 (s, 1 H, 4C,6C-OC*H*Ph), 5.10 (d, 1 H, $J_{H1C, H2C}$ = 0.5 Hz, H1C), 4.97 and 5.72 (each d, each 1 H, *J* = –12.5 Hz, 2A-OCH_2Ph), 4.82 and 4.77

(each d, each 1 H, J = –12.6 Hz, 3B-OCH_2Ph), 4.67 and 4.62 (each d, each 1 H, J = –12.2 Hz, 3A-OCH_2Ph), 4.65 (s, 1 H, $J_{H1B,\ H2B}$ = 0.1 Hz, H1B), 4.56 (dd, 1 H, $J_{H2A,\ H3A}$ = 3.0 Hz, H2A), 4.46 and 4.43 (each d, each 1 H, J = –11.6 Hz, 3C-OCH_2Ph), 4.45 (dd, 1 H, $J_{H2C,\ H3C}$ = 3.2 Hz, H2C), 4.36 (dd, 1 H, $J_{H2B,\ H3B}$ = 3.1 Hz, H2B) 4.34 (ddd, 1 H, $J_{H5A,\ H6Aa}$ = 4.9 Hz, $J_{H5A,\ H4A}$ = 9.2 Hz, $J_{H5A,\ H6Ab}$ = 10.2 Hz, H5A), 4.33 (dd, 1 H, $J_{H6Ca,\ H5C}$ = 4.9 Hz, $J_{H6Ca,\ H6Cb}$ = –10.5 Hz, H6Ca), 4.31 (dd, 1 H, $J_{H6Ba,\ H5B}$ = 4.8 Hz, $J_{H6Ba,\ H6Bb}$ = –10.0 Hz, H6Ba), 4.23 (dd, 1 H, $J_{H6Aa,\ H6Ab}$ = –10.3 Hz, H6Aa), 4.22 (dd, 1 H, $J_{H4C,\ H5C}$ = 9.2 Hz, $J_{H4C,\ H3C}$ = 9.9 Hz, H4C), 4.06 (dd, 1 H, $J_{H4B,\ H5B}$ = 9.3 Hz, $J_{H4B,H3B}$ = 9.8 Hz, H4B), 3.99 (dd, 1 H, $J_{H4A,\ H3A}$ = 10.1 Hz, H4A), 3.98 (dd, 1 H, H3A), 3.97 (dd, 1 H, $J_{H6Cb,\ H5C}$ = 10.1 Hz, H6Cb), 3.77 (dd, 1 H, $J_{H6Ab,\ H5A}$ = 10.2 Hz, H6Ab), 3.72 (dd, $J_{H6Bb,\ H5B}$ = 10.1 Hz, H6Bb), 3.64 (dd, 1 H, H3B), 3.55 (dd, 1 H, H3C), 3.43 (ddd, 1 H, H5C), 3.33 (ddd, 1 H, H5B) ppm.

^{13}C NMR (150.9 MHz, $CDCl_3$, 25 °C): δ = 139.4 – 126.0 (arom. C), 103.0 (C1C), 102.0 (4A,6A-O*C*HPh), 101.6 (4C,6C-O*C*HPh), 101.3 (4B,6B-O*C*HPh), 98.5 (C1B), 85.6 (C1A), 79.3 (C3C), 79.0 (C4A), 78.2 (C4B), 78.1 (C4C), 76.2 (C2B and C2C), 75.7 (C3B), 74.9 (2A-O*C*H_2Ph), 74.8 (C2A), 74.6 (C3A), 72.2 (3C-O*C*H_2Ph), 71.8 (3A-O*C*H_2Ph), 71.0 (3B-O*C*H_2Ph), 68.7 (C6C), 68.6 (C6A and C6B), 67.9 (C5C), 67.8 (C5B), 65.2 (C5A) ppm.

$^1J_{C1A,\ H1A}$ = 165.3 Hz (α), $^1J_{C1B,\ H1B}$ = 155.1 Hz (β), $^1J_{C1C,\ H1C}$ = 158.5 Hz (β)

HRMS: *m/z* calcd. for $C_{73}H_{73}O_{15}SNa$ $[M+ Na]^+$: 1243.4490; Found 1243.4502.

***O*-(2,3-Di-*O*-benzyl-4,6-*O*-benzylidene-β-D-mannopyranosyl)-(1→2)-*O*-(3-*O*-benzyl-4,6-*O*-benzylidene-β-D-mannopyranosyl)-(1→2)-3-*O*-benzyl-4,6-*O*-benzylidene-D-mannopyranose (13):** A solution of **9** (255 mg, 1 equiv.) in a 50:1 mixture of acetone:H_2O (5 mL) was cooled on an ice bath and NBS (69 mg, 2 equiv.) was added and the reaction mixture was stirred ad 0 °C for 30 min after which additional NBS (35 mg, 1 equiv.) was added and the reaction mixture was again stirred for 30 min. Additional NBS (69 mg, 2 equiv.) was added and the reaction mixture was stirred for 30 min after which solid $Na_2S_2O_3$ was added until the yellow color disappeared. The solvent was evaporated and the resulting oil was dissolved in CH_2Cl_2 (50 mL) and washed with H_2O (3 × 20 mL) and dried over Na_2SO_4 after which the solvent was removed. The crude product was purified by column chromatography (hexane:EtOAc 1:1, R_f = 0.36) to yield **13** as a white foam. Yield: 61 mg (28%). Due to the complexity of the NMR spectra caused by a mixture of anomers, the spectra were not fully assigned.

HRMS: *m/z* calcd. for $C_{67}H_{68}O_{16}Na$ $[M + Na]^+$: 1151.4405; Found 1151.4401

***O*-(2,3-Di-*O*-benzyl-4,6-*O*-benzylidene-β-D-mannopyranosyl)-(1→2)-*O*-(3-*O*-benzyl-4,6-*O*-benzylidene-β-D-mannopyranosyl)-(1→2)-3-*O*-benzyl-4,6-*O*-benzylidene-α-D-mannopyranosyl dibenzylphosphate (15): Method 1**: To a solution of **13** (40 mg, 1 equiv.) in dry CH_2Cl_2 under argon was added 1H-tetrazole (9.3 mg, 3.8 equiv.) after which the reaction mixture was cooled down to 0 °C. Dibenzyl(*N*,*N*-diisopropyl) phosphoramidite (30 µl, 2.5 equiv.) was added after which the reaction mixture was allowed to warm up to room temperature and was stirred for 22 h. The reaction mixture was then cooled to –60 °C and *m*-CPBA (20 mg, 2.5 equiv.) was added. The reaction mixture was stirred at 0 °C for 1.5 h and at room temperature for 2 h after which it was diluted with CH_2Cl_2 (40 mL), washed with a saturated solution of $Na_2S_2O_3$ (2 × 15 mL), a saturated solution of $NaHCO_3$ (2 × 15 mL) and H_2O (2 × 10 mL). The organic layer was purified by column chromatography (hexane:EtOAc 1:1, R_f = 0.57) to yield **15** as a white foam. Yield of α-product: 20 mg (41%). $[\alpha]_D^{24}$ = –51.7 ° (c = 1.0 CH_2Cl_2).

Method 2: To a solution of **9** (140 mg, 1 equiv.) in dry CH_2Cl_2 (3 mL) under argon was added $HOPO(OBn)_2$ (94.3 mg, 3 equiv.) and 4 Å molecular sieves. The reaction mixture was cooled to –20 °C and NIS (30.5 mg, 1.2 equiv.) and TfOH, (2.5 µl, 0.12 equiv.) were added. The reaction mixture was stirred at 0 °C for 1 h after which the reaction was quenched by adding pyridine (0.5 mL). The reaction mixture was diluted with CH_2Cl_2 (20 mL) and washed with a saturated solution of $Na_2S_2O_2$ (2 × 15 mL), a saturated solution of $NaHCO_3$ (2 × 15 mL) and H_2O (1 × 15 mL). The organic layer was dried over Na_2SO_4 and the solvent was removed. The crude product was purified by column chromatography (hexane:EtOAc 1:1) to yield **15** as a white foam. Yield of α-product: 64.2 mg (42 %). ^{1}H NMR (600.13 MHz, $CDCl_3$, 25 °C): δ = 7.60 – 7.00 (m, 45 H, arom. H), 5.60 (s, 1 H, 4C,6C-OC*H*Ph), 5.58 (dd, 1 H, $J_{H1A,\ H2A}$ = 1.5 Hz, $J_{H1A,\ P}$ = 6.2 Hz, H1A), 5.45 (s, 1 H, 4B,6B-OC*H*Ph), 5.33 (s, 1 H, 4A,6A-OC*H*Ph), 5.08 and 5.03 [each dd, each, 1 H, J = –11.9 Hz, $J_{CH2a,P}$ = 8.9 Hz, $J_{CH2b,P}$ = 8.2 Hz, PO(OCH_2Ph)], 5.02 and 4.99 [each dd, each, 1 H, J = –11.8 Hz, $J_{CH2a,\ P}$ = 13.6 Hz, $J_{CH2b,P}$ = 9.6 Hz, PO(OCH_2Ph)], 5.00 (d, 1 H, $J_{H1A,\ H2C}$ = 0.1 Hz, H1C), 4.91 and 4.69 (each d, each 1 H, J = –12.5 Hz, 2C-OCH_2Ph), 4.83 and 4.78 (each d, each 1 H, J = –12.5 Hz, 3B-OCH_2Ph), 4.60 and 4.56 (each d, each 1 H, J = –12.2 Hz, 3A-OCH_2Ph), 4.47 (s, 1 H, H1B), 4.45 and 4.42 (each d, each 1 H, J = –11.7 Hz, 3C-OCH_2Ph), 4.39 (dd, 1 H, $J_{H2C,\ H3C}$ = 3.2 Hz, H2C), 4.34 (dd, 1 H, $J_{H6Ca,\ H5C}$ = 4.8 Hz, $J_{H6Ca.\ H6Cb}$ = –10.4 Hz, H6Ca), 4.29 (d, 1 H, $J_{H2B,\ H3B}$ = 3.1 Hz, H2B), 4.26 (dd, 1 H, $J_{H6Ba,\ H5B}$ = 4.8 Hz, $J_{H6Ba,\ H6Bb}$ = –10.2 Hz, H6Ba), 4.22 (dd, 1 H, $J_{H4C,H5C}$ = 9.2 Hz, $J_{H4C,\ H3C}$ = 9.8 Hz, H4C), 4.15 (dd, 1 H, $J_{H2A,\ H3A}$ = 3.3 Hz,

H2A), 4.02 (dd, 1 H, $J_{H4B,\ H5B}$ = 9.4 Hz, $J_{H4B,\ H3B}$ = 9.7 Hz, H4B), 3.99 (dd, 1 H, $J_{H6Aa,\ H5A}$ = 4.9 Hz, $J_{H6Aa,\ H6Ab}$ = –10.3 Hz, H6Aa), 3.97 (dd, 1 H, $J_{H6Cb,\ H5C}$ = 10.2 Hz, H6Cb), 3.85 (dd, 1 H, $J_{H4A,H5A}$ = 9.0 Hz, $J_{H4A,H3A}$ = 10.2 Hz, H4A), 3.84 (ddd, 1 H, $J_{H5A,\ H6Ab}$ = 10.1 Hz, H5A), 3.83 (dd, 1 H, H3A), 3.67 (dd, 1 H, $J_{H6Bb,\ H5B}$ = 10.1 Hz, H6Bb), 3.60 (dd, 1 H, H6Ab), 3.59 (dd, 1 H, H3B), 3.53 (dd, 1 H, H3C), 3.41 (ddd, 1 H, H5C), 3.24 (ddd, 1 H, H5B) ppm.

^{13}C NMR (150.9 MHz, $CDCl_3$, 25 °C): δ = 139.3 – 135.2(arom. C), 103.0 (C1C), 101.9 (4B,6B-O*C*HPh), 101.6 (4A,6A-O*C*HPh), 101.3 (4C,6C-O*C*HPh), 99.6 (C1B), 95.7 ($^2J_{C1A,P}$ = 5.7 Hz, C1A), 79.2 (C3C), 78.1 (C4A, C4B, C4C), 76.2 (C2B), 76.0 (C2C), 75.5 (C3B), 74.9 (2A-O*C*H_2Ph), 73.7 ($^3J_{C2A,P}$ = 9.9 Hz, C2A), 73.5 (C3A), 72.1 (3C-O*C*H_2Ph), 71.9 (3A-O*C*H_2Ph), 71.1 (3B-O*C*H_2Ph), 69.9 [$^2J_{C,P}$ = 6.1 Hz, PO(O*C*H_2Ph)], 69.8 ($^2J_{C,P}$ = 6.1 Hz, PO(O*C*H_2Ph)], 68.7 (C6C), 68.5 (C6B), 68.3 (C6A), 67.9 (C5C), 67.6 (C5B), 65.5 (C5A) ppm.

$^1J_{C1A,\ H1A}$ = 176.4 Hz (α), $^1J_{C1B,\ H1B}$ = 156.2 Hz (β), $^1J_{C1C,\ H1C}$ = 158.6 Hz (β)

^{31}P NMR (242.9 MHz, $CDCl_3$, 25 °C): δ = –2.88 ppm.

HRMS: *m/z* calcd. for $C_{81}H_{81}O_{19}PNa$ $[M+ Na]^+$: 1411.5007; Found 1411.5025.

***O*-(β-D-Mannopyranosyl)-(1→2)-*O*-(β-D-mannopyranosyl)-(1→2)-α-D-mannopyranosylphosphate (17):** Prepared from **15** (22 mg, 0.016 mmol) according to the general procedure for hydrogenolysis of benzyl and benzylidene protecting group. Filtration through celite with water yielded the product as a colorless oil. Yield: 9 mg (97%). Purity: 95 %, with an impurity possibly consisting of a molecule where the phosphate group has been replaced by methyl. $[\alpha]_D^{24}$ = – 13 ° (c = 1.0 H_2O). ^{1}H NMR (600.13 MHz, $CDCl_3$, 25 °C): δ = 5.45 (dd, 1 H, $J_{H1A,\ H2A}$ = 1.5 Hz, $J_{H1A,\ P}$ = 7.9 Hz, H1A), 4.96 (d, 1 H, $J_{H1B,\ H2B}$ = 0.2 Hz, H1B), 4.88 (d, 1 H, $J_{H1C,\ H2C}$ = 0.5 Hz, H1C), 4.32 (dd, 1 H, $J_{H2B,\ H3B}$ = 3.4 Hz, H2B), 4.18 (dd, 1 H, $J_{H2C,\ H3C}$ = 3.3 Hz, H2C), 4.15 (dd, $J_{H2A,\ H3A}$ = 3.1 Hz, H2A), 4.01 (dd, $J_{H3A,\ H4A}$ = 9.8 Hz, H3A), 3.93 (each dd, each 1 H, $J_{H6Ba,\ H5B}$ = 2.1 Hz, $J_{H6Ba,\ H6Bb}$ = –11.9 Hz, $J_{H6Ca,\ H5C}$ = 2.2 Hz, $J_{H6Ca,\ H6Cb}$ = –12.6 Hz, H6Ba and H6Ca), 3.89 (dd, 1 H, $J_{H6Aa,\ H5A}$ = 2.1 Hz, $J_{H6Aa,\ H6Ab}$ = –12.4 Hz, H6Aa), 3.86 (ddd, $J_{H5A,\ H6Ab}$ = 5.6 Hz, $J_{H5A,\ H4A}$ = 9.8 Hz, H5A), 3.77 (dd, 1 H, H6Ab), 3.75 (dd, 1 H, $J_{H6Bb,\ H5B}$ = 5.9 Hz, H6Bb), 3.73 (dd, 1 H, $J_{H6Cb,\ H5C}$ = 6.4 Hz, H6Cb), 3.70 (dd, 1 H, $J_{H3B,\ H4B}$ = 9.9 Hz, H3B), 3.64 (dd, 1 H, $J_{H3C,\ H4C}$ = 9.9 Hz, H3C), 3.61 (each dd, each 1 H, $J_{H4B,\ H5B}$ = 9.7 Hz, H4A and H4B), 3.57 (dd, 1 H, $J_{H4C,\ H5C}$ = 9.8 Hz, H4C), 3.43 (ddd, 1 H, H5B), 3.37 (ddd, 1 H, H5C) ppm.

^{13}C NMR (150.9 MHz, $CDCl_3$, 25 °C): δ = 101.0 (C1C), 98.9 (C1B), 92.9 ($^2J_{C\text{-}1,P}$ = 4.0 Hz, C1A), 78.8 ($^3J_{C2A,P}$ = 6.6 Hz, C2A), 78.7 (C2B), 76.2 (C5C), 76.1 (C5B), 72.9 (C5A), 72.8 (C3C), 72.1 (C3B), 70.4 (C2C), 69.1 (C3A), 67.3 and 66.9 (C4A and C4B), 66.7 (C4C), 61.0 (C6C), 60.7 (C6B), 60.5 (C6A) ppm.

$^1J_{C1A,H1A}$ = 173.4 Hz (α), $^1J_{C1B,H1B}$ = 160.5 Hz (β), $^1J_{C1C,H1C}$ = 160.3 Hz (β)

Phenyl *O*-(2-*O*-(4-methoxybenzyl)-3-*O*-benzyl-4,6-*O*-benzylidene-β-D-mannopyranosyl)-(1→2)-3-*O*-benzyl-4,6-*O*-benzylidene-1-thio-α-D-mannopyranoside (10): Prepared from donor **6** (500 mg 0.876 mmol) and acceptor **5** (455 mg 1.01 mmol) according to the general procedure for β-mannosylation. The crude product was purified by column chromatography (hexane:EtOAc 2:1, R_f = 0.45) Yield: 455 mg (57%). $[\alpha]_D^{24}$ = – 52,5 ° (c = 1.0 CH_2Cl_2). ^{1}H NMR (600.13 MHz, $CDCl_3$, 25 °C): δ = 7.75 – 7.20 (m, 29 H, arom. H), 5.59 (s, 1 H, 4B,6B-OC*H*Ph), 5.52 (s, 1 H, 4A,6A-OC*H*Ph), 5.50 (d, 1 H, $J_{H1A,H2A}$ = 1.5 Hz, H1A), 4.97 and 4.89 (each d, each 1 H, *J* = –11.8, 2B-OC*H*$_2$Ph), 4.80 and 4.75 (each d, each 1 H, *J* = –12.1 Hz, 3A-OC*H*$_2$Ph), 4.67 and 4.59 (each d, each 1 H, *J* = –12.5 Hz, 3B-OC*H*$_2$Ph), 4.61 (d, 1 H, $J_{H1B,H2B}$ = 0.9 Hz, H1B), 4.51 (dd, 1 H, $J_{H2A,H3A}$ = 3.2 Hz, H2A), 4.33 (ddd, 1 H, $J_{H5A,H6Aa}$ = 4.8 Hz, $J_{H5A,H4A}$ = 9.5 Hz, $J_{H5A,HA6b}$ = 10.2 Hz, H5A), 4.24 (each dd, each 1 H, $J_{H6Aa,H6Ab}$ = –10.2 Hz, $J_{H6Ba,H5B}$ = 4.9 Hz, $J_{H6Ba,H6Bb}$ = –10.4 Hz, H6Aa and H6Ba), 4.23 (dd, 1 H, $J_{H4B,H5B}$ = 9.3 Hz, $J_{H4B,H3B}$ = 9.9 Hz, H4B), 4.17 (dd, 1 H, $J_{H4A,H3A}$ = 10.0 Hz, H4A), 3.98 (dd, 1 H, H3A), 3.96 (dd, 1 H, $J_{H2B,H3B}$ = 3.2 Hz, H2B), 3.82 (dd, $J_{H6Bb,H5B}$ = 10.1 Hz, H6Bb), 3.79 (dd, 1 H, H6Ab), 3.73 (s, 3 H, OC*H*$_3$), 3.57 (dd, 1 H, H3B), 3.29 (ddd, 1 H, H5A) ppm.

^{13}C NMR (150.9 MHz, $CDCl_3$, 25 °C): δ = 159.1 – 113.5 (arom. C), 101.7 (4A,6A-O*C*HPh), 101.4 (4B,6B-O*C*HPh), 99.8 (C1B), 86.4 (C1A), 78.7 (C4A), 78.4 (C4B), 77.5 (C3B), 76.1 (C2A), 75.4 (C2B), 74.3 (C3A), 74.2 (2B-O*C*H$_2$Ph), 72.2 (3B-O*C*H$_2$Ph), 71.4 (3A-O*C*H$_2$Ph), 68.6 (C6A), 68.5 (C6B), 67.7 (C5B), 65.4 (C5A), 55.2 (O*C*H$_3$) ppm.

$^1J_{C1A,H1A}$ = 166.9 Hz (α), $^1J_{C1B,H1B}$ = 154.2 Hz (β).

HRMS: *m/z* calcd. for $C_{54}H_{54}O_{11}SNa$ $[M + Na]^+$: 933.3285; Found 933.3228; *m/z* calcd. for $C_{54}H_{58}O_{11}SN$ $[M + NH_4]^+$: 928.3731; Found 928.3634.

Phenyl *O*-(3-*O*-benzyl-4,6-*O*-benzylidene-β-D-mannopyranosyl)-(1→2)-3-*O*-benzyl-4,6-*O*-benzylidene-1-thio-α-D-mannopyranoside (11): A solution of **10** (200 mg, 1 equiv.) in CH_2Cl_2 (3 mL) was cooled down to 0 °C and a suspension of DDQ (74 mg, 1.5 equiv.) in H_2O (3 mL) was added dropwise. The

reaction mixture was stirred for 1 h at 0 °C after which it was diluted with CH_2Cl_2 (25 mL) and washed with of a saturated solution of $NaHCO_3$ (2 × 25 mL). The water layer was extracted with CH_2Cl_2 (2 × 25 mL), dried over Na_2SO_4 and evaporated to dryness. The crude product was purified by column chromatography (hexane:EtOAc 2:1) to yield the **11** as a white foam. Yield: 153 mg (88%). NMR spectra are in accordance with those published previously.[39]

Phenyl *O*-(2,3-di-*O*-benzyl-4,6-*O*-benzylidene-β-D-mannopyranosyl)-(1→2)-*O*-(3-*O*-benzyl-4,6-*O*-benzylidene-β-D-mannopyranosyl)-(1→2)-*O*-(3-*O*-benzyl-4,6-*O*-benzylidene-β-D-mannopyranosyl)-(1→2)-3-*O*-benzyl-4,6-*O*-benzylidene-1-thio-α-D-mannopyranoside (12): Prepared from donor **8** (290 mg, 0.33 mmol) and acceptor **11** (300 mg, 0.38 mmol) according to the general procedure for β-mannosylation. The crude product was purified by column chromatography (hexane:EtOAc 2:1, R_f = 0.50) to afford pure **12**. Yield: 182 mg (35 %). $[\alpha]_D^{24}$ = – 62,0 ° (c = 1.0 CH_2Cl_2). ^{1}H NMR (600.13 MHz, $CDCl_3$, 25 °C): δ = 7.75 – 7.00 (m, 50 H, arom. H), 5.57 (s, 1 H, 4C,6C-OC*H*Ph), 5.54 (s, 1 H, 4A,6A-OC*H*Ph), 5.49 (d, 1 H, $J_{H1A,\ H2A}$ = 1.3 Hz, H1A), 5.44 (s, 1 H, 4B,6B-OC*H*Ph), 5.40 (s, 1 H, 4D,6D-OC*H*Ph), 5.27 (s, 1 H, H1C), 5.07 (d, 1 H, $J_{H1D,\ H2D}$ = 0.1 Hz, H1D), 5.00 and 4.84 (each d, each 1 H, *J* = –12.6 Hz, 2D-OC*H*$_2$Ph), 4.70 (s, 2 H, 3A-OC*H*$_2$Ph), 4.68 and 4.61 (each d, each 1 H, *J* = –12.4 Hz, 3B-OC*H*$_2$Ph), 4.68 (s, 1 H, H1B), 4.62 and 4.44 (each d, each 1 H, *J* = –11.9 Hz, 3C-OC*H*$_2$Ph), 4.54 (d, 1 H, $J_{H2C,\ H3C}$ = 3.0 Hz, H2C), 4.53 (dd, 1 H, $J_{H2A,\ H3A}$ = 3.1 Hz, H2A), 4.50 and 4.40 (each d, each 1 H, *J* = –11.8 Hz, 3D-OC*H*$_2$Ph), 4.48 (d, 1 H, $J_{H2B,\ H3B}$ = 3.4 Hz, H2B), 4.41 (dd, 1 H, $J_{H2D,\ H3D}$ = 3.3 Hz, H2D), 4.33 (dd and ddd, each 1 H, $J_{H6Ca,\ H5C}$ = 4.8 Hz, $J_{H6Ca,\ H6Cb}$ = –10.2 Hz, $J_{H5A,\ H6Aa}$ = 5.0 Hz, $J_{H5A,\ H4A}$ = 9.2 Hz, $J_{H5A,\ H6Ab}$ = 10.2 Hz, H6Ca and H5A), 4.31 (dd, 1 H, $J_{H6Ba,\ H5B}$ = 4.8 Hz, $J_{H6Ba,\ H6Bb}$ = –10.3 Hz, H6Ba), 4.23 (dd, 1 H, $J_{H6Aa,\ H6Ab}$ = –10.3 Hz, H6Aa), 4.19 (each dd, each 1 H, $J_{H4D,\ H5D}$ = 9.3 Hz, $J_{H4D,\ H3D}$ = 9.9 Hz, $J_{H6Da,\ H5D}$ = 4.9 Hz, $J_{H6Da,\ H6Db}$ = –10.3 Hz, H4D and H6Da), 4.06 (dd, 1 H, $J_{H4C,\ H5C}$ = 9.3 Hz, $J_{H4C,\ H3C}$ = 9.8 Hz, H4C), 3.99 (dd, 1 H, $J_{H4A,\ H3A}$ = 9.9 Hz, H4A), 3.97 (dd, 1 H, H3A), 4.93 (dd, 1 H, $J_{H4B,\ H5B}$ = 9.3 Hz, $J_{H4B,\ H3B}$ = 9.8 Hz, H4B), 3.87 (dd, 1 H, $J_{H6Db,\ H5D}$ = 10.1 Hz, H6Db), 3.78 (dd, 1 H, $J_{H6Cb,\ H5C}$ = 10.1 Hz, H6Cb), 3.77 (dd, 1 H, $J_{H6Bb,\ H5B}$ = 10.1 Hz, H6Bb), 3.74 (dd, 1 H, H6Ab), 3.66 (dd, 1 H, H3B), 3.54 (dd, 1 H, H3D), 3.53 (dd, 1 H, H3C), 3.43 (ddd, 1 H, H5C), 3.36 (ddd, 1 H, H5B), 3.32 (ddd, 1 H, H5D) ppm.

^{13}C NMR (150.9 MHz, $CDCl_3$, 25 °C): δ = 139.4 – 126.1 (arom. C), 103.4 (C1D), 102.1 (4A,6A-O*C*HPh), 102.0 (4B,6B-O*C*HPh), 101.8 (C1C), 101.5 (4D,6D-O*C*HPh), 101.3 (4C,6C-O*C*HPh), 99.1 (C1B), 85.7 (C1A), 79.1 (C4A), 79.0 (C3D), 78.4 (C4B), 78.3 (C4D), 78.2 (C4C), 77.0 (C3C), 76.3 (C3B), 76.1

(C2C), 76.0 (C2D), 75.5 (C2A), 74.7 (2D-O*C*H$_2$Ph), 74.5 (C3A), 74.0 (C2B), 72.2 (3D-O*C*H$_2$Ph), 72.1 (3A-O*C*H$_2$Ph), 71.3 (3B-O*C*H$_2$Ph), 70.9 (3C-O*C*H$_2$Ph), 68.8 (C6D), 68.7 (C6C and C-6B), 68.6 (C6A), 68.0 (C5C), 67.9 (C5B), 67.5 (C5D), 65.2 (C5A) ppm.

$^1J_{C1A,\ H1A}$ = 168.2 Hz (α), $^1J_{C1B,\ H1B}$ = 154.5 Hz (β), $^1J_{C1C,\ H1C}$ = 161.0 Hz (β), $^1J_{C1D,\ H1D}$ = 159.6 Hz (β)

HRMS: *m/z* calcd. for $C_{93}H_{92}O_{20}SNa$ $[M + Na]^+$: 1583.5800; Found 1583.5812.

***O*-(2,3-Di-*O*-benzyl-4,6-*O*-benzylidene-β-D-mannopyranosyl)-(1→2)-*O*-(3-*O*-benzyl-4,6-*O*-benzylidene-β-D-mannopyranosyl)-(1→2)-*O*-(3-*O*-benzyl-4,6-*O*-benzylidene-β-D-mannopyranosyl)-(1→2)-3-*O*-benzyl-4,6-*O*-benzylidene-D-mannopyranose (14):** A solution of **12** (250 mg, 1 equiv.) in a 6:1 mixture of acetone:H_2O (5 mL) was cooled on an ice bath and NBS (60 mg, 2 equiv.) was added and the reaction mixture was stirred for 30 min. Additional NBS (30 mg, 1 equiv.) was added and the reaction mixture was again stirred for 30 min after which additional NBS (30 mg, 1 equiv.) was added and the reaction mixture was stirred for 30 min. The reaction was quenched by adding solid $Na_2S_2O_3$ until the yellow color had disappeared. The solvent was evaporated and the residue was dissolved in CH_2Cl_2 (50 mL) and washed with H_2O (2 × 20 mL). The organic layer was dried over Na_2SO_4 and evaporated to dryness. The crude product was purified by column chromatography (hexane:EtOAc 1:1, R_f = 0.38) to yield **14** as a white foam. Yield (62 mg (28%). Due to the complexity of the NMR spectra, caused by a mixture of anomers, the spectra were not fully assigned.

HRMS: *m/z* calcd. for $C_{87}H_{92}O_{21}N$ $[M + NH_4]^+$: 1486.6162; Found 1486.6174.

***O*-(2,3-Di-*O*-benzyl-4,6-*O*-benzylidene-β-D-mannopyranosyl)-(1→2)-*O*-(3-*O*-benzyl-4,6-*O*-benzylidene-β-D-mannopyranosyl)-(1→2)-*O*-(3-*O*-benzyl-4,6-*O*-benzylidene-β-D-mannopyranosyl)-(1→2)-3-*O*-benzyl-4,6-*O*-benzylidene-α-D-mannopyranosyl dibenzylphosphate (16): Method 1**: To a solution of **14** (35 mg, 1 equiv.) in dry CH_2Cl_2 (4 mL) under argon was added 1*H*-tetrazole (6.3 mg, 3.8 equiv.) after which the solution was cooled down to 0 °C. Dibenzyl(*N*,*N*-diisopropyl) phosphoramidite (22 µl, 2.5 equiv.) was added and the reaction mixture was allowed to return to room temperature and was stirred for 2 h. The reaction mixture was cooled down to –60 °C and *m*-CPBA (13.5 mg, 3.8 equiv.) was added and the mixture was stirred at 0 °C for 1 h and then at room temperature for 1 h. The reaction mixture was diluted with CH_2Cl_2 (50 mL) and washed with a saturated solution of $Na_2S_2O_3$ (2 × 15 mL), a saturated solution of $NaHCO_3$ (2 × 15 mL) and H_2O (2 × 10 mL) after which the organic

layer was dried over Na_sSO_4 and concentrated to dryness. The crude product was purified by column chromatography (hexane:EtOAc 1:1, R_f = 0.57) Yield of α-product: 25 mg (60 %). $[\alpha]_D^{24}$ = – 61,2 ° (c = 1.0 CH_2Cl_2).

Method 2: To a solution of **12** (50 mg, 1 equiv.) in dry CH_2Cl_2 (3 mL) under argon was added $PO(OBn)_2Oh$ (26.7 mg, 3 equiv.) and 4 Å molecular sieves. The reaction mixture was cooled down to –50 °C and NIS (8.6 mg, 1.2 equiv.) and TMSOTf (0.7 µl, 0.12 equiv.) were added. The reaction mixture was stirred at –50 °C for 1 h and warmed to –20 °C and stirred for 3.5 h after which additional TMSOTf (0.7 µl, 0.12 equiv.) was added and the reaction mixture was stirred for another 17.5 h at –20 °C. The reaction was quenched by adding pyridine (0.5 mL) after which the reaction mixture was diluted with CH_2Cl_2 (20 mL) and washed with a saturated solution of $Na_2S_2O_3$ (2 × 15 mL), a saturated solution of $NaHCO_3$ (2 × 15 mL) and H_2O (15 mL). The organic layer was dried over Na_2SO_4 and evaporated to dryness. The crude product was purified by column chromatography (hexane:EtOAc 1:1). Yield of α-product: 26 mg (47%). ^{1}H NMR (600.13 MHz, $CDCl_3$, 25 °C): δ =7.75 – 6.75 (m, 55 H, arom. H), 5.59 (dd, 1 H, $J_{H1A,\ H2A}$ = 1.7 Hz, $J_{H1A,\ P}$ = 6.3 Hz, H1A), 5.56 (s, 1 H, 4D,6D-OC*H*Ph), 5.43 (s, 1 H, 4A,6A-OC*H*Ph), 5.41 (each s, each 1 H, 4B,6B-OC*H*Ph and 4C,6C-OC*H*Ph), 5.14 (d, 1 H, $J_{H1C,\ H2C}$ = 0.1 Hz, H1C), 5.08 and 5.02 [each dd, each, 1 H, J = –11.9 Hz, $J_{CH2a,P}$ = 9.1 Hz, $J_{CH2b,P}$ = 8.2 Hz, PO(OCH_2Ph)], 5.06 (d, 1 H, $J_{H1C,\ H2C}$ = 0.1 Hz, H1C), 5.01 and 4.98 [each dd, each, 1 H, J = –11.6 Hz, $J_{CH2a,P}$ = 8.4 Hz, $J_{CH2b,P}$ = 9.9 Hz, PO(OCH_2Ph)], 4.99 and 4.83 (each d, each 1 H, J = –12.5 Hz, 2D-OCH_2Ph), 4.70 and 4.63 (each d, each 1 H, J = –12.4 Hz, 3B-OCH_2Ph), 4.65 and 4.50 (each d, each 1 H, J = –11.9 Hz, 3C-OCH_2Ph), 4.64 and 4.61 (each d, each 1 H, J = –12.4 Hz, 3A-OCH_2Ph), 4.51 (dd, $J_{H2C,\ H3C}$ = 3.1 Hz, H2C), 4.50 (d, 1 H, $J_{H1B,\ H2B}$ = 0.1 Hz, H1B), 4.50 and 4.38 (each d, each 1 H, J = –11.8 Hz, 3D-OCH_2Ph), 4.42 (dd, 1 H, $J_{H2B,\ H3B}$ = 3.3 Hz, H2B), 4.39 (dd, 1 H, $J_{H2D,\ H3D}$ = 3.1 Hz, H2D), 4.36 (dd, 1 H, $J_{H6Ca,\ H5C}$ = 4.6 Hz, $J_{H6Ca,\ H6Cb}$ = –10.2 Hz, H6Ca), 4.26 (dd, 1 H, $J_{H6Ba,\ H5B}$ = 4.8 Hz, $J_{H6Ba,\ H6Bb}$ = –10.2 Hz, H6Ba), 4.18 (dd, 1 H, $J_{H4D,\ H5D}$ = 9.2 Hz, $J_{H4D,\ H3D}$ = 9.9 Hz, H4D), 4.17 (dd, 1 H, $J_{H6Da,\ H5D}$ = 4.8 Hz, $J_{H6Da,\ H6Db}$ = –10.4 Hz, H6Da), 4.10 (dd, 1 H, $J_{H2A,\ H3A}$ = 3.7 Hz, H2A), 4.07 (dd, 1 H, $J_{H4C,\ H5C}$ = 9.3 Hz, $J_{H4C,\ H3C}$ = 9.8 Hz, H4C), 3.98 (dd, 1 H, $J_{H6Aa,\ H5A}$ = 4.9 Hz, $J_{H6Aa,\ H6Ab}$ = –10.3 Hz, H6Aa), 3.88 (dd, 1 H, $J_{H4B,\ H5B}$ = 9.4 Hz, $J_{H4B,\ H3B}$ = 9.9 Hz, H4B), 3.85 (each dd, each 1 H, $J_{H6Db,\ H5D}$ = 10.1 Hz, $J_{H4A,\ H5A}$ = 9.5 Hz, $J_{H4A,\ H3A}$ = 10.1 Hz, H6Db and H4A), 3.82 (ddd, 1 H, $J_{H5A,\ H6Ab}$ = 10.3 Hz, H5A), 3.80 (dd, 1 H, H3A), 3.78 (dd, 1 H, $J_{H6Cb,\ H5C}$ = 10.0 Hz, H6Cb), 3.73 (dd, 1 H, $J_{H6Bb,\ H5B}$ = 10.0 Hz, H6Bb), 3.62 (dd, 1 H,

H3B), 3.55 (dd, 1 H, H6Ab), 3.53 (dd, 1 H, H3C), 3.52 (dd, 1 H, H3D), 3.40 (ddd, 1 H, H5C), 3.31 (ddd, 1 H, H5D), 3.27 (ddd, 1 H, H5B) ppm.

^{13}C NMR (150.9 MHz, $CDCl_3$, 25 °C): δ = 139.4 – 126.1 (arom. C), 103.3 (C1D), 101.9 (C1C, 4A,6A-O*C*HPh, 4B,6B-O*C*HPh), 101.5 (4C,6C-O*C*HPh), 101.2 (4D,6D-O*C*HPh), 100.5 (C1B), 95.7 ($^2J_{C\text{-}1,\ P}$ = 4.9 Hz, C1A), 79.0 (C3D), 78.4 (C4D), 78.3 (C4B), 71.2 (C4A and C4C), 76.8 (C3C), 76.2 (C2C), 76.1 (C3B), 75.9 (C2D), 74.9 ($^3J_{C\text{-}2,\ P}$ = 9.3 Hz, C2A), 74.6 (2D-O*C*H_2Ph), 74.2 (C2B), 73.4 (C3A), 72.2 (3D-O*C*H_2Ph), 72.1 (3A-O*C*H_2Ph), 71.3 (3B-O*C*H_2Ph), 70.8 (3C-O*C*H_2Ph), 69.9 [$^2J_{C,P}$ = 5.4 Hz, $^2J_{C,P}$ = 5.8 Hz, PO(O*C*$_a$$H_2$Ph), PO(O*C*$_b$$H_2$Ph)], 68.8 (C6C), 68.7 (C6D), 68.6 (C6B), 68.3 (C6A), 68.0 (C5C), 67.7 (C5B), 67.5 (C5D), 65.5 (C5A) ppm.

$^1J_{C1A,\ H1A}$ = 175.3 Hz (α), $^1J_{C1B,\ H1B}$ = 155.5 Hz (β), $^1J_{C1C,\ H1C}$ = 161.0 Hz (β), $^1J_{C1D,\ H1D}$ = 158.9 Hz (β).

^{31}P NMR (242.9 MHz, $CDCl_3$, 25 °C): δ = –2.92 ppm.

HRMS: *m/z* calcd. for $C_{101}H_{101}O_{24}PNa$ $[M + Na]^+$: 1751.6318; Found 1751.6341.

***O*-(β-d-Mannopyranosyl)-(1→2)-*O*-(β-D-mannopyranosyl)-(1→2)-*O*-(β-D-mannopyranosyl)-(1→2)-α-D-mannopyranosylphosphate (18):** Prepared from **16** (25 mg, 0.014 mmol) according to the general procedure for hydrogenolysis of benzyl and benzylidene protecting groups. Filtration through celite with a 4:1 mixture of MeOH:H_2O yielded the product as a colorless oil. Yield: 7 mg (67%). Purity: 95 %, with an impurity possibly consisting of a molecule where the phosphate group has been replaced by methyl. $[\alpha]_D^{24}$ = – 15 ° (c = 1.0 H_2O). ^{1}H NMR (600.13 MHz, $CDCl_3$, 25 °C): δ = 5.47 (dd, 1 H, $J_{H1A,\ H2A}$ = 1.4 Hz, $J_{H1A,\ P}$ = 7.8 Hz, H1A), 4.96 (s, 1 H, H1C), 4.94 (s, 1 H, H1D), 4.93 (s, 1 H, H1B), 4.43 (d, 1 H, $J_{H2C,\ H3C}$ = 3.4 Hz, H2C), 4.29 (d, 1 H, $J_{H2B,\ H3B}$ = 3.4 Hz, H2B), 4.16 (dd and d, each 1 H, $J_{H2A,\ H3A}$ = 3.2 Hz, $J_{H2D,\ H3D}$ = 3.4 Hz, H2A and H2D), 4.00 (dd, 1 H, $J_{H3A,\ H4A}$ = 9.9 Hz, H3A), 3.94 (dd, 1 H, $J_{H6Ba,\ H5B}$ = 3.1 Hz, $J_{H6Ba,\ H6Bb}$ = –12.3 Hz, H6Ba), 3.93 (dd, 1 H, $J_{H6Da,\ H5D}$ = 2.5 Hz, $J_{H6Da,\ H\text{-}6Db}$= –12.3 Hz, H6Da), 3.92 (dd, 1 H, $J_{H6Ca,\ H5C}$ = 2.1 Hz, $J_{H6Ca,\ H6Cb}$ = –11.9 Hz, H6Ca), 3.87 (dd, 1 H, $J_{H6Aa,\ H5A}$ = 2.0 Hz, $J_{H6Aa,\ H6Ab}$ = –12.3 Hz, H6Aa), 3.84 (ddd, 1 H, $J_{H5A,\ H6Ab}$ = 4.6 Hz, $J_{H5A,\ H4A}$ = 10.1 Hz, H5A), 3.77 (dd, 1 H, H6Ab), 3.75 (dd, 1 H, $J_{H6Cb,\ H5C}$ = 6.3 Hz, H6Cb), 3.73 (dd and dd, each 1 H, $J_{H6Cb,\ H5C}$ = 6.5 Hz, $J_{H3B,\ H4B}$ = 8.9 Hz, H6Db and H3B), 3.72 (dd, 1 H, $J_{H6Bb,\ H5B}$ = 5.5 Hz, H6Bb), 3.66 (dd, 1 H, $J_{H3C,\ H4C}$ = 10.0 Hz, H3C), 3.62 (dd, 1 H, $J_{H3D,\ H4D}$ = 9.5 Hz, H3D), 3.60 (dd 1 H, H4A), 3.58 (dd, 1 H, $J_{H4C,\ H5C}$ = 9.2 Hz, H4C), 3.56 (dd, 1 H, $J_{H4D,\ H5D}$ = 9.7

Hz, H4D), 3.51 (dd, 1 H, $J_{H4B,\ H5B}$ = 10.2 Hz, H4B), 3.42 (ddd, 1 H, H5B), 3.39 (ddd, 1 H, H5D), 3.38 (ddd, 1 H, H5C) ppm.

^{13}C NMR (150.9 MHz, $CDCl_3$, 25 °C): δ = 101.2 (C1C), 101.0 (C1D), 99.1 (C1B), 93.2 ($^2J_{C1A,\ P}$ = 5.8 Hz, C1A), 79.4 (C2B), 78.9 ($^3J_{C2A,\ P}$ = 8.4 Hz, C2A), 78.4 (C2C), 76.2 (C5C, C5D), 75.9 (C5B), 72.9 (C5A, C3D), 72.1 (C3C), 71.8 (C3B), 70.4 (C2D), 68.9 (C3A), 67.3 (C4A), 67.1 (C4B), 66.9, 66.7 (C4C, C4D), 61.1 (C6B), 60.7 (C6D), 60.5 (C6C), 60.3 (C6A) ppm.

$^1J_{C1A,\ H1A}$ = 172.1 Hz (α), $^1J_{C1B,\ H1B}$ = 159.9 Hz (β), $^1J_{C1C,\ H1C}$ = 162.0 Hz (β), $^1J_{C1D,\ H1D}$ = 160.6 Hz (β)

^{31}P NMR (242.9 MHz, $CDCl_3$, 25 °C): δ = 1.6 ppm.

HRMS: *m/z* calcd. for $C_{24}H_{42}O_{24}P$ $[M - H]^-$: 745.1804; Found 745.1835.

2.8 References

1. Sardi, J. C. O., Scorzoni, L., Bernardi, T., Fusco-Almeida, A. M. & Mendes Giannini, M. J. S. Candida species: Current epidemiology, pathogenicity, biofilm formation, natural antifungal products and new therapeutic options. *Journal of Medical Microbiology* **62,** 10–24 (2013).

2. Samaranayake, Y. H. & Samaranayake, L. P. Experimental Oral Candidiasis in Animal Models. *Clin. Microbiol. Rev.* **14,** 398–429 (2001).

3. Shoham, S. & Marr, K. A. Invasive fungal infections in solid organ transplant recipients. 639–655 (2012).

4. Pfaller, M. A. & Diekema, D. J. Epidemiology of invasive candidiasis: A persistent public health problem. *Clin. Microbiol. Rev.* **20,** 133–163 (2007).

5. Maschmeyer, G., Haas, A. & Cornely, O. A. Invasive aspergillosis: epidemiology, diagnosis and management in immunocompromised patients. *Drugs* **67,** 1567–1601 (2007).

6. Shibata, N., Suzuki, A., Kobayashi, H. & Okawa, Y. Chemical structure of the cell-wall mannan of Candida albicans serotype A and its difference in yeast and hyphal forms. *Biochem. J.* **404,** 365–372 (2007).

7. Johnson, M. A. & Bundle, D. R. Designing a new antifungal glycoconjugate vaccine. *Chem. Soc. Rev.* **42,** 4327–44 (2013).

8. Masuoka, J. Surface Glycans of Candida albicans and Other Pathogenic Fungi : Physiological Roles, Clinical Uses, and Experimental Challenges. *Clin. Microbiol. Rev.* **17,** 281–310 (2004).

9. Scaringi, L. *et al.* Cell wall components of Candida albicans as immunomodulators: induction of natural killer and macrophage-mediated peritoneal cell cytotoxicity in mice by mannoprotein and glucan fractions. *J. Gen. Microbiol.* **134,** 1265–74 (1988).

10. Ponton, J., Omaetxebarria, M. J., Elguezabal, N., Alvarez, M. & Moragues, M. D. Immunoreactivity of the fungal cell wall. *Med.Mycol.* **39 Suppl 1,** 101–110 (2001).

11. Han, Y., Kanbe, T., Cherniak, R. & Cutler, J. E. Biochemical characterization of Candida albicans epitopes that can elicit protective and nonprotective antibodies. *Infect. Immun.* **65,** 4100–4107 (1997).

12. Bundle, D. R., Nycholat, C. M., Costello, C., Rennie, R. & Lipinski, T.

Design of a Candida albicans disaccharide conjugate vaccine by reverse engineering a protective monoclonal antibody. *ACS Chem. Biol.* **7,** 1754–1763 (2012).

13. Nitz, M., Ling, C. C., Otter, A., Cutler, J. E. & Bundle, D. R. The unique solution structure and immunochemistry of the Candida albicans β-1,2-mannopyranan cell wall antigens. *J. Biol. Chem.* **277,** 3440–3446 (2002).

14. Dang, A.-T., Johnson, M. A. & Bundle, D. R. Synthesis of a Candida albicans tetrasaccharide spanning the β1,2-mannan phosphodiester α-mannan junction. *Org. Biomol. Chem.* **10,** 8348 (2012).

15. Lipinski, T., Kitov, P. I., Szpacenko, A., Paszkiewicz, E. & Bundle, D. R. Synthesis and immunogenicity of a glycopolymer conjugate. *Bioconjugate Chem.* **22,** 274–281 (2011).

16. Wu, X. & Bundle, D. R. Synthesis of glycoconjugate vaccines for Candida albicans using novel linker methodology. *J. Org. Chem.* **70,** 7381–7388 (2005).

17. Xin, H., Dziadek, S., Bundle, D. R. & Cutler, J. E. Synthetic glycopeptide vaccines combining β-mannan and peptide epitopes induce protection against candidiasis. *Proc. Natl. Acad. Sci. U. S. A.* **105,** 13526–13531 (2008).

18. Gridley, J. J. & Osborn, H. M. I. Recent advances in the construction of β-D-mannose and β-D-mannosamine linkages. *J. Chem. Soc. Perkin Trans. 1* 1471–1491 (2000).

19. Pozsgay, V. in *Carbohydrates in Chemistry and Biology* (eds. Ernst, B., Hart, G. W. & Sinay, P.) 319–344 (WILEY-VCH Verlag, GmbH & Co. KGaA, 2000).

20. El Ashry, E., Rashed, N. & Ibrahim, E. Strategies of Synthetic Methodologies for Constructing β-Mannosidic Linkage. *Curr. Org. Synth.* **2,** 175–213 (2005).

21. Lichtenthaler, F. W., Schneider-adams, T. & Immel, S. Practical Synthesis of β-D-Xyl-(1-2)-β-D-Man-(1-4)-α-D-Glc-OMe, a Trisaccharide Component of the Hyriopsis schlegelii Glycosphingolipid. *J. Org. Chem.* **59,** 6735–6738 (1994).

22. Nycholat, C. M. & Bundle, D. R. Synthesis of monodeoxy and mono-O-methyl congeners of methyl β-d-mannopyranosyl-(1→2)-β-d-mannopyranoside for epitope mapping of anti-Candida albicans antibodies. *Carbohydr. Res.* **344,** 555–569 (2009).

23. Costello, C. & Bundle, D. R. Synthesis of three trisaccharide congeners to investigate frame shifting of β1,2-mannan homo-oligomers in an antibody binding site. *Carbohydr. Res.* **357,** 7–15 (2012).

24. Dang, A.-T., Johnson, M. A. & Bundle, D. R. Synthesis of a Candida albicans tetrasaccharide spanning the β1,2-mannan phosphodiester α-mannan junction. *Org. Biomol. Chem.* **10,** 8348–60 (2012).

25. Omura, K. & Swern, D. Oxidation of alcohols by 'activated' dimethyl sulfoxide. a preparative, steric and mechanistic study. *Tetrahedron* **34,** 1651–1660 (1978).

26. Romero, J. A. C., Tabacco, S. A. & Woerpel, K. A. Stereochemical reversal of nucleophilic substitution reactions depending upon substituent: Reactions of heteroatom-substituted six-membered-ring oxocarbenium ions through pseudoaxial conformers. *J. Am. Chem. Soc.* **122,** 168–169 (2000).

27. Ayala, L. *et al.* Stereochemistry of Nucleophilic Substitution Reactions Depending upon Substituent: Evidence for Electrostatic Stabilization of Pseudoaxial Conformers of Oxocarbenium Ions by Heteroatom Substituents. *J. Am. Chem. Soc.* **125,** 15521–15528 (2003).

28. Heuckendorff, M., Bendix, J., Pedersen, C. M. & Bols, M. β-Selective Mannosylation With a 4,6-Silylene-Tethered Thiomannosyl Donor. *Org. Lett.* **16,** 1116–1119 (2014).

29. Huang, M., Retailleau, P., Bohé, L. & Crich, D. Cation clock permits distinction between the mechanisms of α- And β-O- and β-C-glycosylation in the mannopyranose series: Evidence for the existence of a mannopyranosyl oxocarbenium ion. *J. Am. Chem. Soc.* **134,** 14746–14749 (2012).

30. Crich, D. in *Glycochemistry: Principles, Synthesis and Applications* (eds. Wang, P. G. & Bertozzi, C. R.) 53–76 (Marcel Dekker, Inc, 2001).

31. Crich, D. & Sun, S. Direct chemical synthesis of β-mannopyranosides and other glycosides via glycosyl triflates. *Tetrahedron* **54,** 8321–8348 (1998).

32. Crich, D. & Sun, S. Formation of β-Mannopyranosides of Primary Alcohols Using the Sulfoxide Method. *J. Org. Chem.* **61,** 4506–4507 (1996).

33. Crich, D. & Sun, S. Direct Formation of β-Mannopyranosides and Other Hindered Glycosides from Thioglycosides. *J. Am. Chem. Soc.* **120,** 435–436 (1998).

34. Crich, D. & Sun, S. Direct Synthesis of -Mannopyranosides by the Sulfoxide Method. *J. Org. Chem.* **62,** 1198–1199 (1997).

35. Crich, D. & Smith, M. 1-Benzenesulfinyl Piperidine/Trifluoromethanesulfonic Anhydride: A Potent Combination of Shelf-Stable Reagents for the Low-Temperature Conversion of Thioglycosides to Glycosyl Triflates and for the Formation of Diverse Glycosidic Linkages. *J. Am. Chem. Soc.* **123,** 9015–9020 (2001).

36. Crich, D., Li, W. & Li, H. Direct chemical synthesis of the β-mannans: Linear and block syntheses of the alternating β-(1→3)-β-(1→4)-mannan common to Rhodotorula glutinis, Rhodotorula mucilaginosa, and Leptospira biflexa. *J. Am. Chem. Soc.* **126,** 15081–15086 (2004).

37. Ekholm, F. S., Sinkkonen, J. & Leino, R. Fully deprotected β-(1→2)-mannotetraose forms a contorted α-helix in solution: convergent synthesis and conformational characterization by NMR and DFT. *New J. Chem.* **34,** 667 (2010).

38. Ekholm, F. S. *et al.* Studies related to Norway spruce galactoglucomannans: Chemical synthesis, conformation analysis, NMR spectroscopic characterization, and molecular recognition of model compounds. *Chem. - A Eur. J.* **18,** 14392–14405 (2012).

39. Poláková, M., Roslund, M. U., Ekholm, F. S., Saloranta, T. & Leino, R. Synthesis of β-(1→2)-linked oligomannosides. *Eur. J. Org. Chem.* 870–888 (2009).

40. Crich, D. & Chandrasekera, N. S. Mechanism of 4,6-O-benzylidene-directed β-mannosylation as determined by α-deuterium kinetic isotope effects. *Angew. Chem., Int. Ed.* **43,** 5386–5389 (2004).

41. Hosoya, T., Kosma, P. & Rosenau, T. Contact ion pairs and solvent-separated ion pairs from d-mannopyranosyl and d-glucopyranosyl triflates. *Carbohydr. Res.* **401,** 127–131 (2015).

42. Oshitari, T. & Kobayashi, S. Preparation of 2-O-(3-O-carbamoyl-α-d-mannopyranosyl)-l-gulopyranose: Synthetic study on the sugar moiety of antitumor antibiotic bleomycin. *Tetrahedron Lett.* **36,** 1089–1092 (1995).

43. Zemplén, G. & Kunz, A. Studien über Amygdalin, IV: Synthese des natürlichen l-Amygdalins. *Ber. Dtsch. Chem. Ges.* **57,** 1357–1359 (1924).

44. Crich, D., Banerjee, A. & Yao, Q. Direct Chemical Synthesis of the β-D-Mannans : The β-(1→2) and β-(1→4) Series. *J. Am. Chem. Soc.* **126,** 14930–14934 (2004).

45. Hanessian, S. The reaction of O-benzylidene sugars with N-bromosuccinimide. *Carbohydr. Res.* **2,** 86–88 (1966).

46. Hanessian, S. & Plessas, N. R. The Reaction of O-Benzylidene Sugars with N-Bromosuccinimide. II. Scope and Synthetic Utility in the Methyl 4,6-O-Benzylidenehexopyranoside Series. *J. Org. Chem.* **34,** 1035–1044 (1969).

47. Veeneman, G. H., van Leeuwen, S. H. & van Boom, J. H. Iodonium ion promoted reactions at the anomeric centre. II An efficient thioglycoside mediated approach toward the formation of 1,2-trans linked glycosides and glycosidic esters. *Tetrahedron Lett.* **31,** 1331–1334 (1990).

48. Konradsson, P., Udodong, U. E. & Fraser-Reid, B. Iodonium promoted reactions of disarmed thioglycosides. *Tetrahedron Lett.* **31,** 4313–4316 (1990).

49. Kocienski, P. J. *Protecting Groups*. (Georg Thieme Verlag, 2005).

50. Podlasek, C. A., Wu, J., Stripe, W. A., Bondo, P. B. & Serianni, A. S. [13C]Enriched Methyl Aldopyranosides: Structural Interpretations of 13C-1H Spin-Coupling Constants and 1H Chemical Shifts. *J. Am. Chem. Soc.* **117,** 8635–8644 (1995).

51. Rees, D. A. & Scott, W. E. Polysaccharide conformation. Part VI. Computer model-building for linear and branched pyranoglycans. Correlations with biological function. Preliminary assessment of inter-residue forces in aqueous solution. Further interpretation of optical rotation in t. *J. Chem. Soc. B Phys. Org.* 469 (1971).

52. Nitz, M. & Bundle, D. R. in *NMR Spectroscopy of Glycoconjugates* (eds. Jiménez-Barbero, J. & Peters, T.) 145–184 (WILEY-VCH Verlag, GmbH & Co. KGaA, 2003).

53. Crich, D. *et al.* Direct synthesis of β-mannans. A hexameric [→3)-β-D-man-(1→4)-β-D-man-(1]3 subunit of the antigenic polysaccharides from Leptospira biflexa and the octameric (1→2)-linked β-D-mannan of the Candida albicans phospholipomannan. X-ray crystal structure of a p. *J. Am. Chem. Soc.* **123,** 5826–5828 (2001).

54. Corey, E. & Feiner, N. Computer-assisted synthetic analysis. A rapid computer method for the semiquantitative assignment of conformation of six-membered ring systems. 2. Assessment of. *J. Org. Chem.* **45,** 765–780 (1980).

55. Maestro, version 8.5, Schrödinger, LCC,New York, NY (USA). (2008).

56. Impact, version 5.0, Schrödinger, LCC,New York, NY (USA). (2005).

3 Multivalency: Introducing the second dimension

Multivalency, as a concept, has received considerable attention ever since its discovery in nature in the 1970s. Typically, a multivalent structure bearing several binding epitopes will interact more strongly with biological receptors than the free binding epitope. Exploiting this property, potentially allows the preparation of more efficient compounds for battling infections and other diseases.

Allergies are an increasing problem in the civilized world, with up to 30% of the population in some regions suffering from nasal allergies. The options for treating the underlying pathological reason for allergies are limited, with specific allergen immunotherapy being the only viable alternative. The method does, however, suffer from drawbacks such as long treatment times and high likelihood of allergic side reactions.

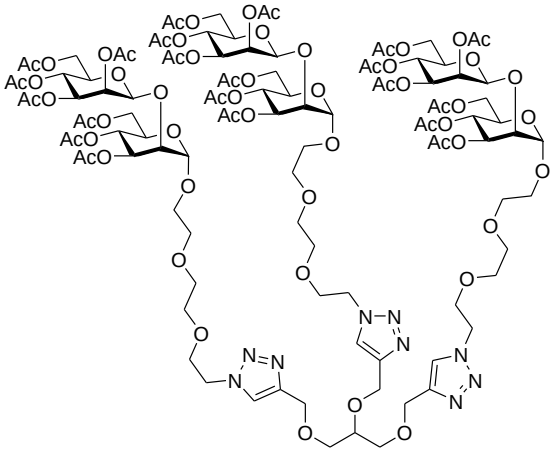

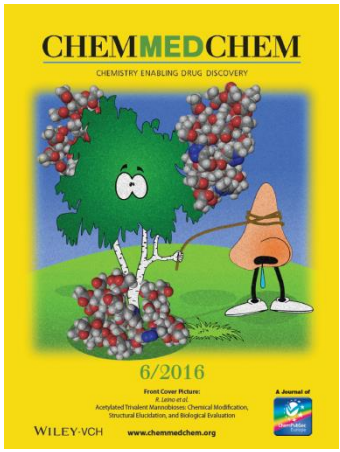

In this chapter, the synthesis and thorough characterization of acetylated trivalent mannobiose glycoclusters will be discussed, together with the potential of using such compounds as adjuvants in specific allergen immunotherapy. Optimally, adjuvants could be used to significantly decrease the amount of time and allergens required for the treatment.

The work in this chapter is based on the previously published paper: **Acetylated Trivalent Mannobioses – Chemical Modification, Structural Elucidation and Biological Evaluation,** J. Rahkila, R. Panchadhayee, A. Ardá, J. Jiménez-Barbero, J. Savolainen, R. Leino, *ChemMedChem*, **2016,** *11*, 562 – 574. Cover picture copyright Wiley-VCH Verlag GmbH & Co. KGaA. Reproduced with permission.

3.1 Introduction

Multivalency, as a term, is used to describe a molecule where several similar structures are attached to a backbone, thus creating a single molecule that can interact with several targets at once. The binding affinity of a multivalent compound to a receptor, is typically significantly higher than that of the free ligand, with respect to the number of binding epitopes present.[1] This phenomenon has become known as the "cluster effect".

Natural glycoproteins, glycolipids, and various polysaccharides make up the glycocalyx, a thick layer that covers all cells. This layer expresses multiple carbohydrate constituents of the same type, and therefore multivalent interactions between carbohydrates and lectins, *i.e.* carbohydrate-binding proteins, are of utmost importance in biological systems. The first steps of the infection process for many pathogens, such as bacteria, viruses, fungi etc. are typically mediated by protein-carbohydrate interactions.[2–6]

The multivalent nature of interactions between carbohydrates and proteins has been known since the 1970s,[7–9] and considerable attention has since then been focused on imitating nature with, synthetic, multivalent structures.[10,11] As mentioned previously, the interactions between carbohydrates and proteins are typically very weak. Since its discovery, multivalency has become a popular solution for overcoming this problem, and over the years a large number of impressive structures based on protein, polymer, dendrimer, cyclodextrin, fullerene, gold nanoparticle, quantum dot and similar scaffolds have been prepared and new technologies are constantly emerging.[6,10,12]

Synthetic, multivalent, carbohydrate structures can be used to prevent pathogens from being able to interact with host cells, therefore preventing an infection. Combining the concept of multivalency with immunogenic carbohydrate structures could, potentially, result in vaccines that imitate the way antigens are presented on a cell surface, without having to use dead or attenuated cells.[13]

The following sections will provide a brief overview of allergic inflammation, and the potential use of immunostimulatory mannose-derived glycoclusters as adjuvants for specific allergen immunotherapy.

3.2 Allergy

The immune system is highly complex, and immune responses are complicated cascades of reactions. Therefore, a detailed description would be beyond the scope of this thesis, and only the most relevant aspects will be discussed.

Immune responses are regulated by a class of cells called helper T cells (T_H), which are further be divided into T_H1, T_H2 and regulatory T_{reg} cells based on their cytokine secretion profiles. T_H1 cells produce interferon-γ (IFN-γ),[14] which activates macrophages, a type of white blood cells that digest foreign particles, cells and in general anything that does not display certain proteins which identify a particle as part of a healthy body. T_H2 cells secrete interleukins (IL) 4, 5 and 13, which are involved in allergic inflammations via activation of immune cells, such as basophils, mast cells and eosinophils.[15–17] The cytokines secreted by T_H1 and T_H2 cells suppress the effects of the reciprocal phenotype.[18] Finally, T_{reg} cells regulate the responses of both T_H1 and T_H2 cells by secreting IL-10, which suppresses both of these responses.[19,20]

The secretion of IL-4 by T_H2 cells stimulates B cells to differentiate into plasma cells, which produce immunoglobulins (Ig), i.e. antibodies. Specifically, the antibody IgE stimulates basophils and mast cells to secrete small-molecular local mediators, such as histamine and serotonin.[16,21] These molecules signal the body, that it has encountered a potentially harmful substance that it needs to dispose of. The response is mucus secretion, coughing, sneezing and diarrhea to expel the detected antigens. IL-5, also secreted by T_H2 cells, causes local inflammation via activation of eosinophils, which release reactive oxygen species, lipid mediators such as prostaglandin, and a number of cytokines, including additional IL-5 and tumor necrosis factor alpha (TNF-α).[21–23] The role of the inflammatory response is to kill any harmful pathogens, but unfortunately it can also cause damage to native cells.

When our bodies encounter foreign substances, the immune response can, in a very simplified scenario, be dominated by either T_H1 or T_H2 type responses. If a particle of pollen enters our body the typical immune response is via the T_H1 pathway, which causes secretion of IgG4 that targets the antigens on the pollen particle and marks it for disposal. This results in the particle being removed from the body in a harmless way. If, for some reason, the response is dominated by the T_H2 pathway, however, the aforementioned inflammatory response takes place.[20] This condition, where the immune system is dominated by T_H2 responses, and reacts excessively towards a normally harmless substance, such

as a pollen particle is known as allergy, or more formally as type I hypersensitivity disorder.

There are many ways of treating the symptoms of allergies, such as antihistamines which act to negate the effects of histamine, decongestants that reduce mucus secretion, steroids that reduce the inflammation and various other pharmaceuticals that counteract the chemicals responsible for the allergic response. There are, however, limited ways of treating the actual cause of allergies. Specific immunotherapy (SIT), also known as hyposensibilization, is a treatment form where patients suffering from allergies are treated with repeated injections (sublingual and oral treatments are emerging but these are typically not as effective)[24] of increasing amounts of a specific allergen. This treatment acts to normalize the response dominated by T_H2 cells, towards a protective T_H1 and T_{reg} response. SIT is a potent method for treating allergies, and typically offers long-lasting protection. This is currently the only way of treating the underlying pathological immune response associated with allergies. The traditional method suffers from some drawbacks, though, as the treatment times are very long, up to five years, and the required amount of allergen is substantial, which can cause severe allergic reactions and in the worst case even anaphylaxis. Because of the long time required for the treatment, and large number of injections, allergic patients might be forced to wait for more than a year to start the treatment. Furthermore, the allergic reactions often cause people to abort the treatment.[25]

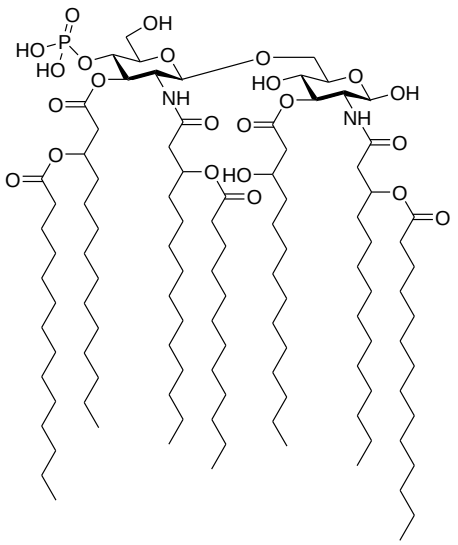

Figure 3.1. General structure of MPLA used as an adjuvant in allergy treatments.

There is, however, great potential in modifying the immune response to optimize the SIT procedure. Adjuvants, are compounds that are added to vaccines to modify how the immune system interacts with the active ingredient in the vaccine. Similar methods can be applied to SIT as well by choosing adjuvants that stimulate the immune system to respond in a desired manner.[26] Because the T_H1 and T_H2 responses suppress the response of the reciprocal phenotype, downregulation of T_H2 or upregulation of T_H1 type responses will yield similar effects.

In human vaccines, the most commonly used adjuvants are based on inorganic salts such as aluminum phosphate and aluminum hydroxide, commonly known as alum. These adjuvants promote T_H2 type responses, causing increased IgE production which, while preferable for conventional vaccines, makes them unsuitable for adjuvants in allergy treatments. There are, however, promising candidates specifically for adjuvants in SIT. Single-strand DNA fragments (CpG-ODN), which act as Toll-like receptor (TLR) 9 agonists have shown promise in phase I and II clinical studies.[27–31] Monophosphoryl lipid A (MPLA, Figure 3.1), a non-toxic modification of the endotoxin lipid A, is a TLR-4 agonist, that has been shown to reduce the number of require injections in SIT from more than 50 to four. MPLA is marketed under the name Pollinex Quattro™ which is a preparation approved for human use.[25]

While both CpG-ODN and MPLA are good candidates for adjuvants, they could encounter some difficulties due to the nature of the compounds. CPG-ODN is essentially a gene, which could result in people regarding it with some reluctance. The MPLA used as an adjuvant is derived from a toxic bacterial compound, and while it has been found to be safe for human use it might, due to its origin, be misinterpreted as harmful.

The β-(1→2) linked mannosides discussed in the previous chapter are known to be immunogenic, and stimulate antibody production. This property could, potentially, be exploited for SIT. A very specific class of compounds that contain such structures will be discussed in the following section.

3.3 Trivalent acetylated mannobiose as adjuvants in specific allergen immunotherapy

In previous work, a large number of carbohydrate-based structures have been screened for potential adjuvant activity in hyposensibilization treatments. The compounds ranged from natural fungal polysaccharides, to synthetic

oligosaccharides and oligovalent structures (Figure 3.2).[32–35] The cytokine responses induced by the compounds were investigated in an *in vitro* model, using peripheral blood mononuclear cell (PBMC) samples from atopic subjects.

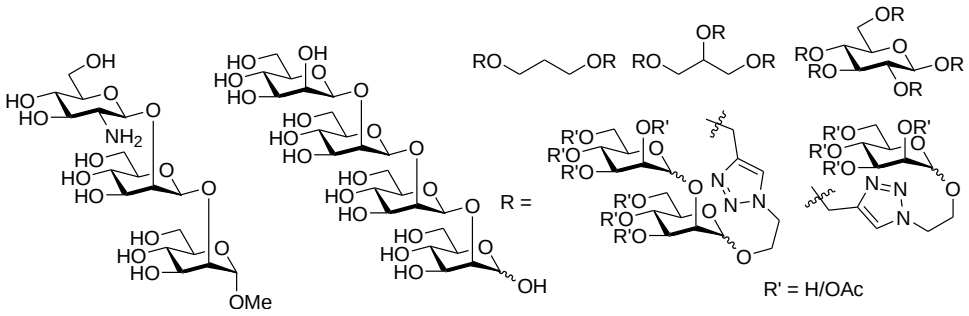

Figure 3.2. Examples of molecules screened in previous studies.

The broad screening allowed for determination of key structural elements, and one particular compound showed great promise as a potential adjuvant in allergen immunotherapy due to its unusually strong ability to induce IL-10 and IFN-γ production, compared to the other compounds. In this particular compound, depicted in Figure 3.3, the key structural elements were identified as 1) β-(1→2) linked mannobiose, 2) α-linkage to the spacer fragment, 3) trivalency and 4) complete acetylation. From here on this compound will be referred to as **1**.

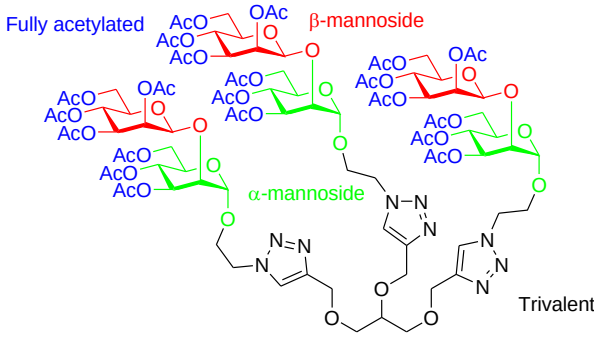

1

Figure 3.3. Structure of the previously discovered lead compound **1**.

If the distance between the mannobiose units is a critical factor in whether the molecule is biologically active or not, it could be reasoned that even a small change in the linker length might cause significant changes in the activity. If on the other hand the activity is not closely linked to the spatial arrangement of the

mannobiose units, a significantly longer linker might be required for achieving a difference in activity. Based on these assumptions, and the structure of **1**, two new molecules, **2** and **3** (Figure 3.4), were designed and prepared. In **2**, the linker is extended by one CH_2 group, and in **3**, the linker is replaced by a triethylene glycol moiety.

The biological screening required the compounds to be at least somewhat soluble in water, which limited the alternatives for the linker structure. Compound **1**, with an ethyl linker, had a solubility of approximately 0.4 mg/mL, and for compound **2** it was even less, close to the limit of the required solubility for the screening. An analogue of **3**, with a nonyl chain instead of the triethylene glycol, would certainly have been, for all practical purposes, completely insoluble in water. Opting to use a triethylene glycol linker instead made the compound soluble enough for the screening.

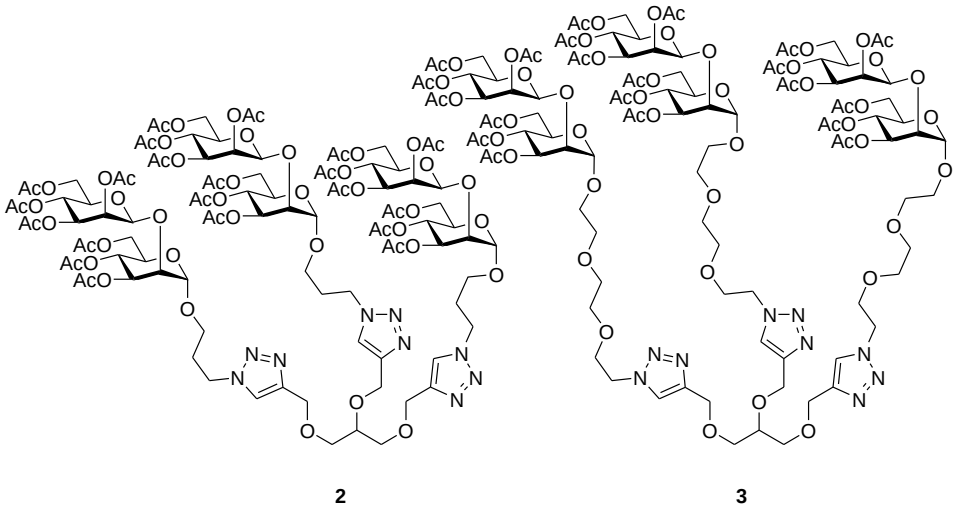

Figure 3.4. Structures of compounds **2** and **3**.

In addition to their biological activities, the behavior of the molecules in solution was investigated by a combination of NMR spectroscopic techniques and molecular dynamics simulations.

3.4 Synthesis of acetylated trivalent mannobioses

The synthetic preparation of compounds **2** and **3** is largely based on the previous synthesis of multivalent mannobioses.[33] The synthesis of the monosaccharide building blocks **4** and **5** (Figure 3.5), which is practically identical to the

synthesis in the previous chapter, has been previously published and will thus not be discussed further here.

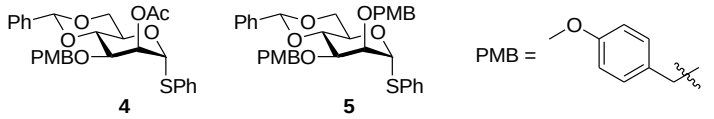

Figure 3.5. Structures of donors **4** and **5**.

The linker moieties were prepared by reacting 3-bromo-1-propanol, and 2-[2-(2-chloroethoxy)ethoxy]ethanol, respectively, with sodium azide to form the azido-functionalized linkers **6** and **7**, according to previously published methods.[36,37] These two compounds were used as acceptors in glycosylation reactions with **4**, using NIS/TMSOTf as the promotor system. The acetyl group on C-2 directed the stereochemical outcome of the reaction via neighboring group participation, resulting in excellent stereoselectivity. After the glycosylation reaction, the acetyl group was removed under Zemplén conditions to afford acceptors **10** and **11** (Scheme 3.1).

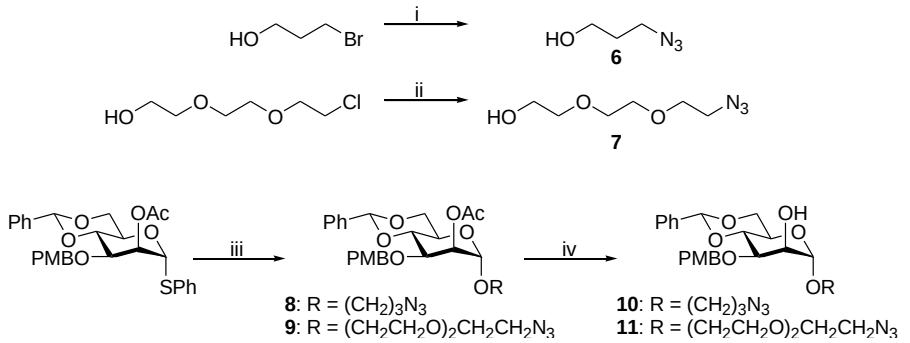

Scheme 3.1. Reagents and conditions: i) NaN_3, H_2O, 80 °C, 48 h (67%); ii) NaN_3, DMF, 90 °C, 19 h (90%); iii) **6** or **7**, NIS/TMSOTf, CH_2Cl_2, –40 °C, 2 h, **8** (70%), **9** (56%); iv) NaOMe/MeOH, r.t., 3 h/30 min (**8**/**9**), **10** (96%), **11** (quantitative).

The β-(1→2) linkage in the disaccharide was constructed in the same way as in the previous chapter, using the Crich β-mannosylation protocol. Monosaccharide donor **5** was activated with BSP and Tf_2O in the presence of TTBP, after which acceptors **10** or **11** were added (Scheme 3.2). The yields of the reactions were not very impressive, and significant decomposition of the activated donor was observed. This could be due to the increased reactivity of the donor caused by the electron-donating PMB groups on C-2 and C-3. The yields of disaccharides **12** and **13** were 57% and 43% respectively.

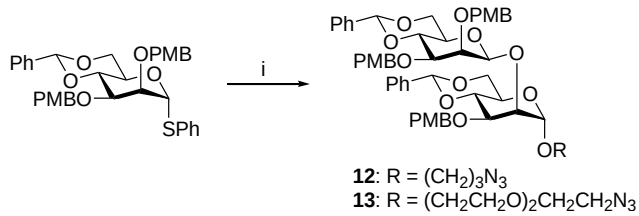

Scheme 3.2. Reagents and conditions: i) 1. BSP, TTBP, Tf_2O, CH_2Cl_2/1-octene 3:1, –60 °C, 30 min, 2. **10**/**11**, –78 °C, 3h/2h, **12** (57%), **13** (43%).

The choice of protecting groups allowed, once again, the removal of all protecting groups in one step. PMB-ethers can be removed by hydrogenation over palladium, but this could have resulted in undesired reduction of the azide to amine, which is why another approach was selected. Furthermore, while deprotection after forming the trivalent compound would have been possible, and this would have circumvented the possibility of reducing the azide, the high probability of causing complex mixtures and poor yields, in case of incomplete deprotection, prompted to replace the protecting groups with acetyl groups before the click reaction. Because hydrogenation to remove the protecting groups was to be avoided, PMB ethers were used instead of benzyl ethers, as these can be easily removed under acidic conditions (TFA in this case), as can the benzylidene acetals.

Upon hydrolysis, the PMB groups form reactive carbocation intermediates, which can, in principle, undergo nucleophilic addition by any free hydroxyl group on the target compound. This is an equilibrium reaction and in order to drive the reaction to completion, a good nucleophile, 1,3-propanedithiol, was used as cation scavenger (Scheme 3.3).

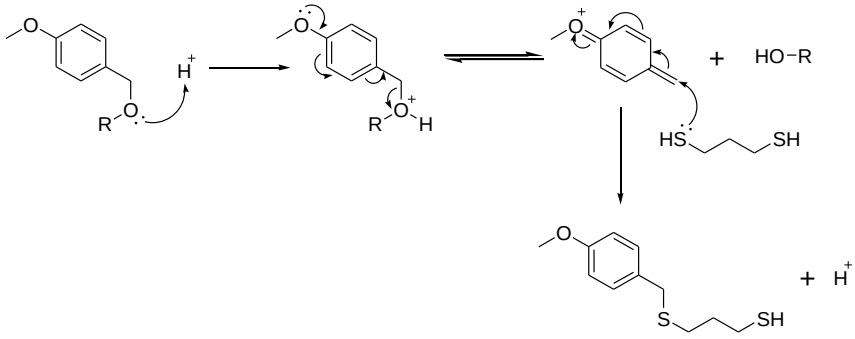

Scheme 3.3. Deprotection of PMB ethers in presence of 1,3-propanedithiol.

The unprotected intermediates were dissolved in water and washed with dichloromethane to remove the byproducts soluble in organic solvents. No further purification or isolation of the intermediates was carried out, and they were used as such in the subsequent acetylation step. The acetylation was carried out by standard protocols using acetic anhydride in pyridine (Scheme 3.4).

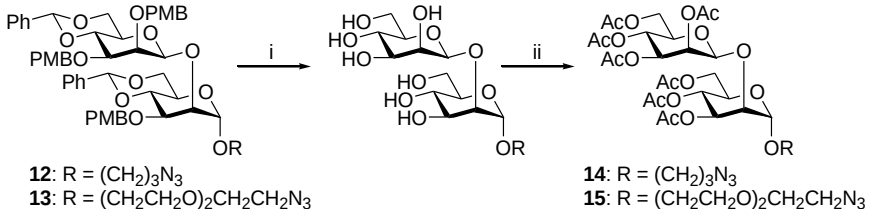

Scheme 3.4. Reagents and conditions: i) 1,3-propanedithiol, TFA/H_2O/CH_2Cl_2 4:1:10, r.t., 3h/2h (**12**/**13**); ii) Ac_2O, pyridine, r.t., 18 h **14** (61%), **15** (75%).

The final trivalent compounds were constructed using copper(I)-catalyzed azide-alkyne cycloaddition ("click" reaction), to attach the finished azido-functionalized acetylated mannobioses to a central glycerol moiety, bearing three propargyl groups. The reaction was carried out under standard conditions, and Cu(I) species were generated *in situ* by reduction of Cu(II) from $CuSO_4$ by Na-ascorbate (Scheme 3.5). The glycerol backbone was prepared by treating glycerol with sodium hydride in DMF, followed by addition of propargyl bromide in toluene according to a previously published method.[38]

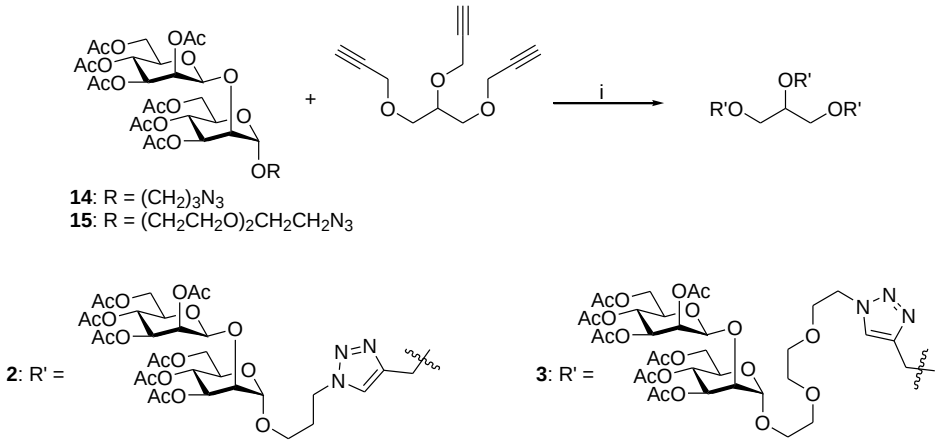

Scheme 3.5. Reagents and conditions: i) $CuSO_4$, Na-ascorbate, CH_2Cl_2/H_2O/*t*-BuOH, 1:1:1, 55 °C, 18 h, **2** (62%), **3** (89%).

All isolated products were thoroughly characterized by NMR spectroscopic methods to assure that the correct products had formed. The anomeric

configurations after the glycosylation reactions were determined by measuring the $^1J_{C1\text{-}H1}$ coupling constants, which were found to be 170.6 Hz and 170.5 Hz for **8** and **9** respectively. For disaccharides **12** and **13**, the $^1J_{C1A\text{-}H1A}$ coupling constants were found to be 171.7 Hz and 171.5 Hz respectively, and $^1J_{C1A\text{-}H1A}$ coupling constants were 155.0 Hz and 154.3 Hz respectively. These coupling constants confirmed the α-linkage to the linker moiety, and β-linkage between mannopyranosyl units.

After the click reaction, the substituent positions on the triazole rings were confirmed, also by NMR methods, using the HMBC experiment which clearly showed a correlation between the CH functionality of the triazole and the closest CH_2 of the linker. This correlation verifies, that the triazoles are 1,4-substituted, as is expected based on the mechanism when copper is used as the catalyst (Scheme 3.6),[39] as opposed to 1,5 substituted triazole, which would be the other alternative commonly obtained when using ruthenium catalysts.[40]

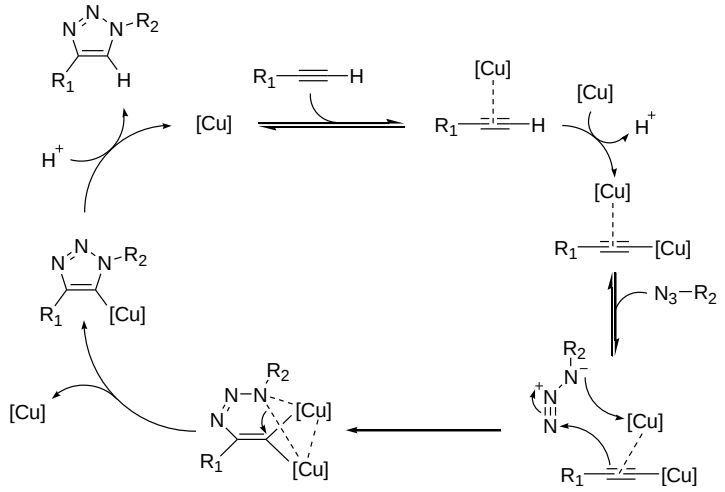

Scheme 3.6. Mechanism of the copper(I) catalyzed azide-alkyne cycloaddition reaction.

To clarify the numbering of the atoms in the molecules, which will be important for the following section, the two mannose moieties are denoted as A and B according to convention. The carbon atoms in the linker are denoted with primed numbers starting from the carbon atom closest to the mannobiose and, finally, the carbon atoms of the glycerol moiety are denoted only as G1 and G2 (as the terminal carbon atoms are not distinguishable by NMR, Figure 3.6)

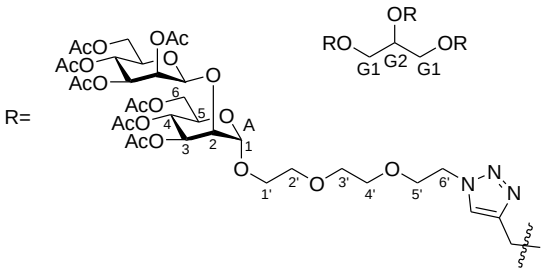

Figure 3.6. Numbering of the atoms in the trivalent compounds.

3.5 Conformational studies

As already discussed in the previous chapter, the three-dimensional structure of molecules is of importance from a biological perspective and plays an important part in how potentially bioactive molecules interact with biological receptors. While it is possible to determine the absolute energy minimum of almost any molecule, such a single conformation would not be of much relevance in molecules like the ones discussed in this chapter. The molecules have a large number of degrees of freedom which typically means that the energy minimum is not well defined, and the molecules are likely to adopt a number of different conformations.

The three molecules **1**, **2** and **3** were investigated by NMR spectroscopic techniques, using Diffusion Ordered SpectroscopY (DOSY) and Rotating frame Overhauser Effect SpectroscopY (ROESY). It is, perhaps, worth noting that the molecular weights of these molecules are significantly larger than those of the tri and tetrasaccharide in the previous chapter, but it was still suspected that the NOE effect would be too close to the zero-crossing, which is why ROESY was used instead of NOESY.

DOSY, is a technique that is used for measuring diffusion coefficients of molecules. The diffusion coefficient gives information about the hydrodynamic radius (volume) of the molecules. In this case, only the relative diffusion coefficients were of interest and because of that no calibration was necessary. The DOSY spectra showed that, even though the length of the linker varies significantly between the molecules, the physical size of all molecules was practically identical. Ultimately, this is not very surprising as the solvent is very polar, and the compounds themselves are rather non-polar. Because of this, the molecules are rather interacting with themselves, exposing as little as possible to the polar solvent. This indicates that the molecules all adopt similar, folded conformations.

While all the biological screenings were performed in water, the NMR spectroscopic experiments were carried out in methanol (d_4) due to the low water solubility of the compounds, which would have resulted in long experiment times, especially for compound **2**. Methanol is quite similar to water with respect to polarity and dielectric constant (p_{H2O} = 1.85 D, ε_{H2O} = 80.1, p_{MeOH} = 1.69 D and ε_{MeOH} = 32.7). Because of this the behavior in methanol is expected to be very similar to that in water.

The signals from the three mannobiose units were practically indistinguishable, which in itself was not surprising, but it complicated the analysis of the ROESY spectra. One advantage of using ROESY (in addition to the obtained correlations always being positive), is that the lack of signals can provide as much information as the signals themselves, as they are not as sensitive to molecular motion as NOESY signals. The severe overlapping in the spectra made it impossible to distinguish correlations between mannobiose units, from those within the same unit, which also makes the accurate calculation of distances practically impossible. It is, however, safe to assume that the distances between atoms of the reported correlations are no more than 4 Å apart, as this is the approximate limit at which range ROESY correlations can be seen in molecules of this size.[41]

In addition to NMR experiments, the conformational behavior of the molecules was also investigated using molecular modelling methods. The exact details are described in the experimental section below. Key intramolecular distances were extracted from the trajectories obtained from molecular dynamics simulations, and these were compared to the correlations seen in the ROESY spectra using well-established approaches.[42]

3.5.1 Conformational behavior of compound 1

As expected, during the molecular dynamics simulation a large number of conformations were observed. During the high-temperature phase of the simulated annealing, the dominating conformation had each of the arms pointing away from the central core of the molecule. When the temperature was lowered, however, the molecule started to fold in on itself. At the final simulation temperature, a folded conformation seemed to be preferred over a spread out conformation.

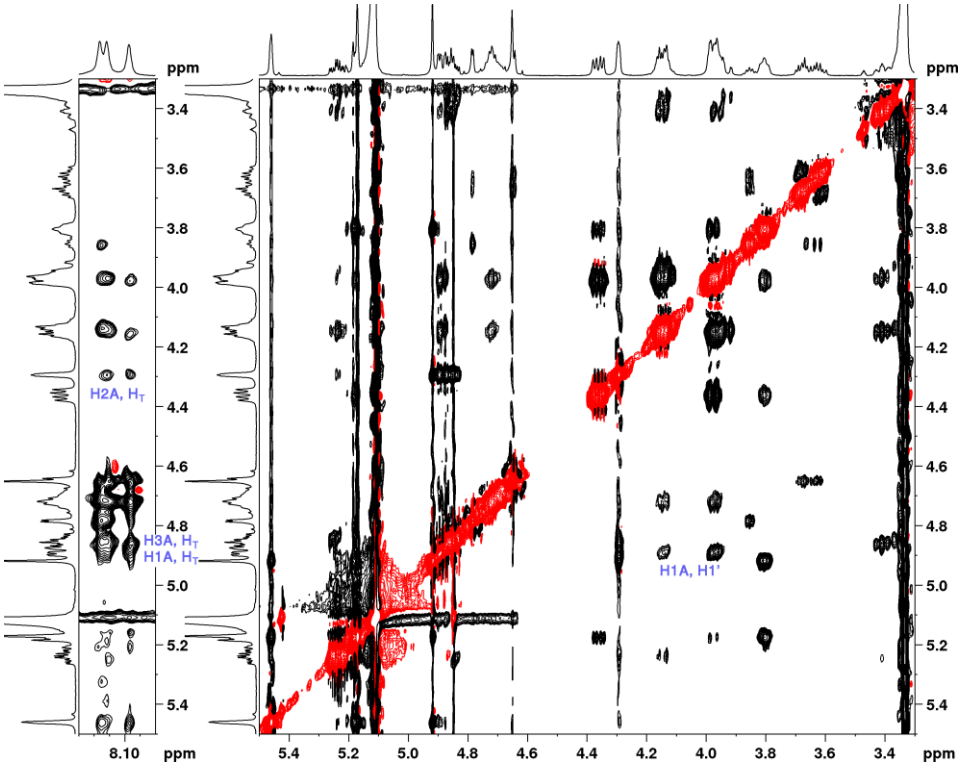

Figure 3.7. ROESY spectrum of compound **1**.

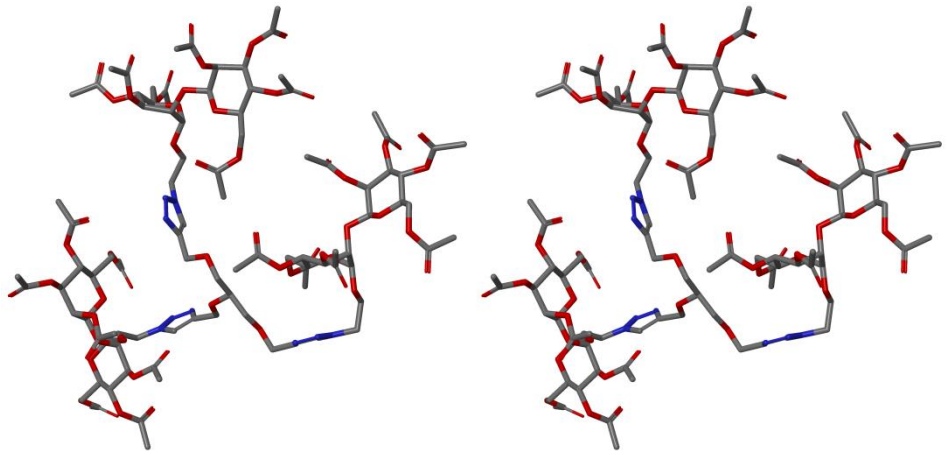

Figure 3.8. Stereoscopic view of **1**. Hydrogens are omitted for clarity.

The most interesting ROESY correlations in this compound were between the triazole protons and parts of the carbohydrate region of the spectrum, namely to H1A, H2A and H3A (Figure 3.7). The distances between the triazole protons

and the carbohydrate protons were, from the molecular dynamics simulations, calculated to be 3.3, 3.2 and 4.0 Å respectively. This supports the hypothesis of a folded structure, and also shows that the MD simulation seems to correctly predict the behavior of the molecule in solution. Furthermore, correlations between H1A and H2B are seen, which is characteristic of the αβ configuration of the glycosidic linkages present in the molecule. Additionally, correlations between protons H3A and H5A, as well as between H1B, H3B and H5B were observed confirming that the individual mannopyranosyl units are in $^4C_1$ conformations. While the exact energy minimum of the molecule is not very well defined, most of the low-energy conformations after the annealing protocol are rather similar. The most populated conformation is depicted in Figure 3.8.

3.5.2 Conformational behavior of compound 2

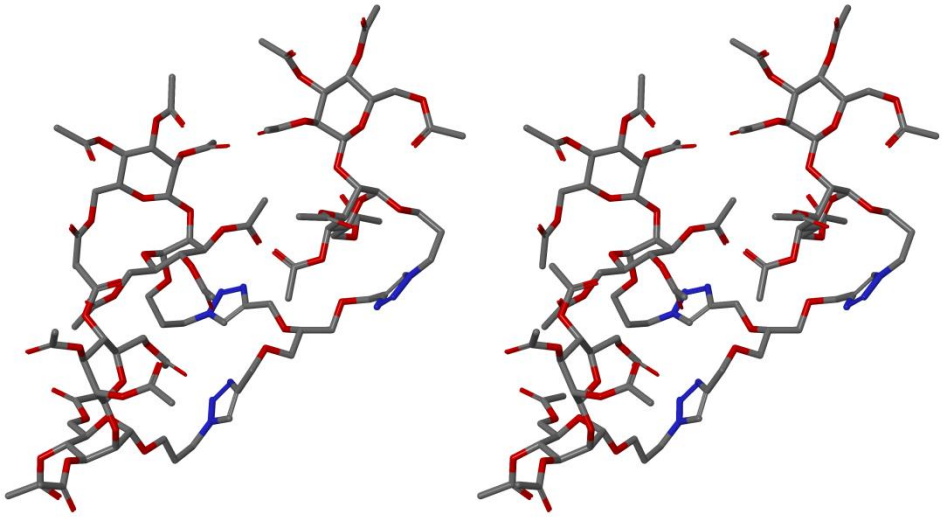

Figure 3.9. Stereoscopic view of **2**. Hydrogens are omitted for clarity.

The overall behavior of **2** is very similar to that of **1**, which is to be expected, as the difference in structure is quite small. The main difference is that the addition of one additional CH_2 moiety appears to move the triazole far enough, that correlations between triazole protons and carbohydrate protons are no longer observed. This is a reasonable result, as the distances in **1** are already close to the limitations of the experiment itself. Several correlations between the linker protons and carbohydrate protons can, however, be seen. The most relevant in this case are H1A–H1′ (2.4 Å), H1A–H2′ (4.0 Å), H5A–H1′ (2.6 Å), H5A–H2′ (3.6 Å) and H5A–H3′ (3.6 Å) (Figure 3.10). This indicates that the linker arms are located close to the underside of the first mannopyranosyl unit, further

supporting a folded conformation. The most populated conformation from the MD simulation is depicted in Figure 3.9.

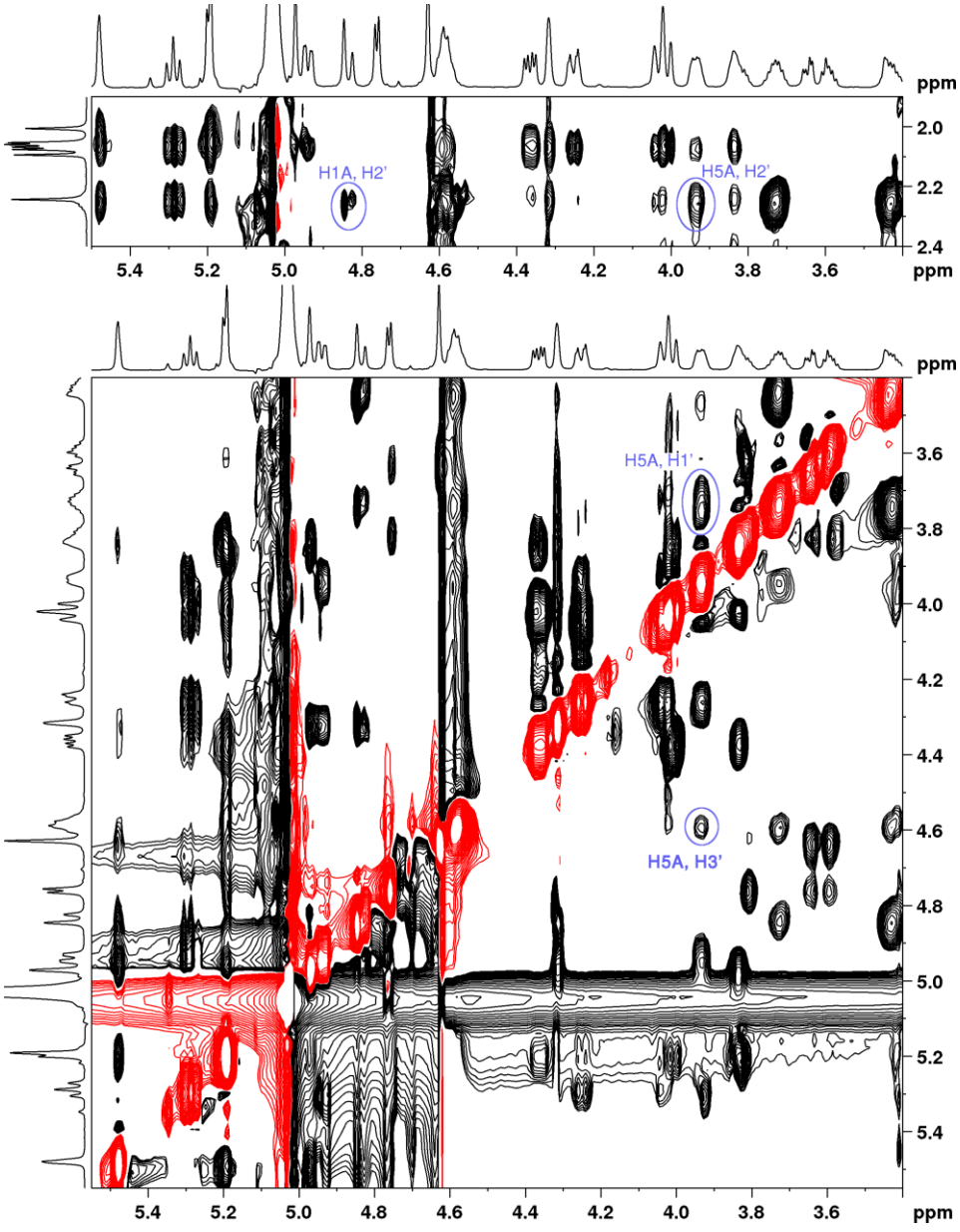

Figure 3.10. ROESY spectrum of compound **2**.

3.5.3 Conformational behavior of compound 3

The significantly longer, and slightly more polar, linker of compound **3** changes the overall behavior of the molecule compared to the other two. There is, as expected, no well-defined energy minimum, and the overlapping of the linker protons in the NMR spectra, makes it difficult to analyze the ROESY spectrum in detail. It does, however, appear that the preferred conformation of **3** is a folded one similar to **1** and **2**, and correlations from the linker protons to almost all carbohydrate protons except H4A and H4B can be seen (Figure 3.11). As discussed in the previous chapter, in the typical conformation of β-(1→2) linked mannosides these two protons are hidden inside the helical structure, making it difficult for them to move close to the linker. The glycosidic angles ϕ and aglyconic angles ψ between the two mannopyranosyl units were found to be ~60° and ~20–30° respectively, consistent with the typical conformation for this class of compounds. One low-energy conformation is depicted in Figure 3.12.

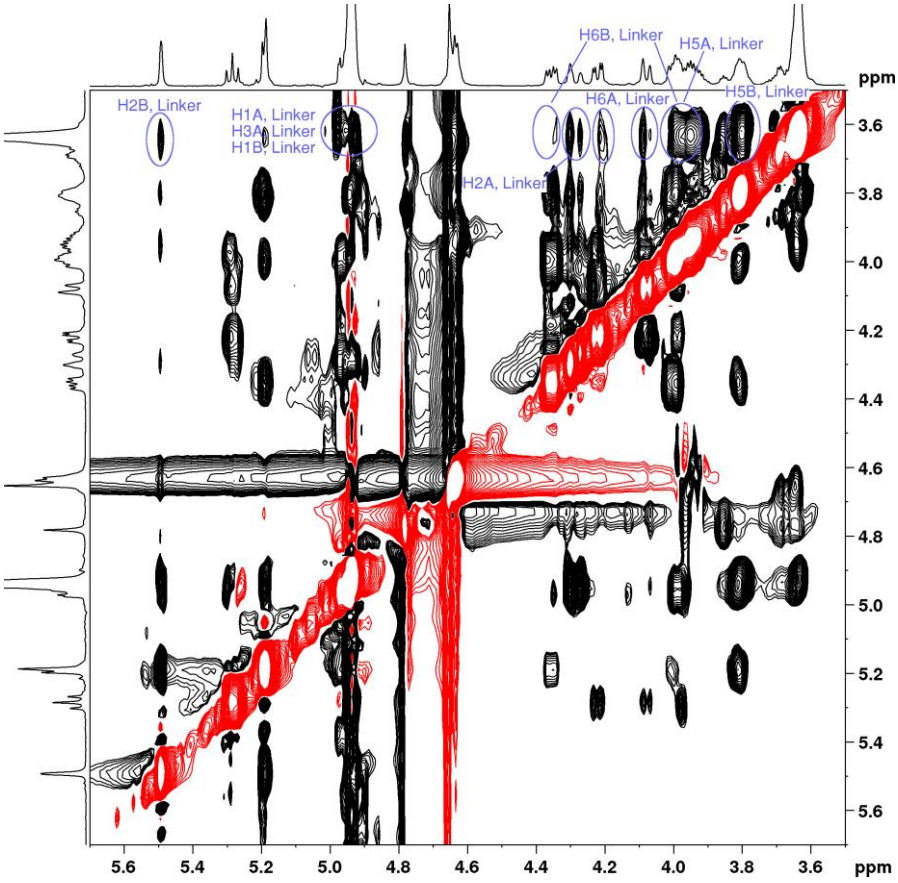

Figure 3.11. ROESY spectrum compound of **3**.

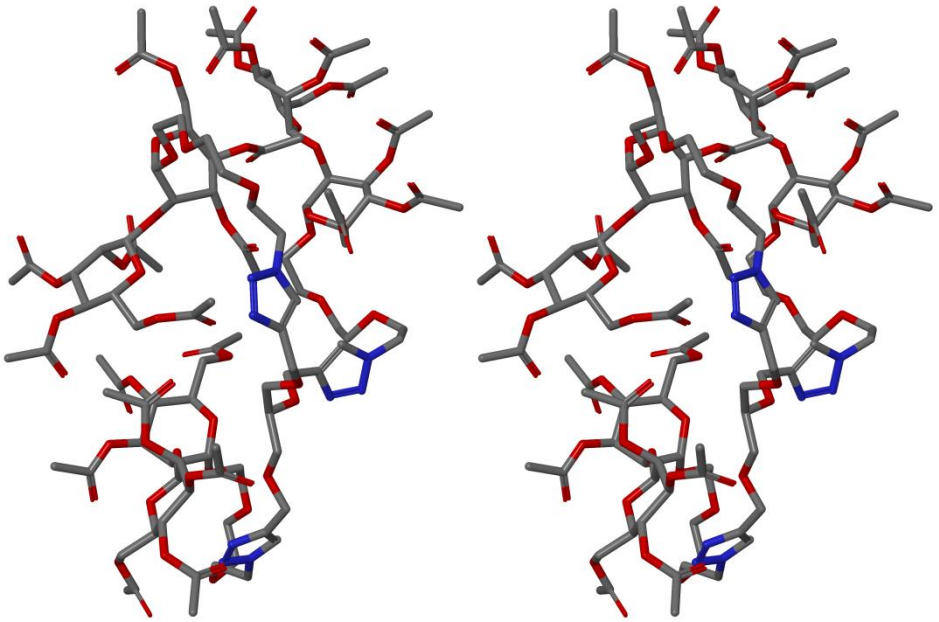

Figure 3.12. Stereoscopic view of **3**. Hydrogens are omitted for clarity.

It should be noted, that none of the ROESY spectra of molecules **1**, **2** and **3**, show correlations between the glycerol backbone and carbohydrate or linker protons. This indicates that the glycerol moiety is on one side of the molecule, and the arms with the mannobioses are on the other side. This is consistent with the molecular dynamics simulations. All molecules also leave the triazole rings on the outside of the structure. This could potentially allow them to interact with biological targets, and it is known that triazoles can participate in this type of interactions. There are a number of pharmaceuticals where triazole moieties play key parts in the biological activity.[43,44] Although the role of the triazole moiety in the biological activity of the trivalent compounds cannot be ruled out completely, it must be emphasized, that out of a large number similar structures, some with triazole moieties and some without, only compound **1** showed significant *in vitro* activity in previous screenings.[32–35] This indicates that the properties described above, and depicted in Figure 3.3 are in key position for the biological activity of this class of compounds.

3.6 Biological studies

3.6.1 PBMC screening.

The effects of **1**, **2**, **3**, MPLA and CpG-ODN on allergen (Bet v) induced cytokine responses in PBMC cultures of 14 birch allergic rhinitis patients were screened, and are presented in Figure 3.13. Stimulation with birch induced significant response of T_H2 cytokine IL-4 (mean 45.3 pg/mL, SEM 11.2 pg mL^{-1}), as compared to non-stimulated culture (mean 0.4 pg mL^{-1}, SEM 0.2 pg mL^{-1}) (p =0.0015). A significant suppression of birch-induced production of IL-4 was seen with 10 ($p < 0.001$) and 100 µg mL^{-1} ($p = 0.036$) of compound **2**, 10 ($p = 0.016$) and 100 µg mL^{-1} ($p = 0.021$) of compound **3**, 10 ($p = 0.016$) and 100 µg mL^{-1} ($p = 0.006$) of **1**, 1 ($p = 0.002$) and 10 µg/ml (p =0.0.013) of MPLA and 200 µg mL^{-1} of CpG-ODN ($p = 0.002$). Dose–response curves of suppression were seen only with compounds **1-3**, as lower concentrations of CpG-ODN increased the IL-4 production, and the highest concentration of MPLA had no suppressive effect (Figure 10). Significantly increased production of pro-inflammatory cytokine TNF was seen with 100 µg mL^{-1} (p=0.021) of compound **2**, 100 µg mL^{-1} ($p = 0.0039$) of compound **3** and 20 ($p = 0.0026$) and 200 µg mL^{-1} ($p < 0.001$) of CpG-ODN (Figure 3.13).

Glycoclusters **1**, **2** and **3** all had a dose-dependent effect on birch-allergen-induced IL-4 production by PBMCs from patients suffering from birch allergy. MPLA was found to only inhibit IL-4 production at lower concentrations, with higher concentrations having no effect. At lower concentrations, CpG-ODN seemed to increase the production of IL-4, but at higher concentration the production was significantly decreased. With IL-4 being the most important cytokine in the development of an allergic inflammation, a clear dose–response allows for specific modulation of its production.

Tumor necrosis factor (TNF) production was not induced by compound **1**, and for compounds **2** and **3** it was induced only at the highest concentrations. CpG-ODN, however, was found to be a strong inducer of TNF, whereas the increase by MPLA was not statistically significant. TNF is a pro-inflammatory cytokine involved in, for example, inflammations in rheumatoid arthritis, cancer, Alzheimer's disease and many others.[45,46] An increased TNF production would, therefore, be considered unfavorable and even harmful, which needs to be taken into account when selecting the adjuvant to use.

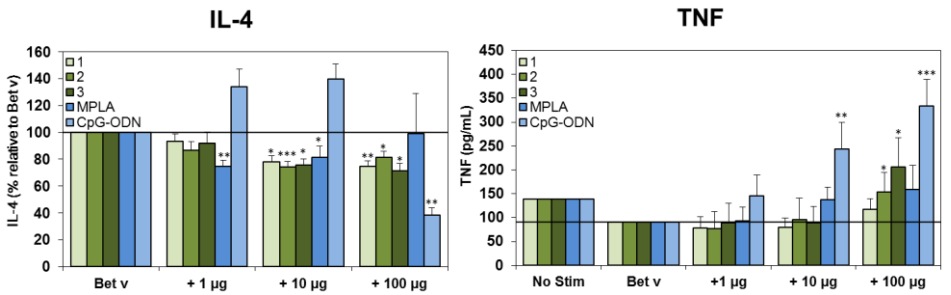

Figure 3.13. IL-4 (left) and TNF (right) responses of PBMCs stimulated with Bet v with and without adjuvants.

3.6.2 TLR ligation screening

CpG-ODN and MPLA act via activation of TLR receptors (TLR-9 and TLR-4 respectively), which prompted to screen compounds **1**, **2** and **3** for binding to human TLRs (TLR 2, 3, 4, 5, 7, 8 and 9) as well. No binding was witnessed between the trivalent mannobioses and any of the TLR receptors. The fate of the acetyl groups under biological conditions is at present unclear, and it is reasonable to assume that they are, at least partially, hydrolyzed. A fully deprotected analogue of **1**, which was previously shown to have no activity in *in vitro* screening,[33] also did not bind any of the TLRs screened.

3.6.3 Possible copper contamination

Copper is an essential trace element, vital for many biological functions, for example metabolism.[47,48] Copper ions also have the ability to generate reactive oxygen species, making them toxic in higher concentrations.[49–51] Because the final synthetic step in preparation of trivalent compounds **1**, **2** and **3** is catalyzed by copper ions, it is crucial to ensure that the copper content in the final compounds is not going to interfere with the biological screening. The copper contents of all three glycoclusters were analyzed by ICP-MS, which showed that the residual copper content after the purification ranged between 7 – 8 mg kg^{-1}. The highest concentrations of the compounds used in the biological screenings were 100 µg mL^{-1}, giving a final concentration of copper as 0.7 – 0.8 ng kg^{-1}. The concentration of copper ions in human blood ranges from ~0.85 µg mL^{-1} to 2 µg mL^{-1},[52–54] which is three orders of magnitude higher than the copper concentration induced by the glycoclusters. It can therefore safely be assumed that the copper content of the investigated molecules is not biologically significant.

3.7 Conclusions

A new trivalent acetylated mannobiose glycoclusters, based on the design of a previously discovered immunostimulatory lead molecule was prepared. The prepared molecules, as well as the previously discovered lead molecule and compound **2**, were subjected to thorough NMR spectroscopic investigations, combined with molecular modelling to elucidate their conformational behavior in solution. The modelling results correlate well with the data extracted from DOSY and ROESY spectra, verifying that the molecular dynamics simulation provides a realistic representation of the molecules.

It was shown that, while both the length and polarity of the linker was varied quite significantly, the conformational behaviors of all three molecules in solution were practically identical. The similar behavior of all compounds correlated well with their similar biological activities.

The prepared glycoclusters were found to be able to suppress Bet v induced IL-4 production by PBMCs from patients with birch allergy, indicating their potential as adjuvants in allergen immunotherapy. The low TNF production induced by the molecules makes them have potentially fewer harmful side effects than currently used adjuvants. Furthermore, the low TNF production induced by the glycoclusters indicates that the mechanism behind the immunostimulatory effect may be different from the previously disclosed adjuvants CpG-ODN and MPLA, which act via TLR activation. This is also consistent with the fact that no binding was witnessed in TLR screening.

3.8 Experimental

3.8.1 Instrumental and general details

Preparation and spectral data of compound **2**, together with some results from the biological screening of compounds **1** and **2** reported here, have also been briefly addressed previously in a patent application.[55] All reagents for synthetic work were purchased from Sigma-Aldrich, and used without further purification. Dry CH_2Cl_2 was obtained by distillation over CaH_2 and dry DMF was purchased as such, and stored over molecular sieves. TLC was performed on aluminum sheets precoated with silica gel 60 F_{254} (Merck) and the spots were visualized by UV, and charring by treatment with H2SO4 in MeOH (20 % v/v) followed by heating. Column chromatography was performed using Silica gel 60 (0.040–0.060 mm Merck).

Optical rotations were measured with a Perkin-Elmer 241 polarimeter using the D-line of sodium at 589 nm at 24 °C, unless mentioned otherwise. HRMS were recorded on a Bruker MicroToF-Q with electrospray ionization operating in positive mode.

NMR spectra were recorded on Bruker Avance spectrometers operating at either 600.13 Hz or 500.13 Hz (^{1}H) and 150.90 Hz or 125.77 Hz (^{13}C). The complete assignment of proton and carbon spectra was carried out by recording a standard set of NMR experiments, ^{1}H NMR, ^{13}C NMR, DQF-COSY, HSQC (both coupled and decoupled) and HMBC. The complexities of the spectra were reduced to monosaccharide level by using 1D-TOCSY. ROESY and DOSY methods were used to help with the conformational studies. The chemical shifts are referenced to an internal standard (tetramethylsilane, δ = 0.0 ppm in both ^{1}H and ^{13}C) or residual solvent signals ($CDCl_3$, δ = 7.26 ppm in ^{1}H and 77.16 ppm in ^{13}C) and reported with two decimals for 1H NMR and one decimal for ^{13}C NMR. Where this was not enough to separate the signals, an additional decimal was reported. Accurate coupling constants were, where possible, determined with the NMR simulation software PERCH[56] and reported with one decimal. To avoid unnecessary bloating of the NMR data, each coupling constant was reported only the first time it is encountered.

The molecular modeling and visualization was done in Maestro, and the calculations were performed by Desmond using the built-in interface in Maestro. Initially, the molecules were constructed in Maestro[57] after which the calculations were carried out using Desmond,[58] controlled via the built-in interface in Maestro. For a good starting point for the molecular dynamics simulations, a quick minimization sequence over 1000 steps was performed after constructing the molecules, and the results visually inspected in order to see if they were reasonable. The molecular dynamics simulations started with a simulated annealing sequence, where the temperature was first raised to 600 K and then slowly lowered from to the final simulation temperature, which in our case was lower than ambient temperature in order to shift the solvent signals, so they do not overlap with important signals in the NMR spectra. Furthermore, the lower temperature caused some of the overlapping proton signals to shift apart, making it easier to extract information from the ROESY spectra. The annealing was repeated to make sure that the molecules were not stuck in a high energy local minimum. After the annealing, the molecular dynamics simulation was run for 2 ns, during which the structures were stored every 1 ps. From these structures, the average distances between protons were measured, and since the NOE effect is proportional to r^{-6},[41] this factor was used as weight when

calculating the average distances. Out of the generated structures, the most populated conformation families were analyzed, and verified using the correlations seen in the recorded ROESY spectra.

3.8.2 Synthetic procedures

3-Azido-1-propyl 2-*O*-acetyl-4,6-*O*-benzylidene-3-*O*-(4-methoxybenzyl)-α-D-mannopyranoside (8): A solution of Phenyl 2-*O*-acetyl-4,6-*O*-benzylidene-3-*O*-(4-methoxybenzyl)-1-thio-α-D-mannopyranoside (2 g, 3.82 mmol, 1 equivalent) and 3-azido-1-propanol (464 mg, 4.59 mmol, 1.2 equivalents) in dry CH_2Cl_2 (15 mL) under argon was cooled down to –40 °C. NIS (1.03 g, 4.59 mmol, 1.2 equivalents) and TMSOTf, (36 µl, 0.20 mmol, 0.05 equivalents) were added and the reaction mixture was stirred at –40 °C for 2 h. The reaction was quenched by adding 100 µl Et_3N. The reaction mixture was filtered and diluted with CH_2Cl_2 (40 mL) and then washed with water (30 mL), satd. $NaHCO_3$ (2 ×30 mL) and brine (2 × 30 mL). The organic layer was dried over Na_2SO_4 and concentrated. The crude mixture was purified by column chromatography (hexane : EtOAc 2 : 1) to afford pure product **8** as a colorless foam. R_f = 0.31. Yield: 1.09 g (56 %). $[\alpha]_D^{25}$ = –3.1° (c 1.0, $CHCl_3$). ^{1}H NMR (600.13 MHz, $CDCl_3$, 25 °C): δ = 7.50 (m, 2 H, arom. H), 7.40–7.35 (m, 3 H, arom. H), 7.27 (m, 2 H, arom. H), 6.84 (m, 2 H, arom. H), 5.62 (s, 1 H, 4,6-OC*H*Ph), 5.36 (dd, 1 H, $J_{H2,\,H1}$ = 1.6 Hz, $J_{H2,\,H3}$ = 3.5 Hz, H2), 4.77 (d, 1 H, H1), 4.63 and 4.58 (each d, each 1 H, J = –11.6 Hz, 3-OCH_2Ph), 4.26 (dd, 1 H, $J_{H6a,\,H5}$ = 4.8 Hz, $J_{H6a,\,H6b}$ = –10.3 Hz, H6a), 4.04 (dd, 1 H, $J_{H4,\,H3}$ = 10.0 Hz, $J_{H4,\,H5}$ = 9.3 Hz, H4), 3.97 (dd, 1 H, H3), 3.83 (dd, 1 H, $J_{H6b,\,H5}$ = 10.4 Hz, H6b), 3.81 (ddd, 1 H, H5), 3.79 (s, 3 H, OCH_3), 3.78 (ddd, 1 H, $J_{H1'a,\,H1'b}$ = –9.8 Hz, $J_{H1'a,\,H2'a}$ = 6.2 Hz, $J_{H1',\,H2'b}$ = 6.1 Hz, H1′a), 3.49 (ddd, 1 H, $J_{H1'b,\,H2'a}$ = 6.8 Hz, $J_{H1'b,\,H2'b}$ = 5.5 Hz, H1′b), 3.78 (ddd, 1 H, $J_{H3'a,\,H2'a}$ = 8.1 Hz, $J_{H3'a,\,H2'b}$ = 8.5 Hz, $J_{H3'a,\,H3'b}$ = –13.0 Hz, H3′a), 3.37 (ddd, 1 H, $J_{H3'b,\,H2'a}$ = 4.1 Hz, $J_{H3'b,\,H2'b}$ = 5.6 Hz, H3′b), 2.16 (s, 3 H, 2-OCOCH_3), 1.87 (ddddd, 1 H, $J_{H2'a,\,H2'b}$ = –7.8 Hz, H2′a), 1.86 (ddddd, 1 H, H2′b).

^{13}C NMR (150.9 MHz, $CDCl_3$, 25 °C): δ = 170.4 (2-O*C*OCH$_3$), 159.4, 137.5, 130.1, 129.5, 129.0, 128.3, 126.2, 113.9 (arom. C), 101.7 (4,6-OCHPh), 99.0 (C1), 78.3 (C4), 73.6 (C3), 72.0 (3-OCH$_2$Ph), 69.8 (C2), 68.8 (C6), 64.8 (C1′), 64.2 (C5), 55.4 (O*C*H$_3$), 48.4 (C3′), 28.9 (C2′), 21.2 (2-OCO*C*H$_3$).

HRSM: *m/z* calcd. for $C_{26}H_{32}N_3O_8$ $[M+H]^+$: 514.2184, found 514.2149; *m/z* calcd. for $C_{26}H_{31}N_3NaO_8$ $[M+Na]^+$: 536.2003, found 536.1952; *m/z* calcd. for $C_{26}H_{31}N_3KO_8$ $[M+K]^+$: 552.1743, found 552.1712.

3-Azido-1-propyl 4,6-*O*-benzylidene-3-*O*-(4-methoxybenzyl)-α-D-mannopyranoside (10): The pH of a solution of **8** (920 mg, 1.79 mmol) in MeOH (20 mL) was adjusted to ~10 – 12 with 0.1 M NaOMe and the reaction mixture was stirred at room temperature for 4 h. The reaction mixture was neutralized with DOWEX-50WX8 H^+ form, filtered and concentrated to afford pure product **10** as a colorless oil. R_f = 0.26 (hexane : EtOAc 2 : 1). Yield: 827 mg (96 %). $[\alpha]_D^{25}$ = +31.3° (c 1.0, $CHCl_3$). ^{1}H NMR (600.13 MHz, $CDCl_3$, 25 °C): δ = 7.42 (m, 2 H, arom. H), 7.32–7.25 (m, 3 H, arom. H), 7.20 (m, 2 H, arom. H), 6.78 (m, 2 H, arom. H), 5.62 (s, 1 H, 4,6-OC*H*Ph), 4.83 (d, 1 H, $J_{H1, H2}$ = 1.5 Hz, H1), 4.80 and 4.66 (each d, each 1 H, J = –11.3 Hz, 3-OCH_2Ph), 4.28 (dd, 1 H, $J_{H6a, H5}$ = 5.0 Hz, $J_{H6a, H6b}$ = –10.4 Hz, H6a), 4.10 Hz (dd, 1 H, $J_{H4, H3}$ = 9.63 Hz, $J_{H4, H5}$ = 9.5 Hz, H4), 5.42 (ddd, 1 H, $J_{H2, H1}$ = 1.5 Hz, $J_{H2, 2\text{-}OH}$ = 1.7 Hz, $J_{H2, H3}$ = 3.5 Hz, H2), 3.90 (dd, 1 H, H3), 3.86 (dd, 1 H, $J_{H6b, H5}$ = 10.4 Hz, H6b), 3.81, (ddd, 1 H, H5), 3.80 (s, 3 H, OCH_3), 3.79 (ddd, 1 H, $J_{H1'a, H1'b}$ = –10.0 Hz, $J_{H1'a, H2'a}$ = 6.1 Hz, $J_{H1'a, H2'b}$ = 6.0 Hz, H1′a), 3.49 (ddd, $J_{H1'b, H2'a}$ = 5.8 Hz, $J_{H1'b, H2'b}$ = 6.5 Hz, H1′b) 3.39 (ddd, 1 H, $J_{H3'a, H2'a}$ = 7.5, $J_{H3'a, H2'b}$ = 6.2 Hz, $J_{H3'a, H3'b}$ = –12.3 Hz, H3′a), 3.37 (ddd, 1 H, $J_{H3'b, H2'a}$ = 6.2, $J_{H3'b, H2'b}$ = 7.0 Hz, H3′b), 1.87 (each dddd, each 1 H, H2′a and H2′b).

^{13}C NMR (150.9 MHz, $CDCl_3$, 25 °C): δ = 159.5, 137.6, 130.1, 129.6, 129.0, 128.3, 126.1, 113.9 (arom. C), 101.6 (4,6-O*C*HPh), 100.2 (C1), 78.8 (C4), 75.4 (C3), 72.9 (3-O*C*H_2Ph), 70.0 (C2), 68.9 (C6), 64.5 (C1′), 63.6 (C5), 55.3 (3 × O*C*H_3), 48.4 (C3′), 28.8 (C2′).

HRSM: *m/z* calcd. for $C_{24}H_{30}N_3O_7$ $[M+H]^+$: 472.2078, found 472.2053; *m/z* calcd. for $C_{24}H_{29}N_3NaO_7$ $[M+Na]^+$: 494.1900, found 494.1849; *m/z* calcd. for $C_{24}H_{29}N_3KO_7$ $[M+K]^+$: 510.1637, found 510.1583.

3-Azido-1-propyl *O*-[4,6-*O*-benzylidene-2,3-di-*O*-(4-methoxybenzyl)-β-D-mannopyranosyl]-(1→2)-4,6-*O*-benzylidene-3-*O*-(4-methoxybenzyl)-α-D-mannopyranoside (12): To a solution of phenyl 4,6-*O*-benzylidene-2,3-di-*O*-(4-methoxybenzyl)-1-thio-α-D-mannopyranoside (1.24 g, 2.03 mmol, 1.2 equivalents) in CH_2Cl_2 (20 mL) was added 4 Å molecular sieves and the solution was stirred at room temperature for 30 min. The solution was then cooled down to –60 °C after which BSP (511 mg, 2.44 mmol 1.4 equivalents), TTBP (727 mg, 2.92 mmol, 1.7 equivalents) and Tf_2O (412 µl, 2.44 mmol, 1.4 equivalents) were added. The reaction mixture was stirred at –60 °C for 30 min (complete activation confirmed by TLC) and then cooled down to –78 °C. Compound **10** (800 mg, 1.69 mmol, 1 equivalent) in CH_2Cl_2 (10 mL) was added slowly. The reaction mixture was then stirred at –78 °C for 2 h and then quenched by adding

Et_3N (1 mL) and stirring for 1 h during which the temperature was allowed to rise to room temperature. The reaction mixture was diluted with CH_2Cl_2 (60 mL) and washed with water (2 × 30 mL) and brine (20 mL). The organic layer was dried over Na_2SO_4 and concentrated. The crude product was purified by column chromatography (hexane : EtOAc 2 : 1) to afford pure **12** as a colorless foam. R_f = 0.3. Yield: 930 mg (57 %). $[\alpha]_D^{25}$ = –61.1° (c 1.0, $CHCl_3$). ^{1}H NMR (600.13 MHz, $CDCl_3$, 25 °C): δ = 7.49 (m, 4 H, arom. H), 7.42 (m, 2 H, arom. H), 7.40–7.32 (m, 8 H, arom. H), 7.19 (m, 2 H, arom. H), 6.85–6.80 (m, 6 H, arom. H), 5.59 (s, 1 H, 4A,6A-OC*H*Ph), 5.51 (s, 1 H, 4B,6B-OC*H*Ph), 4.95 and 4.89 (each d, each 1 H, J = –11.9 Hz, 2B-OCH_2Ph), 4.79 (d, 1 H, $J_{H1A,\ H2A}$ = 1.7 Hz, H1A), 4.70 and 4.65 (each d, each 1 H, J = –11.6 Hz, 3A-OCH_2Ph), 4.61 and 4.54 (each d, each 1 H, J = –12.1 Hz, 3B-OCH_2Ph), 4.59 (s, 1 H, H1B), 4.27 (dd, 1 H, $J_{H6Ba,\ H5B}$ = 4.7 Hz, $J_{H6Ba,\ H6Bb}$ = –10.5 Hz, H6Ba), 4.25 (dd, 1 H, $J_{H6Aa,\ H5A}$ = 4.1 Hz, $J_{H6Aa,\ H6Ab}$ = –9.6 Hz, H6Aa), 4.22 (dd, 1 H, $J_{H4B,\ H3B}$ = 9.8 Hz, $J_{H4B,\ H5B}$ = 9.1 Hz, H4B), 4.18 (dd, 1 H, $J_{H2A,\ H3A}$ = 3.4 Hz, H3A), 4.09 (dd, 1 H, $J_{H4A.\ H3A}$ = 10.0 Hz, $J_{H4A,\ H5A}$ = 8.8 Hz, H4A), 3.93 (d, 1 H, $J_{H2B,\ H3B}$ = 3.3 Hz, H2B), 3.92 (dd, 1 H, H3A), 3.88 (dd, 1 H, $J_{H6Bb,\ H5B}$ = 10.0 Hz, H6Bb), 3.802 (ddd, 1 H, $J_{H1'a,\ H1'b}$ = –9.9 Hz, $J_{H1'a,\ H2'a}$ = 2.3 Hz, $J_{H1'a,\ H2'b}$ = 11.6 Hz, H1′a), 3.801 (s, 3 H, OCH_3), 3.783 (dd, 1 H, $J_{H6Ab,\ H5A}$ = 10.0 Hz, H6Ab), 3.776 (s, 3 H, OCH_3), 3.765 (ddd, 1 H, H5A), 3.763 (s, 3 H, OCH_3), 3.55 (dd, 1 H, H3B), 3.47 (ddd, 1 H, $J_{H1'b,\ H2'a}$ = 7.7 Hz, $J_{H1'b,\ H2'b}$ = 4.5 Hz, H1′b), 3.38 (ddd, 1 H,$J_{H3'a,\ H2'a}$ = 5.1 Hz, $J_{H3'a,\ H2'b}$ = 8.2 Hz, $J_{H3'a,\ H3'b}$ = –12.4 Hz, H3′a), 3.34 (ddd, 1 H, $J_{H3'b,\ H2'a}$ = 5.0 Hz, $J_{H3'b,\ H2'b}$ = 7.5 Hz, H3′b), 3.31 (ddd, 1 H, H5B), 1.86 (each dddd, each 1 H, H2′a and H2′b).

^{13}C NMR (150.9 MHz, $CDCl_3$, 25 °C): δ = 159.12, 159.11, 159.0, 137.6, 137.5, 130.8, 130.6, 130.4, 130.3, 129.3, 129.1, 128.9, 128.8, 128.18, 128.17, 126.1, 126.0, 113.7, 113.54, 113.50 (arom. C), 101.6 (4B,6B-O*C*HPh), 101.3 (4A,6A-O*C*HPh), 100.8 (C1B), 98.5 (C1A), 78.5 (C4A), 78.4 (C4B), 77.2 (C3B), 75.3 (C2B), 75.0 (C2A), 74.0 (2B-O*C*H_2Ph), 73.7 (C3A), 71.9 (3B-O*C*H_2Ph), 71.0 (3A-O*C*H_2Ph), 68.9 (C6A), 68.6 (C6B), 67.8 (C5B), 64.5 (C1′), 64.4 (C5A), 55.26, 55.25, 55.2 (3 × OCH_3), 48.2 (C3′), 28.8 (C2′).

HRSM: *m/z* calcd. for $C_{53}H_{59}N_3NaO_{14}$ $[M+Na]^+$: 984.3890, found: 984.3821; *m/z* calcd. for $C_{53}H_{59}N_3KO_{14}$ $[M+K]^+$: 1000.3629, found: 1000.3596.

3-Azido-1-propyl *O*-(2,3,4,6-tetra-*O*-acetyl-β-D-mannopyranosyl)-(1→2)-3,4,6-tri-*O*-acetyl-α-D-mannopyranoside (14): To a solution of **12** (800 mg, 0.832 mmol, 1 equivalent) in CH_2Cl_2 (10 mL) was added 1,3-propanedithiol (835 µl, 8.32 mmol, 10 equivalents) and the solution was cooled down to –10 °C. TFA (4 mL) and water (1 mL) were added and the reaction mixture was

stirred at room temperature for 2 h. The reaction mixture was then diluted with water (15 mL) and washed with CH_2Cl_2 (4 × 15 mL) to remove all non-polar organic material. The aqueous layer was evaporated and co-evaporated with toluene. The crude product was dissolved in pyridine (15 mL) and cooled down to 0 °C. Ac_2O (10 mL) was added and the reaction mixture was stirred at room temperature for 18 h. The reaction was quenched by adding methanol (10 mL) and then evaporated and co-evaporated with toluene. The crude product was purified by column chromatography (hexane : EtOAc 1 : 1) to afford pure product **14** as a white powder. R_f = 0.3. Yield: 365 mg (61 %). $[\alpha]_D^{25}$ = –46.1° (c 1.0, $CHCl_3$). ^{1}H NMR (600.13 MHz, $CDCl_3$, 25 °C): δ = 5.51 (dd, 1 H, $J_{H2B,\ H1B}$ = 1.0 Hz, $J_{H2B,\ H3B}$ = 3.4 Hz, H2B), 5.26 (t, 1 H, $J_{H4A,\ H3A}$ = $J_{H4A,\ H5A}$ = 10.1, H4A), 5.23 (dd, 1 H, $J_{H4B,\ H3B}$ = 10.0 Hz, $J_{H4B,\ H5B}$ = 9.8 Hz, H4B), 4.81 (d, 1 H, $J_{H1A,\ H2A}$ = 1.9 Hz, H1A), 4.67 (d, 1 H, H1B), 4.32 (dd, 1 H, $J_{H6Bb,\ H5B}$ = 6.0 Hz, $J_{H6Bb,\ H6Ba}$ = –12.2 Hz, H6Bb), 4.31 (dd, 1 H, H2A), 4.24, (dd, 1 H, $J_{H6Ab,\ H5A}$ = 4.2 Hz, $J_{H6Ab,\ H6Aa}$ = –12.3 Hz, H6Ab), 4.08 (dd, 1 H, $J_{H6Aa,\ H5A}$ = 2.3 Hz, H6Aa) 4.03 (dd, 1 H, $J_{H6Ba,\ H5B}$ = 2.5 Hz, H6Ba), 3.85 (ddd, 1 H, H5A), 3.83 (ddd, 1 H, $J_{H1'a,\ H1'b}$ = –9.9 Hz, $J_{H1'a,\ H2'a}$ = 6.2 Hz, $J_{H1'a,\ H2'b}$ = 5.7 Hz, H1′a), 3.63 (ddd, 1 H, H5B), 3.52 (ddd, 1 H, $J_{H1'b,\ H2'a}$ = 5.5 Hz, $J_{H1'b,\ H2'b}$ = 6.6 Hz, H1′b), 3.45 (ddd, 1 H, $J_{H3'a,\ H2'a}$ = 5.8 Hz, $J_{H3'a,\ H2'b}$ = 6.9 Hz, $J_{H3'a,\ H3'b}$ = –12.4 Hz, H3′a), 3.41 (ddd, 1 H, $J_{H3'b,\ H2'a}$ = 7.2 Hz, $J_{H3'b,\ H2'b}$ = 5.8 Hz, H3′b), 2.24, 2.13, 2.10, 2.042, 2.037, 2.03, 2.01 (each s, each 3 H, COCH_3), 1.91 (ddddd, 1 H, $J_{H2'b,\ H2'a}$ = –11.1 Hz, H2′b), 1.90 (ddddd, 1 H, H2′a).

^{13}C NMR (150.9 MHz, $CDCl_3$, 25 °C): δ =171.0, 170.7, 170.30, 170.28, 169.7, 169.3 (O*C*OCH_3), 97.6 (C1A), 96.4 (C1B), 72.3 (C5B), 72.2 (C2A), 70.6 (C3B), 70.3 (C3A), 68.7 (C5A), 68.5 (C2B), 66.1 (C4B), 65.1 (C4A), 64.7 (C1′), 62.4 (C6B), 61.9 (C6A), 48.2 (C3′), 28.7 (C2′).

HRSM: *m/z* calcd. for $C_{29}H_{41}N_3NaO_{18}$ $[M+Na]^+$: 742.2277, found: 724.2282; *m/z* calcd. for $C_{29}H_{41}N_3KO_{18}$ $[M+K]^+$: 758.2017, found: 758.1995.

1,2,3-tris [1-(3-{*O*-(2,3,4,6-tetra-*O*-acetyl-β-D-mannopyranosyl)-(1→2)-3,4,6-tri-*O*-acetyl-α-D-mannopyranosyloxy}propyl)-4-methyloxy-1,2,3-triazolyl]propane (2): To a solution of **14** (300 mg, 0.41 mmol, 3.2 equivalents) and 1,2,3-tris (prop-2-yn-1-yloxy)propane in ^{t}BuOH:H_2O:CH_2Cl_2 (6 mL 1:1:1) were added CuSO4 (6.3 mg, 0.042 mmol, 0.3 equivalents) and sodium ascorbate (15.4 mg 0.08 mmol, 0.6 equivalents). The reaction mixture was stirred at 55 °C for 12 h after which it was quenched by adding satd. NH_4Cl solution and H_2O (20 mL 1:1). The mixture was extracted with CH_2Cl_2 (3 × 20 mL) and the organic layer was dried over Na_2SO_4 and concentrated. The crude mixture was

purified by column chromatography (4 % MeOH in CH_2Cl_2) to afford pure product **10** as a white solid. R_f = 0.20. Yield: 160 mg (62 %). $[\alpha]_D^{25}$ = –53.7° (c 1.0, $CHCl_3$). ^{1}H NMR (600.13 MHz, $CDCl_3$, 25 °C): δ = 7.72 (s, 1 H, triaz. H), 7.65 (s, 2 H, 2 × triaz. H), 5.52–5.49 (m, 3 H, 3 × H2B), 5.26 (m, 3 H, 3 × H4A), 5.25 (m, 3 H, 3 × H4B), 5.08–5.04 (m, 3 H, 3 × H3B), 4.96, (m, 3 H, 3 × H3A), 4.79 (s, 2 H, G2-OC*H*$_2$), 4.79–4.76 (m, 3 H, 3 × H1A), 4.76–4.73 (m, 3 H, 3 × H1B), 4.65 (s, 4 H, G1-OC*H*$_2$), 4.55–4.43 (m, 6 H, 6 × H3′), 4.34 (m, 3 H, 3 × H6Bb), 4.32–4.29 (m, 3 H, 3 × H2A), 4.25 (m, 3 H, 3 × H6Ab), 4.08–4.01 (m, 6 H, 3 × H6Aa, 3 × H6Ba), 3.90–3.85 (m, 3 H, 3 × H5A), 3.83 (m, 1 H, HG2), 3.80–3.73 (m, 3 H, 3 × H1′a), 3.72–3.60 (m, 7 H, 3 × H5B, 4 × HG1), 3.46–3.39 (m, 3 H, 3 × H1′b), 2.28–2.17 (m, 15 H, 6 × H2′, 3 × COC*H*$_3$), 2.11, 2.09, 2.042, 2.038, 2.03, 2.01 (each s, each 9 H, 18 × COC*H*$_3$).

^{13}C NMR (150.9 MHz, $CDCl_3$, 25 °C): δ =171.0, 170.6, 170.34, 170.32, 169.9, 169.7, 169.3 (*C*OCH$_3$), 145.6, 145.2 (C4, triaz.), 122.9, 122.8 (C5, triaz.), 97.8 (C1A), 96.3 (C1B), 77.3 (CG2), 72.14, 72.13 (C5B), 72.1 (C2A), 70.7 (C3B), 70.3 (C3A), 70.3, 70.2 (CG1), 68.8, 68.7 (C5A), 68.5 (C2B), 66.1 (C4B), 65.0 (C4A), 64.8 (G1-O*C*H$_2$), 64.61, 61.58 (C1′), 63.8 (G2-O*C*H$_2$), 62.4 (C6B), 61.8 (C6A), 47.19, 47.16, (C3′), 29.98, 29.95 (C2′), 20.81, 20.76, 20.7, 20.62, 20.58 (CO*C*H$_3$).

HRSM: *m/z* calcd. for $C_{99}H_{138}N_9O_{57}$ $[M+H]^+$: 2364.8171, found: 2364.8168.

2-[2-(2-azidoethoxy)ethoxy]ethyl 2-*O*-acetyl-4,6-*O*-benzylidene-3-*O*-(4-methoxybenzyl)-α-D-mannopyranoside (9): To a solution of Phenyl 2-acetyl-4,6-*O*-benzylidene-3-*O*-(4-methoxybenzyl)-thio-α-D-mannopyranoside (1000 mg, 1.92 mmol, 1 equivalent) and 2-[2-(2-azidoethoxy)ethoxy]ethanol (403 mg, 2.30 mmol, 1.2 equivalents) in dry CH_2Cl_2 (40 mL) at –40 °C were added 4 Å molecular sieves NIS (517 mg, 2.30 mmol, 1.2 equivalents) and TMSOTf (83 µl, 0.23 mmol, 0.24 equivalents). The reaction mixture was stirred at –40 °C for 2 h and then quenched by adding a satd. solution of $NaHCO_3$ (20 mL). The reaction mixture was brought to room temperature and diluted with CH_2Cl_2 (50 mL) and washed with satd. $NaHCO_3$ solution (50 mL) after which the aqueous layer was extracted with CH_2Cl_2 (2 × 50 mL). The combined organic layers were washed with of brine (100 mL), dried over Na_2SO_4 and concentrated. The crude mixture was purified by column chromatography (hexane : EtOAc 2 : 1 → 1 : 1) to afford the pure product **9** as a slightly yellow oil. R_f: 0.33 (hexane: EtOAc 1 : 1). Yield 790 mg (70 %). $[\alpha]_D^{24}$ = +20.0° (c 2.30, $CHCl_3$). ^{1}H NMR (600.13 MHz, $CDCl_3$, 25 °C): δ = 7.50 (m, 2 H, arom. H), 7.40–7.34 (m, 3 H, arom. H), 7.27 (m, 2 H, arom. H), 6.83 (m, 2 H, arom. H), 5.62 (s, 1 H, 4,6-OC*H*Ph), 5.42,

(dd, 1 H, $J_{H2,\ H1}$ = 1.6 Hz, $J_{H2,\ H3}$ = 3.5 Hz, H2), 4.83, (d, 1 H, H1), 4.64 and 4.58 (each d, each 1 H, *J* = –11.56 Hz, 3-OC*H*$_2$Ph), 4.25 (dd, 1 H, $J_{H6a,\ H5}$ = 4.8 Hz, $J_{H6a,\ H6b}$ = –10.24 Hz, H6a), 4.03 (dd, 1 H, $J_{H4,\ H3}$ = 10.0 Hz, $J_{H4,\ H5}$ = 9.5 Hz, H4), 4.01 (dd, 1 H, H3), 3.91 (ddd, 1 H, $J_{H5,\ H6b}$ = 10.4 Hz, H5), 3.83 (dd, 1 H, H6b), 3.80 (m, 1 H, H1′a), 3.79 (s, 3 H, 3-OC*H*$_3$), 3.68–3.61 (m, 9 H, H1′b, H2′, H3′, H4′, H5′), 3.34 (m, 2 H, H6′), 2.15 (s, 3 H, COC*H*$_3$).

^{13}C NMR (150.9 MHz, $CDCl_3$, 25 °C): δ =170.2 (2-O*C*OCH$_3$), 159.2, 137.5, 130.1, 129.3, 128.9, 128.1, 126.1, 113.7 (arom. C), 101.5 (4,6-O*C*HPh), 98-8 (C1), 78.3 (C4) 73.6 (C3), 71.8 (3-O*C*H$_2$Ph), 70.8, 70.7, 70.1 (C2′, C3′, C4′, C5′), 69.7 (C2), 68.7 (C6), 67.0 (C1′), 63.8 (C5), 55.2 (3-O*C*H$_3$), 50.6 (C6′), 21.0 (2-OCO*C*H$_3$).

HRSM: *m/z* calcd. for $C_{29}H_{41}N_4O_{10}$ $[M+NH_4]^+$: 605.2817, found: 605.2829, *m/z* calcd. for $C_{29}H_{37}N_3NaO_{10}$ $[M+Na]^+$: 610.2371, found: 610.2361.

2-[2-(2-azidoethoxy)ethoxy]ethyl 4,6-*O*-benzylidene-3-*O*-(4-methoxybenzyl)-α-D-mannopyranoside (11): The pH of a solution of **9** (490 mg, 0.83 mmol) in dry methanol (4 mL) under argon atmosphere was adjusted to ~10 – 12 by adding a few drops of a 5.4 M solution of NaOMe in MeOH. The reaction mixture was stirred at room temperature for 30 min and then neutralized with DOWEX-50WX8 H^+ form. The reaction mixture was filtered and concentrated to afford the pure product **11** as a yellow/orange oil. Yield: 441 mg (97 %). $[\alpha]_D^{24}$ = +21.0° (c 1.10, $CHCl_3$). ^{1}H NMR (600.13 MHz, $CDCl_3$, 25 °C): δ = 7.51 (m, 2 H, arom. H), 7.42–7.35 (m, 3 H, arom. H), 7.30 (m, 2 H, Arom. H), 6.88 (m, 2 H, arom. H), 5.61 (s, 1 H, 4,6-OC*H*Ph), 4.91 (d, 1 H, $J_{H1,\ H2}$ = 1.5 Hz, H1), 4.78 and 4.65 (each d, each 1 H, *J* = –11.4 Hz, 3-OC*H*$_2$Ph), 4.26 (dd, 1 H, $J_{H6a,\ H5}$ = 4.5 Hz, $J_{H6a,\ H6b}$ = –9.3 Hz, H6a), 4.081 (dd, 1 H, $J_{H2,\ H3}$ = 3.5 Hz, H2), 4.076 (dd, 1 H, $J_{H4,\ H3}$ = 9.6 Hz, $J_{H4,\ H5}$ = 9.5 Hz, H4), 3.93 (dd, 1 H, H3), 3.88 (ddd, 1 H, $J_{H5,\ H6b}$ = 9.6 Hz, H5), 3.84 (dd, 1 H, H6b), 3.85–3.82 (m, 1 H, H1′a), 3.81 (s, 3 H, 3-OC*H*$_3$), 3.71–3.65 (m, 9 H, H1′b, H2′, H3′, H4′, H5′), 3.37 (m, 2 H, H6′)

^{13}C NMR (150.9 MHz, $CDCl_3$, 25 °C): δ = 159.5, 137.7, 130.3, 129.6, 129.0, 128.3, 126.2, 114.0 (arom. C), 101.6 (4,6-O*C*HPh), 101.1 (C1), 79.0 (C4), 75.4 (C3), 72.8 (3-O*C*H$_2$Ph), 70.91, 70.87, 70.4, 70.3 (C2′, C3′, C4′, C5′), 70.0 (C2), 69.0 (C6), 66.9 (C1′), 63.4 (C5), 55.4 (3-O*C*H$_3$), 50.8 (C6′).

HRSM: *m/z* calcd. for $C_{27}H_{39}N_4O_9$ $[M+NH_4]^+$: 563.2712, found: 563.2691, *m/z* calcd. for $C_{27}H_{35}N_3NaO_9$ $[M+Na]^+$: 568.2266, found: 568.2267.

2-[2-(2-azidoethoxy)ethoxy]ethyl *O*-[4,6-*O*-benzylidene-2,3-di-*O*-(4-methoxybenzyl)-β-D-mannopyranosyl]-(1→2)-4,6-*O*-benzylidene-3-*O*-(4-methoxybenzyl)-α-D-mannopyranoside (13): To a solution of Phenyl 4,6-*O*-benzylidene-2,3-di-*O*-(4-methoxybenzyl)-thio-α-D-mannopyranoside (1059 mg, 1.76 mmol, 1.3 equivalents) in dry CH_2Cl_2 (15 mL) and 1-octene (5 mL) was added 4 Å molecular sieves after which the solution was cooled down to –60 °C. BSP (526 mg, 2.12 mmol, 1.56 equivalents), TTBP (568 mg, 2.71 mmol, 2 equivalents) and Tf_2O (386 µl, 2.29 mmol, 1.69 equivalents) were added and the reaction mixture was stirred at –60 °C for 30 min. The reaction mixture was then cooled down to –78 °C and **11** (740 mg, 1.36 mmol, 1 equivalent) in dry CH_2Cl_2 (5 mL) was added. The reaction mixture was stirred at –78 °C for 3 h and then quenched by adding Et_3N (1 mL) and allowing the reaction mixture return to room temperature over 30 min. The reaction mixture was diluted with CH_2Cl_2 (50 mL) and then washed with satd. $NaHCO_3$ solution (50 mL). The water layer was extracted with CH_2Cl_2 (2 × 50 mL) and the combined organic layers were washed with brine (100 mL), dried over Na_2SO_4 and concentrated. Column chromatography (Hexane : EtOAc 2 : 1 → 1 : 1) afforded pure **13** as a clear oil. R_f = 0.35 (Hexane : EtOAc 1 : 1). Yield: 613 mg (43 %). $[\alpha]_D^{24}$ = –36.0° (c 1.36, $CHCl_3$). ^{1}H NMR (600.13 MHz, $CDCl_3$, 25 °C): δ = 7.51–7.47 (m, 4 H, arom. H), 7.43 (m, 2 H, arom. H), 7.40–7.32 (m, 8 H, arom. H), 7.19 (m, 2 H, arom. H), 6.86–6.79 (m, 6 H, arom. H), 5.59 (s, 1 H, 4B,6B-OC*H*Ph), 5.51 (s, 1 H, 4A,6A-OC*H*Ph), 4.96 and 4.89 (each d, each 1 H, J = –11.9 Hz, 2B-OCH_2Ph), 4.84 (d, 1 H, $J_{H1A,\ H2A}$ = 0.7 Hz, H1A), 4.71 and 4.62 (each d, each 1 H, J = –11.5 Hz, 3A-OCH_2Ph), 4.60 and 4.53 (each d, each 1 H, J = –12.0 Hz, 3B-OCH_2Ph), 4.60 (s, 1 H, H1B), 4.27 (dd, 1 H, $J_{H2A,\ H3A}$ = 3.0 Hz, H2A), 4.26 (dd, 1 H, $J_{H6Ba,\ H5B}$ = 5.9 Hz, $J_{H6Ba,\ H6Bb}$ = –10.6 Hz, H6Ba), 4.25 (dd, 1 H, $J_{H6Aa,\ H5}$ = 4.9 Hz, $J_{H6Aa,\ H6Ab}$ = –11.2 Hz, H6Aa), 4.22 (dd, 1 H, $J_{H4B,\ H3B}$ = 9.8 Hz, $J_{H4B,\ H5B}$ = 9.5 Hz, H4b), 4.08 (dd, 1 H, $J_{H4A,\ H3A}$ = 9.9 Hz, $J_{H4A,\ H5A}$ = 9.7 Hz, H4A), 3.96 (dd, 1 H, H3A), 3.93 (d, 1 H, $J_{H2B,\ H3B}$ = 3.1 Hz, H2B) 3.87 (dd, 1 H, $J_{H6Bb,\ H5B}$ = 9,9 Hz, H6Bb), 3.85 (ddd, 1 H, $J_{H5A,\ H6Ab}$ = 9.9 Hz, H5A), 3.82 (m, 1 H, H1′), 3.80 (s, 3 H, OCH_3), 3.774 (s, 3 H, OCH_3), 3.766 (dd, 1 H, H6Ab), 3.76 (s, 3 H, OCH_3), 3.69–3.59 (m, 9 H, H1′b, H2′, H3′, H4′, H5′), 3.55 (dd, 1 H, H3B), 3.32 (m, 2 H, H6′), 3.30 (ddd, 1 H, H5B).

^{13}C NMR (150.9 MHz, $CDCl_3$, 25 °C): δ = 159.23, 159.22, 159.1, 137.71, 137.70, 131.1, 130.7, 130.52, 130.45, 129.3, 129.2, 128.9, 128.30, 128.26, 126.22, 126.15, 113.79, 113.65, 113.6 (arom. C), 101.7 (4A,6A-O*C*HPh), 101.5 (4B,6B-O*C*HPh), 101.0 (C1B), 98.5 (C1A), 78.7 (C4A), 78.6 (C4B), 77.3 (C3B), 75.3 (C2B), 74.9 (C2A), 74.2 (2B-O*C*H_2Ph), 72.0 (3B-O*C*H_2Ph), 70.94

(3A-O*C*H$_2$Ph), 70.91, 70.8, 70.3, 70.2 (C2′, C3′, C4′, C5′), 69.0 (C6A), 68.7 (C6B), 67.9 (C5B), 67.0 (C1′), 64.3 (C5A), 55.38, 55.36, 55,3 (3 × O*C*H$_3$), 50.7 (C6′).

HRSM: *m/z* calcd. for $C_{56}H_{69}N_4O_{16}$ $[M+NH_4]^+$: 1053.4703, found: 1053.4669, *m/z* calcd. for $C_{56}H_{65}N_3NaO_{16}$ $[M+Na]^+$: 1058.4257, found: 1058.4208.

2-[2-(2-azidoethoxy)ethoxy]ethyl *O*-(2,3,4,6-tetra-*O*-acetyl-β-D-mannopyranosyl)-(1→2)-3,4,6-tri-*O*-acetyl-α-D-mannopyranoside (15): To a solution of **13** (200 mg, 0.19 mmol, 1 equivalent) in 10 mL of CH_2Cl_2 was added 1,3-propanedithiol (155 µl, 1,54 mmol, 8 equivalents) and the mixture was cooled down on an ice bath. TFA (4 mL) and H_2O (1 mL) were added and the reaction mixture was stirred at room temperature for 3 h. The reaction mixture was then diluted with H_2O (100 mL) and washed with CH_2Cl_2 (4 × 50 mL) after which the aqueous layer was evaporated and coevaporated with toluene. The residue was dissolved in pyridine (20 mL) and cooled on an ice bath while Ac_2O (10 mL) was added. The reaction mixture was then stirred at room temperature for 18 h after which the reaction was cooled on an ice bath and quenched by adding methanol (10 mL). The reaction mixture was diluted with CH_2Cl_2 (50 mL), washed with H_2O (4 × 50 mL) and brine (50 mL). The organic layer was dried over Na_2SO_4 and concentrated. The crude mixture was purified by column chromatography (hexane : EtOAc 1 : 1 → CH_2Cl_2 : methanol 20 : 1) to afford pure **15** as a clear oil. R_f = 0.34 (CH_2Cl_2 : methanol 20 : 1). Yield: 113 mg (75 %). $[\alpha]_D^{24}$ = –51.5° (c 1.62, $CHCl_3$). ^{1}H NMR (600.13 MHz, $CDCl_3$, 25 °C): δ = 5.51 (dd, 1 H, $J_{H2B, H1B}$ = 0.7 Hz, $J_{H2B, H3B}$ = 3.4 Hz, H2B), 5.27 (t, 1 H, $J_{H4A, H3A}$ = $J_{H4A, H5A}$ = 10.1 Hz, H4A), 5.22 (dd, 1 H, $J_{H4B, H3B}$ = 10.0 Hz, $J_{H4B, H5B}$ = 9.9 Hz, H4B), 5.05 (dd, 1 H, H3B), 5.02 (dd, 1 H, $J_{H3A, H2A}$ = 3.4 Hz, H3A), 4.88 (d, 1 H, $J_{H1A, H2A}$ = 1.8 Hz, H1A), 4.69 (d, 1 H, H1B), 4.36 (dd, 1 H, H2A), 4.32 (dd, 1 H, $J_{H6Bb, H5B}$ = 6.0 Hz, $J_{H6Bb, H6Ba}$ = –12.2 Hz, H6Bb), 4.26 (dd, 1 H, $J_{H6Ab, H5A}$ = 3.8 Hz, $J_{H6Ab, H6Aa}$ = –12.3 Hz, H6Ab) 4.06 (dd, 1 H, $J_{H6Aa, H5A}$ = 2.3 Hz, H6Aa), 4.02 (dd, 1 H, $J_{H6Ba, H5B}$ = 2.4 Hz, H6Ba), 3.94 (ddd, 1 H, H5A), 3.81 (m, 1 H, H1′a), 3.72–3.64 (m, 9 H, H1′b, H2′, H3′, H4′, H5′), 3.64 (ddd, 1 H, H5B), 3.40 (m, 2 H, H6′), 2.25 (s, 3 H, 2B-COC*H*$_3$), 2.13 (s, 3 H, 6A-COC*H*$_3$), 2.10 (s, 3 H, 6B-COC*H*$_3$), 2.05 (s, 3 H, 4A-COC*H*$_3$), 2.03 (s, 3 H, 4B-COC*H*$_3$), 2.02 (s, 3 H, 3A-COC*H*$_3$), 2.01 (s, 3 H, 3B-COC*H*$_3$).

^{13}C NMR (150.9 MHz, $CDCl_3$, 25 °C): δ = 171.0 (6A-*C*OCH$_3$), 170.7 (6B-*C*OCH$_3$), 170.3 (2B-*C*OCH$_3$), 170.2 (3A-*C*OCH$_3$), 170.0 (3B-*C*OCH$_3$), 169.7 (4B-*C*OCH$_3$), 169.3 (4A-*C*OCH$_3$), 97.5 (C1A), 96.3 (C1B), 72.22 (C5B), 72.17 (C2A), 70.73, 70.72 (C3′, C4′), 70.6 (C3B), 70.3 (C3A), 70.2 (C2′), 70.1 (C5′),

68.52 (C2B), 68.50 (C5A), 67.1 (C1′), 66.1 (C4B), 65.1 (C4A), 62.5 (C6B), 61.8 (C6A), 50.7 (C6′), 20.8, 20.74, 20.70, 20.62, 20.57 (CO*C*H_3).

HRSM: *m/z* calcd. for $C_{32}H_{51}N_4O_{20}$ $[M+NH_4]^+$: 811.3091, found: 811.3083, *m/z* calcd. for $C_{32}H_{47}N_3NaO_{20}$ $[M+Na]^+$: 816.2645, found: 816.2621.

1,2,3-tris (1-{2-[2-(2-[*O*-(2,3,4,6-tetra-*O*-acetyl-β-D-mannopyranosyl)-(1→2)-3,4,6-tri-*O*-acetyl-α-D-mannopyranosyloxy]ethoxy)ethoxy]ethyl}-4-methyloxy-1,2,3-triazolyl)propane (3): To a solution of **15** (70 mg, 0.088 mmol, 3.3 equivalents) and 1,2,3-tris (prop-2-yn-1-yloxy)propane (5.5 mg, 0.027 mmol, e equivalent) in of CH_2Cl_2 (2 mL) were added *t*-BuOH (2 mL) and H_2O (2 mL). $CuSO_4$ (2.8 mg, 0.017 mmol, 0.66 equivalents) and Na-ascorbate (7.0 mg, 0.035 mmol, 1.32 equivalents) were added and the reaction mixture was stirred at 55 °C for 18 h. A saturated solution of NH_4Cl (10 mL) and H_2O (10 mL) were added and the reaction mixture was extracted with CH_2Cl_2 (4 × 20 mL). The combined organic layers were dried over Na_2SO_4 and concentrated. The crude mixture was purified by column chromatography (CH_2Cl_2 : methanol 20 : 1 → 5 : 1) to afford the pure product **15** as a white solid. R_f =0.16 (CH_2Cl_2 : methanol 20 : 1). Yield: 62 mg (89 %). $[\alpha]_D^{24}$ = –37.0° (c 1.05, $CHCl_3$). ^{1}H NMR (600.13 MHz, $CDCl_3$, 25 °C): δ = 7.81, 7.772, 7.769 (each s, each 1 H, 3 × triaz. H), 5.52–5.49 (m, 3 H, 3 × H2B), 5.27 (m, 3 H, 3 × H4A), 5.23 (m, 3 H, 3 × H4B), 5.06 (m, 3 H, 3 × H3B), 5.01–4.97 (m, 3 H, 3 × H3A), 4.85 (m, 3 H, 3 × H1A), 4.78 (s, 2 H, G2-OCH_2), 4.72 (m, 3 H, 3 × H1B), 4.64 (s, 4 H, G1-OCH_2), 4.60–4.51 (m, 6 H, 6 × H6′), 4.36–4.30 (m, 6 H, 3 × H6Bb, H2A), 4.24 (m, 3 H, 3 × H6Ab), 4.06 (m, 3 H, 3× H6Aa), 4.03–3.98 (m, 3 H, 3 × H6Ba), 3.95–3.86 (m, 9 H, 3 × H5A, 6 × H5′), 3.85–3.75 (m, 4 H, HG2, 3 × H1′a), 3.68–3.58 (m, 28 H, 3 × H5B, 4 × HG1, 3 × H1′b, 6 × H2′, 6 × H3′, 6 × H4′), 2.24, 2.12, 2.09, 2.04, 2.03, 2.02, 2.01 (each s, each 9 H, 21 × CO*C*H_3).

^{13}C NMR (150.9 MHz, $CDCl_3$, 25 °C): δ = 171.0, 170.6, 170.33, 170.29, 170.0, 169.7, 169.3 (*C*OCH$_3$), 145.1, 144.7 (C4, triaz.), 124.0, 123.9 (C5, triaz.), 97.6 (C1A), 96.29, 96.27 (C1B), 77.2 (CG2), 72.11, 72.08 (C5B, C2A), 70.67, 70.65 (C3B), 70.51, 70.49 (C3′, C4′), 70.29, 70.26 (C3A), 70.2 (CG1), 70.1 (C2′), 69.5 (C5′), 68.53 (C2B), 68.49 (C5A), 67.0 (C1′), 66.1 (C4B), 65.1 (C4A), 64.8 (G1-O*C*H$_2$), 63.8 (G2-O*C*H$_2$), 62.4 (C6B), 61.8 (C6A), 50.2, 50.16 (C6′), 20.79, 20.75, 20.7, 20.62, 20.57 (CO*C*H$_3$).

HRSM: *m/z* calcd. for $C_{108}H_{155}N_9NaO_{63}$ $[M+Na]^+$: 2608.9094, found: 2608.8944.

Biological study subjects: During pollen season, 14 adult birch allergic subjects with allergic rhinoconjunctivitis (12 females and two males) were enrolled in the

study (mean age 42.5 years, SD 12.4 years; mean birch-specific IgE (Immunocap, Thermo Fisher Scientific Phadia, Uppsala, Sweden) 36.1 kU L^{-1}, SD 31.5 kU L^{-1}). They were selected for the study from an earlier cohort based on good birch induced IL-4 responses during pollen season. All samples were taken after informed consent. The study was approved by the local ethics committee.

Adjuvants in the biological studies: Compound **1** was synthesized as previously described.[33] Compounds **2** and **3** were prepared according to the methods described herein. Synthetic MPLA and CpG-ODN (tlrl-2006) were purchased from Invivogen (San Diego, CA, USA). The CpG-ODN had a sequence of 5´-TCG TCG TTT TGT CGT TTT GTC GTT-3´, identical to one used in a previous study.[59]

PBMC cultures: The PBMC were isolated by Ficoll-Paque density gradient centrifugation (Ficoll-Paque PLUS, GE Healthcare Bio-Sciences AB, Uppsala, Sweden) from heparinized blood samples from study subjects during pollen season. The PBMC were washed twice with Hanks' balanced salt solution (HBSS) buffered with $NaHCO_3$ (pH 7.4) and resuspended in RPMI-1640 culture medium (Invitrogen Co., Carlsbad, CA, USA) supplemented with 5% autologous serum, 2.5 mM L-glutamine (Sigma-Aldrich Co., St. Louis, MO) and 100 µg mL^{-1} gentamycin sulfate (Biological Industries Ltd., Kibbutz Beit Haemek, Israel) and applied on 48-well flat-bottomed cell culture plates (Costar, Corning Inc., New York, United States) at a density of 106/ml. Cells were co-cultured in the presence of birch allergen (50 µg mL^{-1}, *Betula verrucosa*, Bet v, Aquagen, ALK-Abelló A/S, Hørsholm, Denmark) and adjuvants **1**, **2**, **3** and MPLA with concentrations 1, 10 and 100 µg mL^{1} and adjuvant CpG-ODN with concentrations 2, 20 and 200 µg mL^{-1} (marked as 1, 10 and 100 µg mL^{-1} in figures 10 and 11 for the sake of simplicity) to achieve equal molarities. Medium alone served as an unstimulated control. All incubations were performed at +37ºC in humidified atmosphere with 5% CO_2. Supernatants from cultures performed in duplicate were collected 72 h after beginning of the stimulation and stored at -70ºC.

IL-4 and TNF production: The cytokines IL-4 and TNF in supernatants were measured with high-sensitivity human cytokine Lincoplex kits (LINCO Research, St. Charles, MO, USA). The assays were performed in accordance with the manufacturer's protocol by employing Luminex technology.

Statistics: Wilcoxon´s Signed Rank test was used to test statistical significance in PBMC experiments. Data are expressed as mean ± SEM and P-values of < 0.05 are considered statistically significant.

TLR ligation screening: Ligation screening was performed with molecules **1**[33] and **3** as well as with the fully deacetylated analogue of **1** by InvivoGen™,[60] using HEK-293 cell lines functionally overexpressing human TLR:s 2,3,4,5,7,8 and 9. Two different concentrations, 4 μM and 40 μM were used which approximately correspond to the concentrations employed in the PBMC screening.

3.9 References

1. Kiessling, L. L., Gestwicki, J. E. & Strong, L. E. Synthetic multivalent ligands in the exploration of cell-surface interactions. *Curr. Opin. Chem. Biol.* **4,** 696–703 (2000).

2. Pieters, R. J. Carbohydrate Mediated Bacterial Adhesion. *Adv. Exp. Med. Biol.* **715,** 227–240 (2011).

3. Karlsson, K.-A. Pathogen-Host Protein-Carbohydrate Interactions as the Basis ofImportant Infections. *Adv. Exp. Med. Biol.* **491,** 431–443 (2001).

4. Sharon, N. *Carbohydrate-Lectin Interactions in Infectious Disease*. *Advances in Experimental Medicine and Biology* **408,** (1996).

5. Imberty, A. & Varrot, A. Microbial recognition of human cell surface glycoconjugates. *Current Opinion in Structural Biology* **18,** 567–576 (2008).

6. Bhatia, S., Dimde, M. & Haag, R. Multivalent glycoconjugates as vaccines and potential drug candidates. *Med. Chem. Commun.* **5,** 862–878 (2014).

7. Krantz, M. J., Holtzman, N. A., Stowell, C. P. & Lee, Y. C. Attachment of thioglycosides to proteins: enhancement of liver membrane binding. *Biochemistry* **15,** 3963–3968 (1976).

8. Chipowsky, S., Lee, Y. C. & Roseman, S. Adhesion of cultured fibroblasts to insoluble analogues of cell-surface carbohydrates. *Proc. Natl. Acad. Sci. U. S. A.* **70,** 2309–12 (1973).

9. Weigel, P. H., Schmell, E., Lee, Y. C. & Roseman, S. Specific Adhesion of Rat Hepatocytes to β-Galactosides Linked to Polyacrylamide Gels*. *J. Biol. Chem.* **253,** 330–333 (1978).

10. Bernardi, A. *et al*. Multivalent glycoconjugates as anti-pathogenic agents. *Chem. Soc. Rev.* **42,** 4709–4727 (2013).

11. Müller, C., Despras, G. & Lindhorst, T. K. Organizing multivalency in carbohydrate recognition. *Chem. Soc. Rev.* **45,** 3275–3302 (2016).

12. Chabre, Y. M. & Roy, R. *Design and creativity in synthesis of multivalent neoglycoconjugates. Advances in carbohydrate chemistry and biochemistry* **63,** (2010).

13. Astronomo, R. D. & Burton, D. R. Carbohydrate vaccines: developing sweet solutions to sticky situations? *Nat. Rev. Drug Discovery* **9,** 308–

324 (2010).

14. Szabo, S. J., Sullivan, B. M., Peng, S. L. & Glimcher, L. H. Molecular mechanisms regulating Th1 immune responses. *Annu. Rev. Immunol.* **21,** 713–58 (2003).

15. Durham, S. R. *et al.* Cytokine messenger RNA expression for IL-3, IL-4, IL-5, and granulocyte/macrophage-colony-stimulating factor in the nasal mucosa after local allergen provocation: relationship to tissue eosinophilia. *J. Immunol.* **148,** 2390–4 (1992).

16. Kay, A. B. Allergy and Allergic Diseases. *N. Engl. J. Med.* **344,** 30–37 (2001).

17. Luzina, I. G. *et al.* Regulation of inflammation by interleukin-4: a review of 'alternatives'. *J. Leukocyte Biol.* **92,** 753–764 (2012).

18. Mosmann, T. R. & Sad, S. The expanding universe of T-cell subsets: Th1, Th2 and more. *Immunol. Today* **17,** 138–146 (1996).

19. Akdis, C. A., Blesken, T., Akdis, M., Wüthrich, B. & Blaser, K. Role of interleukin 10 in specific immunotherapy. *J. Clin. Invest.* **102,** 98–106 (1998).

20. Akdis, M. *et al.* Immune responses in healthy and allergic individuals are characterized by a fine balance between allergen-specific T regulatory 1 and T helper 2 cells. *J. Exp. Med.* **199,** 1567–75 (2004).

21. Galli, S. J., Tsai, M. & Piliponsky, A. M. The development of allergic inflammation. *Nature* **454,** 445–454 (2008).

22. Greenfeder, S., Umland, S. P., Cuss, F. M., Chapman, R. W. & Egan, R. W. Th2 cytokines and asthma. The role of interleukin-5 in allergic eosinophilic disease. *Respir. Res.* **2,** 71–79 (2001).

23. Gould, H. J. *et al.* THE BIOLOGY OF IGE AND THE BASIS OF ALLERGIC DISEASE. *Annu. Rev. Immunol.* **21,** 579–628 (2003).

24. Bousquet, P. J. *et al.* Sub-lingual immunotherapy: World allergy organization position paper 2009. *Allergy Eur. J. Allergy Clin. Immunol.* **64,** 1–59 (2009).

25. Rosewich, M., Lee, D. & Zielen, S. Pollinex Quattro: an innovative four injections immunotherapy in allergic rhinitis. *Hum. Vaccin. Immunother.* **9,** 1523–31 (2013).

26. Moingeon, P. Adjuvants for allergy vaccines. *Hum. Vaccines*

Immunother. **8,** 1492–1498 (2012).

27. Bode, C., Zhao, G., Steinhagen, F., Kinjo, T. & Klinman, D. M. CpG DNA as a vaccine adjuvant. *Expert Rev. Vaccines* **10,** 499–511 (2011).

28. Fonseca, D. E. & Kline, J. N. Use of CpG oligonucleotides in treatment of asthma and allergic disease. *Adv. Drug Delivery Rev.* **61,** 256–262 (2009).

29. Cooper, C. L. *et al.* CPG 7909, an immunostimulatory TLR9 agonist oligodeoxynucleotide, as adjuvant to Engerix-B?? HBV vaccine in healthy adults: A double-blind phase I/II study. *J. Clin. Immunol.* **24,** 693–701 (2004).

30. Jahrsdörfer, B. & Weiner, G. J. CpG oligodeoxynucleotides as immunotherapy in cancer. *Update Cancer Ther.* **3,** 27–32 (2008).

31. Vollmer, J. & Krieg, A. M. Immunotherapeutic applications of CpG oligodeoxynucleotide TLR9 agonists. *Adv. Drug Delivery Rev.* **61,** 195–204 (2009).

32. Ranta, K. *et al.* Evaluation of immunostimulatory activities of synthetic mannose-containing structures mimicking the β-(1→2)-linked cell wall mannans of Candida albicans. *Clin. Vaccine Immunol.* **19,** 1889–1893 (2012).

33. Mukherjee, C., Mäkinen, K., Savolainen, J. & Leino, R. Chemistry and biology of oligovalent β-(1→2)-linked oligomannosides: New insights into carbohydrate-based adjuvants in immunotherapy. *Chem. - A Eur. J.* **19,** 7961–7974 (2013).

34. Ranta, K. *et al.* Evaluation of fungal extracts to determine immunomodulatory properties. *J. Investig. Allergol. Clin. Immunol.* **23,** 226–233 (2013).

35. Mukherjee, C., Ranta, K., Savolainen, J. & Leino, R. Synthesis and Immunological Screening of β-Linked Mono- and Divalent Mannosides. *Eur. J. Org. Chem.* **2012,** 2957–2968 (2012).

36. Fall, A., Sene, M., Gaye, M., Gómez, G. & Fall, Y. Ionic liquid-supported TEMPO as catalyst in the oxidation of alcohols to aldehydes and ketones. *Tetrahedron Lett.* **51,** 4501–4504 (2010).

37. Deng, L. Q., Norberg, O., Uppalapati, S., Yan, M. D. & Ramstrom, O. Stereoselective synthesis of light-activatable perfluorophenylazide-conjugated carbohydrates for glycoarray fabrication and evaluation of structural effects on protein binding by SPR imaging. *Org. Biomol.*

Chem. **9,** 3188–3198 (2011).

38. Mourer, M., Hapiot, F., Tilloy, S., Monflier, E. & Menuel, S. Easily accessible mono- and polytopic β-cyclodextrin hosts by click chemistry. *Eur. J. Org. Chem.* **1,** 5723–5730 (2008).

39. Worrell, B. T., Malik, J. a. & Fokin, V. V. Direct Evidence of a Dinuclear Copper Intermediate in Cu(I)-Catalyzed Azide-Alkyne Cycloadditions. *Science* **340,** 457–460 (2013).

40. Boren, B. C. *et al.* Ruthenium-Catalyzed Azide-Alkyne Cycloaddition: Scope and Mechanism. *J. Am. Chem. Soc.* **130,** 8923–8930 (2008).

41. Weimar, T. & Woods, R. J. in *NMR Spectroscopy of Glycoconjugates* (ed. Jesús Jiménez-Barbero, T. P.) 109–144 (WILEY-VCH Verlag, GmbH & Co. KGaA, 2003).

42. Espinosa, J.-F. *et al.* Conformational Differences Between C- and O-Glycosides: The α-C-Mannobiose/α-O-Mannobiose Case. *Chem. - A Eur. J.* **5,** 442–448 (1999).

43. Zhou, C.-H. & Wang, Y. Recent Researches in Triazole Compounds as Medicinal Drugs. *Curr. Med. Chem.* **19,** 239–280 (2012).

44. Singhal, N., Sharma, P. K., Dudhe, R. & Kumar, N. Recent advancement of triazole derivatives and their biological significance. *J. Chem. Pharm. Res.* **3,** 126–133 (2011).

45. Swardfager, W. *et al.* A meta-analysis of cytokines in Alzheimer's disease. *Biol. Psychiatry* **68,** 930–941 (2010).

46. Locksley, R. M., Killeen, N. & Lenardo, M. J. The TNF and TNF receptor superfamilies: Integrating mammalian biology. *Cell* **104,** 487–501 (2001).

47. Osredkar, J. Copper and Zinc, Biological Role and Significance of Copper/Zinc Imbalance. *J. Clin. Toxicol.* **s3,** (2011).

48. Festa, R. A. & Thiele, D. J. Copper: An essential metal in biology. *Current Biology* **21,** R877–R883 (2011).

49. Scheiber, I., Dringen, R. & Mercer, J. F. B. Copper: Effects of Deficiency and Overload. *Met. Ions Life Sci.* **13,** 359–387 (2013).

50. Masuoka, J. Surface Glycans of Candida albicans and Other Pathogenic Fungi : Physiological Roles, Clinical Uses, and Experimental Challenges. *Clin. Microbiol. Rev.* **17,** 281–310 (2004).

51. McKay, C. S. & Finn, M. G. Click chemistry in complex mixtures: Bioorthogonal bioconjugation. *Chem. Biol.* **21,** 1075–1101 (2014).

52. Lech, T. & Sadlik, J. K. Copper concentration in body tissues and fluids in normal subjects of southern Poland. *Biol. Trace Elem. Res.* **118,** 10–15 (2007).

53. Sachs, A., Levine, V. E., Hill, F. C. & Hughes, R. Copper and Iron in Human Blood. *Arch. Intern. Med.* **71,** 489–501 (1943).

54. Tompsett, S. L. The copper content of blood. *Biochem. J.* **28,** 1544–9 (1934).

55. Savolainen, J., Ranta, K., Leino, R. & Mukherjee, C. Multivalent [beta] - 1 - 2 - linked mannose oligosaccharides as immunostimulatory compounds and uses thereof. (2012).

56. PERCH, PERCH Solutions Ltd., Kuopio (Finland). (2010).

57. Maestro, version 8.5, Schrödinger, LCC,New York, NY (USA). (2008).

58. Desmond, version 3.9, Schrödinger, LCC,New York, NY (USA). (2013).

59. Marshall, J. D. *et al.* Immunostimulatory sequence DNA linked to the Amb a 1 allergen promotes T(H)1 cytokine expression while downregulating T(H)2 cytokine expression in PBMCs from human patients with ragweed allergy. *J. Allergy Clin. Immunol.* **108,** 191–7 (2001).

60. InvivoGen, Toulouse, France, http://www.invivogen.com/. (2015).

4 Size matters (or does it?)

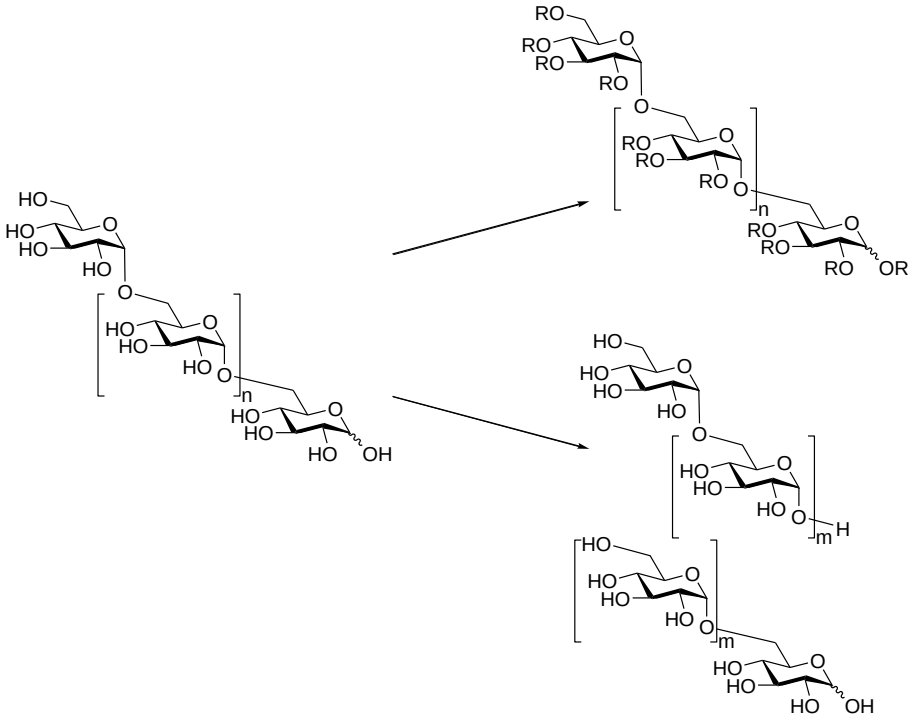

Polysaccharides are one of the most important renewable resources, and new applications are sought constantly. Their important roles in biological systems make them attractive targets for investigating biological events and developing treatments for various conditions. Natural polysaccharides are, however, inherently heterogeneous, which often complicates the use of them as such. In this chapter, preparation of well-defined natural polysaccharide mimics is explored and their interactions with biological targets are investigated. Furthermore, a new method for fragmenting polysaccharides into regularly sized fragments using readily available reagents is presented.

This chapter is based on unpublished results: **Mimicking Saccharide Interactions in Nature: NMR Studies of Dextran-Supported Multivalent Molecular Probes Show Distinct Glycan-Lectin Recognition Features,** J. Rahkila, F. S. Ekholm, J. Savolainen, A. Ardá, S. Delgado, J. Jiménez-Barbero, R. Leino, *manuscript submitted*; **Cu(I) Mediated Degradation of Polysaccharides Leads to Fragments With Narrow Polydispersities,** J. Rahkila, F. S. Ekholm, R. Leino, *Eur. J. Org. Chem.* **2018,** Accepted manuscript online: 17 Jan 2018, DOI: 10.1002/ejoc.201800033.

4.1 Introduction

Polysaccharides play many important roles in nature, for example as structural components, such as cellulose in plants and chitin in the exoskeletons of arthropods, as well as energy storage molecules in the form of starch and glycogen. Additionally, polysaccharides are involved in a number of cell-recognition and cell-signaling events. The surface of cells is covered with a thick layer of complex polysaccharides, the glycocalyx, that can reach out up to 3 µm from the cell surface.[1,2]

Bacterial capsular polysaccharides cover the cells of several types of bacteria, *e.g. Escherichia coli*, *Neisseria meningitidis*, *Haemophilus influenzae*, and many others.[3,4] These polysaccharides allow the bacteria to very efficiently avoid the immune system, by hiding antigenic proteins and other molecules on the cell surface. This prevents the cells from being internalized, and subsequently destroyed by immune cells.[3,5,6]

The biological roles of polysaccharides are an attractive area of research that can provide in-depth understanding of biological systems. The study of natural polysaccharides is, however, often complicated by the inherent difficulties of working with them. Polysaccharides from natural sources are typically heterogeneous, which complicates the purification procedures and analytical work. Isolating sufficient quantities, pure enough for biological investigations is difficult. Furthermore, the intrinsic heterogeneity of this class of compounds makes it difficult to interpret the analytical data, and it is often difficult to determine which part of the polysaccharides interact with for example proteins in biological systems.

Synthetic approaches can provide solutions to problems associated with heterogeneity and availability of compounds. As discussed in the first chapter of this thesis, however, the chemical synthesis of even smaller oligosaccharides can be highly time consuming and expensive. Furthermore, small oligosaccharides do not necessarily act in the same way in a biological environment as large polysaccharides. Because of this, a hybrid method might provide insight in biological mechanisms while avoiding the high cost and time requirements for synthetic compounds, as well as the problems with acquiring natural polysaccharides.

There exists a number of linear, or almost linear, polysaccharides consisting of a single type of monosaccharide moiety. Two examples of such homogeneous polysaccharides are the previously mentioned cellulose and chitin. These two

polysaccharides have rather low water solubility, which could potentially complicate the use of them as biological probes. Dextran, however, is a highly homogeneous water-soluble polysaccharide, produced by *Leuconostoc* species. Structurally, it is an α-(1→6) linked glucopolysaccharide with occasional α-(1→3) branches. Its commercially availability makes it an attractive starting material for further modifications.

As discussed previously, the interactions between ligands and receptors in nature typically occur in a multivalent manner. This concept has been widely utilized by attaching a vast array of carbohydrates to various scaffolds and backbones, ranging from small-molecular compounds to large macromolecules such as peptides, nanoparticles etc.[7–9]

Modification of natural polysaccharides has found, in addition to applications based purely on material properties, numerous biological applications both as such,[10] and as scaffolds for drugs or other biologically relevant compounds. Polysaccharides typically have high biocompatibility, biodegradability, meaning that they are not immunogenic, and are ultimately metabolized in the body. Furthermore, Polysaccharides are often water-soluble, making them excellent carriers for ligands in a biological environment.[11]

In addition to purely biological applications, polysaccharides are, due to their renewable nature and material properties, attractive targets for various research fields.[12–14] These applications suffer from the same problems associated with natural polysaccharides as described above. High heterogeneity and polydispersity makes behavior of the bulk material unpredictable, and while there are methods for fractionation and fragmentation of polysaccharides to obtain more evenly sized polysaccharide fragments, these are typically expensive and often difficult to control. New and more efficient methods are thus needed.

In the following sections, a novel approach combining the use of biologically active carbohydrate-based ligands and polysaccharide-based scaffolds will be discussed. The preparation of polysaccharide mimics based on a dextran backbone, functionalized with three biologically important disaccharides is presented. All prepared compounds are thoroughly characterized by NMR spectroscopic and chromatographic methods. Furthermore, the ability of the modified dextran to interact with human Galectin-3 (Gal-3) will be discussed. Finally, the degradation of polysaccharides under conventional “click” chemistry conditions will be explored.

4.2 Functionalization of dextran

As mentioned above, the high heterogeneity of natural polysaccharides is a common problem for biological investigations. A homogeneous polysaccharide with well-defined binding epitopes would thus be preferable as it would simplify the analysis of results. To this end, compounds that mimic natural polysaccharides were designed, based on smaller, well-defined, oligosaccharide fragments attached to a homogeneous polysaccharide backbone. For reliability of the obtained data, it is important to ensure that the interactions between the biological target molecule and the polysaccharide-based backbone are kept to a minimum. In this work, Galectin-3, a lectin that binds β-D-galactopyranosyl units, was selected as the biological target. Accordingly, dextran consisting of α-D-glucopyranosyl units was deemed a suitable scaffold. The dextran selected for this work had an average molecular weight of 70 kDa, which corresponds to approximately 430 glucose units. Dextran typically has occasional α-(1→3) branches, and in this particular case they were found on approximately every 25 glucose units.

The method for functionalizing dextran with disaccharides consisting of lactose, maltose and a β-(1→2) linked mannobiose, was based on a copper(I) catalyzed azide-alkyne cycloaddition (CuAAC) approach similar to that presented in the previous chapter. Dextran was selected to carry the alkyne functionalities required for the reaction, and the disaccharides were functionalized with azide groups.

4.2.1 Propargylation of dextran

The initial modification of dextran was carried out by introducing alkyne functionalities to the dextran with propargyl bromide under alkaline conditions in water, according to a modification of a previously published method.[15] Dextran was dissolved in water and cooled on an ice bath, after which solid potassium hydroxide was added. When everything had dissolved propargyl bromide was added, and the reaction mixture was allowed to return to room temperature and stirred overnight. The reaction was quenched by neutralization using acetic acid, which formed potassium acetate as a byproduct. The reaction mixture was purified by precipitation into ethanol to remove any unreacted propargyl bromide, as well as the potassium bromide produced during the neutralization. A small amount of potassium acetate remained in the propargylated dextrans, but this constituted a few mass-percent at most and further purification was deemed unnecessary (Scheme 4.1).

Modification of polysaccharides is in many ways similar to modification of smaller molecules. There are, however, some factors that need to be considered. With large molecules, it is often difficult to drive a reaction to completion and because of this it is of utmost importance to determine the degree of substitution (DS) after a reaction. The DS indicates how complete the reaction has been, and determines the reaction parameters (such as equivalents of reagent) for subsequent modifications. Herein DS will refer to the number of substitutions per monosaccharide unit, *i.e.* 0 – 3.

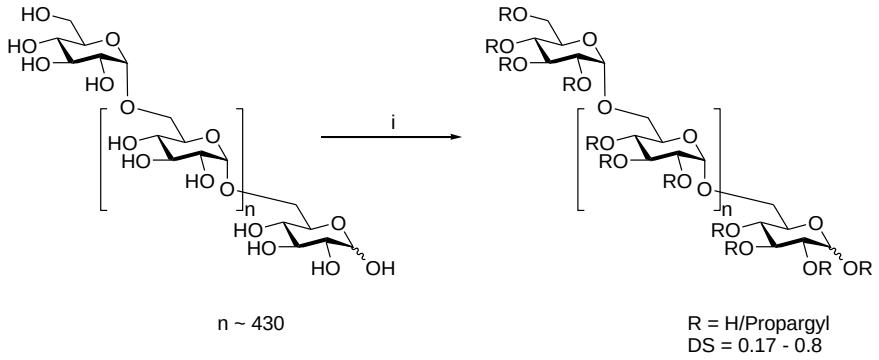

Scheme 4.1. Reagents and conditions: i) PgBr, KOH, H_2O, 0 °C → r.t., 19 h.

The DS of the propargylation reaction was easily varied by using different amounts of propargyl bromide in the reaction. Six different degrees of substitution were prepared, ranging from 0.17 to 0.8 (**P1**: DS = 0.17; **P2**: DS = 0.25; **P3**: DS = 0.41; **P4**: DS = 0.51; **P5**: DS = 0.60; **P6**: DS = 0.80) which seemed to be the practical upper limit. Above DS = 0.8 the solubility of the polysaccharide decreased to a level where analysis and subsequent modification became difficult, and because of this a higher DS was not pursued.

4.2.2 Preparation of azido-functionalized disaccharides

Three azido-functionalized disaccharides: lactose, maltose and β-(1→2) linked mannobiose were selected for this work (Figure 4.1). The preparation of all of these is slightly different, and the selected approaches will be discussed next.

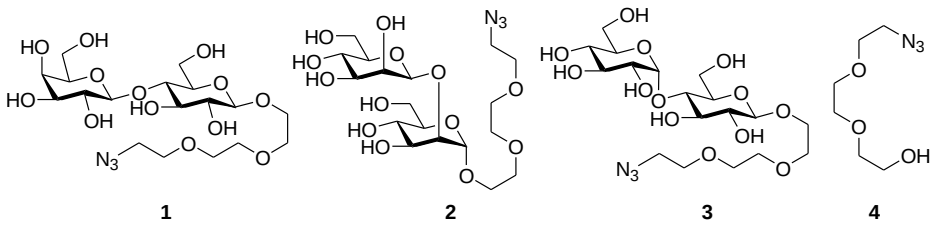

Figure 4.1. Azido-functionalized disaccharides.

Lactose was first benzoylated using benzoyl chloride in pyridine. The anomeric position on the glucopyranosyl unit was selectively deprotected using (N,N-dimethylamino)-1-propylamine (DMAPA), a cheap alternative to the commonly used methylamine, which in some regions is a regulated compound due to its use in the production of methamphetamine. The hemiacetal was then reacted with trichloroacetonitrile in presence of a strong base DBU, which promotes the formation of the α-product. The finished glycosyl donor was glycosylated using **4** as the acceptor (preparation of which is escribed in the previous chapter), and TMSOTf as promotor after which the product was deprotected under Zemplén conditions, affording the final azido-functionalized lactose **1** (Scheme 4.2).

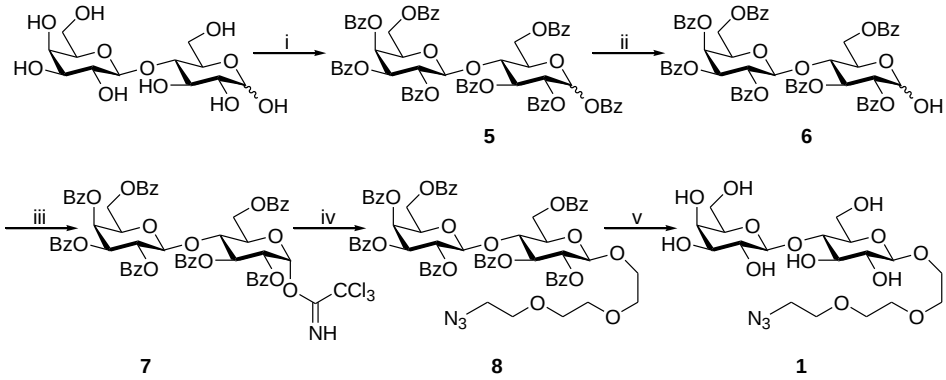

Scheme 4.2. Reagents and conditions: i) BzCl, Pyridine, r.t., 1.5 h (96%); ii), DMAPA, THF, r.t., 24 h (54%); iii) Trichloroacetonitrile, DBU, CH_2Cl_2, 0 °C, 1.5 h (77%), iv) **4**, TMSOTf, CH_2Cl_2, 4 Å MS, –30 °C, 2 h (81%); v) NaOMe, MeOH/THF, r.t., 2.5 h (94%).

Azido-functionalized β-(1→2) linked mannobiose **2** was prepared by deprotection of the benzyl protected analogue discussed in the previous chapter (compound **13** in the previous chapter, Scheme 4.3).

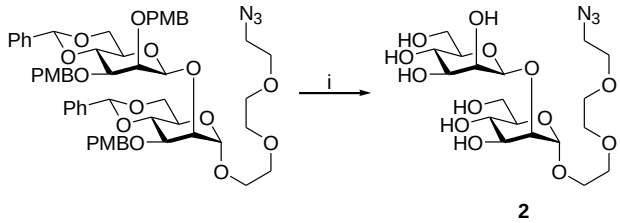

Scheme 4.3. Reactions and conditions: i) 1,3-propanedithiol, TFA/H_2O/CH_2Cl_2, 4:1:10, 0 °C → r.t., 24 h (74%).

The maltose derivative was prepared by reacting peracetylated maltose with 2[-2-(chloroethoxy)ethoxy]ethanol, promoted by $BF_3{\cdot}OEt_2$, after which the chloride was replaced by azide, by reacting it with NaN_3 in DMF in the presence of Bu_4NI. The acetyl groups were removed under Zemplén conditions to afford the final azido-functionalized maltose **3** (Scheme 4.4).

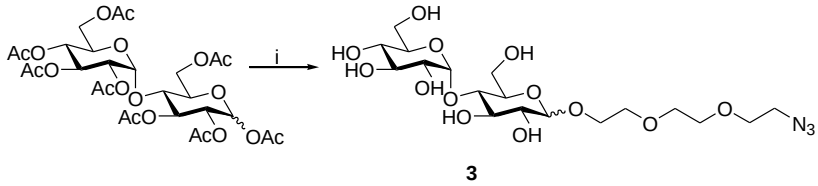

Scheme 4.4. Reagents and conditions: i) 1) 2[-2-(chloroethoxy)ethoxy]ethanol, $BF_3{\cdot}OEt_2$, CH_2Cl_2, 0 °C → r.t., 5 h; 2) NaN_3, TBAI, DMF, 87 °C, o/n; 3) NaOMe, MeOH, r.t., 1.5 h (27% over three steps).

4.2.3 Click reactions

Azides **1** – **4** were attached to the dextran backbone by conventional CuAAC reactions, using copper sulfate and sodium ascorbate. The reactions were carried out in water using two equivalents of azide for each propargyl group. Cu(I) required for the reaction was produced *in situ* via reduction of Cu(II) from $CuSO_4$ by Na-ascorbate (Scheme 4.5).

The compounds were purified by precipitating into, and washing with, methanol to remove unreacted azide after which they were passed through Sephadex PD-15 G-25 columns to remove other small-molecular compounds. Finally, the compounds were treated with a generous amount of Quadrapure™ TU thiourea-based metal ion chelator to remove any copper residues. The prepared compounds are presented in Table 4.1 below.

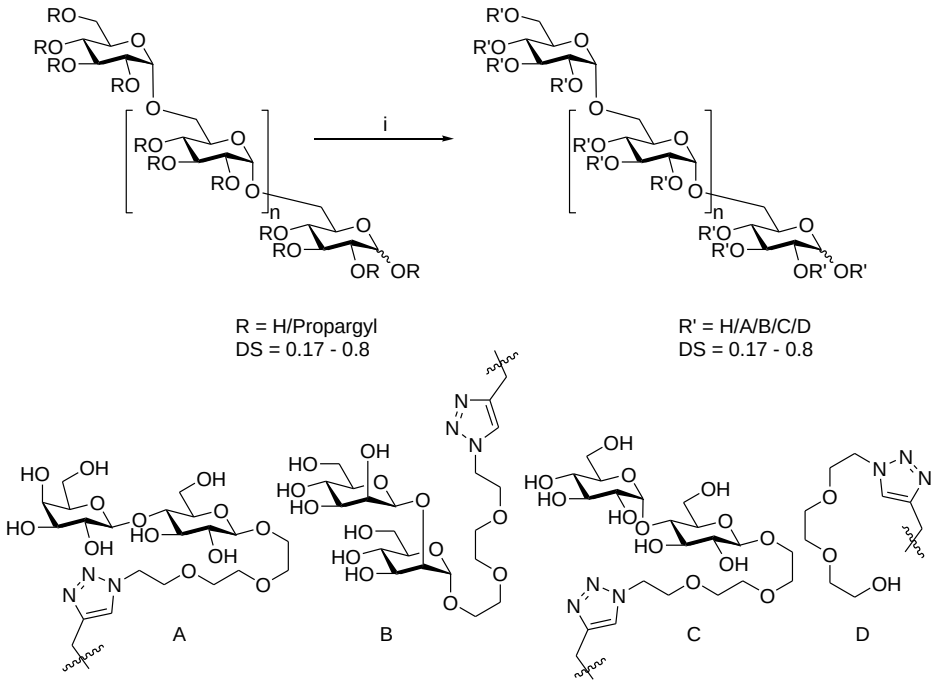

Scheme 4.5. Reagents and conditions: i) **1**, **2**, **3** or **4**, $CuSO_4$, Na-ascorbate, H_2O, 55 °C, 20 h.

Table 4.1. List of final compounds prepared in this work.

Compound	Dextran	Ligand	DS	Yield
Lac1	**P1**	**A**	0.17	64%
Lac2	**P2**	**A**	0.25	66%
Lac3	**P3**	**A**	0.41	57%
Lac4	**P4**	**A**	0.51	59%
Lac5	**P5**	**A**	0.60	57%
Lac6	**P6**	**A**	0.80	62%
Man	**P6**	**B**	0.80	87%
LM1	**P6**	**A**:**C**; 1:3	0.80	58%
LM2	**P6**	**A**:**C**, 3:1	0.80	62%
T	**P6**	**D**	0.80	60%

4.3 Characterization

All isolated new compounds were thoroughly characterized by NMR spectroscopic methods, using a set of standard experiments: 1H, 13C, DQF-COSY, HSQC and HMBC. The complexities of the spectra were reduced to monosaccharide level by using 1D-TOCSY. Accurate coupling constants and

shifts for the small-molecular compounds were extracted by using the NMR simulation software PERCH.[16]

While the spectra of the small-molecular compounds **1**, **2**, and **3** are not particularly difficult to assign, extracting coupling constants and even accurate chemical shifts, is virtually impossible without quantum-mechanical simulation. Compound **1** in particular, shows very significant second order effects caused by the close proximity of coupled signals. Even simulation does not provide a perfect fit for the triethylene glycol moiety, due to overlapping in the spectrum which results in information being lost due to insufficient resolution.

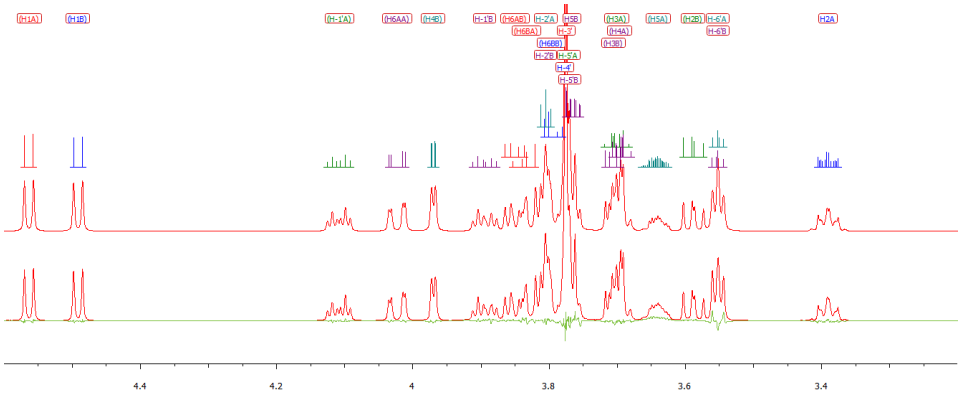

Figure 4.2. Experimental ^{1}H NMR spectrum of **1** (bottom) and simulated spectrum (top).

Typically, the signals H2A, H3A, H4A and H5A in compound **1** would be expected to appear as dd (except for H5A which would be expected to appear as ddd). As can be seen in the ^{1}H spectrum (Figure 4.2 and Figure 4.3), however, this is not the case and the signals are far more complex than expected. This is due to signals H3A (at 3.701 ppm) and H4A (3.697 ppm) being very close to one another, and sharing a strong scalar coupling constant. The signals are separated by only 2.5 Hz (on a 600 MHz instrument) and have a coupling constant of 8.8 Hz. Since the difference in chemical shift is of the same order as the coupling constant (and in this case even smaller), the nuclei are said to be strongly coupled and strong second order effects will be seen in the form of so-called "virtual coupling".[17] This effect significantly complicates the appearance of the affected signals, and makes extraction of coupling constants challenging as they can no longer be reliably measured manually. This effect has previously been reported for carbohydrates, for example in N,N'-diacetyl chitobiose, where the anomeric signal at the reducing end of the β-anomer is not a simple doublet as expected.[18,19] Virtual coupling can cause unexpected peaks in the spectra, and

such peaks could incorrectly be assigned as impurities, unless proper multiplet analysis is done.

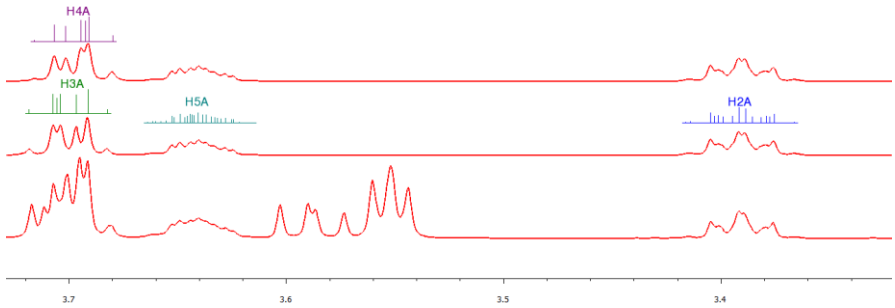

Figure 4.3. Selected region of the ^{1}H NMR spectrum of **1** showing the unexpected shape of signals H2A, H3A, H4A and H5A due to virtual coupling (overlapping signals have been removed in the top two spectra to show the true shape of H3A and H4B).

The DS of the propargylated dextrans could not accurately be determined by ^{1}H NMR due to overlapping of the HDO signal with both the anomeric region, and the CH_2 group of the propargyl side chains. Because of this, quantitative ^{13}C NMR was utilized instead. In the carbon spectrum the anomeric signals are well separated at around 93 – 102 ppm, as are the CH_2 signals from the propargyl side chains at 57 – 62 ppm. This made the integration of these regions easy and reliable (Figure 4.4).

The substitution pattern was determined by using a combination of DQF-COSY, HSQC, HSQC-TOCSY and HMBC. To increase the resolution of the HMBC spectra without suffering from folding effects, a band selective modification was used and spectra were recorded of regions 54 – 64 ppm and 75 – 85 ppm on the F1 axis. The HSQC spectra showed that some signals shifted approximately 7 – 8 ppm downfield in the carbon spectrum during the propargylation reaction, and HMBC was used to verify that this shift was due to a propargyl group being added. The position on the glucose unit was determined by a combination of DQF-COSY, HSQC, and HSQC-TOCSY (Figure 4.5). The dextran that was used in this work had an α-(1→3) branch approximately every 25 glucose units. The cross-peaks from the branching overlap with the cross-peaks from propargylated C3-H3 correlations in the HSQC spectra. The high homogeneity of the starting material allowed for fairly simple characterization of the propargylated products.

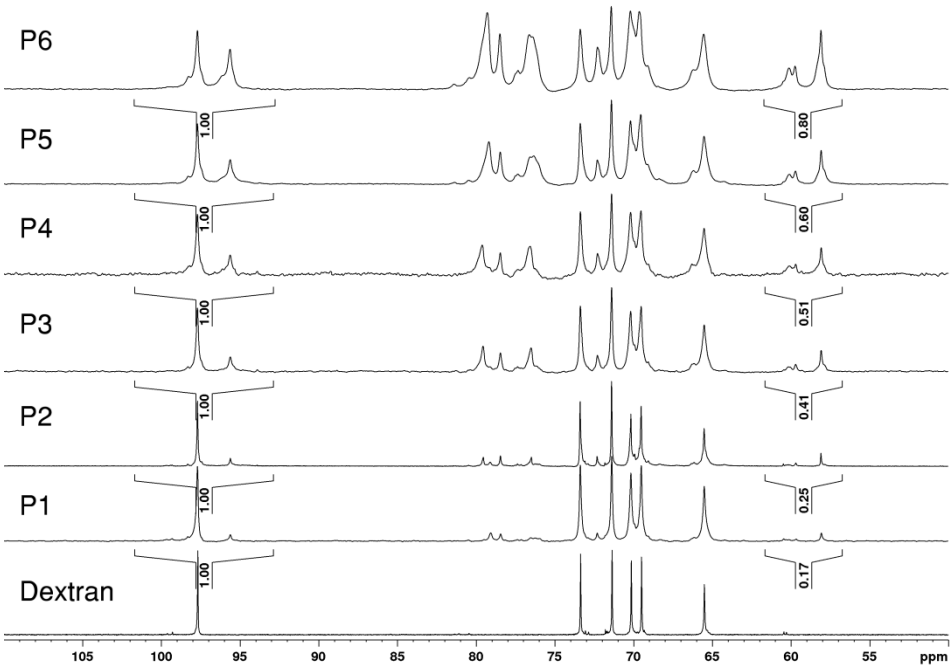

Figure 4.4. Quantitative ^{13}C spectra of the propargylated dextrans.

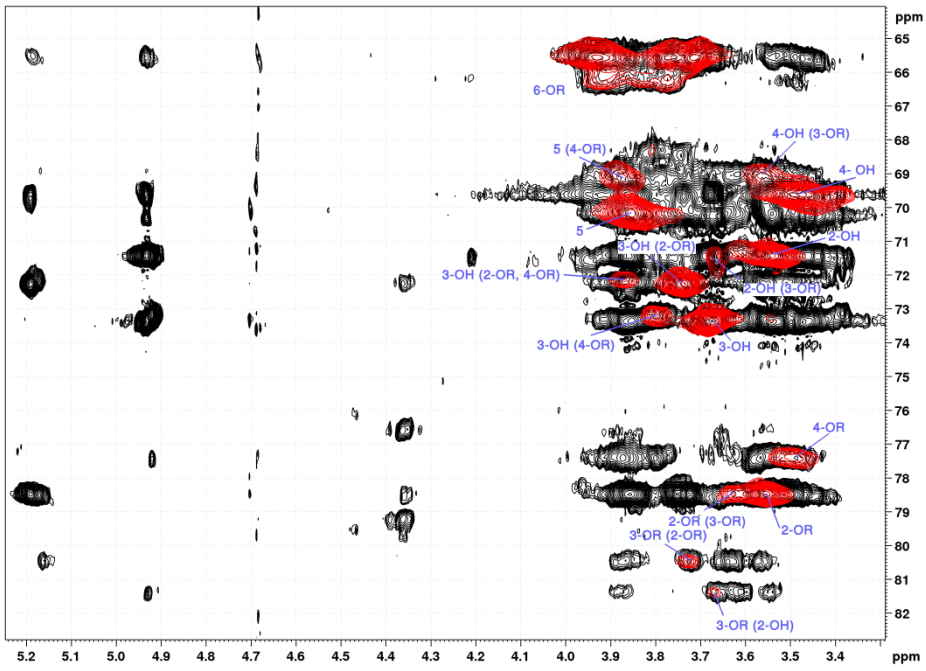

Figure 4.5. HSCQ-TOCSY (black) and HSQC (red) spectra of **P6**.

The majority of the propargyl groups were located on C-2 (~59%), which is also seen in the quite significant change in the shift of the anomeric signal (~0.25 ppm in proton and ~2 ppm in carbon spectra). The remaining substituents are on C-3 and C-4 but due to overlapping, the ratio of these could not be determined.

The final products were, like the intermediates, characterized by NMR spectroscopic methods. In this case the combination of ^{1}H, ^{13}C and HSQC proved to be the most useful. The ^{1}H and ^{13}C spectra are strongly dominated by the attached disaccharides, as is to be expected as these fragments are more homogeneous than the dextran backbone, and will thus give sharper peaks. The rather long linkers ensure that all attached disaccharide moieties behave in identical fashion. It can clearly be seen in the proton spectra, that the CH_2 of the propargyl groups at approximately 4.5 ppm, shifts downfield (and ends up beneath the water signal), and that the CH_2N_3 of **1** shifts from 3.55 ppm to 4.7 ppm, in the final products (Figure 4.6). These shifts are to be expected, as the triazole ring is aromatic, and therefore more electron-withdrawing than the alkyne and azide present in the starting materials. Similar changes can be seen in the carbon spectra. The two alkyne signals at 79 ppm and 77 ppm in the spectrum of **P6** disappear, and are replaced by two triazole signals at 125 ppm and 144 ppm. The proton spectrum also shows a new peak at 8.17 ppm which is the signal from the triazole proton (the terminal alkyne proton in the starting material is typically not present due to its acidic nature and slow relaxation). The same changes can also be seen when comparing the HSQC spectra of the azido-sugars, propargylated dextrans, and final compounds (Figure 4.7).

The carbohydrate region in the HSQC spectra is quite visually complex, due to the presence of several types of carbohydrate moieties. The disappearance of signals from starting materials, mainly the disappearance of the CH_2 of the propargyl moieties, indicates full conversion and no free propargyl groups left on the polysaccharide. This is further confirmed by quantitative ^{13}C NMR, which shows that the ratio between attached disaccharide and glucose signals from dextran is the same as the ratio of propargyl groups to glucose in the starting materials.

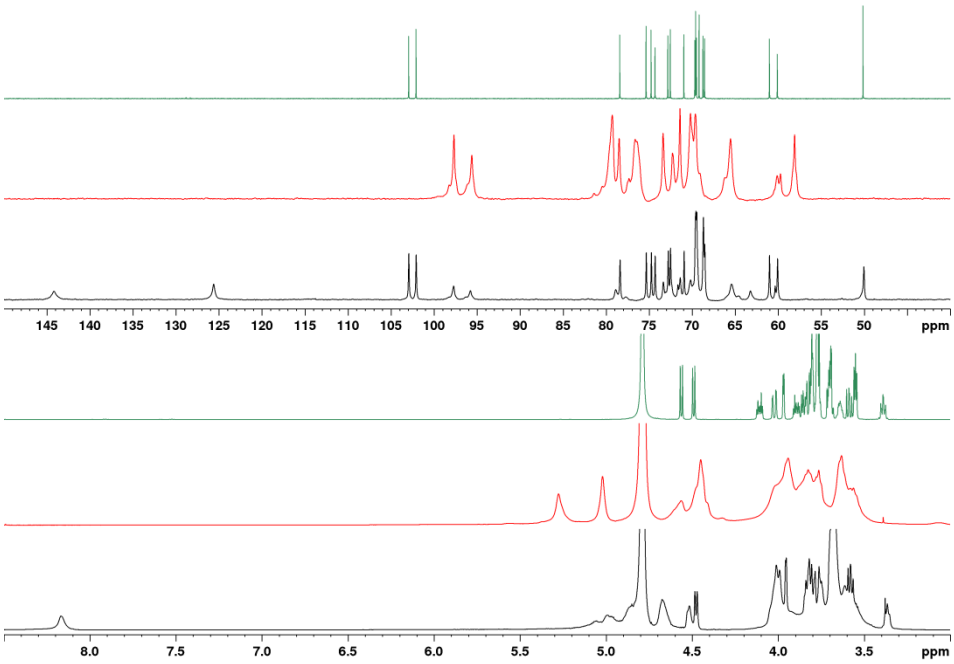

Figure 4.6. ^{1}H (bottom) and ^{13}C (top) spectra of **Lac6** (black), **P6** (red) and **1** (green).

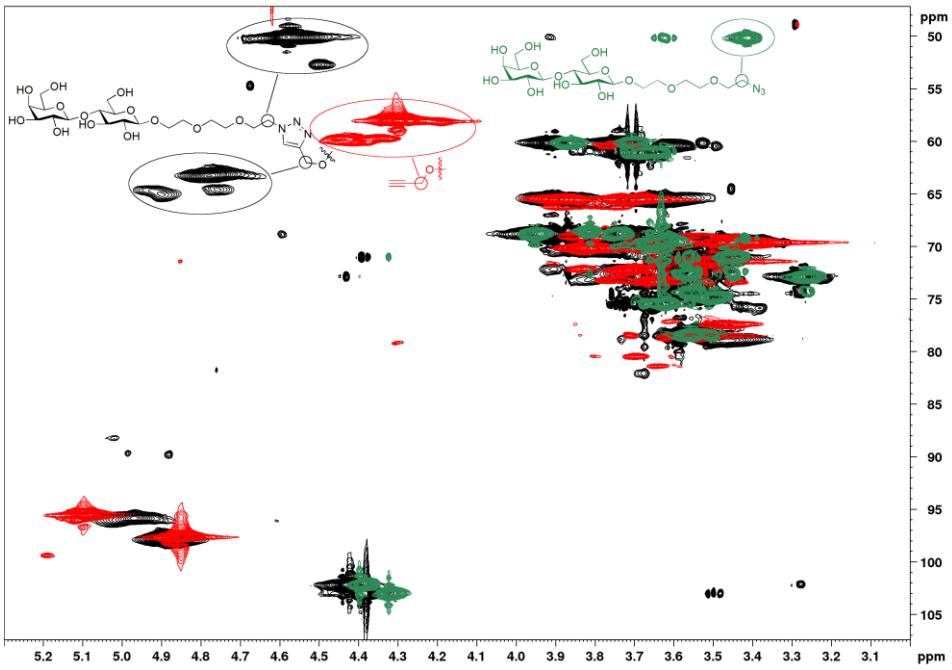

Figure 4.7. HSQC spectra of **Lac6** (Black), **P6** (red) and **1** (green).

Finally, the final compounds were characterized by high-pressure size-exclusion chromatography (HPSEC) and multiangle laser light scattering (MALLS), to determine the size of the polymers. The expected size of the polymers, based on the DS lies approximately between 110 – 250 kDa. The observed size for the polymers was, however, found to be 40 – 50 kDa.

It is known that that carbohydrates can degrade in strongly alkaline conditions, such as those used in the propargylation reaction, via a so called peeling reaction by β-elimination.[20,21] This is, however, only possible if the anomeric position of the reducing end is a free hydroxyl. In the case of these polysaccharides, the anomeric position at the reducing end is expected to be the first one to react, and therefore the peeling reaction should have minimal effect on the final polymer size. HPSEC/MALLS analysis showed that no significant degrading took place during this step.

It has also been reported that Cu(I) species can produce reactive oxygen species that can be detrimental to biomolecules,[22,23] and the depolymerization of polysaccharides by such species can be traced back to the 1960's.[24,25] It does, indeed, seem that the conditions used for the click reaction can degrade the polysaccharide backbone. The degradation of biomolecules under such conditions has, however, previously been prevented by using copper chelators that trap the Cu(I) species and keep them in this oxidation state.[26,27] In this work, similar methods for preventing the degradation was explored using a TGTA[26] chelator which did prevent the degradation to some degree. Even a five-fold excess of the chelator in relation to the copper was, however, not enough to completely prevent the degradation. Since, rather serendipitously, the final compounds were all of very similar size, making them optimal for biological studies, no further effort was put towards trying to completely prevent the degradation. The fact that the molecules all degraded to very similar sizes, prompted further investigations into this phenomenon, the results of which will discussed in more detail in section 4.5.

4.4 Interactions of modified dextrans with galectin-3

Interactions between the modified dextrans and human galectin-3 (Gal-3) were investigated using NMR spectroscopic techniques. To simplify the analysis of data, only the carbohydrate-recognition domain (CRD) of the protein was used. Samples of the protein were titrated with the polysaccharides and ^{15}N – ^{1}H HSQC spectra were recorded after each addition. The cross peaks in the spectra were monitored, and any changes during the titration were recorded.

If a ligand is in close proximity to the protein, the change in chemical environment of the NH cross-peaks close to the site of interaction will cause the NH correlations to shift. The chemical shift perturbation can be used to determine the binding site of the protein and, provided that the binding process is in the fast regime, the binding affinity can be estimated by fitting the data to the function $\Delta\delta/\Delta\delta_{max} = [L]/(K_d + [L])$ where [L] is the free ligand concentration ($[L] = [L_{tot}] - [L_{bound}]$) and K_d is the dissociation constant.[28,29]

4.4.1 Galectin-3

Gal-3, is a lectin that recognizes β-D-galactopyranosides. Out of the 14 mammalian galectins it is probably the most studied one, known to play important parts in biological systems such as cell differentiation, growth, and apoptosis, as well as in inflammatory responses. Structurally it is a chimera type lectin with a single carbohydrate recognition domain, consisting of approximately 150 amino acids and an N-terminal tail consisting of collagen-like repeats, the length of which depends on the species (nine in human Gal-3).[30,31]

An increase in the expression of Gal-3 is commonly associated with cancer,[32] and it is known to inhibit antitumor immunity and promote tumor growth via T-cell activation and apoptosis.[33,34] Competitive inhibition of Gal-3 in mice has been shown to slow down the growth of cancer cells *in vivo*.[33,35] Furthermore, *in vitro* studies using human breast carcinoma cells have shown, that inhibition of Gal-3 also prevents the adhesion of the cells to endothelial cells.[35] The increasing number of cancer patients demands new treatments for this group of diseases. The properties of Gal-3 make it an attractive target for developing such treatments.

In addition to β-D-galactopyranosyl units, Gal-3 has, on multiple occasions, been suggested to also recognize the cell wall of *C. albicans*[36–40] which is quite unexpected as lectins are typically highly specific for their substrates. The cell-wall of *Saccharomyces cerevisiae*, however, is not recognized by the lectin.[41] One of the major differences between the cell walls of these two yeasts, is the presence of β-(1→2) linked mannose units on the cell wall polysaccharide of *C. albicans*.[41–43] Since, as discussed previously, β-(1→2) linked mannosides are known to be immunogenic[44,45] and Gal-3 is involved in modulating the immune system[46,47] investigation of this rather unusual binding phenomenon could lead to better understanding of the interactions between proteins and carbohydrates.

4.4.2 Lactose-containing dextrans

One of the great benefits of using synthetically modified polysaccharides is that the ligand content can easily be calculated. The DS of the modified dextrans were, for convenience, converted to µmol ligand/mg polysaccharide. This made it possible to compare results between different polysaccharides, considering only the actual ligand concentration.

Samples of the ^{15}N labeled Gal-3 was titrated with lactose-containing dextrans up to a lactose:protein ratio of 50:1, which caused the chemical shift perturbations to flatten out to a horizontal line indicating saturation of the protein (Figure 4.8).

As mentioned above, multivalency typically results in stronger binding, compared to increasing the concentration of a monovalent ligand. In this case, however, the determined K_D values were in the range of 0.25 – 0.45 mM for all lactose samples. This is approximately the same as the binding affinity of Gal-3 to pure lactose,[48,49] i.e. no cluster effect was observed for the lactose-functionalized dextran. The dextrans with lower degree of substitution showed somewhat higher binding affinity than the dextrans with higher DS, but the overall small differences correspond only to a small difference in binding energy. Due to the similarity in K_D values observed for the lactose-functionalized compounds, not all of them were analyzed as no large deviations are to be expected. The results are summarized in Table 4.2.

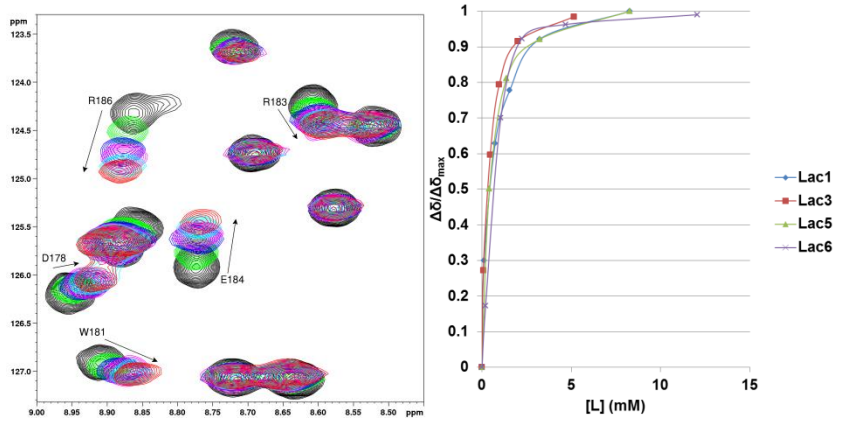

Figure 4.8. Chemical shift perturbations of a selected region in the HSQC spectrum of Gal-3CRD (left), and binding curves (right), upon titration with lactose-functionalized dextran.

Table 4.2. Binding affinities of the lactose-functionalized dextrans.

Compound	K_D (mM)	C_{Gal-3} (μM)
Lac1	0.44	169
Lac3	0.25	105
Lac5	0.32	169
Lac6	0.45	246
LM1	0.38	169
LM2	0.37	97

Only the most affected cross-peaks were monitored during the titration. The most perturbed signals were found to be from the amino acids associated with the canonical galactose binding site of the protein (Figure 4.9). This is, naturally, the expected result as the ligands contain a β-D-galactopyranosyl moiety.

As a negative control, dextran modified by only the triethylene glycol linker was used. This compound caused no changes in the shifts of the protein signals, which verified that any interactions between Gal-3 and the modified dextrans does, indeed, stem from the carbohydrate moieties attached, and not the linker or the dextran backbone.

4.4.3 β-(1→2) linked mannoses

No significant chemical shift perturbations were observed upon titration of Gal-3 with the dextran functionalized with β-(1→2) linked mannobiose. Approximately 15 signals (Figure 4.10) did, however, decrease in intensity compared to the other signals. Typically, a decrease in signal intensity of a binding site is witnessed if the exchange rate is slow, *i.e.* if k_{off} is slow. In such cases new signals from the bound protein should appear, however, and the total intensity associated with a signal should remain constant, and the ratio represents the fraction of bound protein.[28,29] Furthermore, decrease in all the protein signals could be indicative of non-specific binding, and generally all protein signals will decrease somewhat over the course of a titration.

The observations during the titration suggests, that the protein does indeed interact with the β-(1→2) linked mannobiose units on the dextran, but the type of binding is different than for the galactose-functionalized dextrans. The decrease in signal intensity is likely due to broadening, caused by an interconversion of an ensemble of different complexes between the protein and ligand. The ligand is interacting with a specific region of the protein, defined by the affected residues, but in multiple orientations. This could be seen as nonspecific binding from the ligand perspective.[50]

All the affected signals corresponded to amino acids located in the same region of the protein (Figure 4.9). The affected region was, however, not the canonical binding site responsible for binding β-D-galactopyranosyl units, but located on the opposite side of the CRD. Visual inspection of the site does not indicate the presence of a clear binding pocket, as is the case for the canonical binding site. This could explain why the ligands can interact with the site in multiple orientations. Gal-3 has previously been reported to also bind mannose-containing polysaccharides.[49]

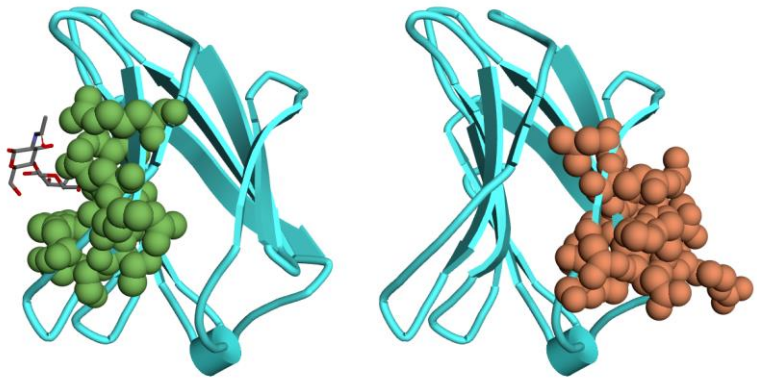

Figure 4.9. Gal-3 CRD displaying the canonical binding site (left) and non-canonical binding site (right).

The galectin was titrated to a ligand/protein ratio of 100:1 and the intensities of the signals were monitored. As mentioned previously, the overall intensity of the protein signals typically decreases over the course of the titration and because of this, the intensities of the signals of interest were normalized against signals unaffected by the binding. This indicated that the binding clearly depends on the concentration of the ligand. Reliable quantification of such binding is, however, difficult, and no K_D values are reported here.

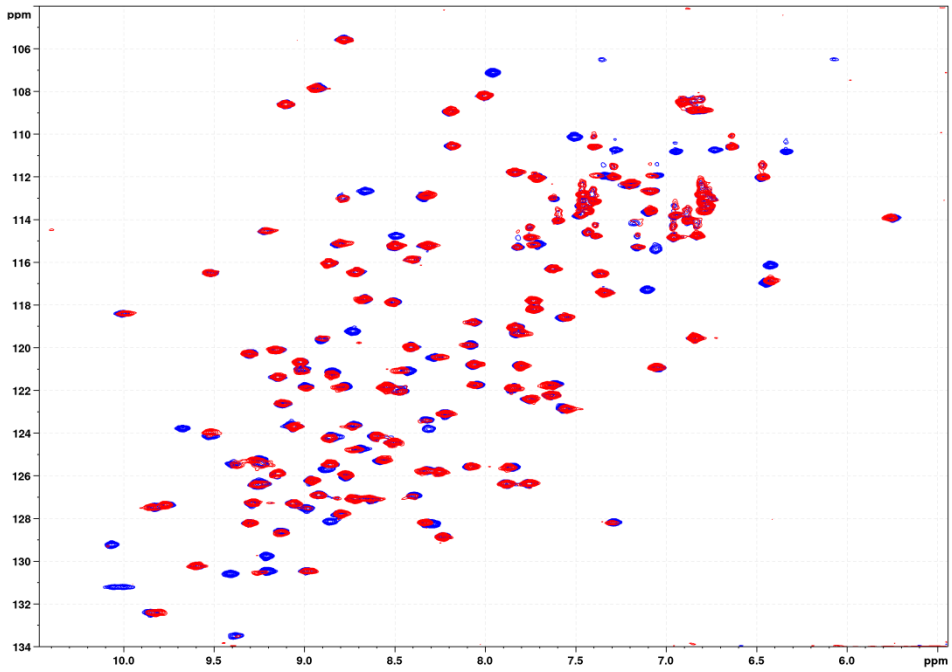

Figure 4.10. ^{15}N–^{1}H HSQC spectra of Gal-3 (blue) and the endpoint of the titration with mannose-functionalized dextran (red).

In addition to the mannose-functionalized dextran, the binding of Gal-3 to mannans extracted from the *C. albicans* cell wall was investigated. These polysaccharides did, however, not appear to interact with the galectin to any noticeable degree. In previous studies, the interactions of Gal-3 with mannose-containing polysaccharides has only been investigated using full-length Gal-3[37,38,49] whereas in this study only the CRD of Gal-3 was used. It is possible that the collagen-like tail of Gal-3 facilitates the binding of larger mannans. In this work, the disaccharide units are located quite far from the dextran backbone, and are thus allowed to behave more freely than they would if they were incorporated into the backbone itself. This might also explain the difference between these results and those published before.

Rather surprisingly, the dextrans functionalized with both maltose and lactose seemed, in addition to the galactose binding site, also to interact with the same region of the protein as the mannose-functionalized dextran.

The unexpected binding of Gal-3 to various carbohydrates suggests that the understanding of interactions between carbohydrates and proteins is far from

being complete, and further investigations into the binding phenomenon are required.

4.5 Depolymerization of polysaccharides

As mentioned in the introduction to this chapter, polysaccharides are valuable targets for development of renewable materials. Obtaining oligosaccharide fragments with desired size and properties is not always straightforward, however. Synthetic procedures for combining monosaccharides or small oligosaccharides into larger structures exist, but these are typically laborious and expensive if larger quantities are required. Even with the emergence of automated systems as discussed in the first chapter of this thesis, preparation of large structures in desired amounts for material purposes is often not feasible.

Fragmentation of natural polysaccharides into smaller structures can be achieved in multiple ways, but the generally applied methods typically suffer from some drawbacks. Enzymatic methods are highly selective which, while often desired, can cause problems as natural polysaccharides typically contain many different types of linkages, and glycosylases (enzymes that hydrolyze glycosidic linkages) are typically specific for a certain type of linkage. Because of this, a mixture of enzymes is often required.[51] Furthermore, non-selective methods such as hydrolysis by strong mineral acids, or under oxidative conditions are often difficult to control, and produce fragments with large polydispersities.[20,52] Due to the problems associated with the existing methods, new approaches are needed for processing polysaccharides from natural sources.

During the final step in the functionalization of dextran, *i.e.* the CuAAC reaction, significant degradation of the dextran backbone was observed. This prompted a more thorough investigation into the reaction and its effect on other polysaccharides. The phenomenon itself, can be traced back to the 1960s when it was discovered that polysaccharides can be depolymerized by a combination of ascorbic acid and copper ions.[24,25] Even though the degradation of polysaccharides under these conditions has been known for over 50 years, it is still regularly neglected today.[53–58] Furthermore, the potential applications of this reaction for intentional degradation of polysaccharides have not been addressed previously.

4.5.1 Dextran as a model compound

The high homogeneity of dextran makes it an excellent model compound for this study. The fragments created by the degradation are very similar in structure,

which makes the analysis of results straightforward, and the commercial availability of analytical standards of various sizes of dextran allows for obtaining of reliable calibration curves.

To investigate the roles of the different reagents and reaction times, different conditions were screened while keeping the solvent (water), temperature (55 °C), and starting material (70 kDa dextran) fixed (the general scheme for the reaction is shown in Scheme 4.6). Neither $CuSO_4$ nor Na-ascorbate caused any significant depolymerization on their own (entry 6 and 7 in Table 4.3). CuCl, however, caused significant fragmentation resulting in smaller polymers with molecular weights of approximately 17 – 18 kDa (entry 8 in Table 4.3). This suggests that Cu(I) ions are the active species in the reactions. This is in accordance with previous results where Cu(I) ions have been suggested to generate reactive oxygen species, that are the driving force of the degradation.[22,23] In the reagent system consisting of $CuSO_4$ and Na-ascorbate, Cu(II) gets reduced to Cu(I). The degradation was studied by varying the amounts of these reagents. All experiments resulted in fragments of approximately 7 – 10 kDa, i.e. the exact amount of reagents did not seem to be very significant (entries 2 – 4 in Table 4.3).

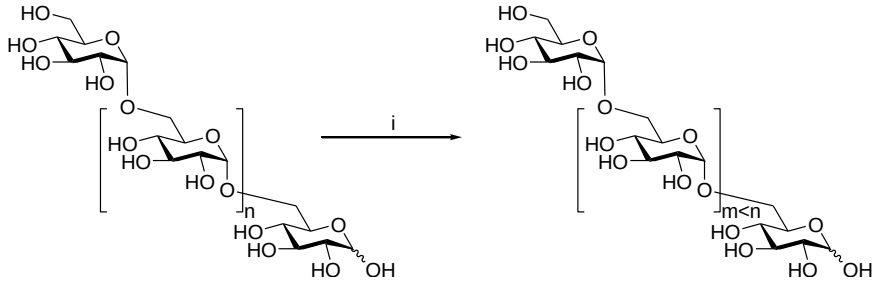

Scheme 4.6. Degradation of dextran. Reagents and conditions: i) 70 kDa dextran, 55 °C, H_2O, reagents (Table 4.3).

From these results it is quite clear that Cu(I) ions are the active species in the reaction. The reason why the reagent system consisting of $CuSO_4$ and Na-ascorbate is more effective than using CuCl, could be explained by the fact that Cu(I) species are readily oxidized to Cu(II) species in the presence of water and oxygen. The combined effect of Cu(I) species and Na-ascorbate cannot, however, be ruled out completely.

Table 4.3. Degradation of dextran under different reaction conditions.

Entry	$CuSO_4$ (equiv)	Na-asc (equiv)	t (h)	M_{HPSEC} (kDa)	M_{MALLS} (kDa)	M_w/M_n	~DP
1	0	0	0	70	72	1.20	430
2	0.1	0.2	20	12.8	15.9	1.43	100
3	0.3	0.6	20	10.3	11.1	1.34	70
4	0.5	1.0	20	9.1	10.2	1.22	65
5	0.5	1.0	48	7.1	10.9	1.55	65
6	0.5	0	20	67	71	1.21	430
7	0	1.0	20	68	71	1.21	430
8	0.5 (CuCl)	0	20	18	17	1.67	105

All equivalents are given as equivalents per monosaccharide unit. The data is visualized in Figure 4.11.

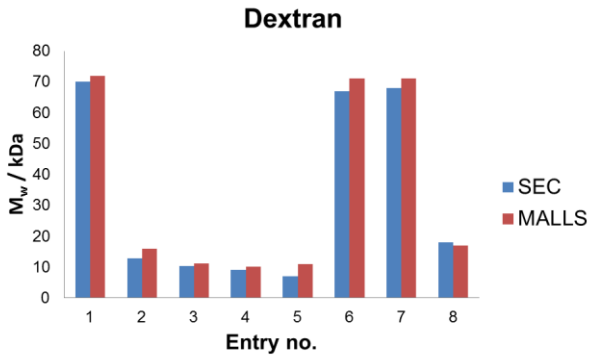

Figure 4.11. Visualization of the data in Table 4.3.

Based on the results from the initial screening, the reagent system consisting of $CuSO_4$ and Na-ascorbate was selected for all the remaining experiments. The degradation of dextran was repeated on 200 mg scale using 0.05 equivalents of $CuSO_4$ and 0.1 equivalents of Na-ascorbate, and the reaction progress was monitored for five days to investigate the degradation over time. The results from this experiment are shown in Figure 4.12. It was found that at a certain point, interpreted herein as terminal oligomer size, the degradation rate decreased significantly. Neither using large excess of reagents or long reactions times were found to have a large impact on this size (entries 2 – 5 in Table 4.3). For dextran, this limit was found to be approximately 7 – 10 kDa, corresponding to a degree of polymerization (DP) of approximately 40 – 60 (The starting material with a molecular weight of 70 kDa has a DP of ~400). To verify the existence of a terminal oligomer size, the reaction was repeated using a

commercial maltoheptaose. In this case no degradation was detected which confirmed the hypothesis.

Figure 4.12 shows that the degradation has a rather strict logarithmic dependency on the reaction time. This could, in principle, allow the calculation of the time required to produce polysaccharides of desired length, by applying a simple mathematical function. The predictability combined with the low polydispersity of the produced fragments, makes this a promising method for fragmenting polysaccharides into smaller structures with desired properties. The predictable behavior may, however, be limited to linear polysaccharides. Nonetheless, intrigued by these findings, the behaviors of three other polysaccharides under the same reaction conditions were investigated, the results of which will be discussed next.

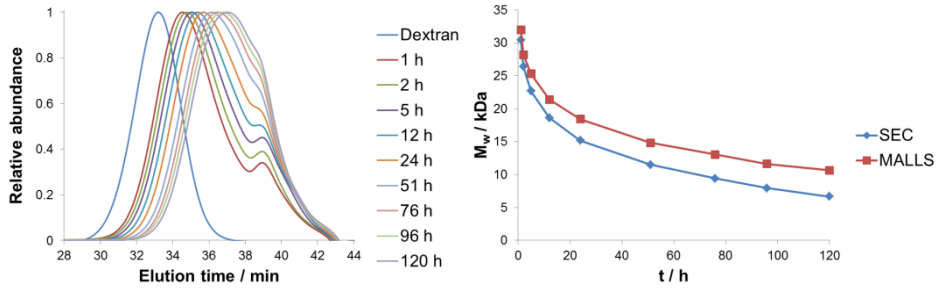

Figure 4.12. Degradation of dextran over five days.

4.5.2 Polysaccharides from biomass feedstock

To investigate the applicability of the method for processing polysaccharides from biomass feedstock, three naturally occurring polysaccharides: xylan, starch, and galactoglucomannan (GGM), were subjected to the degradation conditions. The chemical structures of the polysaccharides are displayed in Figure 4.13.

Xylans, are a group of hemicelluloces found in plant cell walls, where they can constitute up to 10 – 35% of the total hemicellulose content.[59] Due to their abundance, they are a relevant renewable source of polysaccharides. Structurally, this class of compounds consists of a β-(1→4) linked xylose backbone, with various branches depending on the species of origin.[60] In this particular study, 36 kDa birchwood xylan with α-(1→2) linked branches of 4-O-methyl-D-glucuronic acid units approximately 10 xylan residues was used.[61,62]

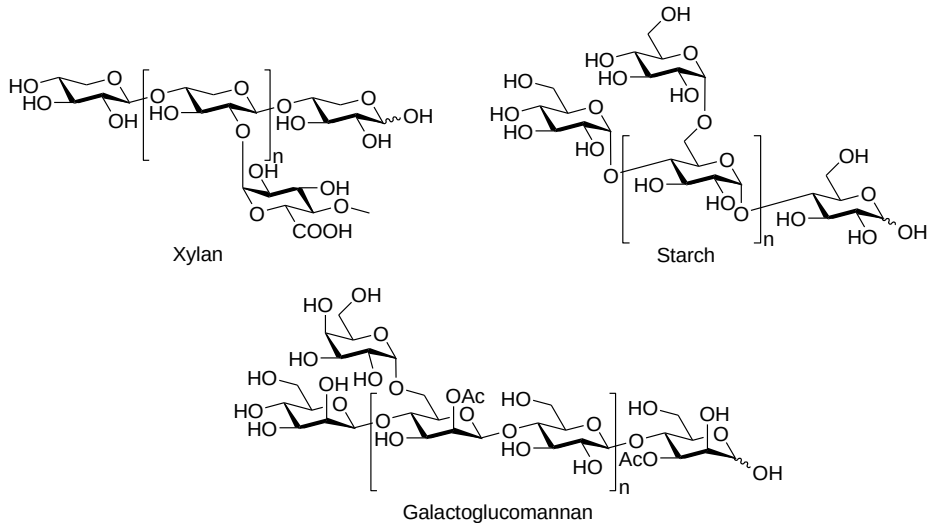

Figure 4.13. Chemical structures of xylan, starch and GGM.

Starch is the energy storage molecule in most green plants, and is thus one of the most abundant naturally occurring polysaccharides, and an important raw material in food and paper industries.[63] Starch consists of two types of molecules, linear α-(1→4)-D-glucopyranan (amylose) that is insoluble due to the ordered helical conformation it forms, and amylopectin that in addition to the α-(1→4)-linked backbone, also contains branches connected via α-(1→6)-linkages. The branching breaks the regular structure of starch, and makes amylopectin water soluble. The wide industrial applicability of starch makes it an excellent substrate for this investigation, and a 70 kDa starch polysaccharide was thus used here for degradation studies.

Finally, GGM is a hemicellulose commonly found in softwoods, where it can constitute up to 10-20% of the dry weight.[62,64] Structurally it is a polysaccharide, with a backbone consisting of β-(1→4) linked glucopyranosyl and mannopyranosyl units, with occasional galactopyranosyl units attached to the mannoses via α-(1→6) linkages. The Man/Glc/Gal ratio of the GGM can vary slightly depending on the isolation procedure and source.[65,66] The ratio in the GGM used in this study was 4:1:0.1. Similar to xylan, GGM is also an important starting material for future biorefineries. The industrial applications, as well as the potential biological applications make it an attractive target for future research.[67] Previously a 22 step synthetic protocol was devised for preparation of a tetrasaccharide fragment present in GGM.[68] Understandably, more feasible ways of preparing such fragments would be preferred for large-scale production.

Table 4.4. Results from degradation of xylan, starch and GGM.

Entry	Polysaccharide	$CuSO_4$ (equiv.)	Na-asc (equiv.)	t (h)	M_{HPSEC} M_{MALLS} M_{DOSY}	M_w/M_n	DP
1a	Xylan	0	0	0	- - 36		- - 200
1b	Xylan	0.1	0.2	18	5.5 12[a] 6.4	1.29	35 75 40
1c	Xylan	0.5	1.0	18	5.0 11[a] 6.3	1.32	30 70 40
2a	Starch	0	0	0	- - 70		- - 430
2b	Starch	0.1	0.2	19	- - 5.5		- - 35
2c	Starch	0.5	1.0	19	- - 5.5		- - 35
3a	GGM	0	0	0	12 11 -	1.38	75 70 -
3b	GGM	0.1	0.2	18	4.2 3.9 -	2.01	25 24 -
3c	GGM	0.5	1.0	18	2.0 2.3 -	1.38	12 14 -

[a]The large deviation is probably caused by an incorrect dn/dc value. Reaction conditions: starting material, H_2O, 55 °C, reagents. The data are visualized in Figure 4.14.

The three polysaccharides; xylan, starch and GGM, were subjected to the degradation conditions using two different concentrations of $CuSO_4$ and Na-ascorbate. The results of these reactions are summarized in Table 4.4 and Figure 4.14. The xylan and starch were degraded into approximately 5 – 6 kDa polysaccharide fragments, corresponding to DPs of 30 – 40 (Figure 4.15). These fragments are similar to those obtained from dextran. The GGM, however, was degraded into even smaller fragments of approximately 2 – 2.5 kDa,

corresponding to a DP of 10 – 15 (Figure 4.15). The difference could stem from the fact that GGM is significantly more heterogeneous than xylan or starch, and thus has a less ordered structure in solution, which might allow the reaction to proceed further than for the more homogeneous polysaccharides. It has been reported previously, that the ability of the polysaccharides to form complexes with copper is a crucial part of the degradation reaction.[69] Complexation would allow the generation of oxidative species in close proximity of the glycosidic linkages, where they can hydrolyze the bonds. The requirement for complexation would, at least in part, explain the existence of a terminal oligomer size. In addition to what has been mentioned previously, it also appears that the stereochemistry of the monosaccharide units can have a significant impact on the final oligomer size. The polysaccharides consisting of monosaccharides with "gluco"-stereochemistry, i.e. dextran, starch and xylan, had a final DP of approximately 30 – 60 whereas GGM, which is dominated by mannose units, had a final DP of only 10 – 15. More detailed studies about the reaction, its mechanism, and the correlation to the final oligomer size are, however, required.

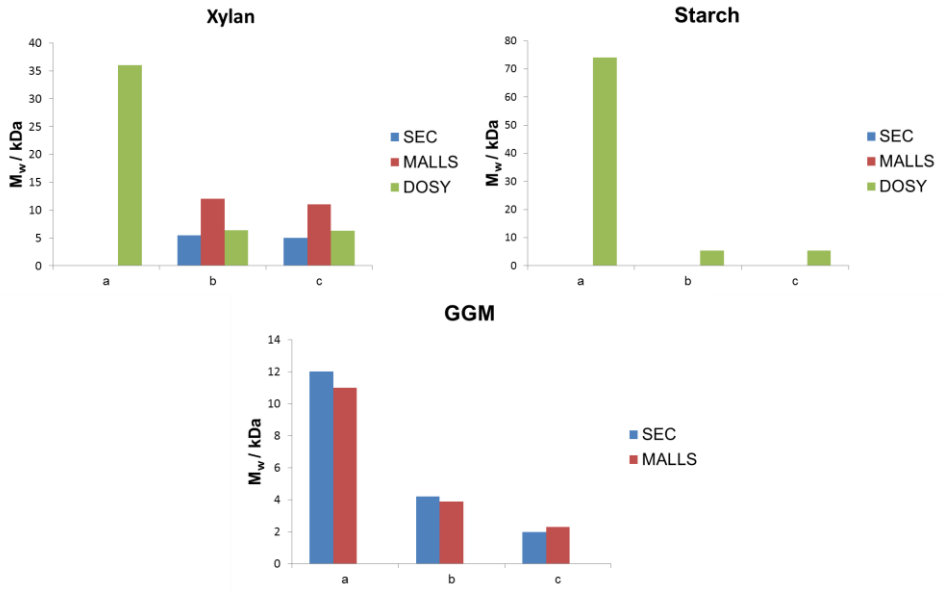

Figure 4.14. Visualization of the data in Table 4.4.

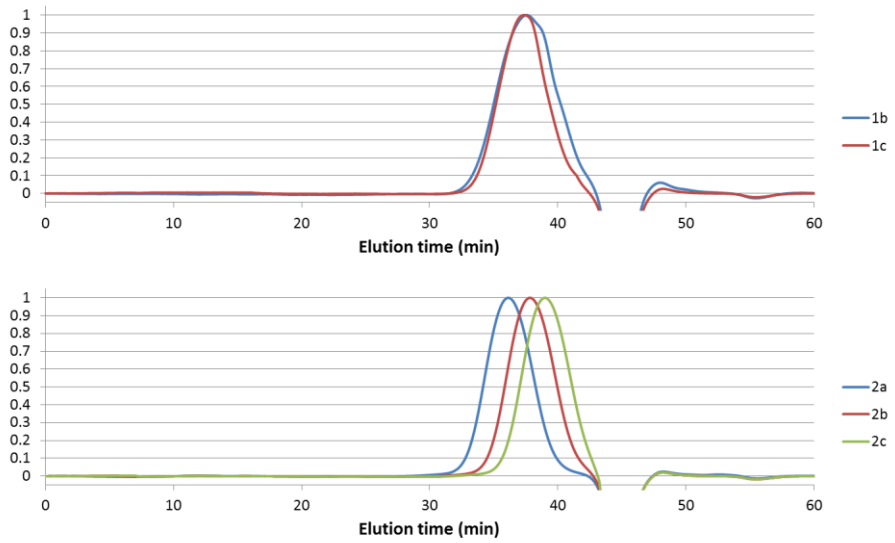

Figure 4.15. Normalized SEC chromatograms for degraded xylan (top) and GGM (bottom).

4.5.3 Analysis of degradation products.

The degradation products were mainly analyzed with high pressure size exclusion chromatography (HPSEC) and multiangle laser light scattering (MALLS). HPSEC is a method that separates molecules based on their size, and MALLS is a method that measures how molecules in solution scatter light. The light scattering can be related to molecular weight, if the so-called Rayleigh ratio Rθ (also known as dn/dc), which relates the molecular weight to the scattering angle and intensity, is known. By this method, molecular weights and polydispersities can be calculated. There are tables of dn/dc values available, but these are dependent on several other factors such as solvent, buffer, temperature, and exact polysaccharide type as well. Because of this, there might be slight errors in the calculated molecular weights, but by analyzing also the starting materials, and combining the MALLS data with HPSEC and NMR data, the degradation is quite evident. All methods used in the analysis are in good agreement, indicating that the methods are reliable at least in a qualitative manner. The HPSEC and DOSY data was calibrated using dextran standards ranging from 50 – 270 kDa (Figure 4.16).

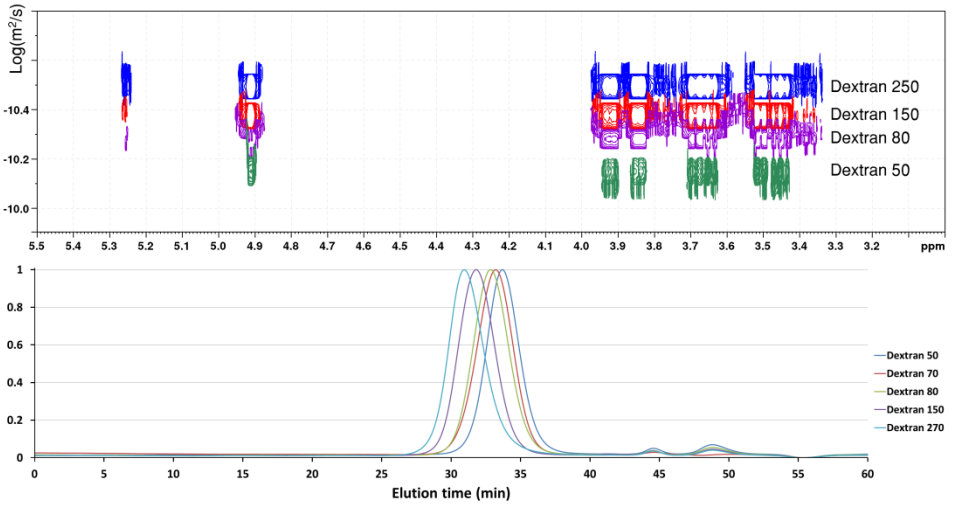

Figure 4.16. DOSY spectra (top) and normalized SEC chromatograms (bottom) of dextran standards.

The most useful NMR techniques for this type of analysis are DOSY and HSQC. DOSY, is a technique that separates compounds in the sample based on their diffusion coefficients, and thus it gives data similar to that from HPSEC. Over the years DOSY has become a frequently used method for polymer analysis in solution.[70,71] Conventional ^{1}H and ^{13}C spectra are not of much use in this type of analysis due to severe overlapping in the spectra, which complicates the comparison of spectra. HSQC, however, can be used to detect an increasing number of end-groups, which indicates depolymerization.

The poor solubility of starch and xylan, resulted in some analytical problems, especially in the case of starch which did not become appreciably soluble at room temperature even after the reaction. Both of these could be dissolved by briefly heating the samples to 80 °C, but upon cooling some precipitate appeared in the samples. To avoid the risk of precipitating the compounds on the SEC column, the unreacted xylan and all starch samples were analyzed by NMR techniques alone. HSQC and DOSY spectra of starch, xylan and degradation products 2c and 1c can be seen in Figure 4.17 and Figure 4.18.

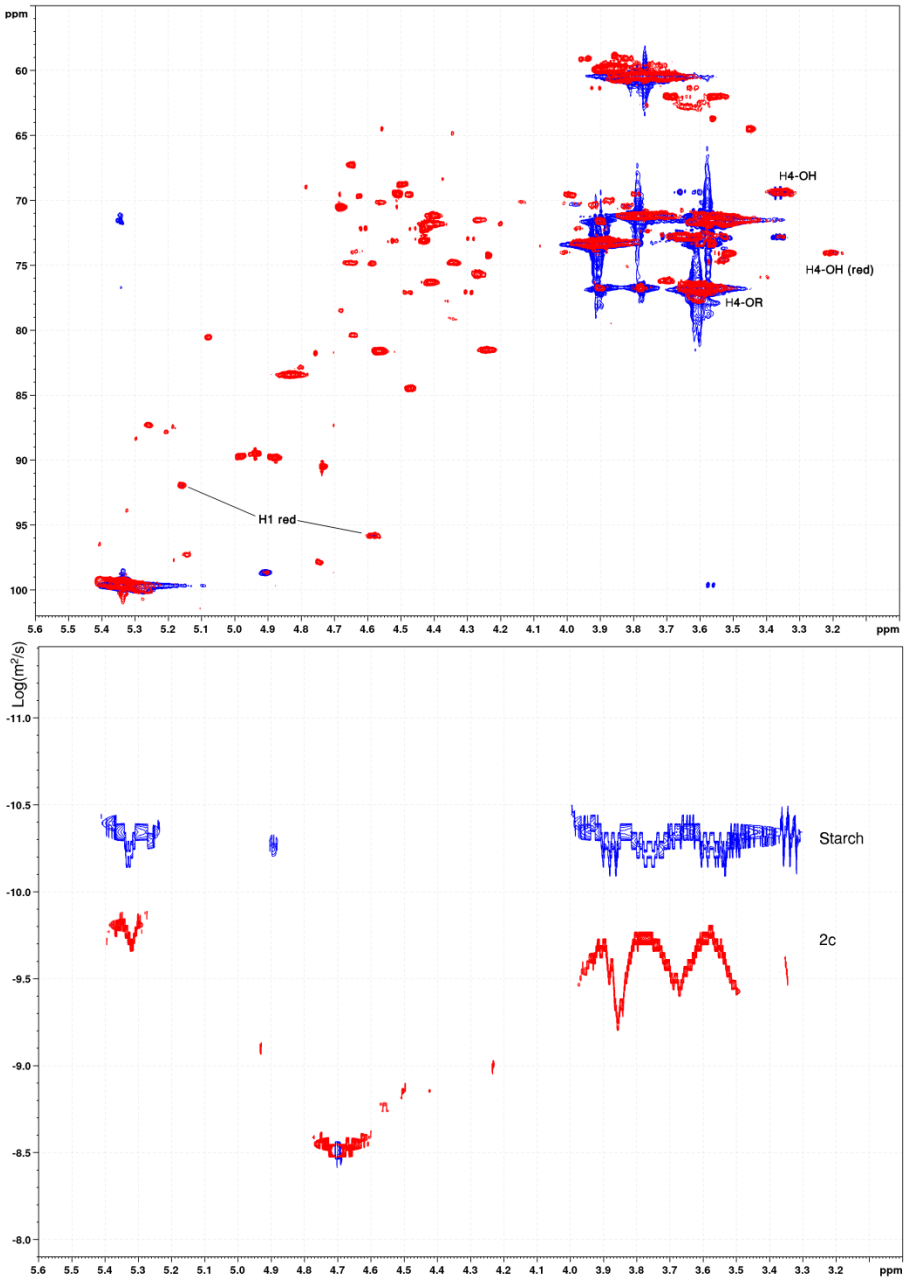

Figure 4.17. HSQC (top) and DOSY (bottom) spectra of starch (blue) and degradation product 2c (red).

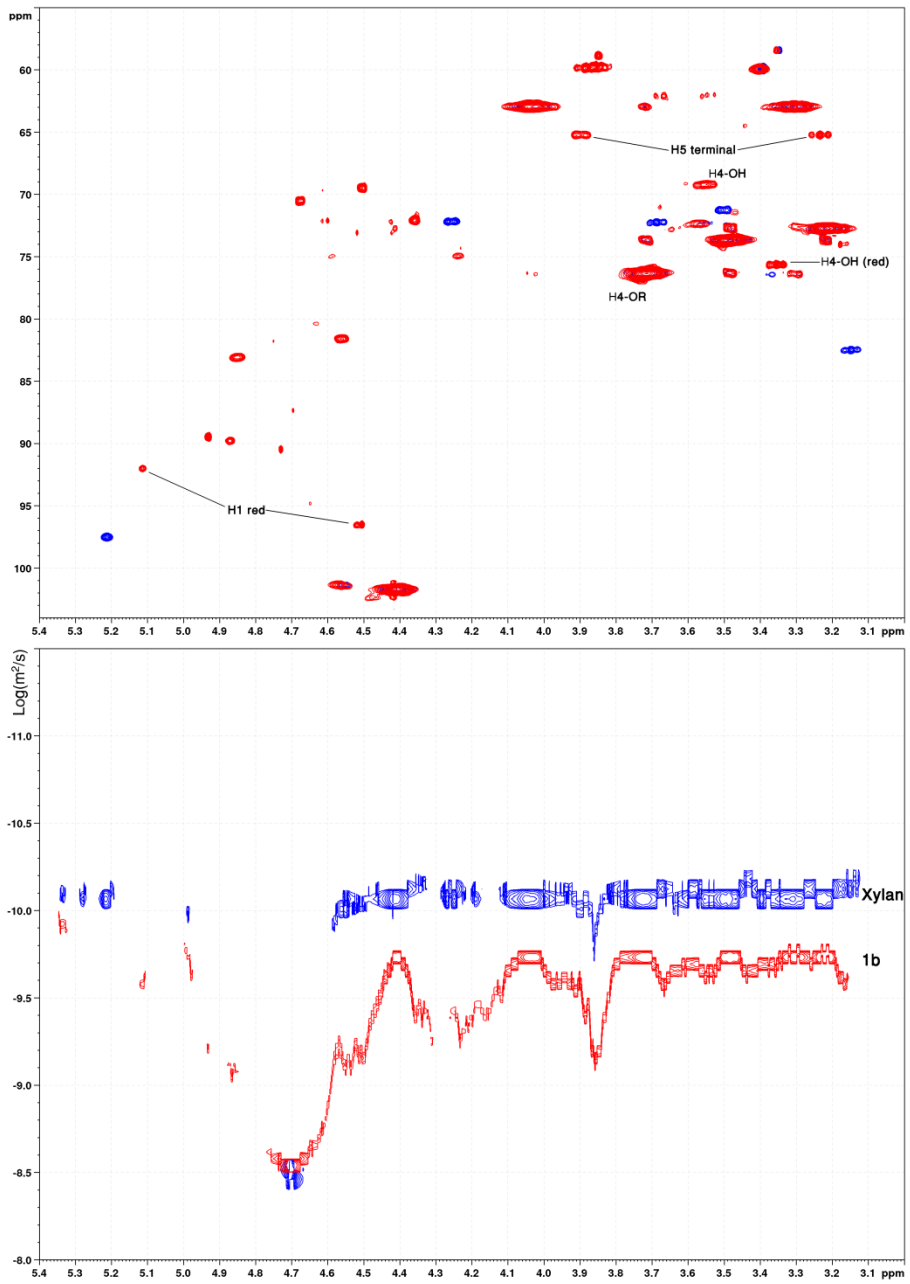

Figure 4.18. HSQC (top) and DOSY (bottom) spectra of xylan (blue) and degradation product 1b (red).

4.6 Conclusions

By combining the concepts of using carbohydrate-based ligands for protein receptors and carbohydrates as carriers for biomolecules a method for preparing natural polysaccharide mimics has been developed. The potential applicability of the method has been evaluated, by investigating the binding between Gal-3 and dextran functionalized with various disaccharide fragments. All compounds have been meticulously characterized by NMR, HPSEC and MALLS to assure that they correctly represent the assumed structures.

In the binding studies, unexpected interactions between Gal-3 and dextrans functionalized with other than galactose-containing disaccharides was witnessed, suggesting that the interactions between carbohydrate ligands and protein receptors might be a more complex phenomenon, than what is typically assumed. These findings might also, due to the nature of the studied protein, in the future provide insights into the complicated mechanisms of cancerous diseases.

During the modification of dextran, one of the most well-known and widely applied "click" reactions, the copper(I)-catalyzed azide-alkyne cycloaddition (CuAAC), was found to be detrimental to the polysaccharide backbone. These findings prompted a more in-depth investigation into the applicability of the same conditions, for obtaining well-defined polysaccharide fragments from natural polysaccharides. The reaction was found to generate fragments of well-defined size, and thus these findings could provide access to molecules that are extremely laborious to prepare by conventional methods.

4.7 Experimental

4.7.1 Instrumental and general information

All reagents for synthetic work were purchased from Sigma-Aldrich, unless mentioned otherwise, and used without further purification. GGM was obtained from the Laboratory of Wood and Paper chemistry at Åbo Akademi University. Dry solvents were either distilled (CH_2Cl_2 Over CaH_2). TLC was performed on aluminum sheets precoated with Silica gel 60 F_{254} (Merck) and the spots were visualized by UV and charred by using a 1:4 solution of H_2SO_4 in MeOH, followed by heating. Column chromatography was carried out using Silica gel 60 (0.040 – 0.060 mm, Merck) for normal phase and silica gel 100 C_{18} (0.015 – 0.035 mm, Fluka) for reverse phase.

NMR spectra were recorded on a Bruker AVANCE III spectrometer operating at 500.20 MHz (^{1}H) and 125.78 MHz (^{13}C) equipped with a Prodigy BBO CryoProbe or a Bruker AVANCE III spectrometer operating at 600.16 MHz (^{1}H) and 150.9 MHz (^{13}C) equipped with a Prodigy TCI inverted CryoProbe optimized for proton detection. ^{15}N-^{1}H HSQC experiments were performed on a Bruker Avance II instrument with a standard triple-channel probe operating at 600.13 MHz (^{1}H) and 60.8 MHz (^{15}N). Coupling constants in the NMR data are reported only the first time they are encountered to avoid unnecessary bloating of the NMR data. Accurate chemical shifts and coupling constants were obtained with the NMR simulation software PERCH.[16]

K_d values of the interactions between Gal-3 and the ligands were estimated by plotting $\Delta\delta/\Delta\delta_{max}$ vs [L] and fitting a function $\Delta\delta/\Delta\delta_{max} = [L]/(K_d+[L])$ to the plot. The $\Delta\delta$ values were measured as weighted average values for ^{1}H and ^{15}N shifts using $\alpha = 0.2$ as weighting factor for the ^{15}N shifts.[29,72]

DOSY spectra were recorded at a concentration of approximately 2 mg/mL and HSQC at a concentration of 10 mg/mL. The starch samples and the unreacted xylan sample had to be heated to approximately 80 °C to make everything dissolve. Upon cooling some precipitate was observed, which could mean that the lower molecular-weights might be slightly overrepresented in these samples.

HPSEC/MALLS analysis was performed on an Agilent 1260 series (G1311B) instrument equipped with a refractive index detector (Shimadzu RID-10A) and MALLS detector (Wyatt Technology miniDAWN Tristar). The setup consisted of a guard column (Waters, Ultrahydrogel 6 mm × 40 mm) and two columns (2 × Ultrahydrogel linear 7.8 mm × 300 mm) connected in series. Eluent: 100 mM $NaNO_3$; flow rate: 0.5 mL/min; injection volume: 200 µL.

HRMS were recorded on a Bruker MicroToF-Q with electrospray ionization operating in positive mode.

4.7.2 Synthetic procedures

2-[2-(2-Azidoethoxy)ethoxy)ethyl *O*-(2,3,4,6-tetra-*O*-benzoyl-β-D-galactopyranosyl)-(1→4)-2,3,6-tri-*O*-benzoyl-β-D-glucopyranoside (5): To a solution of 1-O-(2,3,4,6-Tetra-O-benzoyl-β-D-galactopyranosyl)-(1→4)-2,3,6-tri-O-benzoyl-α-d-glucopyranosyl Trichloroacetimidate (4.00 g, 3.29 mmol, 1 equiv.) and 2-[2-(2-azidoethoxy)ethoxy)ethanol (864 mg, 4.94 mmol, 1.5 equiv.) in freshly distilled CH_2Cl_2 (40 mL) was added 4 Å molecular sieves after which the solution was cooled down to –30 °C and TMSOTf (60 µL, 0.33 mmol, 0.1

equiv.) was added. The reaction mixture was stirred at –30 °C for 2 h and then quenched with Et_3N and evaporated. The crude product was purified by column chromatography (hexane : EtOAc, 1 : 1) which yielded pure **1** as a white foam. Yield 3.18 g (81%), R_f = 0.39.

^{1}H NMR (600.16 MHz, $CDCl_3$, 25 °C): δ = 8.05 – 7.10 (m, 35 H, arom. H), 5.80 (1 H, dd, $J_{H3A,\ H2A}$ = 9.9 Hz, $J_{H3A,\ H4A}$ = 9.1 Hz, H3A), 5.73 (dd, 1 H, $J_{H4B,\ H3B}$ = 3.4 Hz, $J_{H4B,\ H5B}$ = 1.1 Hz, H4A), 5.72 (dd, 1 H, $J_{H2B,\ H1B}$ = 7.9 Hz, $J_{H2B,\ H3B}$ = 10.3 Hz, H2B), 5.46 (dd, 1 H, $J_{H2A,\ H1A}$ = 7.9 Jz, H2A), 5.37 (dd, 1 H, H2B), 4.88 (d, 1 H, H1B), 4.82 (d, 1 H, H1A), 4.60 (dd, 1 H, $J_{H6Aa,\ H5A}$ = 1.9 Hz, $J_{H6Aa,\ H6Ab}$ = –12.1 Hz, H6Aa), 4.49 (dd, 1 H, $J_{H6Ab,\ H5A}$ = 4.3 Hz, H6Ab), 4.25 (dd, 1 H, $J_{H4A,\ H5A}$ = 9.9 Hz, H4A), 3.90 (ddd, 1 H, $J_{H1'a,\ H1'b}$ = –11.5 Hz, $J_{H1'a,\ H2'a}$ = 4.83 Hz, $J_{H1'a,\ H2'b}$ = 3.4 Hz, H1′a), 3.88 (ddd, 1 H, $J_{H5B,\ H6Ba}$ = 6.7 Hz, $J_{H5B,\ H6Bb}$ = 6.6 Hz, H5B), 3.83 (ddd, 1 H, H5A), 3.73 (dd, 1 H, $J_{H6Ba,\ H6Bb}$ = –11.4 Hz, H6Ba), 3.71 (ddd, 1 H, $J_{H1'b,\ H2'a}$ = 3.3 Hz, $J_{H1'a,\ H2'b}$ = 7.4 Hz, H1′b), 3.69 (dd, 1 H, H6Bb), 3.57 (ddd, 1 H, $J_{H2'a,\ H2'b}$ = –11.4 Hz, H2′a), 3.53 (ddd, 1 H, H2′b), 3.499 (ddd, 1 H, $J_{H5'a,\ H5'b}$ = –13.2 Hz, $J_{H5'a,\ H6'a}$ = 6.5 Hz, $J_{H5'a,\ H6'b}$ = 7.0 Hz, H5′a), 3.497 (ddd, 1 H, $J_{H5'b,\ H6'a}$ = 4.2 Hz, $J_{H5'b,\ H6'b}$ = 7.0 Hz, H5′b), 3.44 (ddd, 1 H, $J_{H3'a,\ H3'b}$ = –10.9 Hz, $J_{H3'a,\ 4'a}$ = 6.4 Hz, $J_{H3'a,\ H4'b}$ = 3.2 Hz, H3′a), 3.43 (ddd, 1 H, $J_{H3'b,\ H4'a}$ = 3.1 Hz, $J_{H3'b,\ H4'b}$ = 6.0 Hz, H3′b), 3.36 (ddd, 1 H, $J_{H4'a,\ H4'b}$ = –10.9 Hz, H4′a), 3.35 (ddd, 1 H, H4′b), 3.284 (ddd, 1 H, $J_{H6'a,\ H6'b}$ = –8.5 Hz, H6′a), 3.282 (ddd, 1 H, H6′b) ppm.

^{13}C NMR (150.9 MHz, $CDCl_3$, 25 °C): δ = 165.8, 165.6, 165.40, 165.39, 165.22, 165.16, 164.8 (O*C*OPh), 133.5, 133.40, 133.38, 133.37, 133.3, 133.17. 133.15 (arom. C), 130.0 – 128.8 (35 C, arom. C), 101.2 (C1A), 101.0 (C1B), 76.1 (C4A), 73.0 (C5A), 72.9 (C3A), 72.0 (C2A, C2B), 71.4 (C5B), 70.6 (C3′), 70.5 (C4′), 70.4 (C2′), 69.90 (C3B), 69.88 (C5′), 69.4 (C1′), 67.5 (C4B), 62.4 (C6A), 61.1 (C6B), 50.6 (C6′) ppm.

HRMS: *m/z* calcd. for $C_{67}H_{61}N_3NaO_{20}$ $[M + Na]^+$ = 1250.3741, found 1350.3742.

2-[2-(2-Azidoethoxy)ethoxy)ethyl *O*-(β-D-galactopyranosyl)-(1→4)-β-D-glucopyranoside (1): To a solution of **5** (3.10 g, 1.59 mmol) in THF (5 mL) and MeOH (10 mL) was added 5.4 M NaOMe/MeOH solution (0.5 mL) and the reaction mixture was stirred at ambient temperature for 2.5 h. The mixture was then neutralized with DOWEX 50WX8 H^+ form and evaporated to dryness to obtain pure **1** as a white powder. Yield 1.22 g (94%).

^{1}H NMR (600.16 MHz, D_2O, 25 °C): δ = 4.56 (d, 1 H, $J_{H1A,\ H2A}$ = 8.0 Hz, H1A), 4.49 (d, 1 H, $J_{H1B,\ H2B}$ = 7.9 Hz, H1B), 4.11 (ddd, 1 H, $J_{H1'a,\ H1'b}$ = –11.6 Hz, $J_{H1'a,\ H2'a}$ = 4.0 Hz, $J_{H1'a,\ H2'b}$ = 4.4 Hz, H1′a), 4.02 (dd, 1 H, $J_{H6Aa.\ H5A}$ = 2.3 Hz, $J_{H6Aa,\ H6Ab}$ = –12.3 Hz, H6Aa), 3.97 (dd, 1 H, $J_{H4B,\ H3B}$ = 3.4 Hz, $J_{H4B,\ H5B}$ = 0.2 Hz, H4B), 3.89 (ddd, 1 H, $J_{H1'b,\ H2'a}$ = 4.9 Hz, $J_{H1'b,\ H2'b}$ = 4.7 Hz, H1′b), 3.85 (dd, 1 H, $J_{H6Ab,\ H5A}$ = 5.4 Hz, H6Ab), 3.83 (dd, 1 H, $J_{H6Ba,\ H5B}$ = 8.8 Hz, $J_{H6Ba,\ H6Bb}$ = –12.2 Hz, H6Ba), 3.804 (each dd, each 1 H, H2′a, H2′b), 3.796 (dd, 1 H, $J_{H6Bb,\ H5B}$ = 3.9 Hz, H6Bb), 3.79 – 3.75 (m, 6 H, H3′a, H3′b, H4′a, H4′b, H5′a, H5′b), 3.77 (ddd, 1 H, H5B), 3.71 (dd, 1 H, $J_{H3B,\ H2B}$ = 9.9 Hz, H3B), 3.701 (dd, 1 H, $J_{H3A,\ H2A}$ = 9.6 Hz, $J_{H3A,\ H4A}$ = 8.8 Hz, H3A), 3.967 (dd, 1 H, $J_{H4A,\ H5A}$ = 9.4 Hz, H4A), 3.64 (ddd, 1 H, H5A), 3.59 (dd, 1 H, H2B), 3.55 (m, 2 H, H6′a, H6′b), 3.39 (dd, 1 H, H2A) ppm.

^{13}C NMR (150.9 MHz, D_2O, 25 °C): δ =103.0 (C1B), 102.1 (C1A), 78.4 (C4A), 75.4 (C5B), 74.8 (C5A), 74.3 (C3A), 72.8 (C2A), 72.6 (C3B), 71.0 (C2B), 69.7 (C2′), 69.6, 69.5 (C3′, C4′), 69.2 (C5′), 68.8 (C1′), 68.6 (C4B), 61.0 (C6B), 60.1 (C6A), 50.2 (C6′) ppm.

HRMS: *m/z* calcd. for $C_{18}H_{33}N_3NaO_{13}$ $[M + Na]^+$ = 522.1906, found 522.1934.

2-[2-(2-Azidoethoxy)ethoxy)ethyl *O*-(β-D-mannopyranosyl)-(1→2)-α-D-mannopyranoside (2): To a solution of 2-[2-(2-azidoethoxy)ethoxy]ethyl *O*-[4,6-*O*-benzylidene-2,3-di-*O*-(4-methoxybenzyl)-β-D-mannopyranosyl]-(1→2)-4,6-*O*-benzylidene-3-*O*-(4-methoxybenzyl)-α-D-mannopyranoside (1.00 g, 0.97 mmol, 1 equiv.) in CH_2Cl_2 (10 mL) was added 1,3-propanedithiol (775 µL, 7.7 mmol, 8 equiv.) and then the mixture was cooled on an ice bath. H_2O (1 mL) and TFA (4 mL) were added and the reaction was stirred at ambient temperature for 24 h. The reaction mixture was then diluted with H_2O (50 mL) and washed with CH_2Cl_2 (4 × 50 mL) after which the water layer was evaporated. The crude product was purified by reverse phase column chromatography (H_2O : MeOH, 3 : 1) which yielded pure **2** as a white powder. Yield: 360 mg (74%), R_f = 0.56.

^{1}H NMR (600.16 MHz, D_2O, 25 °C): δ = 5.03 (d, 1 H, $J_{H1A,\ H2A}$ = 1.7 Hz, H1A), 4.80 (s, 1 H, H1B), 4.21 (dd, 1 H, $J_{H2A,\ H3A}$ = 3.4 Hz, H2A), 4.08 (d, 1 H, $J_{H2B,\ H3B}$ = 3.3 Hz, H2B), 3.96 (dd, 1 H, $J_{H6Ba,\ H5B}$ = 2.3 Hz, $J_{H6Ba,\ H6Bb}$ = –12.0 Hz, H6Ba), 3.93 (ddd, 1 H, $J_{H1'a,\ H1'b}$ = –11.7 Hz, $J_{H1'a,\ H2'a}$ = 4.5 Hz, $J_{H1'a,\ H2'b}$ = 4.0 Hz, H1′a), 3.91 (dd, 1 H, $J_{H6Aa,\ H5A}$ = 2.1 Hz, $J_{H6Aa,\ H6Ab}$ = –12.3 Hz, H6Aa), 3.88 (dd, 1 H, $J_{H3A,\ H4A}$ = 9.4 Hz, H3A), 3.82 (dd, 1 H, $J_{H6Ab,\ H5A}$ = 5.7 Hz, H6Ab), 3.78 (each dd, each 1 H, $J_{H2'a,\ H1'b}$ = 7.2 Hz, $J_{H2'b,\ H1'b}$ = 2.8 Hz, H2′a, H2′b), 3.78 – 3.75 (m, 6 H, H3′a, H3′b, H4′a, H4′b, H5′a, H5′b), 3.77 (dd, 1 H, $J_{H6Bb,\ H5B}$ = 7.0 Hz,

H6Bb), 3.74 (dd, 1 H, $J_{H4A,\ H5A}$ = 10.6 Hz, H4A), 3.72 (ddd, 1 H, H1′b), 3.70 (ddd, 1 H, H5A), 3.68 (dd, 1 H, $J_{H3B,\ H4B}$ = 9.7 Hz, H3B), 3.61 (dd, 1 H, $J_{H4B,\ H5B}$ = 9.8 Hz, H4B), 3.53 (m, 2 H, H6′a, H6′b), 3.41 (ddd, 1 H, H5B) ppm.

^{13}C NMR (150.9 MHz, D_2O, 25 °C): δ = 98.6 (C1B), 97.8 (C1A), 77.1 (C2A), 76.4 (C5B), 72.80 (C5A), 72.76 (C3B), 70.8 (C2B), 69.9 (C3A), 69.6 (C2′), 69.53, 69.47 (C3′, C4′), 69.3 (C5′), 67.0 (C4A), 66.7 (C4B), 66.6 (C1′), 61.0 (C6B), 60.6 (C6A), 50.1 (C6′) ppm.

$^1J_{C1A,\ H1A}$ = 171.1 Hz, $^1J_{C1B,\ H1B}$ = 160.9 Hz.

HRMS: *m/z* calcd. for $C_{18}H_{33}N_3NaO_{13}$ $[M + Na]^+$ = 522.1906, found 522.1905.

2[2-(2-azidoethoxy)ethoxy]ethyl *O*-(α-D-glucopyranosyl)-(1→4)-β-D-glucopyranoside (3). Peracetylated maltose (4.4 g, 6.4 mmol) was dissolved in dry CH_2Cl_2 (20 mL, under an argon atmosphere). 2-[2-(2-chloroethoxy)ethoxy]ethanol (5 ml, 35 mmol, 5.5 equiv.) was added to the solution and the reaction mixture was cooled on an ice bath. $BF_3{\cdot}OEt_2$ (6.5 ml, 53 mmol, 8.3 equiv.) was added dropwise and the reaction mixture was slowly warmed to r.t. and left to stir for 5 hours (MALDI-TOF analysis was utilized to monitor the reaction progress: $[M+Na]^+$ calculated for $C_{32}H_{47}ClO_{20}Na$: 809.22; observed: 809.65). The reaction mixture was cooled on an ice bath and neutralized with Et_3N. The mixture was brought to rt, diluted with CH_2Cl_2 (30 mL) and washed with satd. $NaHCO_3$-solution (30 mL) and brine (30 mL). The organic phase was separated dried over Na_2SO_4, filtered and concentrated. The crude product was partially purified by column chromatography (EtOAc:hexane 2:1; R_f = 0.35 in EtOAc:hexane 1:1) to give an oil (4.6 g). The partially purified product was utilized as such in the following step.

The oil (4.6. g) was dissolved in dry DMF (30 mL) and Bu_4NI (2 g, 5.85 mmol, ~ 1 equiv.) and NaN_3 (2.3 g, 35 mmol, ~ 6 equiv.) was added. The resulting mixture was refluxed at 87 °C overnight (MALDI-TOF analysis was utilized to monitor the reaction progress; $[M+Na]^+$ calculated for $C_{32}H_{47}N_3O_{20}Na$: 816.26; observed: 816.47) and concentrated. The crude product was filtered through a pad of silica (EtOAc:hexane 3:1; R_f = 0.39 in EtOAc:hexane 3:1) (impurities still present). The partially purified product was utilized as such in the following step.

The crude product was dissolved in dry MeOH (10 mL) and the pH was adjusted to 10-11 with a 5 M solution of NaOMe. TLC-monitoring (MeOH:CH_2Cl_2 1:3) of the reaction progress indicated that the reaction was complete after 1.5 hours.

The reaction mixture was neutralized with AG 50-X8 (H^+-form), diluted with MeOH (20 mL), filtered and concentrated to give the crude product. The crude product was purified by column chromatography (MeOH:CH_2Cl_2 1:3; R_f = 0.42 in MeOH:CH_2Cl_2 1:3) to give the title compound as a white foam (870 mg, 1.7 mmol, yield over three steps: 27 %).

^{1}H NMR (500.10 MHz, D_2O, 25 °C): δ = 5.41 (d, 1 H, $J_{H1B,\ H2B}$ = 4.0 Hz, H1B), 4.52 (d, 1 H, $J_{H1A,\ H2A}$ = 8.0 Hz, H1A), 4.08 (ddd, 1 H, $J_{H1'a,\ H1'b}$ = –11.7 Hz, $J_{H1'a,\ H2'a}$ = 4.0 Hz, $J_{H1'a,\ H2'b}$ = 4.6 Hz, H1′a), 3.94 (dd, 1 H, $J_{H6Aa,\ H5A}$ = 2.1 Hz, $J_{H6Aa,\ H6Ab}$ = –12.2 Hz, H6Aa), 3.863 (dd, 1 H, $J_{H6Ba,\ H5B}$ = 2.2 Hz, $J_{H6Ba,\ H6Bb}$ = –12.4 Hz), 3.860 (ddd, 1 H, $J_{H1'b,\ H2'a}$ = 7.9 Hz, $J_{H1'b,\ H2'b}$ = 1.4 Hz, H1′b), 3.79 (dd, 1 H, $J_{H3A,\ H2A}$ = 8.8 Hz, $J_{H3A,\ H4A}$ = 9.8 Hz, H3A), 3.78 (dd, 1 H, $J_{H6Ab,\ H5A}$ = 5.5 Hz, H6Ab), 3.773 (each dd, each 1 H, H2′a, H2′b), 3.772 (dd, 1 H, $J_{H6Bb,\ H5B}$ = 5.4 Hz, H6Bb), 4.744 (s, 4 H, H3′a, H3′b, H4′a, H4′b), 4.738 (each 1 H, each dd, $J_{H5'a,\ H6'a}$ = 7.5 Hz, $J_{H5'a,\ H6'b}$ = 2.3 Hz, $J_{H5'b,\ H6'a}$ = 2.6 Hz, $J_{H5'b,\ H6'b}$ = 7.3 Hz, H5′a, H5′b), 3.72 (ddd, 1 H, $J_{H5B,\ H4B}$ = 10.1 Hz, H5B), 3.69 (dd, 1 H, $J_{H3B,\ H2B}$ = 9.9 Hz, $J_{H3B,\ H4B}$ = 9.2 Hz, H3B), 3.64 (dd, 1 H, $J_{H4A,\ H5A}$ = 9.8 Hz, H4A), 3.60 (ddd, 1 H, H5A), 3.59 (dd, 1 H, H2B), 3.524 (ddd, 1 H, $J_{H6'a,\ H6'b}$ = –11.6 Hz, H6′a), 3.519 (ddd, 1 H, H6′b), 3.43 (dd, 1 H, H4B), 3.34 (dd, 1 H, H2A) ppm.

^{13}C NMR (125.8 MHz, D_2O, 25 °C): δ = 102.1 (C1A), 99.6 (C1B), 76.8 (C4A), 76.1 (C3A), 74.5 (C5A), 73.0 (C2A), 72.8 (C3B), 72.7 (C5B), 71.6 (C2B), 69.7 (C2′), 69.6, 69.5 (C3′, C4′), 69.3 (C4B), 69.2 (C5′), 68.7 (C1′), 60.7 (C6A), 60.5 (C6B), 50.1 (C6′) ppm.

HRMS: *m/z* calcd. for $C_{18}H_{33}N_3NaO_{13}$ $[M + Na]^+$ = 522.1906, found 522.1906.

Propargylated dextran: KOH (4.85 g, 86 mmol, 14 equiv.) was dissolved in 8 ml H_2O and cooled on an ice bath, after which 70 kDa dextran (1 g, 6 mmol glucose units, 1 quivalent) was added and the mixture was stirred until everything dissolved. Propargyl bromide (80% in toluene, 0.33 – 2.67 mL, 3 – 24 mmol, 0.5 – 4 equivalents) and the mixture was stirred on an ice bath for 1 h and at room temperature for 19 h. The reaction mixture was then neutralized by adding acetic acid followed by precipitation int 100 mL EtOH. The residue was dissolved in 10 mL H_2O and precipitated into 100 mL EtOH two more times.

Click reactions: Propargylated dextran (1 equiv. propargyl groups) was dissolved in 3 ml H_2O after which one of the azidofunctionalized disaccharides (2 equiv./propargyl group), CuSO4 (0.3 equiv.) and Na-ascorbate (0.6 equiv.) were added. The reaction mixture was stirred at 55 °C for 19 h after which the mixture was evaporated down to a few drops. MeOH (5 mL) was added, and the

precipitate was collected and washed with additional MeOH (5 mL). The residue was then passed through a PD-10 G-25 desalting column according to manufacturer instructions. Any remaining copper residues were removed by QuadraPure® TU thiourea-based metal ion chelator.

4.8 References

1. Nieuwdorp, M. *et al.* The endothelial glycocalyx: a potential barrier between health and vascular disease. *Curr. Opin. Lipidol.* **16,** 507–511 (2005).

2. Reitsma, S., Slaaf, D. W., Vink, H., Van Zandvoort, M. A. M. J. & Oude Egbrink, M. G. A. The endothelial glycocalyx: Composition, functions, and visualization. *Pflugers Arch. Eur. J. Physiol.* **454,** 345–359 (2007).

3. Willis, L. M. & Whitfield, C. Structure, biosynthesis, and function of bacterial capsular polysaccharides synthesized by ABC transporter-dependent pathways. *Carbohydr. Res.* **378,** 35–44 (2013).

4. Kröncke, K. D., Golecki, J. R. & Jann, K. Further electron microscopic studies on the expression of Escherichia coli group II capsules. *J. Bacteriol.* **172,** 3469–72 (1990).

5. Spinosa, M. R. *et al.* The Neisseria meningitidis capsule is important for intracellular survival in human cells. *Infect. Immun.* **75,** 3594–3603 (2007).

6. Noel, G. J., Hoiseth, S. K. & Edelson, P. J. Type b capsule inhibits ingestion of haemophilus influenzae by murine macrophages: Studies with isogenic encapsulated and unencapsulated strains. *J. Infect. Dis.* **166,** 178–182 (1992).

7. Bernardi, A. *et al.* Multivalent glycoconjugates as anti-pathogenic agents. *Chem. Soc. Rev.* **42,** 4709–4727 (2013).

8. Cecioni, S., Imberty, A. & Vidal, S. Glycomimetics versus multivalent glycoconjugates for the design of high affinity lectin ligands. *Chemical Reviews* **115,** 525–561 (2015).

9. Renaudet, O. & Roy, R. Multivalent scaffolds in glycoscience: an overview. *Chem. Soc. Rev.* **42,** 4515 (2013).

10. Li, S. *et al.* Molecular Modification of Polysaccharides and Resulting Bioactivities. *Compr. Rev. Food Sci. Food Saf.* **15,** 237–250 (2016).

11. Wen, Y. & Oh, J. K. Recent Strategies to Develop Polysaccharide-Based Nanomaterials for Biomedical Applications. *Macromol. Rapid Commun.* **35,** 1819–1832 (2014).

12. Lapasin, R. & Pricl, S. in *Rheology of Industrial Polysaccharides: Theory and Applications* 134–161 (Springer US, 1995).

13. Lapasin, R. & Pricl, S. in *Rheology of Industrial Polysaccharides: Theory and Applications* 1–133 (Springer US, 1995).

14. Stephen, A. M. & Churms, S. C. in *Food Polysaccharides and Their Applications* (eds. Stephen, A. M., Phillips, G. O. & Williams, P. A.) 1–24 (Taylor & Francis Group, 2006).

15. Grischenko, L. A. *et al.* Propargylation of arabinogalactan with propargyl halides-a facile route to new functionalized biopolymers. *Carbohydr. Res.* **376,** 7–14 (2013).

16. *PERCH*. (PERCH Solutions Ltd., 2014).

17. Musher, J. I. & Corey, E. J. Virtual long-range spin-spin couplings in NMR. *Tetrahedron* **18,** 791–809 (1962).

18. Bruch, R. C., Burch, M. D., Noggle, J. H. & White, H. B. Characterization of virtual coupling in the proton nuclear magnetic resonance spectrum of N,N'-diacetylchitobiose by two-dimensional J-resolved spectroscopy. *Biochem. Biophys. Res. Commun.* **123,** 555–561 (1984).

19. Brisson, J.-R. & Carver, J. P. Virtual coupling in the 1H NMR spectrum of N,N'-diacetyl chitobioside. *J. Biol. chemsitry* **257,** 11207–11209 (1982).

20. Whistler, R. L. & BeMiller, J. N. Alkaline Degradation of Polysaccharides. *Adv. Carbohydr. Chem.* **13,** 289–329 (1958).

21. Mozdyniewicz, D. J. & Sixta, H. Carbohydrate degradation reactions during alkaline steeping of dissolving pulp- Influence of air exclusion. *Lenzinger Berichte* **90,** 103–107 (2012).

22. Lallana, E., Riguera, R. & Fernandez-Megia, E. Reliable and efficient procedures for the conjugation of biomolecules through huisgen azide-alkyne cycloadditions. *Angew. Chem., Int. Ed.* **50,** 8794–8804 (2011).

23. McKay, C. S. & Finn, M. G. Click chemistry in complex mixtures: Bioorthogonal bioconjugation. *Chem. Biol.* **21,** 1075–1101 (2014).

24. Matsumura, G. & Pigman, W. Catalytic role of copper and iron ions in the depolymerization of hyaluronic acid by ascorbic acid. *Arch. Biochem. Biophys.* **110,** 526–533 (1965).

25. Herp, A., Rickards, T., Matsumura, G., Jakosalem, L. B. & Pigman, W. Depolymerization of some polysaccharides and synthetic polymers by L-ascorbic acid. *Carbohydr. Res.* **4,** 63–71 (1967).

26. Ekholm, F. S. *et al.* Synthesis of the copper chelator TGTA and evaluation of its ability to protect biomolecules from copper induced degradation during copper catalyzed azide-alkyne bioconjugation reactions. *Org. Biomol. Chem.* **14,** 849–852 (2015).

27. Hong, V., Udit, A. K., Evans, R. A. & Finn, M. G. Electrochemically protected copper(I)-catalyzed azide-alkyne cycloaddition. *ChemBioChem* **9,** 1481–1486 (2008).

28. Fielding, L. NMR methods for the determination of protein-ligand dissociation constants. *Prog. Nucl. Magn. Reson. Spectrosc.* **51,** 219–242 (2007).

29. Williamson, M. P. Using chemical shift perturbation to characterise ligand binding. *Prog. Nucl. Magn. Reson. Spectrosc.* **73,** 1–16 (2013).

30. Henderson, N. C. & Sethi, T. The regulation of inflammation by galectin-3. *Immunol. Rev.* **230,** 160–171 (2009).

31. Kopitz, J. *et al.* Human chimera-type galectin-3: Defining the critical tail length for high-affinity glycoprotein/cell surface binding and functional competition with galectin-1 in neuroblastoma cell growth regulation. *Biochimie* **104,** 90–99 (2014).

32. Zeinali, M., Adelinik, A., Papian, S., Khorramdelazad, H. & Abedinzadeh, M. Role of galectin-3 in the pathogenesis of bladder transitional cell carcinoma. *Hum. Immunol.* **76,** 770–774 (2015).

33. Peng, W., Wang, H. Y., Miyahara, Y., Peng, G. & Wang, R. F. Tumor-associated galectin-3 modulates the function of tumor-reactive T cells. *Cancer Res.* **68,** 7228–7236 (2008).

34. Cardoso, A. C. F., Andrade, L. N. de S., Bustos, S. O. & Chammas, R. Galectin-3 Determines Tumor Cell Adaptive Strategies in Stressed Tumor Microenvironments. *Front. Oncol.* **6,** 127 (2016).

35. Nangia-Makker, P., Nakahara, S., Hogan, V. & Raz, A. Galectin-3 in apoptosis, a novel therapeutic target. *J. Bioenerg. Biomembr.* **39,** 79–84 (2007).

36. Jouault, T. *et al.* β-1,2-linked oligomannosides from Candida albicans act as signals for tumor necrosis factor alpha production. *Infect. Immun.* **63,** 2378–2381 (1995).

37. Jouault, T. *et al.* Specific Recognition of Candida albicans by Macrophages Requires Galectin-3 to Discriminate Saccharomyces cerevisiae and Needs Association with TLR2 for Signaling. *J. Immunol.*

177, 4679–4687 (2006).

38. Fradin, C., Poulain, D. & Jouault, T. beta -1,2-Linked Oligomannosides from Candida albicans Bind to a 32-Kilodalton Macrophage Membrane Protein Homologous to the Mammalian Lectin Galectin-3. *Infect. Immun.* **68,** 4391–4398 (2000).

39. Netea, M. G., Brown, G. D., Kullberg, B. J. & Gow, N. A. R. An integrated model of the recognition of Candida albicans by the innate immune system. *Nat. Rev. Microbiol.* **6,** 67–78 (2008).

40. Gow, N. A. & Hube, B. Importance of the Candida albicans cell wall during commensalism and infection. *Curr. Opin. Microbiol.* **15,** 406–412 (2012).

41. Jawhara, S. *et al.* Murine model of dextran sulfate sodium-induced colitis reveals Candida glabrata virulence and contribution of β-mannosyltransferases. *J. Biol. Chem.* **287,** 11313–11324 (2012).

42. Klis, F. M., de Koster, C. G. & Brul, S. Cell wall-related bionumbers and bioestimates of Saccharomyces cerevisiae and Candida albicans. *Eukaryotic Cell* **13,** 2–9 (2014).

43. Chaffin, W. L., López-Ribot, J. L., Casanova, M., Gozalbo, D. & Martínez, J. P. Cell wall and secreted proteins of Candida albicans: identification, function, and expression. *Microbiol. Mol. Biol. Rev.* **62,** 130–180 (1998).

44. Nelson, R. D., Shibata, N., Podzorski, R. P. & Herron, M. J. Candida mannan: Chemistry, suppression of cell-mediated immunity, and possible mechanisms of action. *Clin. Microbiol. Rev.* **4,** 1–19 (1991).

45. Shibata, N., Kobayashi, H. & Suzuki, S. Immunochemistry of pathogenic yeast, Candida species, focusing on mannan. *Proc. Japan Acad. Ser. B* **88,** 250–265 (2012).

46. Rabinovich, G. A. & Toscano, M. A. Turning 'sweet' on immunity: galectin-glycan interactions in immune tolerance and inflammation. *Nat. Rev. Immunol.* **9,** 338–352 (2009).

47. Chung, A. W. *et al.* Galectin-3 Regulates the Innate Immune Response of Human Monocytes. *J. Infect. Dis.* **207,** 947–956 (2013).

48. Diehl, C. *et al.* Protein flexibility and conformational entropy in ligand design targeting the carbohydrate recognition domain of galectin-3. *J. Am. Chem. Soc.* **132,** 14577–14589 (2010).

49. Miller, M. C. *et al.* Binding of polysaccharides to human galectin-3 at a noncanonical site in its carbohydrate recognition domain. *Glycobiology* **26,** 88–99 (2015).

50. Park, S. J., Borin, B. N., Martinez-Yamout, M. A. & Dyson, H. J. The client protein p53 adopts a molten globule–like state in the presence of Hsp90. *Nat. Struct. Mol. Biol.* **18,** 537–541 (2011).

51. Stone, B. A., Svensson, B., Collins, M. E. & Rastall, R. A. in *Glycoscience: Chemistry and Chemical Biology* (eds. Fraser-Reid, B. O., Tatsuta, K. & Thiem, J.) 2325–2375 (Springer-Verlag Berlin Heidelberg, 2008).

52. Duan, J. & Kasper, D. L. Oxidative depolymerization of polysaccharides by reactive oxygen/nitrogen species. *Glycobiology* **21,** 401–409 (2011).

53. Hein, C. D., Liu, X.-M. & Wang, D. Click chemistry, a powerful tool for pharmaceutical sciences. *Pharm. Res.* **25,** 2216–30 (2008).

54. Liebert, T., Hänsch, C. & Heinze, T. Click chemistry with polysaccharides. *Macromol. Rapid Commun.* **27,** 208–213 (2006).

55. Hafrén, J., Zou, W. & Córdova, A. Heterogeneous 'organoclick' derivatization of polysaccharides. *Macromol. Rapid Commun.* **27,** 1362–1366 (2006).

56. Hasegawa, T. *et al.* 'Click chemistry' on polysaccharides: A convenient, general, and monitorable approach to develop (1→3)-β-d-glucans with various functional appendages. *Carbohydr. Res.* **341,** 35–40 (2006).

57. Sawa, M. *et al.* Glycoproteomic probes for fluorescent imaging of fucosylated glycans in vivo. *Proc. Natl. Acad. Sci. U. S. A.* **103,** 12371–6 (2006).

58. Tanaka, H., Tago, H., Adachi, Y., Ohno, N. & Takahashi, T. Synthesis of a β-glucan polysaccharide analogue by an iterative copper-catalyzed azide-acetylene coupling reaction. *Tetrahedron Lett.* **53,** 4104–4107 (2012).

59. Ebringerová, A. & Heinze, T. Xylan and xylan derivatives – biopolymers with valuable properties, 1. Naturally occurring xylans structures, isolation procedures and properties. *Macromol. Rapid Commun.* **21,** 542–556 (2000).

60. Koch, G. in *Handbook of Pulp* (ed. Sixta, H.) 21–68 (WILEY-VCH Verlag, GmbH & Co. KGaA, 2006).

61. Lebel, R. G., Goring, D. A. I. & Timell, T. E. Solution properties of birch xylan . I. measurement of molecular weight. *J. Polym. Sci.* **28,** 9–28 (1963).

62. Timell, T. E. Recent progress in the chemistry of wood hemicelluloses. *Wood Sci. Technol.* **1,** 45–70 (1967).

63. Koch, H. & Röper, H. New Industrial Products from Starch. *Starch* **40,** 121–131 (1988).

64. Willför, S., Sundberg, K., Tenkanen, M. & Holmbom, B. Spruce-derived mannans - A potential raw material for hydrocolloids and novel advanced natural materials. *Carbohydr. Polym.* **72,** 197–210 (2008).

65. Lundqvist, J. *et al.* Isolation and characterization of galactoglucomannan from spruce (Picea abies). *Carbohydr. Polym.* **48,** 29–39 (2002).

66. Lundqvist, J. *et al.* Characterization of galactoglucomannan extracted from spruce (Picea abies) by heat-fractionation at different conditions. *Carbohydr. Polym.* **51,** 203–211 (2003).

67. Ebringerová, A. *et al.* Norway spruce galactoglucomannans exhibiting immunomodulating and radical-scavenging activities. *Int. J. Biol. Macromol.* **42,** 1–5 (2008).

68. Ekholm, F. S. *et al.* Studies related to Norway spruce galactoglucomannans: Chemical synthesis, conformation analysis, NMR spectroscopic characterization, and molecular recognition of model compounds. *Chem. - A Eur. J.* **18,** 14392–14405 (2012).

69. Uchida, K. & Kawakishi, S. Oxidative depolymerization of polysaccharides induced by the ascorbic acid-copper ion systems. *Agric. Biol. Chem.* **50,** 2579–2583 (1986).

70. Morris, K. F. & Johnson, C. S. J. Resolution of Discrete and Continuous Molecular Size Distributions by Means of Diffusion-Ordered 2D NMR Spectroscopy. *J. Am. Chem. Soc.* **115,** 4291–4299 (1993).

71. Jerschow, A. & Müller, N. Diffusion-separated nuclear magnetic resonance spectroscopy of polymer mixtures. *Macromolecules* 6573–6578 (1998).

72. Wang, W. *et al.* Fast conformational exchange between the sulfur-free and persulfide-bound rhodanese domain of E. coli YgaP. *Biochem. Biophys. Res. Commun.* **452,** 817–821 (2014).

5 Summary, conclusions and future prospects

The aim of this thesis was to gain a fundamental understanding of carbohydrate chemistry: protecting group strategies, stereoselective glycosylations and analysis of products. These concepts were then expanded into developing carbohydrate-based structures for potential biological applications and exploring the interactions between carbohydrates and other macromolecules.

The first chapter of this thesis provided an overview of carbohydrate chemistry starting from the pioneering work of Emil Fischer towards the end of the 19th century and into the 20th century. Fundamental concepts about the structure, nomenclature and methods for modification were introduced. Furthermore, the biological importance and existing, as well as emerging, carbohydrate-based therapeutics were discussed. Finally, new emerging technologies, such as automated synthesis, were discussed.

The second chapter introduced a cornerstone of this thesis: β-(1→2) linked mannosides derived from the cell wall of *Candida albicans* together with their structure and biological properties. The synthetic challenges associated with creating *cis*-glycosides were assessed and the effect of a charged phosphate group on the unique structure of this class of compounds was investigated by NMR and molecular modelling methods. All prepared compounds were thoroughly characterized by NMR spectroscopic techniques and complete assignment of shifts and coupling constants was done by quantum-mechanical simulation of the spectra by the NMR simulation software PERCH.

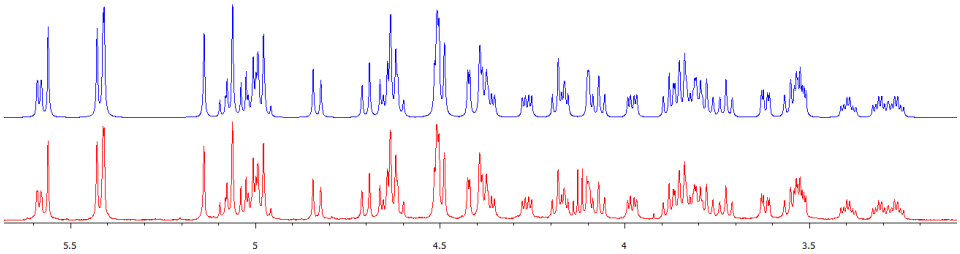

Figure 5.1. NMR spectrum from 5.7 ppm to 3.1 ppm of compound **16** in chapter 2 (bottom) and simulated spectrum (top).

It was discovered that the previously used methods for introducing an anomeric phosphate group to β-(1→2) linked mannosides were not applicable to trisaccharides and tetrasaccharides due to unwanted side reactions during the hydrolysis of the thiophenol group resulting in low yields in this step. A new

method based on direct activation of the thioglycosides towards glycosylation was devised and the target compounds were obtained in satisfactory yields. Conformational studies showed that the anomeric phosphate group has no significant impact on the overall conformation of β-(1→2) linked mannosides.

The third chapter introduced the concept of multivalency. This can be seen as the second dimension of carbohydrate chemistry, with the first dimension being oligosaccharides. Multivalency is a prevalent phenomenon in nature where it increases the affinity of ligands towards their target receptors. The potential applications of multivalent β-(1→2) linked mannosides as adjuvants for specific allergen immunotherapy were explored and first steps towards elucidating their mechanism of action were taken. Conformational behavior of the compounds was investigated by a combination of NMR spectroscopy and molecular dynamics simulations.

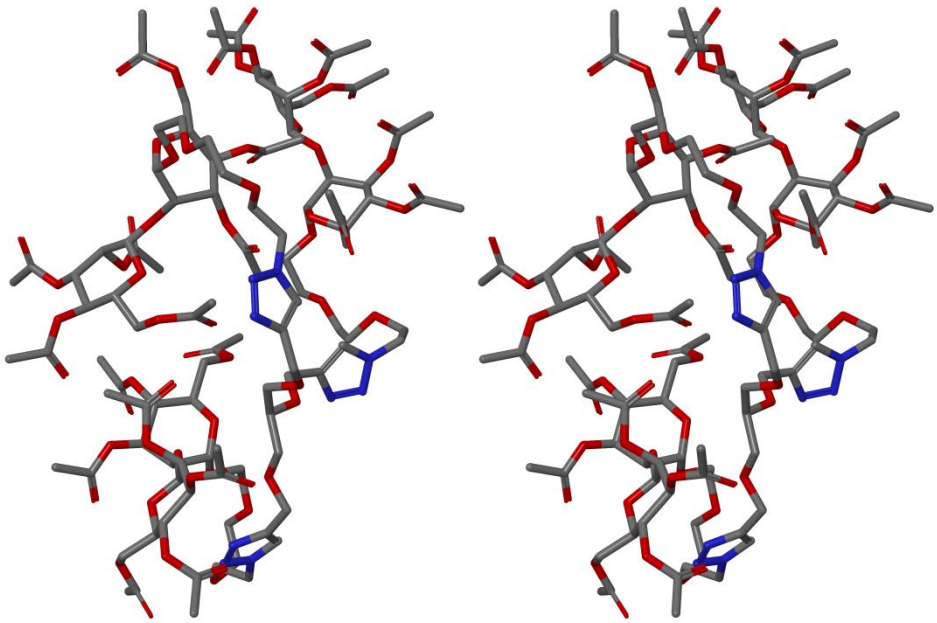

Figure 5.2. Stereoscopic view of compound **3** in chapter 3.

The new compounds **2** and **3** were shown to have similar biological activity as the previously prepared lead compound **1**. The similar activity is explained by all three compounds adopting similar conformations in solution. Preliminary steps towards elucidating the mechanisms behind the biological activity of the compounds were taken in the form of TLR ligation screening which showed that the compounds do not interact with Toll-like receptors, suggesting a different

mechanism than those of CpG-ODN and MPLA. This is supported by the fact that compounds **1**-**3** do not induce TNF production at lower concentrations.

The fourth and final chapter of this thesis expanded the concepts introduced in the two previous chapters. Methods for circumventing the intrinsic heterogeneity of many natural polysaccharides have been developed and well-defined natural polysaccharide mimics have been prepared by attaching various disaccharides to a highly homogenic linear polysaccharide. The interactions between the modified polysaccharides and a protein, human galectin-3, have been investigated by using NMR techniques. Furthermore, a commonly used protocol for convenient polysaccharide functionalization, copper(I)-catalyzed dipolar azide-alkyne cycloaddition, was found to be detrimental to the structural integrity of polysaccharides. The ability of the reaction conditions to degrade polysaccharides into smaller structures of regular size was investigated using industrially and biologically important polysaccharides.

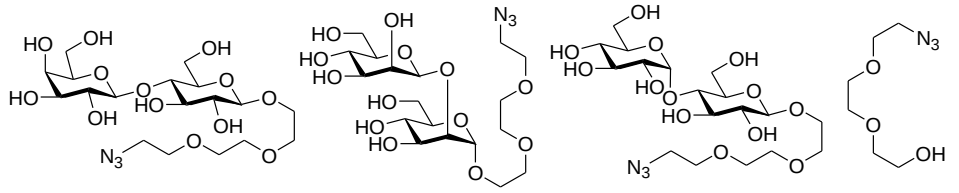

Figure 5.3. The compounds used for functionalization of dextran in chapter 4.

The binding studies showed that Gal-3 binds lactose-functionalized dextran in its canonical binding pocket as expected. Dextrans functionalized with β-(1→2) linked mannosides and maltose, however, were found to interact with a different part of the protein, on the opposite side of the CRD from the canonical binding site. This unusual binding could indicate that protein-carbohydrate interactions may have hitherto unknown impacts on biological systems. Furthermore, the degradation of polysaccharides under typical CuAAC conditions shows that great care should be taken and all available analytical methods should be used to verify the structures of prepared compounds. Conventional NMR spectroscopic methods might hide effects such as degradation of large heterogeneous molecules due to the severe overlapping in the spectra. This phenomenon could, however, be used for controlled depolymerization of polysaccharides into fragments with low polydispersities which could make it applicable for processing of biomass.

To conclude, β-(1→2) linked mannosides analogous to those found in the cell wall of *C. albicans* and derivatives of these have been prepared and their

potential biological applications have been evaluated. The conformational behavior of the molecules in solution has been studied by NMR spectroscopic techniques combined with molecule modelling methods. Furthermore, methods for modifying polysaccharides and preparing structures that imitate natural polysaccharides have been developed. Throughout the thesis, particular attention has been focused on thorough characterization of prepared compounds, especially by NMR spectroscopic methods. A wide array of one and two dimensional methods has been used and quantum mechanical simulation has enabled the extraction of information from complex spectra.

Carbohydrate chemistry dates back over a hundred years and many great discoveries have been made in this field. Even with the increasing knowledge of carbohydrates, many questions remain unanswered and scientific breakthroughs are to be expected in the future. The importance of carbohydrates cannot be denied and in the future their importance might be emphasized due to modern lifestyles contributing to an increase in allergies and antibiotic resistance. The applicability of carbohydrates as vaccines and other immunomodulators makes carbohydrate chemistry an attractive field for future research and the skills developed during the work of this thesis make a solid foundation for such.

Appendix

List of conference contributions

1. **Synthesis of Phosphorylated β-(1→2) Linked Mannosides.** J. Rahkila, R. Panchadhayee, F. S. Ekholm, R. Leino, *COST CM1102 MultiGlycoNano Meeting,* February 2 – 4, 2012, Berne, Switzerland (poster presentation).

2. **Synthesis and Conformational Analysis of Phosphorylated Mannosides.** J. Rahkila, R. Panchadhayee, F. S. Ekholm, A. Ardá, J. Jiménes-Barbero, R. Leino, *Russian-Finnish Scientific Seminar "Renewable Resources Chemistry",* September 19 – 21, 2012, St. Petersburg, Russia (poster presentation).

3. **Conformational analysis of β-(1→2) Linked Mannosides.** J. Rahkila, R. Panchadhayee, F. S. Ekholm, A. Ardá, J. Jiménes-Barbero, R. Leino, *COST CM1102 Multiglyconano Workshop,* September 26 – 28, 2012, Birmingham, United Kingdom (flash presentation).

4. **Immunostimulatory Oligovalent β-(1→2) Linked Mannosides: Synthetic Studies on the Linked Length.** J. Rahkila, R. Leino, *COST CM1102 MultiGlycoNano Meeting,* April 19 – 21, 2013, Prague, Czech Republic (poster presentation).

5. **Benzoylated Glycosyl Trichloroacetimidate Derivatives as Potent Donors for Glycosylations of Phenolic Acceptors.** J. Rahkila, A. K. Misra, R. Leino, *Cost CM1102 MultiGlycoNano Winter Training School*, November 4 – 6, 2013, Grenoble, France (flash presentation).

6. **Immunostimulatory Oligosaccharides – An Update.** J. Rahkila, R. Leino, *Glycoscience Graduate School – Glycobiology in Life Sciences*, December 13, 2013, Helsinki, Finland (oral presentation).

7. **Conformational Studies on Immunostimulatory Glycoclusters.** J. Rahkila, A. Ardá, J. Jiménez-Barbero, R. Leino, *COST CM1102 MultiGlycoNano Meeting*, June 25 – 28, 2014, Siena, Italy (oral presentation).

8. **Conformational Studies on Trivalent Acetylated Mannobiose Clusters.** J. Rahkila, R. Panchadhayee, A. Ardá, J. Jiménez-Barbero, R. Leino, *11th Carbohydrate Bioengineering Meeting*, March 10 – 13, 2015, Otaniemi, Espoo, Finland (oral presentation).

9. **Conformational Studies on Trivalent Acetylated Mannobiose Clusters.** J. Rahkila, A. Ardá, J. Jiménez-Barbero, R. Leino, *COST CM1102/IBCarb – Spring Training School,* April 9 – 11, 2015, Bangor, Wales (flash presentation and poster).

10. **Multivalent Molecular Probes for Investigating Carbohydrate – Lectin Interations.** J. Rahkila, F. Ekholm, A. Ardá, J. Jiménez-Barbero, R. Leino, *XXXIX Finnish NMR Symposium*, June 7 – 9, 2017, Turku, Finland (Oral Presentation).

Other publications by the author

I **Increasing the Amphiphility of an Estradiol Based Steroid Structure By Barbier-Allylation – Ring-Closing Metathesis – Dihydroxylation sequence,** T. Saloranta, I. Zupkó, J. Rahkila, G. Schneider, J. Wölfling, R. Leino, *Steroids*, **2011,** *77*, 110 – 117.

II **Cytotoxicity and Anti-Cancer Activity of Ruthenium Half-Sandwich Cyclopentadiene Complexes,** D. Mavrynsky, J. Rahkila, I. Zupkó, M. J. Calhorde, R. Leino, *Organometallics*, **2013,** *32*, 35 – 46.

III **Ultrasonic Energy Promoted Allylation to Generate 1-*C*-(2,3,4,6-Tetra-*O*-Benzyl-α-D-Glucopyranosyl)prop-2-ene,** M. Farrell, C. O'Reilly, D. V. Jarikote, J. Rahkila, P. V. Murphy, in *Carbohydrate Chemistry Proven Synthetic Methods, Vol 2*, (eds. Gijsbert van der Marel, Jeroen Codee); CRC Press/Taylor & Francis Group, 2014, Chapter 4, pp 33 – 37.

IV **Structural Characterization of Birch Lignin Isolated from a Pressurized Hot Water Extraction and Mild Alkali Pulped Biorefinery Process,** L. Lagerquist, A. Pranovich, A. Smeds, S. von Schultz, L. Vähäsalo, J. Rahkila, I. Kilpeläinen, T. Tamminen, S. Willför, P. Eklund, *Ind. Crops. Prod.* **2018,** *111*, 306–316.

ISBN 978-951-765-886-7